Fifth Annual Science Day
Faculty of Science-Sohag University

March 18, 2020

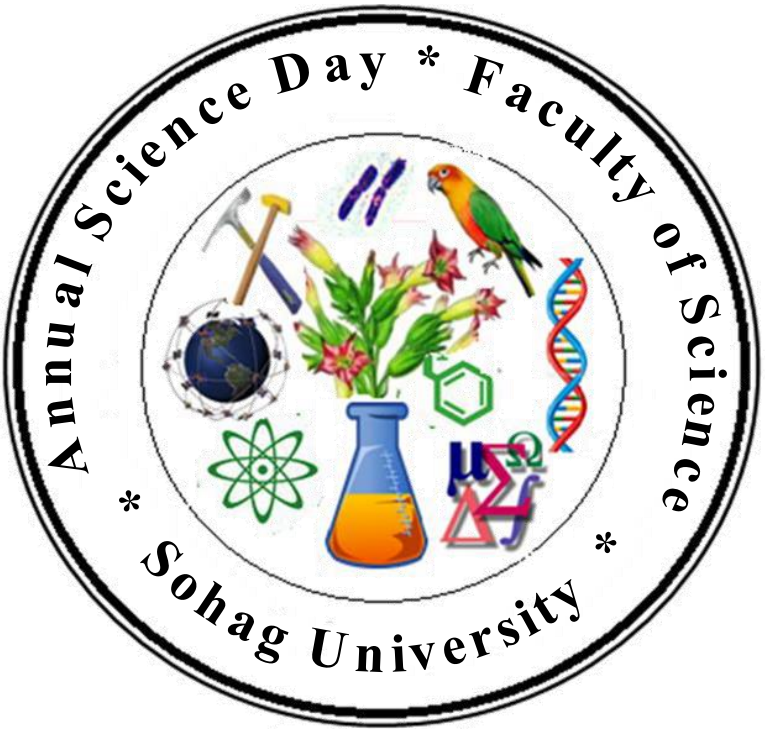

المؤتمر العلمى السنوى الخامس لكلية العلوم
جامعة سوهاج

Abstract Book for Papers Published by Staff Members of Faculty of Science during 2019

PREFACE

This abstract book is compiled of **300** abstracts of the published articles in international journals by Staff members of Faculty of Science, Sohag University during 2019. The book was made on the sidelines of the 5th Annual Science Day ceremony held on, 18 March, 2020 at Sohag Faculty of Science under the patronage of General. **Tarek El Feqi**, the Governor of Sohag, Prof. Dr. **Ahmed Aziz Abdel-Monem**, President of Sohag University, and Prof. Dr. **Ahmed Mohamed Soliman**, Vice President Post-Graduate and Research Affairs.

Besides emerging the scientific research activities of staff members, the Abstract book as a whole is an important reference of the recent advances in research. Furthermore, the Annual Science Day meeting offers an opportunity for researchers from different departments who work on similar research problems but rarely cross paths, to connect with each other. Science Day event is also a great opportunity to share the value of our research with different sectors of community services.

Congratulations to all who participated, and thanks to everyone made this event such a huge success.

Dean of Faculty of Science
Prof. Dr. Ahmed M. Ahmed Ali

Organizing Committee

Prof. Dr. Ahmed M. Ahmed Ali	Dean of Faculty of Science
Prof. Dr. Kamal M. S. Khalil	Vice-Dean for Education & Students Affairs
Prof. Dr. Abdel Baset Abu Deif	Vice-Dean for Community & Environmental Affairs
Prof. Dr. Zakaria A. Mohamed	Chairman of Botany & Microbiology Department
Prof. Dr. Lobna A. E. Naser	Director of Quality Assurance Unit
Prof. Dr. Hazem Elmeshneb	Physics Department
Prof. Mahrous Rashad Ahmed	Physics Department
Prof. Dr. Alaa Y. Fahmey	Zoology Department
Dr. Mohamed Ismael	Chemistry Department
Dr. Mostafa G. Redwan	Geology Department
Dr. Mahmoud Abdel Aleem Ali	Chemistry Department
Dr. Emad F. Newir	Chemistry Department
Dr. Naglaa Yousef	Botany & Microbiology Department
Dr. Mahmoud S. Bakheit	Botany & Microbiology Department
Dr. Mohamed Alaraby	Zoology Department
Dr. Mohamed Attef	Geology Department
Dr. Al-Wageh A. Farghal	Mathematics Department
Dr. Mostafa Abd Allah	Mathematics Department
Dr. Miran Mostafa Khalef	Geology Department
Mrs. Elham A. Abd El-Hameed	Quality Assurance Unit
Mr. Ahmed M. Abdel-Mawgoud	Quality Assurance Unit

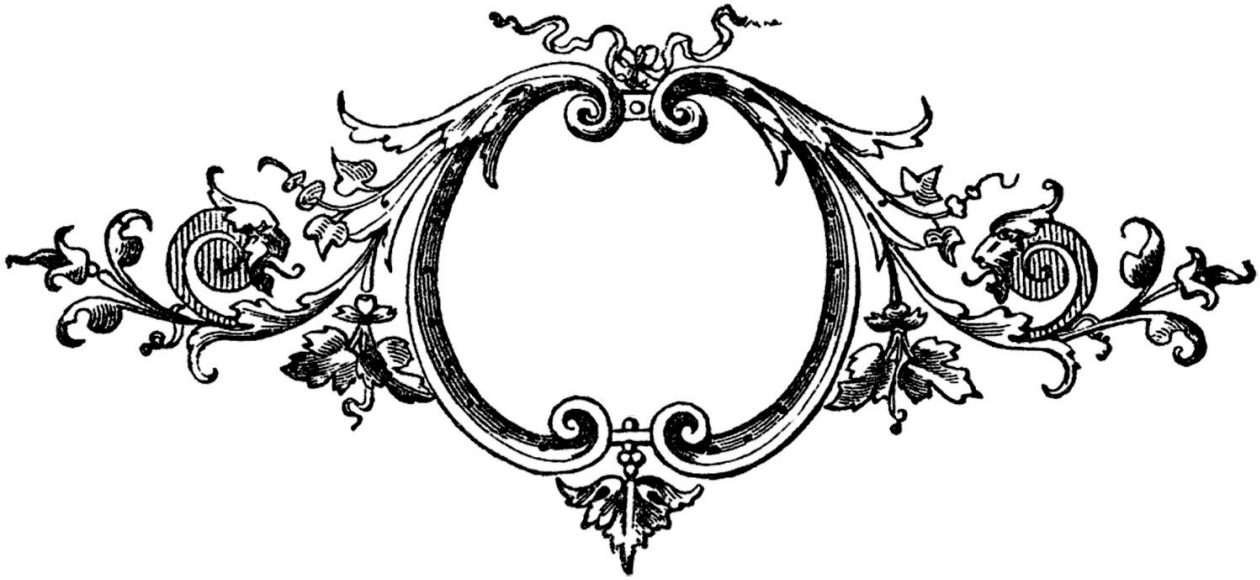

List of Publications

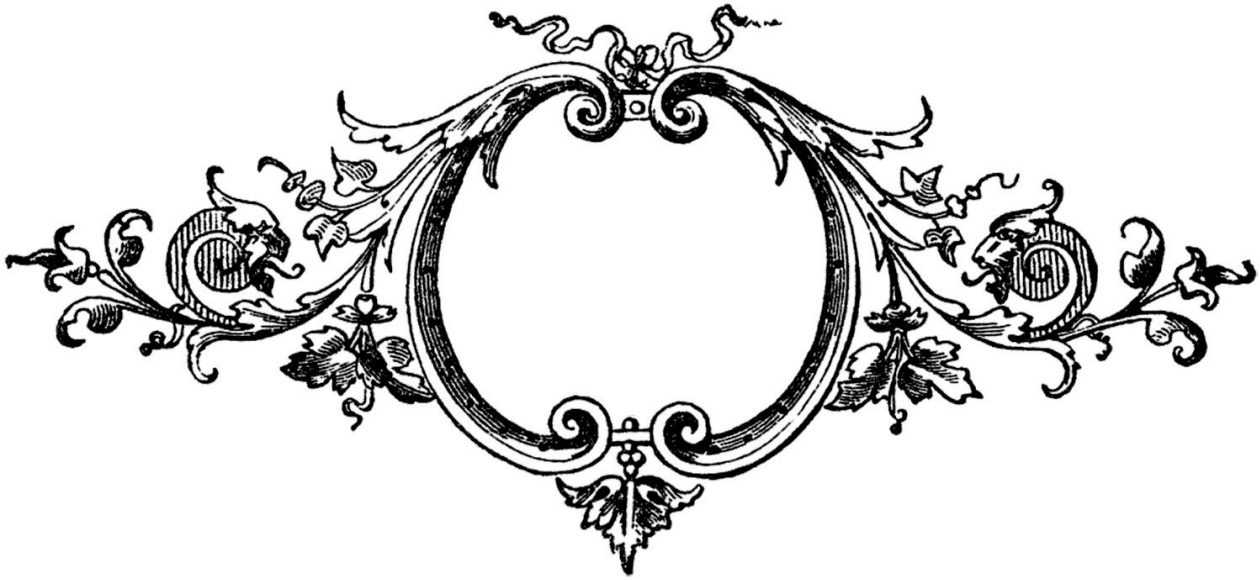

List of papers published by Staff members of Mathematics Department (P. 1-48)

1	**A new general fractional-order derivative with rabotnov fractional-exponential kernel appliedto model the anomalous heat transfer** ***Xiao-Jun Yang, Mahmoud Abdel-Aty, Carlo Cattani***
2	**Direct Observation of Dissipation in Dynamical Search Algorithm using Transmon Qubits** ***Ali H. Homid, Mahmoud Abdel-Aty, Ahmed Farouk, Abdel-Shafy F. Obada***
3	**Reflection and refraction of incident p-, T-, and SVwaves at interface between magnetized two solidliquid media with heat sources and initial stress with and without thermal relaxation times Reflection and refraction of incident p-, T-, and SVwaves at interface between magnetized two solidliquid media with heat sources and initial stress with and without thermal relaxation times** ***Sayed M. Abo-Dahab, Mohamed. N. M. Allam, Mahmoud Abdel-Aty***
4	**New Design of Reversible Full Adder/Subtractor Using R Gate** ***Rasha Montaser, Ahmed Younes, Mahmoud Abdel-Aty***
5	**Controlling steady-state entanglement and quantum discord through squeezing angle** ***Eman G. El-Hadidy, Ahmed Farouk, Mahmoud Abdel-Aty, S. Ghose***
6	**A quantum algorithm based on entanglement measure for classifying Boolean multivariate function into novel hidden classes** ***Mohammed Zidan[a,b], Abdel-Haleem Abdel-Aty[c,d], Duc Manh Nguyen[e], Ahmed S.A. Mohamed[a,f], Yazeed Al-Sbou[g], Hichem Eleuch[h,i], Mahmoud Abdel-Aty[a,b,j]***
7	**Multistability of Stationary Motions for Darcy Convection Anisotropic Problem** ***Abdelhafez M. A.[12], Tsybulin V.G.[1]***
8	**Anisotropy Effects and Cosmymetry of Convective Flows for Nanofluids in Porous Medium** ***Abdelhafez M. A.***
9	**C-fuzzy Soft Closure Operators and Fuzzy Soft Closure Systems** ***El-Sayed El-Sanousy***
10	**Fuzzy soft upper and lower semi-continuous Multifunctions** ***S. E. Abbas, E. El-sanowsy, A. Atef***
11	**On (L;M)-Fuzzy Convex Structures** **Osama Rashed Sayed[a], EL − Sayed EL − Sanousy [b],Yaser Hassanein Sayed[b]**
12	**Stratified Soft L-fuzzy Quasi-proximities** ***El-Sayed El-Sanousy***
13	**A modified shrinking projection methods for numerical reckoning fixed points of g-nonexpansive mappings in hilbert spaces with graphs** ***H. A. Hammad, W. Cholamjiak, D. Yambangwai, And H. Dutta***
14	**Fixed point results for$\emptyset-(\gamma,\mu,n,m)$ contractions with applications to nonlinear integral equations** **Hasanen A. Hammad[1], Manuel De la Sen[2]**
15	**Solution of Nonlinear Integral Equation via Fixed Point of Cyclic α_L^{Ψ} -Rational Contraction Mappings in Metric-Like Spaces** ***Hasanen A. Hammad[1], Manuel De la Sen[2]***
16	**Analytical Solution for a Periodic Boundary Random-value Problem Via Stochastic Fixed Points with PPF Dependence Technique** ***Hasanen Abuelmagd Hammad[1] AND Rashwan A.Rashwan[2]***
17	**Solving a coupled system of functional equations using coupled coincidence point technique in metric-like spaces** ***Dhekra M.Albaqeri[1],Hasanen A.Hammad[2] AND Rashwan A.Rashwan[3]***

18	**PPF-Dependent Fixed Point Results for New Multi-Valued Generalized F-Contraction in the Razumikhin Class with an Application** **HASANEN A. HAMMAD[1] AND MANUEL DE LA SEN[2]**
19	**A Coupled Fixed Point Technique for Solving Coupled Systems of Functional and Nonlinear Integral Equations** **HASANEN A. HAMMAD[1] AND MANUEL DE LA SEN[2]**
20	**Analytical Solution of Urysohn Integral Equations by Fixed Point Technique in Complex Valued Metric Spaces** **HASANEN A. HAMMAD[1] AND MANUEL DE LA SEN[2]**
21	**C-class functions on common fixed point theorems for weak contraction mapping of integral type in modular spaces** **HASANEN A. HAMMAD[1] , R. A. Rashwan[2] , A. H. Ansari[3]**
22	**Coincidence and Fixed Point of Nonexpansive Type Mappings in 2-Metric Spaces** **H. A. Hammad1[1] , A. H. Ansari[2] and R. A. Rashwan[3],**
23	**Analytical solution for a coupled of nonlinear integral equations via coupled fixed point technique** **RASHWAN A. RASHWAN[1] , HASANEN A. HAMMAD[2] and SLOBODANKA MITROVI[3]**
24	**Common fixed point theorems for weakly compatible mappings satisfying a general contractive condition of integral type** **RASHWAN A. RASHWAN[1] *and* HASANEN A. HAMMAD[2],**
25	**Common Fixed Point Theorems in Complex-Valued S-Metric Spaces via Implicit Relations with Applications** **RASHWAN A. RASHWAN[1] , HASANEN A. HAMMAD[2], and M. G. Mahmoud [3]**
26	**Generalized Contractive Mappings and Related Results in b-Metric Like Spaces with an Application** **HASANEN A. HAMMAD[1] AND MANUEL DE LA SEN[2]**
27	**A Solution of Fredholm Integral Equation by Using the Cyclic μ_s^q -Rational Contractive Mappings Technique in b-Metric-Like Spaces** **HASANEN A. HAMMAD[1] AND MANUEL DE LA SEN[2]**
28	**Analytical approximations to nonlinear oscillation of nanoelectro-mechanical resonators** **G. M. Ismail[1], M. Abul − Ez[1], N. M. Farea[1] and N. Saad[2]**
29	**Higher-order approximate periodic solution for the oscillator with strong nonlinearity of polynomial type** **L. Cveticanin[1,2] and G. M. Ismail[3]**
30	**On involute-evolute curve couple in the hyperbolic and de Sitter spaces** H. S. Abdel − Aziz[1], M. Khalifa Saad[1,2] **and** A. A. Abdel − Salam[1]
31	**On the Jacobian of Kuribayashi curves** ***Alwaleed Kamel and Waleed Khaled Elshareef***
32	**Inextensible flows of curves in three-dimensional light cone** ***H. S. Abdel-Aziz, M. Khalifa Saad and Haytham. A. Ali***
33	**Image Pixel Permutation Operation Based on Elliptic Curve Cryptography** Omar Reyad[1,2] , Hany S. Khalifa[3] **and** Radwan Kharabsheh[4]
34	**An Efficient Deep Convolutional Neural Network for Visual Image Classification** Basma Abd El − Rahiem[1], Muhammad Atta Othman Ahmed[2], Omar Reyad[3] Hani Abd El − Rahaman[1], Mohamed Amin1, **Fathi Abd El-Samie[1]**

35	**Image Encryption Algorithm Methodology Based on Multi-mapping Image Pixel** W. M. Abd − Elhafiez[1,2] , Omar Reyad [1] , M. A. Mofaddel [1]
36	**High Efficient Haar Wavelets for Medical Image Compression** ***E. A. Zanaty***
37	**Initial Energy Value Effects on the Performance of Some Heterogeneous Protocols Levels in Wireless Sensor Network** ***Hamdy H. El-Sayed***
38	**Some WSN characteristics effects on the performance of LEACH and MODLEACH protocols** ***Hamdy H. El-Sayed***
39	**Minutiae-Based Fing erprint Extraction: An EffectiveMethod Based on Harris Corner Detector** ***Samy Bakheet, Mahmoud A. Mofaddel, and Rehab Youssef***
40	**A new memristive model with complex variables and its generalized complex synchronizations with time lag** ***Emad E.Mahmoud, Ohood A.Althagafi***
41	**A New Nine-Dimensional Chaotic Lorenz System with Quaternion Variables: Complicated Dynamics, Electronic Circuit Design, Anti-Anticipating Synchronization, and Chaotic Masking Communication Application** ***Emad E. Mahmoud, M. Higazy , Turkiah M. Al-Harthi***
42	**Fuzzy ideal topological spaces** ***Ali N.A. Koam, Ismail Ibedou, S.E. Abbas***
43	**Complex anti-synchronization of two indistinguishable chaotic complex nonlinear models** ***Emad E Mahmoud, Madeha A Al-Adwani***
44	**Connectedness in Fuzzy Soft Topological Spaces** ***S. E. Abbas· El-sayed El-sanowsy· A. Atef***
45	**A general formula of complex synchronizations with complex scaling diagonal matrix and time lag** ***Emad E.Mahmoud Fatimah S.Abood***
46	**Initial fuzzy soft closure structures** ***Ali N. Koam, Ismail Ibedou, S. E. Abbas***
47	**A phenomenal form of complex synchronization and chaotic masking communication between two identical chaotic complex nonlinear structures with unknown parameters** ***Emad E.Mahmoud, Bushra H.AL-Harthi***
48	**Further Results on the Inverse Base of Axially Monogenic Polynomials** ***Mohamed Abdalla · Mahmoud Abul-Ez · Aida Al-Ahmadi***
49	**Effect of a magnetic field on the propagation of waves in a homogeneous isotropic thermoelastic half-space** ***AM Abd-Alla, SM Abo-Dahab, SM Ahmed, MM Rashid***
50	**Rayleigh surface wave propagation in an orthotropic rotating magneto-thermoelastic medium subjected to gravity and initial stress** ***AM Abd-Alla, SM Abo-Dahab, SM Ahmed, MM Rashid***
51	**A magneto–thermo-elastic problem for a half-space without energy dissipation subjected to rotation and gravity field** ***AM Abd-Alla, SM Abo-Dahab, SM Ahmed, MM Rashid***
52	**Effect of magnetic field and three-phase-lag in a rotating micropolar thermo-viscoelastic half-space homogeneous isotropic material** ***SM Abo-Dahab, AM Abd-Alla, SM Ahmed, MM Rashid***

53	**Solution of a problem of thermal stresses in a non-homogeneous thermoelastic infinite medium of isotropic material by finite difference method** ***A.M.Farhan, AM Abd-Alla, MoaiadA.Khder***
54	**Effects of rotation and gravity on an electro-magneto-thermoelastic medium with diffusion and voids by using the Lord-Shulman and dual-phase-lag models** **SM Abo-Dahab, AM Abd-Alla, A. A. KILANY**
55	**Effect of rotation on wave propagation through a poroelastic wet bone with cavity** ***AM Abd-Alla, SM Abo-Dahab, Roqia Ateeq, MoaiadA.Khder***
56	**On problem of the stresses in a non-homogeneous composite of an infinite cylinder of orthotropic material** ***A.M.Farhan, AM Abd-Alla, MoaiadA.Khder***
57	**Effect of heat laser pulse on wave propagation of generalized thermoelastic micropolar medium with energy dissipation** ***Mohamed I. A. Othman, Abo-el-nour N. Abd-alla, Elsayed M. Abd-Elaziz***
58	**Shear horizontal waves in composite materials: Behavior under rotation and initial stress** ***Abo-el-nour N. Abd-alla, Mohamed I. A. Othman, NF Hasbullah***
59	**Analytical solutions of fractional bioheat model in a spherical tissue** **Aatef Hobiny, Ibrahim Abbas**
60	**A GN model on photothermal interactions in a two-dimensions semiconductor half space** **Aatef Hobiny, Ibrahim Abbas**
61	**Photo-thermo-elastic interactions without energy dissipation in a semiconductor half-space** ***Faris S. Alzahrani, Ibrahim Abbas***
62	**Analytical solutions of thermal damage in living tissues due to laser irradiation** ***Faris S. Alzahrani, Ibrahim Abbas***
63	**Analytical estimations of temperature in a living tissue generated by laser irradiation using experimental data** ***Faris S. Alzahrani [1] and Ibrahim Abbas***
64	**Global properties of latent virus dynamics with B-cell impairment** ***A. M. Elaiw, S. F. Alshehaiween, Aatef Hobiny, Ibrahim Abbas***
65	**An analytical solution of the bioheat model in a spherical tissue due to laser irradiation** ***Ibrahim Abbas, Aatef Hobiny, Faris S. Alzahrani***
66	**Two-Temperature Photothermal Interactions in a Semiconducting Material with a 3D Spherical Cavity** ***Aatef Hobiny, Ibrahim Abbas***
67	**Fractional Order Thermoelastic Wave Assessment in a Nanoscale Beam Using the Eigenvalue Technique** ***Ibrahim Abbas, Faris S. Alzahrani , Abo-el-nour N. Abd-alla, F. Berto***
68	**An analytical study on the fractional transient heating within the skin tissue during the thermal therapy** ***Abdeljabbar Ghanmi, Ibrahim Abbas***
69	**Solutions of Some Difference Equations Systems and Periodicity** ***Elsayed M Elsayed, Faris S. Alzahrani , Ibrahim Abbas, NH Alotaibi***
70	**Dynamical Behavior and Solution of Nonlinear Difference Equation Via Fibonacci Sequence** ***Elsayed M Elsayed, Faris S. Alzahrani, Ibrahim Abbas, NH Alotaibi***
71	**Fractional Order GN Model on Photo-Thermal Interaction in a Semiconductor Plane** ***Aatef Hobiny, Ibrahim Abbas***

72	**Модель двухфазного сдвига фототермоупругих волн в двумерной полупроводниковой среде** ***Aatef Hobiny, Ibrahim Abbas***
73	**Analysis of photo-thermo-elastic response in a semiconductor media due to moving heat source** ***Faris S. Alzahrani, Ibrahim Abbas***
74	**Eigenvalue approach for generalized thermoelastic porous medium under the effect of thermal loading due to a laser pulse in DPL model** ***Mohamed IA Othman, Ibrahim Abbas***
75	**A DPL model of photothermal interaction in a semiconductor material** ***Ibrahim Abbas, Faris S. Alzahrani, Ahmed Elaiw***
76	**The Matrix of Matrices Exponential and Application** ***Z. Kishka, M. Saleem, A. Elrawy***
77	**Quantum Fisher information of atomic system interacting with a single cavity mode in the presence of Kerr medium** **N. Zidan[1,2], H. F. Abdel-Hameed[1,3], N. Metwally**
78	**Dynamics of the entanglement and teleportation of thermal state of a spin chain with multiple interactions** ***Ahmad Redwan, Abdel-Haleem Abdel-Aty, Nour Zidan, Tarek El-Shahat***
79	**Entanglement, photon statistics and Wehrl entropy for a time-dependent qubit–field system in the presence of phase decoherence effect** ***S. Abdel-Khalek***
80	**Quantum correlation and non-classical properties in semiconductor microcavities for multi-photon excitation** ***S. Abdel-Khalek, K. Berrada, H. Eleuch***
81	**Optical tomography for excited coherent states associated to deformed oscillators** ***Abdullah M.Almarashi, Ali Algarni, Fahad M.Alaboud, S.Abdel-Khalek, K.Berrada***
82	**Interaction between two two-level atoms coupled to N-level quantum system** ***A.-S. F. Obada, Abdullah F. Al Naim, E. M. Khalil, S. Abdel-Khalek, H. Eleuch***
83	**Quantum Fisher Information And Tomographic Entropy Of A Single Qubit In Excited Binomial And Negative Binomial Distributions** ***Abdullah M. Almarashi, Ali Algarni, S. Abdel-Khalek, Hon Keung Tony Ng***
84	**Entanglement and physical attributes of the interaction between two SC-qubits and thermal field in the presence of a magnetic field** ***Abdullah F.AlNaim, Javed Y.Khan, S.Abdel-Khalek, E.M.Khalil***
85	**Nonclassical properties and field entropy squeezing of the dissipative two-photon JCM under Kerr like medium based on dispersive approximation** ***Haifa S.Alqannas, S.Abdel-Khalek***
86	**Entanglement, nonclassical properties, and geometric phase in circuit quantum electrodynamics with relativistic motion** ***S.Abdel-Khalek, K.Berrada***
87	**Physical and nonclassical properties of the interaction between a four-level atom and field in coherent state of Morse potential** ***Haifa S.Alqannas, S.Abdel-Khalek***
88	**Effects of Kerr Medium and Stark Shift Parameter on Wehrl Entropy and the Field Purity for Two-Photon Jaynes–Cummings Model Under Dispersive Approximation** ***Abdullah F.AlNaim, Javed Y.Khan, S.Abdel-Khalek, E.M.Khalil***
89	**Some features of the geometric phase and entanglement of three-level atom under cavity damping effects** ***S Abdel-Khalek, Y S El-Saman, I Mechai, M Abdel-Aty***

90	**Some features of the nonlocal correlation and geometric phase of the quantum system in two-mode nondegenerate entangled states** ***S Abdel-Khalek, Sadah A. Alkhateeb***
91	**Computing special smarandache curves according to darboux frame in euclidean 4-space** ***M. Khalifa Saad, M. A. Abd-Rabo***
92	**Estimation of Generalized Inverted Exponential Distribution based on Adaptive Type-II Progressive Censoring Data** ***Ahmed A. Soliman, Essam. A. Ahmed, Al-Wageh A. Farghal, Abdulgalil A. AL-Shibany***
93	**A new chaotic system with line of equilibria: dynamics, passive control and circuit design** ***Aceng Sambas, Mustafa Mamat, Ayman Ali Arafa, Gamal M Mahmoud, Mohamad Afendee Mohamed, W. S. Mada Sanjaya***
94	**Thermomechanical response in a two-dimension porous medium subjected to thermal loading** ***Tareq Saeed, Ibrahim Abbas***
95	**Thermal response of cylindrical tissue induced by laser irradiation with experimental study** ***Aatef Hobiny, Ibrahim Abbas***

List of papers published by Staff members of Physics Department (P. 49-63)

1	**Optical, Electrical, and Thermoelectric Properties of Hydrothermally Synthesized Bi_2Te_3 Nanoflakes** ***Mohamed Abdullah Abdullah Mohamed, Hazem Mahmoud Ali, Eslam Mohamed Mohamed Ibrahim, and Moustafa Mohamed Wakkad***
2	**Optical and transport properties of few quintuple-layers of $Bi_{2-x}Sb_xSe_3$ nanoflakes synthesized by hydrothermal method** ***E. M. M. Ibrahim, M. A. A. Mohamed, H. M. Ali, Vyacheslav O. Khavrus, Silke Hampel, M. M. Wakkad***
3	**Structure, Optical, Corrosion, and Photocatalytic Properties of Thermally Evaporated Molybdenum Trioxide Thin Films deposited on different substrates** ***Sh. A. Elkot, W. S. Mohamed, Mahmoud Elrouby, H. M. Ali, E. Kh. Shokr***
4	**Study the effect of the sintering temperature on the microstructure and optical reflectance of the compacted bulk $CuAlS_2$ fabricated by powder metallurgy technique (p/m)** ***Elsayed A. Ahmed, Moataz H. Ata, Mahmoud El-Rouby Mohammed, Hazem M. Ali***
5	**Near-Threshold Incoherent Pion Photoproduction on The Deuteron With Final-State Interaction Effects** ***E. M. Darwish, M. M. Almarashi, E. M. Mahrous, M. A. Hassanain, M. Saleh Yousef***
6	**Analyzing Powers in Elastic e-d Scattering and Their Sensitivity to Nucleon Form Factors** ***E. M. Mahrous, E. M. Darwish, H. M. Abou-Elsebaa, A. Hemmdan***
7	**Analysis of Elastic $^{16}O + ^{40}Ca$ Refractive Scattering at 214 MeV** ***M. A. Hassanain, H. F. A. Alshrani, A. A. Ibraheem, M. Anwar, K. O. Behairy, Z. M. M. Mahmoud, E. M. Darwish***
8	**Influence of Nucleon Structure on Tensor and Vector Analyzing Powers in Elastic Electron–Deuteron Scattering** **E. M. Mahrous, E. M. Darwish, H. M. Abou-Elsebaa, A. Hemmdan**
9	**Sensitivity of Beam-Target Polarized Response Functions in Elastic Electron–Deuteron Scattering to Nucleon Structure and Modern *NN* Potentials** ***E. M. Darwish, A. Hemmdan, K. O. Behairy, E. M. Mahrous, Kh. S. Alsadi, M. A. Hassanain***
10	**Sensitivity of Tensor and Vector Analyzing Powers in Elastic e-d Scattering to Modern Local and Nonlocal NN Potentials** ***E. M. Darwish, H. M. Abou-Elsebaa, E. M. Mahrous, S. S. Al-Thoyaib***
11	**Coherent π^0-Photoproduction on The Deuteron Near Threshold and The Role of D-Wave Component of The Deuteron Wave Function** ***E. M. Darwish, M. Saleh-Yousef***
12	**Study of Microstructural, Electrical and Dielectric Properties of $La_{0.9}Pb_{0.1}MnO_3$ and $La_{0.8}Y_{0.1}Pb_{0.1}MnO_3$ Ceramics** ***S. A. Saleh***
13	**Enhancing the capability of plasma treated austenite stainless steels as thermal reactor materials** ***S U El-Kameesy, F M El-Hossary, M M Eissa, A A Abd El-Moula, Samah A Al-Shelkamy***
14	**Influence of Rf plasma carbonitriding on AISI304L, SSMn6Ni and SSMn10Ni for nuclear applications** ***F M El-Hossary, S U El-Kameesy, M M Eissa, A A Abd El-Moula, Samah A Al-Shelkamy***
15	**Mechanical and Gamma Ray Attenuation Properties of N316L Steel Treated by RF Plasma as a Nuclear Material** ***M. M. Eissa, F. M. El-Hossary, S. U. El-Kameesy, Aly Saeed, Al-Zahraa A. Abd Elmoula, Samah A. Al- Shelkamy***
16	**Optical, water splitting and wettability of titanium nitride/titanium oxynitride bilayer films for hydrogen generation and solar cells applications** ***S. H. Mohamed, Huaping Zhao, Henry Romanus, F. M. El-Hossary, M. Abo EL Kassem, M. A. Awad Mohamed Rabia, Yong Lei***
17	**Use of Magnetocaloric Material for Magnetic Refrigeration System: A Review** **A. Abdel-Latif, Mahrous R. Ahmed**

18	**One-Dimensional Metallo-Superconductor Photonic Crystals as a Smart Window** ***Arafa H. Aly, Ayman A. Ameen, Hussein A. Elsayed, S. H. Mohamed, Mahi R. Singh***
19	**TiO_2/TiO_xN_Y hollow mushrooms-like nanocomposite photoanode for hydrogen electrogeneration** ***M. Rabia, S. H. Mohamed, H. Zhao, M. Shaban, Y. Lei, A. M. Ahmed***
20	**Study of the effects of both film thickness and annealing time on $Cu_xS_yO_z$thin films for the possibility of usage as solar control coatings** ***S. H. Mohamed, N. M. A. Hadia, M. A. Awad, Mohamed Ismail Hafez***
21	**Effects of Thickness and Ag Layer Addition on the Properties of ZnS Thin Films** ***S.H. Mohamed, N.M.A. Hadiaa, M.A. Awad, Essam R. Shaaban***
22	**Experimental and theoretical studies of *hybrid multifunctional* TiO_2/ *TiN* / TiO_2** ***M. A. Awad, Arafa H. Aly***
23	**Simultaneous synthesis of various Sb_2S_3 nanostructures by vapor transport technique** ***N. M. A. Hadia, W.S.Mohamed, M.S.Abd El-sadek***
24	**Composition dependence of structural and linear and non-linear optical properties of $CdS_{1-x}Mn_x$ semiconducting thin films** ***Mansour Mohamed, A. M. Abdelraheem, M. I. Abd-Elrahman, N.M.A. Hadia, E. R. Shaaban***
25	**Cross sectional complex structure analysis is a key issue of thin film research: A case study on the preferential orientation crossover in TiN thin films** ***P. B. Barna, D. Biro, M. F. Hasaneen, L. Székely, M. Menyhárd, A. Sulyok, Z. E. Horváth, P. Pekker, I. Dódony, G. Radnóczi***
26	**Investigating the structure and tribo-mechanical performance of PVD TiN onbearing TiN substrate constructed by rf plasma** ***M. Raaif***
27	**Impact of Co^{2+} Substitution on Microstructure and Magnetic Properties of $Co_xZn_{1-x}Fe_2O_4$ Nanoparticles** **W. S. Mohamed, Meshal Alzaid, Mohammed S. M. Abdelbaky, Zakariae Amghouz,Santiago García-Granda, Ahmed M. Abu-Dief**
28	**Physical, Electrochemical and Biocompatibility Characteristics of Ti-Al-N Thin Film Synthesized by DC Pulsed Magnetron Sputtering** ***F. M. El-Hossary, A. M. Abd El-Rahman, M. Raaif, M. Abo El-Kassem***
29	**Thermoelectric properties of enhanced phonon scattering Hf-doped FeVSb Half-Heuslералloys** ***A. M. Adam, A. El-Khouly, A.P. Novitskii, E. M. M. Ibrahim, A. V. Kalugina, D. S. Pankratova, A. I. Taranova, A. A. Sakr, A. Trukhanov, M. M. Salem, V. Khovaylo***
30	**H_2 sensing characteristics in glass-removed amorphous $Co_{60.51}Fe_{3.99}Cr_{12.13}B_{13.53}Si_{9.84}$ microwires** ***S.A. El-Demrdash, A.M. Adam, L.V. Panina***
31	**Crossover effect of magnetotransport and magnetocaloric effect in $(La_{0.7}Ba_{0.3}MnO_3)1\text{-}x/(Al_2O_3)_x$ composites** ***A.M. Ahmed, H.F. Mohamed*, A.K. Diab, Esraa Y. Omar***
32	**Tuning electrical conductivity of β-Ga_2O_3 single crystals by Ta doping** ***Huiyuan Cui[ab] H. F. Mohamed[bc] Changtai Xia Qinglin Sai Wei Zhou Hongji Qi Jingtai Zhao Jiliang Si Xiao li Ji***
33	**Growth and fundamentals of bulk *β*-Ga_2O_3 single crystals** ***H. F. Mohamed, Changtai Xia, Qinglin Sai, Huiyuan Cui, Mingyan Pan, Hongji Qi***
34	**Crossover effect of magnetotransport and magnetocaloric effect in $(La_{0.7}Ba_{0.3}MnO_3)_{1-x}/(Al_2O_3)_x$ composites** ***A. M.Ahmed, H. F. Mohamed, A. K. Diab, Esraa Y. Omar***
35	**Impact of aluminum on the Seebeck coefficient and magnetic properties of $La_{0.7}Ba_{0.3}MnO_3$ manganites** ***H. F. Mohamed, A. M. Ahmed, A. K. Diab, Esraa Y. Omar***
36	**Modelling of high-efficiency substrate CIGS solar cells with ultra-thin absorber layer** ***A S Mohamed, H A Mohamed***

37	**Radioactivity Concentrations in Dust and Soil of Enhanced Naturally Occurring Radionuclides and their Transfer Factors to Urban Trees in Phosphate Polluted Areas** ***M. El-Zohry & M. H. El-Zayat***
38	**The Annual Effective Dose of Natural Radioactivity Intake from Animal Products Consumption in Phosphate Polluted Area** ***Abdelmonem A M, El-Zohry M, El-Zayat M H***
39	**Inactivation by helium cold atmospheric pressure plasma for Escherichia coli and Staphylococcus aureus** ***Khaled Lotfy[1,2], Sayed Mohammed Khalil, Hany Abd El-Raheem***
40	**Enhanced thermoelectric figure of merit in Bi-containing Sb_2Te_3 bulk crystalline alloys** ***M. Adam[1, 2], A. El-Khouly, A. P. Novitskii, E. M. M. Ibrahim, A. V. Kalugina, D. S. Pankratova, A. I. Taranova, A. A. Sakr, A. Trukhanov, M. M. Salem, V. Khovaylol***
41	**Influence of nickel doping on the energy band gap, luminescence, and magnetic order of spray deposited nanostructured ZnO thin films** ***H. Ali, A. M. Alsmadi, B. Salameh, M. Mathai, M. Shatnawi, N. M. A. Hadia, E. M. M. Ibrahim***
42	**Magnetic Sm-BFO and Ce-BFO nanoflakes as protective coating layers for C-steel in acidic chloride environments** ***Mai M. Khalaf, Hany M. Abd El-Lateef, G. Farghal, E. M. M. Ibrahim***
43	**Sonochemically synthesized Ni-doped ZnS nanoparticles: structural, optical, and photocatalytic properties** ***A. A. Othman, M. A. Osman, Manar A. Ali, W. S. Mohamed, E. M. M. Ibrahim***
44	**Enhanced magnetic and DC electrical properties of Sm-doped $Bi_2Fe_4O_9$ nanoplates synthesized by a sol-gel method** ***E. M. M. Ibrahim, G. Farghal, Mai M. Khalaf, Hany M. Abd El-Lateef***
45	**Linear and Non-linear Optical Parameters of Diluted Magnetic Semiconductor CdS0.9Mn0.1 Thin Film: Influence of the Film Thickness** ***A. M. Abdelraheem, M. I. Abd-Elrahman, Mansour Mohamed, N. M. A. Hadia, E. R. Shaaban***
46	**Radiation shielding, mechanical and tribological properties of treated $AISI_{304}L$ using H_2/N_2 rf plasma** ***S U El-Kameesy, F M El-Hossary, M M Eissa, A A Abd El-Moula, Samah A Al-Shelkamy, A Saeed***
47	**Tuning the optical, electrical resistivity and structural properties of DC magnetron sputtered aluminum zinc oxide films by changing the oxygen flow rate** ***Mohammed S. Alqahtani, N. M. A. Hadia, S. H. Mohamed***

List of papers published by Staff members of Chemistry Department (P. 65-105)

1	**A robust in vitro Anticancer, Antioxidant and Antimicrobial Agents Based on New Metal-Azomethine Chelates Incorporating Ag(I), Pd (II) and VO (II) Cations: Probing the Aspects of DNA Interaction** ***Ahmed M. Abu-Dief, Laila H. Abdel-Rahman, Azza A. Hassan Abdel-Mawgoud***
2	**Kinetic study of humic acid adsorption onto smectite: The role of individual and blend background electrolyte** ***Laila H. Abdel-Rahman[1] ,Ahmed M. Abu-Dief[1] Badriah Saad Al-Farhan***
3	**Synthesis and characterization of new Cr(III), Fe(III) and Cu(II) complexes incorporating multi-substituted aryl imidazole ligand: Structural, DFT, DNA binding, and biological implications** ***Ahmed M. Abu-Dief, Laila H. Abdel-Rahman, Antar A.Abdelhamid, Adel A. Marzouk, Mohamed R. Shehata, Mohamed Abdelaal Bakheet, Omar A. Almaghrabi, Ayman Nafady***
4	**Impact of Co^{2+} Substitution on Microstructure and Magnetic Properties of $Co_xZn_{1-x}Fe_2O_4$ Nanoparticles** ***W. S. Mohamed, Meshal Alzaid, Mohammed S. M. Abdelbaky, Zakariae Amghouz, Santiago García-Granda, Ahmed M. Abu-Dief***
5	**Novel Di- and Tri-azomethine Compounds as Chemo Sensors for the Detection of Various Metal Ions** ***Ahmed M. Abu-Dief and Azza A. Hassan Abdel-Mawgoud Laila H. Abdel-Rahman***
6	**A Simple and Reliable Synthesis of Superparamagnetic Magnetite Nanoparticles by Thermal Decomposition of $Fe(acac)_3$** ***C. Toyos-Rodríguez, J. Calleja-García, L. Torres-Sánchez, A. López, Ahmed M. Abu-Dief, A. Costa, L. Elbaile, R. D. Crespo, J. S. Garitaonandia, E. Lastra, J. A. García, F. J. García-Alonso***
7	**Synthesis, catalysis, antimicrobial activity, and DNA interactions of new Cu(II)-Schiff base complexes** ***Mohamed Shaker S. Adam, Laila H. Abdel-Rahman,Ahmed M. Abu-Dief, Nahla A. Hashem***
8	***Catalytic Potential of Mononuclear Cr(III)-Imine Complexes for Selective Oxidation of Benzyl Alcohol by Aqueous H_2O_2*** ***Laila H. Abdel-Rahman, Mohamed Shaker S. Adam, Ahmed M. Abu-Dief, Azza A. H. Abdel-Mawgoud***
9	**Novel azomethine Pd (II)- and VO (II)-based metallo-pharmaceuticals as anticancer, antimicrobial, and antioxidant agents: Design, structural inspection, DFT investigation, and DNA interaction** ***Ahmed M. Abu-Dief, Laila H. Abdel-Rahman, Mohamed R. Shehata, Azza A. Hassan Abdel-Mawgoud***
10	**Design, synthesis and structural inspection of some novel di- and tri-azomethene compounds as chemo sensors for the detection of various metal ions** ***Laila H. Abdel-Rahman, Ahmed M. Abu-Dief, Azza A. Hassan Abdel-Mawgoud***
11	**Some new Ag(I), VO(II) and Pd(II) chelates incorporating tridentate imine ligand: Design, synthesis, structure elucidation, density functional theory calculations for DNA interaction, antimicrobial and anticancer activities and molecular docking studies** ***Laila H. Abdel-Rahman Ahmed M. Abu-Dief, Mohamed R. Shehata, Faten M. Atlam, Azza A. Hassan Abdel-Mawgoud***
12	**Azomethine Metal Chelates as an Efficient Catalyst for Oxidation of Organic Compounds** ***Ahmed M. Abu-Dief***
13	**Antimicrobial and anticancer activities of cobalt (III)-hydrazone complexes: Solubilities and chemical potentials of transfer in different organic co-solvent-water mixtures** ***Ahmad Desoky M. Mohamad, M. J. A. Abualreish, Ahmed M. Abu-Dief***

14	**Green synthesis of TiO_2 nanoparticles as an efficient heterogeneous catalyst with high reusability for synthesis of 1, 2-dihydroquinoline derivatives** ***Mahmoud Abd El Aleem Ali Ali El-Remaily, Ahmed M. Abu-Dief, O.M Elhady***
15	**Iron (III)-porphyrin Complex FeTSPP as an efficient catalyst for synthesis of tetrazole derivatives via [2 + 3]cycloaddition reaction in aqueous medium** ***M. A. E. A. A. A. El-Remaily, O. M. Elhady***
16	**Development of DNA Nanotechnology for Cancer Therapy** ***Ahmed M. Abu- Dief***
17	**Development, structural investigation, DNA binding, antimicrobial screening and anticancer activities of two novel quari-dentate VO (II) and Mn (II) mononuclear complexes** ***Laila H Abdel-Rahman, Ahmed M Abu-Dief, Azza A Hassan Abdel-Mawgoud***
18	**Fabrication, spectroscopic characterization, calf thymus DNA binding investigation, antioxidant and anticancer activities of some antibiotic azomethine Cu(II), Pd(II), Zn(II) and Cr(III) complexes** ***Ahmed M. Abu-Dief, Hussein M. El-Sagher, Mohamed R. Shehata***
19	**Electrochemical methods for fabrication of polymers/calcium phosphates nanocomposites as hard tissue implants** ***Hany M. Abd El-Lateef, Ahmed H. Touny, Mohamed M. Saleh, Mahmoud M. Saleh***
20	**Comparative study of synergistic inhibition of mild steel and pure iron by 1-hexadecylpyridinium chloride and bromide ions** ***Hany M. Abd El-Lateef, M.M. Saleh, Manal G. Mahmoud***
21	**Solvent-free synthesis and corrosion inhibition performance of Ethyl 2-(1,2,3,6-tetrahydro-6-oxo-2-thioxopyrimidin-4-yl)ethanoate on carbon steel in pickling acids: Experimental, quantum chemical and Monte Carlo simulation studies** ***Hany M.Abd El-Lateef, Zeinab A.Abdallah, Mohamed S.Mohamed Ahmed***
22	**Sulfonated salicylidene thiadiazole complexes with Co (II) and Ni (II) ions as sustainable corrosion inhibitors and catalysts for cross coupling reaction** ***Hany M. Abd El-Lateef, Abdelwahed R. Sayed, Mohamed Shaker S. Adam***
23	**Magnetic Fe_3O_4 nanocubes coated by SiO_2 and TiO_2 layers as nanocomposites for Cr (VI) up taking from wastewater** ***Mai M. Khalaf, Kawther Al-Amer, Hany M. Abd El-lateef***
24	**Novel dispersed Tl_2O_3-SiO_2/polyaniline nanocomposites: in-situ polymerization, characterization and enforcement as a corrosion protective layer for carbon-steel in acidic chloride medium** ***Hany M. Abd El-Lateef, MaiM. Khalaf***
25	**Removal of cationic surfactants from dilute solutions using nanoporous nickel phosphate: A structural, kinetic and thermodynamic study** ***Hany M. Abd El-Lateef, M.M. Saleh, Ahmed H. Touny***
26	**Efficient route synthesis of new polythiazoles and their inhibition characteristics of mild-steel corrosion in acidic chloride medium** ***Hany M. Abd El-Lateef, Abdelwahed R. Sayed, Mahmoud M. Saleh, Mohammed A. Al-Omair***
27	**Synthesis of crystalline and amorphous iron phosphate nanoparticles by simple low-temperature method** ***Hany M. Abd El-Lateef, M. M. Saleh, Ahmed H. Touny***
28	**Magnetic Sm-BFO and Ce-BFO nanoflakes as protective coating layers for C-steel in acidic chloride environments** ***Mai M. Khalaf, Hany M. Abd El-Lateef, G. Farghal, E.M.M. Ibrahim***
29	**Electrodeposited Pt nanorods on a novel flowered-like nanostructured Ni e Co alloy as an electrocatalyst for methanol oxidation** ***Mahmoud Elrouby, Hany M. Abd El-Lateef, Mansour Sadek***

30	**Antimicrobial activities of mesoporous nickel phosphate synthesized with low-temperature method** ***Mai M. Khalaf, Mohammed A. Al-Omair, A. H. Touny, H. Elsawy, M. M. Saleh***
31	**Experimental Design Modeling of the Effect of Hexagonal Wurtzite-ZnO Synthesis Conditions on Its Characteristics and Performance as a Cationic and Anionic Adsorbent** ***Mai M.Khalaf, Enshirah Da'na, Kawther Al-Amer, Manal Hessien***
32	**Sustainable dipolar homo-dicopper (II) dihydrazone complex as a catalyst for Sonogashira cross couplings** ***Mohamed Shaker S. Adam***
33	**Chemical design and bioefficacy screening of new insect growth regulators as potential insecticidal agents against Spodoptera littoralis (Boisd.)** ***Abdelhamid A. A., Elwassimy M. M, Aref, S. A., Gad M. A.***
34	**Biocatalysis explained: From pharmaceutical to bulk chemical production(Review)** ***Abdelraheem E. M. M., Busch H., Hanefeld U., Tonin F.***
35	**Novel Cr (III), Fe (III) and Ru (III) Vanillin Based Metallo-Pharmaceuticals for Cancer and Inflammation Treatment: Experimental and Theoretical Studies** ***L.H. Abdel-Rahman, R.M. El-Khatib, S.M. Abdel-Fatah, H. Moustafa, A.M. Alsalme, A. Nafady***
36	**Biogenic silver nanoparticles for trace colorimetric sensing of enzyme disrupter fungicide vinclozolin** ***Hussain M., Nafady A., Sirajuddin, Avcı A., Pehlivan, E., Nisar J., Sherazi S.T.H., Balouch A., Shah M.R., Almaghrabi, O.A.,Ul-Haq, M.A.***
37	**An efficient synthesis of benzylidene-2-alkoxy-4-aryl-2,3-cycloalkenopyridine-3-carbonitrile derivatives** ***Albayati M. R., Moustafa A. H, Abdelhamed A. A***
38	**Iridium complex immobilization on covalent organic framework for effective C-H borylation** ***Vardhan H., Pan Y., Yang Z., Verma G., Nafady A., Al-Enizi A. M., Alotaibi T. M. Almaghrabi O. A., Ma S.***
39	**A regioselective and convenient one-pot multicomponent synthesis of polyfunctionalized 4-aryl-2-cyanoimino-3,4-dihydro-1H-pyrido[2,3-d] pyrimidines** ***Hussein B. R. M., Moustafa A. H.***
40	**Theoretical insight into the structure-property relationship of mixed transition metal oxides nanofibers doped in activated carbon and 3D graphene for capacitive deionization** ***Yasin A. S., Mohamed A. Y., Mohamed I. M. A., Cho D.-Y., Park C. H., Kim C. S.***
41	**Catalytic comparison of various polar Zn(II)-Schiff base complexes and VO(II)-Schiff base complexes in (ep)oxidation processes of 1,2-cyclohexene and cyclohexane** ***Adam M. S. S., Al-Omair M. A., Ullah F.***
42	**Near UV-Irradiation of CuO_x-Impregnated TiO_2 Providing Active Species for H_2 Production Through Methanol Photoreforming** ***Vitiello G., Clarizia L., Abdelraheem W., Esposito S., Bonelli B., Ditaranto N., Vergara A., Nadagouda M., Dionysiou D. D., Andreozzi R., Luciani G., Marotta R.***
43	**Synthesis of electrospun 1D-photoanode nanocomposite based on electrospinning followed by hydrothermal treatment for highly efficient liquid-junction photovoltaic devices** ***Mohamed I. M. A., Dao V.-D., Liu C., Barakat N. A. M., Choi H.-S.***
44	**Electrospun carbon nanofiber-encapsulated NiS nanoparticles as an efficient catalyst for hydrogen production from hydrolysis of sodium borohydride** ***Al-Enizi A. M., Nafady A., El-Halwany M. M., Brooks R. M., Abutaleb A., Yousef A.***
45	**Facile synthesis, characterizations, and impedance spectroscopic features of Zn(II)-bis Schiff base complex films towards photoelectronic applications** ***Shehata M. M., Adam M. S. S., Abdelhady K., Makhlouf M. M.***

46	**Mechanistic Investigations of Photoelectrochemical Water and Methanol Oxidation on Well-Defined TiO_2 Anatase (101) and Rutile (110) Surfaces** ***Ahmed A. Y., Kandiel T. A., Oekermann T., Günnemann C., Bahnemann D.***
47	**Sub-ppt level voltammetric sensor for Hg^{2+} detection based on nafion stabilized l-cysteine-capped Au@Ag core-shell nanoparticles** ***Siddiqui S., Nafady A., El-Sagher H. M., Al-Saeedi S. I., Alsalme A. M., Sirajuddin, Talpur F. N., Sherazi S. T. H., Kalhoro M. S., Shah M. R., Shaikh T., Arain M., Bhargava S. K.***
48	**Efficient Aerobic Oxidation of trans-2-Hexen-1-ol using the Aryl Alcohol Oxidase from Pleurotus eryngii** ***de Almeida T. P., van Schie M. M. C. H., Ma A., Tieves F., Younes S. H. H., Fernández-Fueyo E., Arends I. W. C. E., Riul A. Jr.[c], Hollmann F.***
49	**Formate Oxidase (FOx) from Aspergillus oryzae: One Catalyst Enables Diverse H_2O_2-Dependent Biocatalytic Oxidation Reactions** ***Tieves F., Willot S. J.-P., van Schie M. M. C. H., Rauch M. C. R., Younes S. H. H., Zhang W., Dong J., Gomez de Santos P., Robbins J. M., Bommarius B., Alcalde M., Bommarius A. S., Hollmann F.***
50	**Electrochemical determination of antihypertensive drugs by employing costless and portable unmodified screen-printed electrodes** ***Khorshed A. A., Khairy M., Banks C. E.***
51	**Multi-component Reactions, Solvent-free Synthesis of Substituted Pyrano-pyridopyrimidine under Different Conditions Using ZnO Nanoparticles** ***Mahmoud N. F. H., El-Saghier A. M.***
52	**Nano ZnO (hexagonal wurtzite) of different shapes under various conditions: Fabrication and characterization** ***Hessien M., Da'Na E., Al-Amer K., Khalaf M. M.***
53	**Synthesis, structural characterization, DFT calculations, biological investigation, molecular docking and DNA binding of Co(II), Ni(II) and Cu(II) nanosized Schiff base complexes bearing pyrimidine moiety** ***Basha M. T., Alghanmi R. M., Shehata M. R., Abdel-Rahman L. H.***
54	**Piperidinium Hydrogen Sulfate (PHS) as an Efficient Ionic Liquid Catalyst for the Synthesis of Imidazole Derivative under Solvent-Free Condition** ***Albayati M. R., Marzouk A. A., Abdelhamid A. A.***
55	**Chemical design of novel electrospun CoNi/Cr nanoparticles encapsulated in C-nanofibers as highly efficient material for urea oxidation in alkaline media** ***Mohamed I. M. A., Liu C.***
56	**Photochemical treatment of tyrosol, a model phenolic compound present in olive mill wastewater, by hydroxyl and sulfate radical-based advanced oxidation processes (AOPs)** ***Kilic M. Y., Abdelraheem W. H., He X., Kestioglu K., Dionysiou D. D.***
57	**Multicomponent Reaction for Synthesis of Novel 2-Tosyloxyphenylpyridines** ***Hussein B. R. M., Ali A. M.***
58	**Novel aryl carboximidamide and 3-aryl-1,2,4-oxadiazole analogues of naproxen as dual selective COX-2/15-LOX inhibitors: Design, synthesis and docking studies** ***Youssif B. G. M., Mohamed M. F. A., Al-Sanea M. M., Moustafa A. H., Abdelhamid A. A., Gomaa H. A. M.***
59	**Novel adsorbents derived from recycled waste polystyrene via cross-linking reaction for enhanced adsorption capacity and separation selectivity of CO_2** ***Fu Z., Mohamed I. M. A., Li J., Liu C.***
60	**Structure-Activity Relationships of Hierarchical Three-Dimensional Electrodes with Photosystem II for Semiartificial Photosynthesis** ***Fang X., Sokol K. P., Heidary N., Kandiel, T. A., Zhang J. Z., Reisner E.***
61	**Design and Synthesis of Some New Analgesic Azole Derivatives Containing Tramadol Moiety** ***Khodairy A., Ahmed E. A., Ismael M., Mohamed K. M., Thabet S. A.***

62	**Green synthesis, antileishmanial activity evaluation, and in silico studies of new amino acid-coupled 1,2,4-triazoles** ***El-Saghier A. M., Mohamed M. A., Abd-Allah O. A., Kadry A. M., Ibrahim T. M., Bekhit A. A.***
63	**Surface activation of wood plastic composites (WPC) for enhanced adhesion with epoxy coating** ***Mohamed M. R., Naguib H. M., El-Ghazawy R. A., Shaker N. O., Amer A. A., Soliman A. M., Kandil U. F.***
64	**New Route for the Synthesis of Hetaryl-1,5-benzodiazepines: Part 2** ***Ahmed A. M., Abdel-Ghany H., Moustafa H. M., Khodairy A.***
65	**Hydrothermal synthesis of photoactive nitrogen- and boron- codoped TiO_2 nanoparticles for the treatment of bisphenol A in wastewater: Synthesis, photocatalytic activity, degradation byproducts and reaction pathways** ***Abdelraheem W. H. M., Patil M. K., Nadagouda M. N., Dionysiou D. D.***
66	**Synthesis, characterization of novel p-tert-butylthiacalix[4]arene derivatives and its application for extraction of alkali and transition elements** ***Ahmad Desoky M. Mohamad · Omran A. Omran***
67	**Incorporating zirconia nanoparticles into activated carbon as electrode material for capacitive deionization** ***Yasin A. S., Mohamed I. M. A., Amen M. T., Barakat N. A. M., Park, C.H., Kim C. S.***
68	**Disposable screen-printed electrodes modified with uniform iron oxide nanocubes for the simple electrochemical determination of meclizine, an antihistamine drug** ***Khorshed A. A., Khairy M., Elsafty S. A., Banks C. E.***
69	**Green Synthesis of new Trizole Based Heterocyclic Amino Acids Ligands and their Transition Metal Complexes. Characterization, Kinetics, Antimicrobial and Docking Studies** ***El-Saghier A. M., Abd El-Halim H. F., Abdel-Rahman L. H., Kadry A.***
70	**Biological and catalytic potential of sustainable low and high valent metal-Schiff base sulfonate salicylidene pincer complexes** ***Adam M. S. S, El-Hady O. M., Ullah F.***
71	**Investigation of the anticancer activity of coordination-driven self-assembledtwo-dimensional ruthenium metalla-rectangle** ***Vardhan H., Nafady A., Al-Enizi A. M., Khandke K., El-Sagher H. M., Verma G., Acevedo-Duncan M., Alotaibi T. M., Ma, S.***
72	**Investigation of the electrochemical reduction process of the molybdate ions in the tartaric electrolytes** ***Majidzade V. A., Aliyev A. S., Babanly D. M., Elrouby M., Tagiyev D. B.***
73	**Pore environment engineering in metal-organic frameworks for efficient ethane/ethylene separation** ***Wang X., Niu Z., Al-Enizi A. M., Nafady A., Wu Y., Aguila B., Verma G., Wojtas L., Chen Y.-S., Li Z., Ma S.***
74	**Antibacterial and photocatalytic activities of controllable (anatase/rutile) mixed phase TiO_2 nanophotocatalysts synthesized: Via a microwave-assisted sol-gel method** ***Almashhori K., Ali T. T., Saeed A., Alwafi R., Aly M., Al-Hazmi F.E.***
75	**Ranolazine-functionalized copper nanoparticles as a colorimetric sensor for trace level detection of As^{3+}** ***Laghari G. N., Nafady A., Al-Saeedi S. I., Sirajuddin, Sherazi S. T. H., Nisar J., Shah M. R., Abro M. I., Arain M., Bhargava S. K.***
76	**Copper (I) Nicotinate complex Abrogates Acrylamide Induced Hepatotoxicity in Male Rats: Biochemical and Histological Studies** ***Nagwa M. Elsawi, Wejdan, A. Aldajani, Mounir A. A. Mohamed, Ahmed. M. Ali, Gamal S. A., Soad Shaker Ali, Sabra A. Abd El lah***
77	**Biochemical Analysis of C-X-C Motif Chemokine Ligand 10 (CXCL10) as a Biomarker in Patients with Rheumatoid Arthritis** ***Amal M. Imam, Amany M. Hamed, Samah I. Nasef, Amany M. Hassan, Hanan H. Omar***

78	**Structure, Optical, Corrosion, and Photocatalytic Properties of Thermally Evaporated Molybdenum Trioxide Thin Films Deposited on Different Substrates** ***Sh. A. Elkot, W. S. Mohamed, Mahmoud Elrouby, H. M. Ali, E. Kh. Shokr***
79	**Study the Effect of the Sintering Temperature on the Microstructure and Optical Reflectance of the Compacted Bulk $CuAlS_2$ Fabricated by Powder Metallurgy Technique (P/M)** ***Elsayed Abd Ellatif Ahmed, Moataz H. Ata, Mahmoud Elrouby, Hazem M. Ali***
80	**Simultaneous Voltammetric Determination of Gallic and Protocatechuic Acids in Mango Juice Using a Reduced Graphene Oxide-Based Electrochemical Sensor** ***Refat Abdel-Hamid, Ahmed Bakr, Emad F. Newair, François Garcia***
81	**Template Assisted Microwave Synthesis of rGO-ZrO2 Composites: Efficient Photocatalysts Under Visible Light** ***Tarek T. Ali, Katabathini Narasimharao, Sulaiman N. Basahel, Mohamed Mokhtar, Edreese H. Alsharaeh, Hatem A. Mahmoud***
82	**Morphology, Histology, and Chemistry of the wings of Tribolium castanaeum and Tribolium confusum (Coleoptera: Tenebrionidae)** ***Nasra M. H. Zohry[1], Ahmed Mohamed El-Sayed***
83	

List of papers published by Staff members of Botany&Microbiology Department (P. 107-118)

1	**Additions to the genus *Savoryella* (*Savoryellaceae*), with the asexual morphs *Savoryella nypae comb. nov.* and *S. sarushimana sp. nov.*** ***Sheng-Nan Zhang, Mohamed A. Abdel-Wahab, E.B. Gareth Jones, Kevin D. Hyde, Jian-Kui (Jack) Liu***
2	**Natural products of *Alternaria* sp., an endophytic fungus isolated from *Salvadora persica* from Saudi Arabia** ***Abdallah M.Elgorban, Ali H.Bahkali, Dunia A.Al Farraj, Mohamed A.Abdel-Wahab***
3	***Saturnispora mangrovi* f.a., sp. nov. from Syhat mangrove, Saudi Arabia** ***Abd El-Rahim M. A. El-Samawaty, Teun Boekhout, Mohamed A. Yassin, Mohamed A. Abdel-Wahab***
4	***Nia lenicarpa* sp. nov.** (Niaceae, Agaricales) from Red Sea mangroves in Saudi Arabia with comments on ***Nia vibrissa*** ***Mohamed A. Abdel-Wahab, E. B. Gareth Jones, Faten A. Abdel-Aziz, Ali H. Bahkali***
5	**An online resource for marine fungi** ***E. B. Gareth Jones • Ka-Lai Pang • Mohamed A. Abdel-Wahab et al.***
6	**Phylogeny of new marine Dothideomycetes and Sordariomycetes from mangroves and deep-sea sediments** ***Evan Benjamin Gareth Jones, Bandarupalli Devadatha, Mohamed A. Abdelwahab, Monika C. Dayarathne, Sheng-Nan Zhang, Kevin D. Hyde, Jian-Kui Liu, Ali Hassan Bahkali, V. Venkateswara Sarma, Sanja Tibell, Leif Tibell, Meng-meng Wang, Fang Liu, Lei Ca***
7	***Phaeonectriella alba* sp. nov. from the River Nile, Egypt** ***Ahmed E. Abdel-Aziz, Sabah S. Mohamed, Ahmed M. Abdel-Raheem, Mohamed A. Abdel-Wahab***
8	**Marine fungi from Red Sea mangroves in Saudi Arabia with Fulvocentrum rubrum sp. nov. (Torpedosporales, Ascomycota)** ***Abdel-Wahab Mohamed A., Jones E. B. Gareth, Bahkali Ali H. A., El-Gorban Abdallah M.***
9	**Biosynthesis of cadmium selenide quantum dots by *Providencia vermicola*** ***Abou-Assy Rawan S., Bahig A. El-Deeb, Abdullah D. Al-Talhi, Nasser Y. Mostafa.***
10	**Potassium Synergize the Positive Effect of Ascorbic Acid on some Morpho-physiological Parameters of Salt Stressed Faba Bean Cultivars** ***Naglaa Loutfy, M. M. Azooz, A. M. Hassanein, A. Bassiony***
11	**Oxidative stress caused by Basagran® herbicide is altered by salicylic acid treatments in peanut plants** ***D E M Radwan, A K Mohamed, K A Fayez, A M Abdelrahman***
12	**Isolation and Characterization Of Novel Egyptian Regulatory Gene Tri 10 From *Fusarium fujikuroi* (MG211161)** ***Samia El-Rabbat, Osman El-Maghraby, Samah El-Debaiky, Ashraf Haider***
13	**Floristic Diversity and Phytogeography of Mil steppe-Azerbaijan** ***Gurbanov E. M., Naglaa Y. Abdallah, Mammadova Z. J., Asadova K. A., Ahmed Elkordy***
14	**Bioaccumulation of heavy metals air pollutants by Urban trees** ***Ahmed Ali El-Khatib, Nasser A. Barakat, Naglaa A. Youssef & Nesrin A. Samir***
15	**Fine-template synthetic process of mesoporous TiO_2 using ionic/nonionic surfactants as potential remediation of Pb(II) from contaminated soil** ***M. M. Khalaf · N. Y. Abdallah · H. M. Abd El-Lateef***
16	**Floristic diversity and vegetation analysis of riparian and aquatic plants of the canals in the Sohag Governorate, Egypt** ***Ahmed Elkordy, Omer Elshikh & Naglaa Abdallah***

17	**Detection of free and bound microcystins in tilapia fish from Egyptian fishpond farms and its related public health risk assessment** ***Zakaria Mohamed, • Zeinab Ahmed, • Asmaa Bakr, • Mohamed Hashem, • Saad Alamri***
18	**Direct transesterification of fatty acids produced by *Fusarium solani* for biodiesel production: Effect of carbon and nitrogen on lipid accumulation in the fungal biomass** ***Abdel-Hamied M. Rasmey, Mostafa A. Tawfik, Marwa M. Abdel-Kareem***
19	**Assessment of phytoplankton species in gut and feces of cultured tilapia fish in Egyptian fishponds: Implications for feeding and bloom control** ***Zakaria Mohamed, Zeinab Ahmed and Asmaa Bakr***
20	**Exogenous application of zinc mitigates the deleterious effects in eggplant grown under salinity stress** ***Abdelnasser Galal***
21	**Some important aspects in Moringa oleifera Lam. micropropagation** ***Ahmed Hassanein, Jehan Salem, Fayza Faheed, Abdullah El-Nagish***
22	**The action mechanism and biocontrol potentiality of novel isolates of Saccharomyces cerevisiae against the aflatoxigenic *Aspergillus flavus*** ***M. Marwa Abdel-Kareem, A.M. Rasmey, A. A. Zohri***
23	**Metabolic profiling of endophytic *Bacillus subtilis* US2 isolated from *Rosmarinus officinalis* leaves with potential antimicrobial activity** ***Magdy A. Abu-Gharbia, Rehab M. Mohamed, Mohamed A. Awad***

List of papers published by Staff members of Zoology Department (P. 119-128)

1	**Induction of hyperpigmentation and heat shock protein 70 response to the toxicity of methomyl insecticide during the organ development of the Arabian toad, Bufo arabicus (Heyden,1827)** ***Amin Abdou Seleem***
2	**Teratogenicity and neurotoxicity effects induced by methomyl insecticide on the developmental stages of Bufo arabicus** ***Amin A. Seleem***
3	**Evaluation of Leiurus quinquestriatus scorpion venom anticancer potential against Prostate Cancer Cell Lines (PC3)** ***Tito N. Habib, Hemely A. Hassan, Fayza M. Ali, Nadia S. Mahrous***
4	**Marine Pollution of Chemicals Detergents Contamination Induced Apoptosis and Necrosis in Fish Liver (Sardine aurita) by Flow Cytometry DNA Measurements** ***Tito N. Habib* Mohamed F. El-Sayed, Fathi M. Ali, Tawfiq M. Almsatar***
5	**RAPD-Contaminant Indicative Bands Induced by Sodium Lauryl Sulfate of Economic Fish (Sardine Aurita) from Libyan Coasts** ***Tito N. Habib, Mohamed F. El-Sayed, Fathi M. Ali, Tawfiq M. Almsatar***
6	**Toxic impacts of the neem biopesticide (Triology®) on the histological structure of gills and intestine in the Grass Carp " Ctenopharyngodon idella".** ***Hamdy M.A. Hassanein, El-Sabry Abu_Amra, Faiza M. Soliman, Hanan A. Okail***
7	**Cypris polygoniae n. sp. (Ostracoda: Cyprididae) collected from wastewater of sewage station, Sohag, Egypt** ***Somaia A. Ramadan, Ebtesam A. Yousef, Amal M. Mohamed***
8	**Studies on the cuticle and musculature of freshwater mite, Unionicola aegyptiaca** ***Somaia A. Ramadan, Tarek G. Ismail, Asmaa N. Mustafa***
9	**Ameliorative effect of Spirulina platensis against lead nitrate–induced cytotoxicity and genotoxicity in catfish Clarias gariepinus** ***Mohamed Hamed, Hamdy A. M. Soliman, Alaa El-Din H. Sayed***
10	**Assessment the effect of exposure to microplastics in Nile Tilapia (Oreochromis niloticus) early juvenile: I. blood biomarkers** ***Mohamed Hamed, Hamdy A.M. Soliman, Alaa G.M. Osman, Alaa El-Din H. Sayed***
11	**Protective effects of a novel pyrazolecarboxamide derivative against lead nitrate induced oxidative stress and DNA damage in Clarias gariepinus** ***Hamdy A.M. Soliman , Mohamed Hamed , Jae-Seong Lee, Alaa El-Din H. Sayed***
12	**Recent progress in biomedical applications of chitosan and its nanocomposites in aquaculture: A review** ***Fatma Ahmed, Faiza M.Solim, Mohamed A. Adly, Hamdy A.M.Solim, Mansour El-Matboulia, Mona Saleha***
13	**Toxic and Genotoxic Effects of Silver Nanoparticles in Drosophila.** ***Alaraby M, Romero S, Hernández A, Marcos R***
14	**Ultrastructural studies on the sensilla of the mouth parts and antennae of the pre-adult stages of sitophilus granarius (coleoptera: curculionidae)** ***Nasra M. H. Zohry***
15	**Morphology, Histology, and Chemistry of the wings of Tribolium castanaeum and Tribolium confusum (Coleoptera: Tenebrionidae)** ***Nasra M. H. Zohry, Ahmed Mohamed El-Sayed***
16	**Carcinoembryonic Cell Adhesion-Related Molecule 2 Regulates Insulin Secretion and** ***Energy Balance Salaheldeen Elsaid, Alexa Jaume, Sonia Michael Najjar***
17	**Protective Effects of Melatonin and Thymoquinone on Hematological Parameters, Hepatic and Renal Activities against Lithium-Chloride Toxicity in Male Albino Rats.** ***Mohamed F. El-Sayed, Sary Kh. Abd El-ghaffar, Aziz Awaad, Mohamed M. Mahmoud***

18	**Molecular Method vs. Traditional Methods for Estimating the Prevalence of Larval Trematode Infections in Some Red Sea Snails** ***Muslimah, N. ALsulami, Sabah M. Hassan, Amaal Hassan***
19	**Corynebacterium tuberculostearicum, a human skin colonizer, induces the canonical nuclear factor kappa B inflammatory signaling pathway in human skin cells** ***Altonsy Mohammed Omar, Kurwa, Habib A.***
20	**Copper (I) Nicotinate complex Abrogates Acrylamide Induced Hepatotoxicity in Male Rats: Biochemical and Histological Studies** ***Nagwa M. Elsawi, Wejdan, A. Aldajani, Mounir A. A. Mohamed, Ahmed. M. Ali, Gamal S. A., Soad Shaker Ali, Sabra A. Abd El lah***

List of papers published by Staff members of Geology Department (P. 129-143)

1	**Expansive potentiality of sabkha soils of Rabigh Lagoon, Saudi Arabia: a case study** ***Bader A. Hakami, El-Sayed Sedek Abu Seif***
2	**Derivation of empirical relationships between geotechnical parameters and resistivity using electrical resistivity tomography (ERT) and borehole data at Sohag University site, Upper Egypt** **Mohammed M.A., Sensoy M. M., Abudeif A.M.**
3	**Geotechnical performance of sandy bricks made with fine aggregates of sand dunes, Saudi Arabia** ***El-Sayed Sedek Abu Seif, Abdullah Rashed Sonbul***
4	**Pleistocene aquifer sediments at sohag region, nile valley, egypt: a statistical approach** ***Shaymaa Rezk , Ahmed.A.Abdel Moneim, Abdallah M. Hassan, Mohamed H. Ali***
5	**Rockfall hazards assessment along the Aswan–Cairo highway, Sohag Governorate, Upper Egypt** ***Abu Seif, E.-S. S., Bahabri A. A.***
6	**Characterization and environmental impact assessment of gold mine tailings in arid regions: A case study of Barramiya gold mine area, Eastern Desert, Egypt** ***Mostafa Redwan, Abdullah O. Bamousa***
7	**Chemical characteristics and assessment of groundwater quality in Halayieb area, southeastern part of the Eastern Desert, Egypt** ***Sameh R. Zaki, Mostafa Redwan, Ahmed M. Masoud, Ahmed A. Abdel Moneim***
8	**Tracking the transition from subduction-related to post-collisional magmatism in the north Arabian–Nubian Shield: A case study from the Homrit Waggat area of the Eastern Desert of Egypt** ***Mokhles K. Azer, Khaled M. Abdelfadil, Paul D. Asimow, Ahmed E. Khalil***
9	**Geochemistry and Petrogenesis of Late Ediacaran Rare-Metal Albite Granite of the Nubian Shield: Case Study of Nuweibi Intrusion, Eastern Desert, Egypt** ***Azer M. K., Abdelfadil K. M., Ramadan A. A.***
10	**Electrical resistivity tomography applications for the construction an educational building in New Sohag University at Al Kawamil area, Sohag, Upper Egypt** **Mohammed Atef Elsayed, Abdelbaset Mohamed Abudeif**
11	**Single and multi-channel passive source methods for calculating the shallow S-wave velocity structure and site effect parameters at 15th May City, Egypt** ***A. M. Abudeif, M. A. Mohammed, A. K. Abd el-aal, Kh. A. Omar***
12	**Geotechnical aspects and associated problems of Al-Shuaiba Lagoon soil, Red Sea coast, Saudi Arabia** ***Bader A. Hakami, El-Sayed Sedek Abu Seif***
13	**Geotechnical engineering evaluation of soil utilizing 2D Multichannel Analysis of Surface Waves (MASW) technique in New Akhmim City, Sohag, Upper Egypt** **A.M. Abudeif, R. E. Fat-Helbary, H.M. Alkhashab, M.A. Mohammed, M. M. Masoud**
14	**Revised (miospores-based) stratigraphy of the Lower Cretaceous succession of the Minqar-IX well, Shushan Basin, north Western Desert, Egypt: Biozonation and correlation approach** ***Magdy S. Mahmoud, Amr S. Deaf, Mohamed A. Tamam, Miran M. Khalaf***
15	**Geoelectrical Characterization of the Al-Kawamil New Settlement, Sohag, Egypt** ***Mohammed A. Mohammed, Abdelbaset M. Abudeif***
16	**Pore and fracture pressure modeling using direct and indirect methods in Badri Field, Gulf of Suez, Egypt** ***A. E. Radwan, A. M. Abudeif, M. M. Attia, M. A. Mohammed***

17	**Development of formation damage diagnosis workflow, application on Hammam Faraun reservoir: A case study, Gulf of Suez, Egypt** ***A. E. Radwan, A. M. Abudeif, M. M. Attia, M. A. Mahmoud***
18	**Chemical speciation of heavy metals of quaternary sediments in Sohag Governorate, Egypt** ***Shaymaa Montaser AbdelRaheem, Mohamed Hassan Ali***
19	**Remote sensing-based geological mapping and petrogenesis of Wadi Khuda Precambrian rocks, South Eastern Desert of Egypt with emphasis on leucogranite** ***Asran M. Asran, S.M. Hassan***
20	**Alluvial karstification and paleodoline development in Eocene limestones, a case study from west Sohag City, Egypt: implications for causes and impacts** ***Tawfiq M. Mahran, Abdallah M. Hassan***
21	**Flood-Hazard Assessment Modeling Using Multicriteria Analysis and GIS: A Case Study-Ras Gharib Area, Egypt** ***Ahmed M.Youssef, Mahmoud A.Hegab***
22	**Chemical speciation of heavy metals of Quaternary sediments in Sohag Governorate, Egypt.** ***Ahmed.A.Abdel Moneim, A.M. Hassan, Mohamed H. Ali, Shaymaa Rezk***
23	**Multi-hazard assessment modeling via multi-criteria analysis and GIS: a case study** ***Hariklia D. Skilodimou, George D. Bathrellos, Konstantinos Chousianitis, Ahmed M. Youssef, Biswajeet Pradhan***
24	**Environmental Hazards of Sand Dunes, South Jeddah, Saudi Arabia: An Assessment and Mitigation Geotechnical Study** ***Ammar Amin, El-Sayed Sedek Abu Seif***
25	**Statistical Analysis of Rainfall Patterns in Jeddah City, KSA: Future Impacts** ***Mazen M. Abu Abdullah, Ahmed M. Youssef, FawzyNashar, Emad Abu AlFadail***
26	**Flood Hazard Assessment of the Urban Area of Tabuk City, Kingdom of Saudi Arabia by Integrating Spatial-Based Hydrologic and Hydrodynamic Modeling** ***Ashraf Abdelkarim, Ahmed F. D. Gaber, Ahmed M. Youssef, Biswajeet Pradhan***
27	**Agriculture Sprawl Assessment Using Multi-Temporal Remote Sensing Images andIts Environmental Impact; Al-Jouf, KSA** **Ahmed M. Youssef, Mazen M. Abu Abdullah, Biswajeet Pradhan, Ahmed F. D. Gaber**
28	**Desertification Risk Assessment of Sand Dunes in Middle Egypt: A Geotechnical Environmental Study** ***El-Sayed Sedek Abu Seif· Mohamed H. El-Khashab***
29	**Sources and behavior of trace elements in groundwater in the South Eastern Desert, Egypt** ***Embaby A., Redwan M.***
30	**Geological and Engineering Characteristics of Expansive Soils in Western Desert, Egypt** ***A. Elshater, M. A. Khashab, M. A. El-Sherif, E. S. Abu Seif***

List of Cook Chapters published by Staff members at Faculty of Science (P. 145-147)

Physics	**Encyclopaedia of Nuclear Physics of Stars** **Ritu Tamta, Khaled S. A. Hassaneen, Johan H. Knapen**
Physics	**Nuclear Physics the Core of Matter and the Fuel of Stars** ***Khaled S. A. Hassaneen***
Botany	**Cyanotoxins in Egypt and Saudi Arabia** ***Zakaria A Mohamed***

Number of published papers by staff members of Faculty of Science during 2019

Department	Number
Mathematics	95
Physics	47
Chemistry	82
Botany & Microbiology	23
Zoology	20
Geology	30
Book Chapters	3
Total	300

- **Collaborative publications within 2019 include:**

  Departments of Physics and Chemistry collaborate and success to publish 5 articles.

  Departments of Chemistry and Zoology collaborate and success to publish 2 articles.

Mathematics

A new general fractional-order derivative with rabotnov fractional-exponential kernel appliedto model the anomalous heat transfer

Xiao-Jun YANG [a], Mahmoud ABDEL-ATY [b,c,d], and Carlo CATTANI [e,f]

[a]*State Key Laboratory for GeoMechanics and Deep Underground Engineering, China University of Mining and Technology, Xuzhou, China*

[b]*Center for Photonics and Smart Materials (CPSM), Zewail City of Science and Technology, Zewail, Egypt*

[c]*Mathematics Department, Faculty of Sciences, Sohag University, Sohag, Egypt*

[d]*Applied Science University, Sitra, Kingdom of Bahrain*

[e]*Engineering School, DEIM, University of Tuscia, Viterbo, Italy*

[f]*Ton Duc Thang University, HCMC, Ho Chi Minh City, Vietnam*

Abstract: In this paper, we consider a general fractional-order derivataive of the Liouville-Caputo type with the non-singular kernel of the Rabotnov fractional-exponential function for the first time. A new general fractional-order derivataive heat transfer model is discussed in detail. The general fractional-order derivataive formula is a new mathematical tool proposed to model the anomalous behaviors in complex and power-law phenomena.

Keywords: power law Rabotnov fractional-exponential function, general fractional-order derivataive, heat transfer,non-singular kernel

A New General Fractional-Order Derivative with Rabotnov .THERMAL SCIENCE: Year 2019, Vol. 23, No. 3A, pp. 1677-1681

Direct Observation of Dissipation in Dynamical Search Algorithm using Transmon Qubits

Ali H. Homid [a], Mahmoud Abdel-Aty [b,c,d], Ahmed Farouk [e], and Abdel-Shafy F. Obada [f]

[a] *Faculty of Science Al-Azhar University Assiut 71524, Egypt*

[b] *Center for Photonics and Smart Materials (CPSM), Zewail City of Science and Technology, Zewail, Egypt*

[c] *Mathematics Department, Faculty of Sciences, Sohag University, Sohag, Egypt*

[d] *Applied Science University, Sitra, Kingdom of Bahrain*

[e] *Department of Physics and Computer Science Wilfrid Laurier University Waterloo ON N2L 3C5, Canada*

[f] *Faculty of Science Al-Azhar University Nasr city 11884, Cairo, Egypt*

Abstract: Following recent work [Fortschritte der Physik 66, 1700080 (2018)], the dissipation effect of the dynamical quantum search algorithm (DQSA) is investigated. Such an algorithm is realized with the interaction of multi superconducting transmon qubits inside a 3D bus cavity. The dissipation of such system is caused by managing the sensitivity to charge noise via tuning the qubit frequency by employing Josephson energy. The probabilities of marked and unmarked states for the present algorithm have been calculated analytically and numerically. Such probabilities of marked states are sensitive to any change in the dissipation parameter. A deficiency causes the dissipation for the marked states, and that deficiency is added to the unmarked states. It is interesting to mention that one of the datasets at large dissipation rates gives an observation of the marked states probabilities which is related to the decoherence free subspace. It is predicted that the algorithm can be successfully implemented in the current experiments.

Keywords: dissipation, dynamical quantum search algorith, superconducting transmon qubits

Dynamical Quantum Search Algorithm: Year 2019,

Reflection and refraction of incident p-, T-, and SVwaves at interface between magnetized two solidliquid media with heat sources and initial stress with and without thermal relaxation times
Reflection and refraction of incident p-, T-, and SVwaves at interface between magnetized two solidliquid media with heat sources and initial stress with and without thermal relaxation times

Sayed M. Abo-Dahab [a,b], Mohamed. N. M. Allam [c] & Mahmoud Abdel-Aty[d]
[a] *Mathematics Department, Faculty of Science, South Valley University, Qena, Egypt;*
[b] *Mathematics Department, Faculty of Science, Taif University, Taif, Saudi Arabia;*
[c] *Mathematics Department, Faculty of Science, Mansoura University, Mansoura, Egypt*
[d]*Deanship of Research and Graduate Studies, Applied Science University, Bahrain and Sohag University, Egypt*

Abstract: We investigate the problem of reflection and refraction of thermoelastic waves at a magnetized solid-liquid interface in presence of initial stress. In the context of Green-Lindsay and coupled thermoelastic theories of thermoelasticity, the problem has been solved and the effect of magnetic field, external heat sources, and initial stress on p-, T-, and SV-waves propagation have been discussed. The boundary conditions at the interface for displacement continuity, vanishing the tangential displacement, continuity of normal force, tangential force, and continuity of temperature are applied. The amplitudes ratios for the incident p-, T-, and SV-waves have been obtained. The effect of the initial stress, heat sources, and magnetic field on the reflection and transmitted coefficients for the incident waves have been discussed.

Keywords: CT theory; Green-Lindsay; heat sources; initial stress; magnetic field; reflection; refraction; thermoelasticity
JOURNAL OF THERMAL STRESSES, 2019, VOL. 42, NO. 2, 233–253:

New Design of Reversible Full Adder/Subtractor Using R Gate

Rasha Montaser[1] · Ahmed Younes[1,2] ·Mahmoud Abdel-Aty[3,4]
[1]*Department of Mathematics and Computer Science, Faculty of Science, Alexandria University,*
[2]*School of Computer Science, University of Birmingham, Birmingham, B15 2TT, UK*
[3]*University of Science and Technology, Zewail City of Science and Technology, Zewail, Egypt*
[4]*Department of Mathematics, Faculty of Science, Sohag University, Sohag, Egypt*

Abstract: Quantum computers require quantum processors. An important part of the processor of any computer is the arithmetic unit, which performs binary addition, subtraction, division and multiplication, however multiplication can be performed using repeated addition, while division can be performed using repeated subtraction. In this paper we present two designs using the reversible R3 gate to perform the quantum half adder/subtractor and the quantum full adder/subtractor. The proposed half adder/subtractor design can be used to perform different logical operations, such as AND, XOR, NAND, XNOR, NOT and copy of basis. The proposed design is compared with the other previous designs in terms of the number of gates used, the number of constant bits, the garbage bits, the quantum cost and the delay. The proposed designs are implemented and tested using GAP software.

Keywords: Reversible gates · Quantum processors · Arithmetic unit · Reversible adder · Reversible subtractor
International Journal of Theoretical Physics (2019) 58: 167–183

Controlling steady-state entanglement and quantum discord through squeezing angle

Eman G. El-Hadidy [a], Ahmed Farouk [b,e], Mahmoud Abdel-Aty [c,d], S. Ghose [b]
[a] *Department of Mathematics, Faculty of Science, Damietta University, Egypt*
[b] *Department of Physics and Computer Science, Wilfrid Laurier University, Waterloo, Canada*
[c] *Applied Science University, Kingdom of Bahrain; Center for Photonics and Smart Materials, Zewail City for Science and Technology, Giza, Egypt*
[d] *Mathematics Department, Faculty of Sciences, Sohag University, Egypt*
[e] *Center for Quantum Computing and Artificial Intelligent, Faculty of Science, Sohag University, Egypt*

Abstract: We analyze the dynamics of entanglement and quantum discord in a two-qubit system coupled to squeezed reservoirs. We present analytical expressions that can be used to efficiently calculate the evolution of quantum discord and entanglement between the two qubits. Our results show that quantum discord is a more general and robust measure of quantum correlations than entanglement. Furthermore, there is a relationship between the time before sudden death of entanglement and the reservoir squeezing angle. Additionally, the increase of squeezing angle accelerates the decay of quantum discord. These results provide new avenues for controlling quantum correlations and designing quantum states that can be used for various quantum computing applications.
Keywords: Steady-state entanglement Quantum discord Squeezing angle
Chaos, Solitons and Fractals 128 (2019) 382–389

A quantum algorithm based on entanglement measure for classifying Boolean multivariate function into novel hidden classes

Mohammed Zidan[a,b], Abdel-Haleem Abdel-Aty[c,d], Duc Manh Nguyen[e], Ahmed S.A. Mohamed[a,f], Yazeed Al-Sbou[g], Hichem Eleuch[h,i], Mahmoud Abdel-Aty[a,b,j]
[a] *University of Science and Technology, Zewail City of Science and Technology, October Gardens 12578, 6th of October City, Giza, Egypt*
[b] *Center for Photonics and Smart Materials (CPSM), Zewail City of Science and Technology, October Gardens, 6th of October City, Giza 12578, Egypt*
[c] *Department of Physics, College of Sciences, University of Bisha, Bisha 61922, P.O. Box 344, Saudi Arabia*
[d] *Physics Department, Faculty of Science, Al-Azhar University, 71524 Assiut, Egypt*
[e] *Coding and Information Theory Lab, University of Ulsan, Ulsan 44610, South Korea*
f Department of Engineering Mathematics and Physics, Faculty of Engineering, Cairo University, Giza 12613, Egypt
[g] *Deanship of Research and Graduate Studies, Applied Science University, P.O. Box 5055, 55222 Manama, Bahrain*
[h] *Department of Applied Sciences and Mathematics, College of Arts and Sciences, Abu Dhabi University, Abu Dhabi, United Arab Emirates*
[i] *Institute for Quantum Science and Engineering, Texas A&M University, College Station, TX 77843, USA*
[j] *Department of Mathematics, Faculty of Science, Sohag University, Sohag, Egypt*

Abstract In this paper, we propose a novel algorithm that solves a generalized version of the Deutsch-Jozsa problem. The proposed algorithm has the potential to classify an oracle U_F , that represents an unknown Boolean function on n Boolean variables, to one of 2^n different classes instead of only two classes which are constant and balanced classes in the case of Deutsch-Jozsa algorithm. The proposed algorithm is based on the use of entanglement measure to explore 2^n 2 additional classes compared to the standard Deutsch-Jozsa algorithm. In addition, the comparison between the proposed quantum algorithm and the classical one is investigated in details. The comparison shows that the proposed algorithm is faster when the number of Boolean variables exceed 14 variables.
Keywords: Quantum information, Quantum algorithm, Deutsch-Jozsa algorithm, Quantum entanglement measure
Results in Physics 15 (2019) 102549

Multistability of Stationary Motions for Darcy Convection Anisotropic Problem

Abdelhafez M. A.[12], Tsybulin V.G.[1]

[1] *Southern Federal University, Rostov-on-Don, 344006, Russia*

[2] *Sohag University, Sohag, 82524, the Arab Republic of Egypt*

Abstract Based on the Darcy model, _uid convection in a porous rectangle is analyzed taking into account anisotropy of thermal characteristics and permeability. Relations between parameters for which the problem belongs to the class of cosymmetric systems are derived. For this case explicit formulas for the critical numbers of the loss of stability of mechanical equilibrium are found. Using a _nite-di_erence method that preserves the cosymmetry of the problem, family of stationary convective regimes is computed. Through the computational experiment the destruction of families is demonstrated in the case of violation of the conditions of cosymmetry.

As result the appearance of a _nite number of stationary regimes are obtained.

EPH - International Journal of Mathematics and Statistics, Volume-5, Issue-5, pp. 23—27.

Anisotropy Effects and Cosmymetry of Convective Flows for Nanofluids in Porous Medium

Abdelhafez M. A.

Sohag University, Sohag, 82524, the Arab Republic of Egypt

Abstract The planar problem of convection in a porous rectangle saturated with a heat-conducting nanofluid is considered. Based on the Darcy-Boussinesq equations, taking into account the Soret effect and assuming the anisotropy of a fluid and a medium, an instability analysis of quiescent state is studied. The conditions under which the problem is being cosymmetric one are established and explicit formulas for the critical Rayleigh numbers are derived. The finite difference methods are developed with preservation of cosymmetry property.

Keywords: Convection; Nanofluid; Porous media; Anisotropy; Cosymmetry

Evolutions in Mechanical Engineering 3(1).2019, pp. 1-3

C-fuzzy Soft Closure Operators and Fuzzy Soft Closure Systems

El-Sayed El-Sanousy
Mathematics Department, Faculty of Science, Sohag University, 82524 Sohag, Egypt

Abstract: In this paper, we introduce the concepts of C -fuzzy soft closure spaces, fuzzy soft closure systems and study the relationships between them. Also, we introduce the notions of r -fuzzy soft T0 -space and r -fuzzy soft T1 -space in C-fuzzy soft closure space. Several results have been proved which establish the appropriatness of the defnitions.

Keywords: Fuzzy soft closure systems; fuzzy soft closure operators; r -fuzzy soft T0 -space and r -fuzzy soft T1 -space.
The Journal of Fuzzy Mathematics Vol. 27, No. 1, 2019

Fuzzy soft upper and lower semi-continuous Multifunctions

S. E. Abbas, E. El-sanowsy, A. Atef
Mathematics Department, Faculty of Science, Sohag University, 82524 Sohag, Egypt

Abstract In this paper, we de_ne the upper and lower inverse of a fuzzy soft multifunction and prove some basic identities. Then by using these ideas we introduce the concept of fuzzy soft continuity and obtain many interesting properties of fuzzy soft upper and lower semi-continuous multifunctions. Also, we de_ne the notions of fuzzy soft lower (A; B; C;D; I)-continuity and fuzzy soft upper (A; B; C;D; I)-continuity. Moreover, we present di_erent cases of upper and lower fuzzy soft continuous multifunctions.

Keywords: Fuzzy soft set, Fuzzy soft multifunctions, Fuzzy soft continuity..
Annals of Fuzzy Mathematics and Informatics, Volume 17, No. 1, (February 2019) pp. 1{15

On (L;M)-Fuzzy Convex Structures

Osama Rashed Sayed[a], EL − Sayed EL − Sanousy [b],Yaser Hassanein Sayed[b]
[a] *Department of Mathematics, Faculty of Science, Assiut University, Assiut 71516, Egypt*
[b] *Department of Mathematics, Faculty of Science, Sohag University, Sohag, 82524, Egypt*

Abstract This paper defines a new class of L-fuzzy sets called r-L-fuzzy biconvex sets in (L;M)-fuzzy convex structures (X;C); where C is an (L;M)-fuzzy convexity on X; and some of their properties were studied. In addition, weintroduce (L;M)-fuzzy topological convexity space and study some of its properties. Finally, we introduce locally (L;M)-fuzzy topology (L;M)-fuzzy convexity space and study some of its properties.

Keywords: r-L-fuzzy biconvex sets, (L;M)-fuzzy topological convexity space, locally fuzzy convex.
Faculty of Sciences and Mathematics, University of Niˇs, Serbia, Filomat 33:13 (2019), 4151–4163

Stratified Soft L-fuzzy Quasi-proximities

El-Sayed El-Sanousy
Mathematics Department, Faculty of Science, Sohag University, 82524 Sohag, Egypt

Abstract: In this paper, the notion of soft L -fuzzy quasi-proximity to be stratified and the related notion of stratification are introduced and studied. Also, we studied the relation between soft L -quasi-proximity and the soft L -grill. Using the notion of soft L –grill to be stratified and the related notion of stratification we show that the soft L –grill associated to both of stratified soft L -quasi-proximity and stratified soft L -grill also is stratified.

Keywords: Soft L -fuzzy quasi-proximities, L -grill, stratification, soft L -Fuzzy proximily continuous
The Journal of Fuzzy Mathematics Vol. 27, No. 1, 2019

A modified shrinking projection methods for numerical reckoning fixed points of g-nonexpansive mappings in hilbert spaces with graphs

H. A. Hammad, W. Cholamjiak, D. Yambangwai, And H. Dutta
Department of Mathematics, Faculty of Science, Sohag University, Sohag 82524, Egypt
Department of Mathematics, School of Science, University of Phayao, Phayao 56000, Thailand
Department of Mathematics, School of Science, University of Phayao, Phayao 56000, Thailand
Department of Mathematics, Faculty of Science, Gauhati University, Guwahati-781014, India

Abstract: In this paper, we introduce four new iterative schemes by modifying the shrinking projection method with Ishikawa iteration and S-iteration. The strong convergence theorems are given for obtaining a common fixed point of two G-nonexpansive mappings in a Hilbert space with a directed graph. We also give some numerical experiments for supporting our main theorems and compare convergence rate between them.

Keywords: strong convergence, shrinking projection, G-nonexpansive mappings, modified iterations, numerical discussion
Miskolc Mathematical Notes Vol. 20 (2019), No. 2, pp. 941–956

Fixed point results for$\emptyset-(\gamma,\mu,n,m)$ contractions with applications to nonlinear integral equations

Hasanen A. Hammad[1], Manuel De la Sen[2]
[1]Department of Mathematics, Faculty of Science, Sohag University, Sohag 82524, Egypt
[2]Institute of Research and Development of Processes University of the Basque Country 48940- Leioa (Bizkaia), Spain

Abstract: The aim of this paper is to introduce a new class of pair of contraction mappings, called $\emptyset-(\gamma,\mu,n,m)$ contraction pairs, and obtain common _xed point theorems for a pair of mappings in this class, satisfying a weakly compatible condition. As an application, we use mappings of this class to _nd the existence of solutions for nonlinear integral equations on the space of continuous functions and in some of its subspaces. Moreover, some examples are given here to illustrate the applicability of these results.

Keywords: $\emptyset-(\gamma,\mu,n,m)$ contraction pairs; weakly compatible mappings; nonlinear integral equations.
International Journal of Analysis and Applications Volume 17, Number 3 (2019), 448-463

Solution of Nonlinear Integral Equation via Fixed Point of Cyclic α_L^{ψ} -Rational Contraction Mappings in Metric-Like Spaces

Hasanen A. Hammad[1], Manuel De la Sen[2]
[1]Department of Mathematics, Faculty of Science, Sohag University, Sohag 82524, Egypt
[2]Institute of Research and Development of Processes University of the Basque Country 48940- Leioa (Bizkaia), Spain

Abstract: In this paper, we introduce the notions of α_L^{ψ} -rational contractive and cyclic α_L^{ψ} - rational contractive mappings and establish the existence and uniqueness of fixed points for such mappings in complete metric-like spaces (dislocated metric spaces). The results presented here substantially generalize and extend several comparable results in the existing literature. As an application, we prove new fixed point results for ψL-graphic and cyclic ψL-graphic rational contractivemappings.Moreover, some examples and an application to integral equation are presented here to illustrate the usability of the obtained results.

Keywords: Cyclic contractive mapping · α-Admissible mapping · Nonlinear integral Equations
Bull Braz Math Soc, New Series

Analytical Solution for a Periodic Boundary Random-value Problem Via Stochastic Fixed Points with PPF Dependence Technique

Hasanen Abuelmagd Hammad[1] AND Rashwan A.Rashwan[2]
[1]Department of Mathematics, Faculty of Science, Sohag University, Sohag 82524, Egypt
[2]Department of Mathematics, Faculty of Science, Assuit University, Assuit 71516, Egypt

Abstract: In this paper, some random common fixed point and coincidence point theorems are established with PPF dependence for generalized random contractions in a separable Banach space. Our results introduce stochastic versions and extensions of recent results as [3, 21, 25] and others. In addition, an application to establish PPF dependent solution of a periodic boundary random-valued problem is given to illustrate the usability of obtained results.

Keywords: PPF dependent Random fixed point with a PPF dependent, Random generalized contractive mappings, The Razumikhin class.
Stat., Optim. Inf. Comput., Vol. 7, December 2019, pp 653–668.

Solving a coupled system of functional equations using coupled coincidence point technique in metric-like spaces

Dhekra M.Albaqeri[1], Hasanen A.Hammad[2] AND Rashwan A.Rashwan[3]

[1]Department of Mathematics, Faculty of Education, Sana'a University, Sana'a 1247, Yemen

[2]Department of Mathematics, Faculty of Science, Sohag University, Sohag 82524, Egypt

[3]Department of Mathematics, Faculty of Science, Assuit University, Assuit 71516, Egypt

Abstract: In this article, we study some new coupled coincidence and coupled common fixed point theorems in metric-like spaces for integral type contraction condition involving a pair of mappings satisfying the CRL1 property. As an application, we discuss the existence of the solution for a coupled system of functional equations arising in dynamic programming. Our results generalize and modify several comparable results in the literature. Finally, two examples are given to illustrate the usefulness of the theoretical results.

Keywords: Common coupled fixed point, w-compatible mappings, CRL1 property, system of functional equations, dynamic programming, metric-like spaces.
Journal of Advanced Studies in Topology 10:1 (2019), 96–108

PPF-Dependent Fixed Point Results for New Multi-Valued Generalized F-Contraction in the Razumikhin Class with an Application

HASANEN A. HAMMAD[1] AND MANUEL DE LA SEN[2]

[1]Department of Mathematics, Faculty of Science, Sohag University, Sohag 82524, Egypt

[2]Institute of Research and Development of Processes University of the Basque Country 48940- Leioa (Bizkaia), Spain

Abstract: In this paper, a new multi-valued generalized F-contraction mapping is given. Using it, the existence of PPF-dependent fixed point for such mappings in the Razumikhin class is obtained. Moreover, an application for nonlinear integral equations with delay is presented here to illustrate the usability of the obtained results.

Keywords: PPF-dependent fixed point; multi-valued generalized F-contraction; Razumikhin class; nonlinear integral equations
Mathematics 2019, 7, 52

A Coupled Fixed Point Technique for Solving Coupled Systems of Functional and Nonlinear Integral Equations

HASANEN A. HAMMAD[1] AND MANUEL DE LA SEN[2]

[1]Department of Mathematics, Faculty of Science, Sohag University, Sohag 82524, Egypt
[2]Institute of Research and Development of Processes University of the Basque Country 48940- Leioa (Bizkaia), Spain

Abstract: In this paper, we obtain coupled fixed point results for F-contraction mapping satisfying a nonlinear contraction condition in the framework of complete metric space without and with a directed graph. As applications of our results, we study a problem of existence and uniqueness of solutions for a class of systems of functional equations that appears in dynamic programming and nonlinear integral equations. Finally, illustrative examples to support some our results are discussed.

Keywords: coupled common fixed point; F-contraction mapping; dynamic programming; nonlinear integral equations
Mathematics 2019, 7, 634

Analytical Solution of Urysohn Integral Equations by Fixed Point Technique in Complex Valued Metric Spaces

HASANEN A. HAMMAD[1] AND MANUEL DE LA SEN[2]

[1]Department of Mathematics, Faculty of Science, Sohag University, Sohag 82524, Egypt
[2]Institute of Research and Development of Processes University of the Basque Country 48940- Leioa (Bizkaia), Spain

Abstract: The purpose of this article is to introduce a fixed point result for a general contractive condition in the context of complex valued metric spaces. Also, some important corollaries under this contractive condition are obtained. As an application, we find a unique solution for Urysohn integral equations, and some illustrative examples are given to support our obtaining results. Our results extend and generalize some other known results in the literature.

Keywords: single-valued mappings; complex valued metric spaces; common fixed point; nonlinear integral equations
Mathematics 2019, 7, 852

C-class functions on common fixed point theorems for weak contraction mapping of integral type in modular spaces

HASANEN A. HAMMAD[1] , R. A. Rashwan[2] , A. H. Ansari[3]

[1]Department of Mathematics, Faculty of Science, Sohag University, Sohag 82524, Egypt

[2]Department of Mathematics, Faculty of Science, Assuit University, Assuit 71516, Egypt.

[3]Department of Mathematics, Karaj Branch, Islamic Azad University, Karaj, Iran.

Abstract: In this paper, we use the concept of C-class functions introduced by Ansari [4] to prove the existence and uniqueness of common _xed point for self-mappings in modular spaces of integral inequality. Our results extended and generalized previous known results in this direction.

Keywords: Common fixed point, modular spaces, p-compatible maps, comparison function, Lebesgue-Stieltjes integrable mapping, C-class functions.

Journal of Linear and Topological Algebra Vol. 08, No. 04, 2019, 265- 285

Coincidence and Fixed Point of Nonexpansive Type Mappings in 2-Metric Spaces

H. A. Hammad1[1] , A. H. Ansari[2] and R. A. Rashwan[3],

[1]Department of Mathematics, Faculty of Science, Sohag University, Sohag 82524, Egypt

[2]Department of Mathematics, Karaj Branch, Islamic Azad University, Karaj, Iran.

[3]Department of Mathematics, Faculty of Science, Assuit University, Assuit 71516, Egypt.

Abstract: The aim of this paper is to prove a coincidence point theorem for a class of self mappings satisfying nonexpansive type condition under various conditions and a fixed point theorem is also obtained. Our results extend and generalize the corresponding result of Singh and Chandrashekhar [7].

Keywords: coincidence point, fixed point, nonexpansive type mapping, 2-metric space.

Earthline Journal of Mathematical Sciences ISSN (Online): 2581-8147 Volume 2, Number 1, 2019, Pages 191-206

ANALYTICAL SOLUTION FOR A COUPLED OF NONLINEAR INTEGRAL EQUATIONS VIA COUPLED FIXED POINT TECHNIQUE

RASHWAN A. RASHWAN[1] , HASANEN A. HAMMAD[2] and SLOBODANKA MITROVI[3],

[1]Department of Mathematics, Faculty of Science, Assuit University, Assuit 71516, Egypt.

[2]Department of Mathematics, Faculty of Science, Sohag University, Sohag 82524, Egypt

[3]Faculty of Forestry Kneza Vi_seslava 1, University of Belgrade, Beograd Serbia

Abstract: In this paper, we obtain a result of coupled _xed point for F-contractionmapping satisfying a nonlinear contraction condition in the framework of complete metric space. We also demonstrate a result of existence and uniqueness for solutions of a system of nonlinear integral equations. Finally, explained examples are given to strong our findings.

Keywords: Coupled fixed point, F-contraction, nonlinear integral equations.
J. Adv. Math. Stud. Vol. 12(2019), No. 1, 13-21

COMMON FIXED POINT THEOREMS FOR WEAKLY COMPATIBLE MAPPINGS SATISFYING A GENERAL CONTRACTIVE CONDITION OF INTEGRAL TYPE

RASHWAN A. RASHWAN[1] *and* HASANEN A. HAMMAD[2],

[1]Department of Mathematics, Faculty of Science, Assuit University, Assuit 71516, Egypt.

[2]Department of Mathematics, Faculty of Science, Sohag University, Sohag 82524, Egypt

Abstract: In this paper, we establish common fixed point theorems for weakly compatible mappings satisfying a general contractive condition of integral form in rational setting. Some examples to justify our results are given. The mapping involved here generalized various type of contractive mapping of integral inequality.

Keywords: Complete metric space, Lebesgue integrable mapping, monotonically decreasing function, weakly compatible mappings..
Palestine Journal of Mathematics, Vol. 8(2)(2019) , 114–126

Common Fixed Point Theorems in Complex-Valued S-Metric Spaces via Implicit Relations with Applications

RASHWAN A. RASHWAN[1] , HASANEN A. HAMMAD[2], and M. G. Mahmoud [3]

[1]Department of Mathematics, Faculty of Science, Assuit University, Assuit 71516, Egypt.

[2]Department of Mathematics, Faculty of Science, Sohag University, Sohag 82524, Egypt

[3]Department of Mathematics, South Valley University, Luxor, Egypt.

Abstract: The aim of this paper is to present some common fixed point results for four weakly compatible mappings in complex valued S-metric spaces. Also, new contraction conditions in this space are given. Finally, as applications of our results,
we give the existence and uniqueness of common solution of Hammerstein and
Urysohn integral equations.

Keywords: Complex valued S-metric spaces; common fixed point; nonlinear integral equations..
Res. Fixed Point Theory Appl.Volume 2019, Article ID 2018034, 17 pages

Generalized Contractive Mappings and Related Results in b-Metric Like Spaces with an Application

HASANEN A. HAMMAD[1] AND MANUEL DE LA SEN[2]

[1]Department of Mathematics, Faculty of Science, Sohag University, Sohag 82524, Egypt

[2]Institute of Research and Development of Processes University of the Basque Country 48940- Leioa (Bizkaia), Spain

Abstract: In this article, a general contractive mapping is presented and some fixed point results in complete b-metric-like spaces are studied. The results obtained here extend and improve some related results in the literature. Also, new common fixed point results for a graphic contraction mappings are proved. Some comparative examples are given to support the obtained results. Moreover, an analytical solution of an integral equation has been presented as an application.

Keywords: : a b-metric-like space; general contractive mappings; graphic contraction mappings; an integral equation
Symmetry 2019, 11, 667; doi:10.3390/sym11050667

A Solution of Fredholm Integral Equation by Using the Cyclic μ_s^q -Rational Contractive Mappings Technique in b-Metric-Like Spaces

HASANEN A. HAMMAD[1] AND MANUEL DE LA SEN[2]

[1]Department of Mathematics, Faculty of Science, Sohag University, Sohag 82524, Egypt

[2]Institute of Research and Development of Processes University of the Basque Country 48940- Leioa (Bizkaia), Spain

Abstract: In this article, the notion of cyclic μ_s^q-rational contractive mappings is discussed and some fixed point theorems in the context of complete b-metric-like spaces are showed. Here, the obtained consequences unify, extend and generalize various comparable known results. Furthermore, new common fixed point outcomes in a directed graph are demonstrated. Moreover, some useful examples are discussed to justify our theoretical results and finding a solution of Fredholm integral equation was discussed as enforcement.

Keywords: : cyclic μ_s^q -rational contractive mapping; a directed graph; fixed point technique; Fredholm integral equation; b-metric-like spaces

Symmetry 2019, 11, 1184

Analytical approximations to nonlinear oscillation of nanoelectro-mechanical resonators

G. M. Ismail[1], M. Abul − Ez[1], N. M. Farea[1] and N. Saad[2]

[1]Department of Mathematics, Faculty of Science, Sohag University, Sohag 82524, Egypt

[2]School ofMathematical and Computational Sciences, University of Prince Edward Island, 550 University Avenue, Charlottetown, PEI, Canada

Abstract: We introduce a new analytical-approximate method based on the global residue harmonic balance method (GRHBM) to study the oscillation of nonlinear nanoelectromechanical resonators. The proposed method is efficiently implemented and evaluated numerically. An illustrative example demonstrates the validity and applicability of the method, further discussed in detail. A highly remarkable agreement found between the approximated solution obtained with the first-order approximation of the present approach and the numerical solutions deduced by other methods that also show the effectiveness of the current approach.

Eur. Phys. J. Plus (2019) 134: 47

Higher-order approximate periodic solution for the oscillator with strong nonlinearity of polynomial type

L. Cveticanin[1,2] and G. M. Ismail[3]

[1]Faculty of Technical Sciences, 21000 Novi Sad, Trg D. Obradovica 6, Serbia

[3]Obuda University, Doctoral School on Safety and Security Sciences, 1081 Budapest, Nepszinhaz u. 8, Hungary

[3]Department of Mathematics, Faculty of Science, Sohag University, Sohag 82524, Egypt

Abstract: In this paper the harmonic balance method (HBM) is adopted for solving a special group of oscillators with strong nonlinear damping and elastic forces. The nonlinearity is of polynomial type. The motion is described with a strong nonlinear differential equation, whose approximate solution is assumed as a suitable sum of trigonometric functions. To find the most convenient combination of trigonometric functions as the probe function is the most important part of this investigation. Introducing the procedure of equating the terms with the same order of the trigonometric functions to zero, the problem is transformed into solving a system of nonlinear algebraic equations. Solving these equations the parameters of the solution up to high-order approximation are obtained. In the paper, the suggested solving procedure is applied for two nonlinear oscillator problems: free vibrations of a restrained uniform beam carrying an intermediate lumped mass and of a particle on a rotating parabola. The obtained approximate analytic solutions are compared with the already published results and with the numerically obtained solution. The solution up to third-order approximation is calculated. It is proved that the HBM with the suggested function gives more accurate results than the previous applied ones. Besides, the difference between the third-order approximate analytical solution and the numerical one is negligible. The method works well for different, even high, values of initial amplitudes

Eur. Phys. J. Plus (2019) 134: 266

On involute-evolute curve couple in the hyperbolic and de Sitter spaces

H. S. Abdel − Aziz[1], M. Khalifa Saad[1,2] **and** A. A. Abdel − Salam[1]

[1]Department of Mathematics, Faculty of Science, Sohag University, Naser Street, Sohag, 82524, Egypt

[2]Department of , Mathematics, Faculty of Science, Islamic University of Madinah, 170 Madinah, Kingdom of Saudi Arabia

Abstract: This paper aims at showing that Frenet apparatus of an evolute curve can be formed in terms of Frenet apparatus of its involute curve in the hyperbolic (de Sitter) space. Also, we establish relationships among Frenet frame of the considered curve couple. Finally, we defray some examples to confirm our main results.

Keywords: Frenet frames, Involute-evolute curves, Hyperbolic space
Journal of the Egyptian Mathematical Society (2019) 27:25

On the Jacobian of Kuribayashi curves

Alwaleed Kamel[a] and Waleed Khaled Elshareef[b]
a) Department of Mathematics, Faculty of Science, Sohag University, Egypt and Islamic University of Madinah, Saudi Arabia, Email: wld_kamel22@yahoo.com
b) Department of Mathematics, Faculty of Science, Sohag University, Sohag, Egypt, Email: waleed@aims.ac.za

Abstract: Kuribayashi quartic curves:
$C_a: = X^4 + Y^4 + Z^4 + a(X^2Y^2 + X^2Z^2 + Y^2Z^2)$,
have total sextactic points if and only if $a = 14$ or a is a zero of $P(a) = a^3 + 68a^2 - 91a + 98$. In [1], the first author described the group generated by the total sextactic points in the Jacobian of Kuribayashi quartic when if $a = 14$. In this paper, we describe this group when a is a zero of $P(a)$:

Keywords: Algebraic curves; Jacobian; sextactic points
COMMUNICATIONS IN ALGEBRA

Inextensible flows of curves in three-dimensional light cone

H. S. Abdel-Aziz, M. Khalifa Saad and Haytham. A. Ali
Department of Mathematics, Faculty of Science, Sohag University, Sohag, 82524, Egypt

Abstract: In this paper, we study inextensible flows of spacelike and lightlike (null) curves in 3-dimensional light cone Q_3 of Minkowiski 4-space E^4_1. We introduce the necessary and sufficient conditions for inextensible flows of these curves which can be expressed as partial differential equations involving the curvatures.

Keywords:: Spacelike and null curves, Frenet frame, Inextensible flow, Minkowski space.
International Journal of Mathematics and Computation, Vol. 30; Issue No. 1; Year 2019,

Image Pixel Permutation Operation Based on Elliptic Curve Cryptography

Omar Reyad[1,2], Hany S. Khalifa[3] **and** Radwan Kharabsheh[4]

[1]*Computer Science Department, Faculty of Science, Sohag University, Sohag, Egypt*
[2]*College of Computing & Information Technology, Shaqra University, Shaqra, Kingdom of Saudi Arabia*
[3]*Computer Science Department, Misr Higher Institute of Commerce and Computers, Egypt*
[4]*Department of Business Administration, Applied Science University, Bahrain*

Abstract: In this paper, elliptic curve (EC) based pseudo-random bit generator is used to control the group operation (GRP) method which has good inherent cryptographic properties. The new proposed method named EC-GRP operation combines the cryptographic properties of both elliptic curve cryptography (ECC) and the group bit permutation operation. When applied to image pixels, the proposed EC-GRP bit-level permutation method controlled by the EC pseudo-random bit generator, presented higher performance characteristics in terms of security analysis test benchmarking.

Keywords: Elliptic Curve Cryptography, Group Permutation, Pseudo-random Bit Generator, Image Encryption
Applied Mathematics & Information Sciences, 13, No. S1, 183-189 (2019)

An Efficient Deep Convolutional Neural Network for Visual Image Classification

Basma Abd El – Rahiem[1], Muhammad Atta Othman Ahmed[2], Omar Reyad[3]
Hani Abd El – Rahaman[1], Mohamed Amin[1], Fathi Abd El-Samie[1]
[1]Faculty of Science, Menoufia University, Shibin El Kom, Egypt
[2]Faculty of Computers and Information, South Valley University, Luxor, Egypt
[3]Faculty of Science, Sohag University, Sohag, Egypt
[4]Faculty of Electronic Engineering, Menoufia University, Shibin El Kom, Egypt

Abstract: . Such a hot open issue in the area of computer vision is the classification of visual images especially in Internet of Things (IoT) and remote mid-band and high-band based connections. In this paper, we propose a robust and efficient taxonomy framework. The proposed model utilizes the well-known convolutional neural network composites to construct a robust Visual Image Classification Network (VICNet). The VICNet consists of three convolutional layers, four Relu/Leaky Relu activation layers, three max-pooling layers and only two fully connected layers for extracting expected input image features. To make the training process faster, we used non-saturating neurons with a very efficient Graphics Processing Unit (GPU) implementation for the convolution operation. To minimize over-fitting issue in the fully-connected layers, we utilized a recently-developed regularization approach “dropout” with a dropping probability of 50%. The proposed VICNet framework has a high potential capability in the recognition of test images. The experimental and simulations results proven the efficacy of the proposed model.

Keywords: Deep learning · Visual image classification Convolutional neural network · Deep feature extraction Transfer learning
Proceedings of the International Conference on Advanced Intelligent Systems and Informatics 2019

Image Encryption Algorithm Methodology Based on Multi-mapping Image Pixel

W. M. Abd – Elhafiez[1,2] , Omar Reyad [1], M. A. Mofaddel [1],
[1]Faculty of Science, Sohag University, Sohag, Egypt
[2]College of Computer Science and Information Systems, Jazan University, Jazan, Kingdom of Saudi Arabia

Abstract: . Image encryption and decryption using a key sequence based on the multi-mapping method of an image pixel is proposed in this paper. The generated key sequences are based on the logistic map, elliptic curves (EC) and Henon map. In the beginning, the one-dimensional sequence is generated using logistic map for the bifurcation parameter and initial value. The generated sequences are XORed with image pixels as a first mapping step. Then the resulted pixels are XORed with key sequence based on elliptic curve random number generator (ECRNG) as a second mapping step. Finally, the resulted pixels XORed with key sequence generated by Henon map. The obtained cipher image introduces good cryptographic properties in the case of multi-mapping. The performance of the proposed scheme is analyzed by computing Histogram, Entropy, and Correlation between the original and encrypted images. The proposed method provides an immense improvement in the encrypted image.

Keywords: Encryption _ Gray image _ Henon map _ Logistic map _Elliptic curves
The International Conference on Advanced Machine Learning Technologies and Applications (AMLTA2019) pp 645-655

High Efficient Haar Wavelets for Medical Image Compression

E. A. Zanaty
Computer Science Department, Faculty of Science, Sohag University, Sohag, Egypt

Abstract: In this paper, we proposed an improved high efficient Haar wavelets (HEHW) algorithm to improve the quality of image compression ratio (CR) rate and peak signal to noise ratio for medical imaging. The proposed algorithm starts by partitioning the original image into 2 * 2 submatrices. Then the wavelets transform coefficients obtained by working on the submatrices instead of the rows and on the columns in the original image. We re-compute the resulting coefficients for sub-matrices to obtain the approximation and the sub details of the original image. Then, we calculate statistical thresholds on the details sub bands to complete the compression process. The proposed algorithm is applied to five different medical image structures to prove its efficiency using the evaluation factors like CR, peak signal to noise ratio, mean square error and transform time. The comparison between the proposed and the well-known modified Haar method also compared to the results of existing wavelets techniques: like Coiflet, Daubechies, Biorthogonal, Dmeyer, and Symlets to prove the proposed algorithm efficiency.

Keywords: Haar transform (HT) , Compression ratio (CR) ,Peak signal to noise ratio (PSNR) High efficient haar wavelet (HEHW) ,Statistical thresholds
Proceedings of the International Conference on Advanced Intelligent Systems and Informatics 2019

Initial Energy Value Effects on the Performance of Some Heterogeneous Protocols Levels in Wireless Sensor Network

Hamdy H. El-Sayed
Computer Science Department, Faculty of Science, Sohag University, Sohag, Egypt

Abstract :This paper presents the simulating of 2-level heterogeneous network model for Wireless Sensor Networks (WSNs) to enhance the network life-time, dead nodes number and packet to base station with different value of initial energy which is characterized by a single parameter. The heterogeneous network model also helps to select cluster heads and different nodes sends to base station with different initial values. The network lifetime, number of dead nodes and number of packet send to base station have been computed by implementing Low Energy Adaptive Clustering Hierarchy (LEACH) and Distributed energy-efficient clustering (DEEC) protocols for our network. Low Energy Adaptive Clustering Hierarchy (LEACH) and Distributed energy-efficient clustering (DEEC) protocols have been implemented for the existing 1-level and 2-level heterogeneous network models it is denoted as LEACH-level1, LEACH-level2, DEEC-level1 and DEEC-level2, respectively. The network lifetime and the rate of packet to Base station increased with increasing initial energy on the other side dead nodes number decreased with increasing initial energy. Different values and new results are presented in our article it is recommends adequate initial energy use to increase the network lifetime of WSN.

Keywords: 2-level heterogeneous, LEACH, DEEC, alive nodes, dead nodes, packet to BS, WSN.
Egyptian Computer Science Journal Vol. 43 No.1 January 2019 ISSN-1110-2586

Some WSN characteristics effects on the performance of LEACH and MODLEACH protocols

Hamdy H. El-Sayed
Computer Science Department, Faculty of Science, Sohag University, Sohag, Egypt

Abstract: This paper studies a number of network characteristics of Low Energy Adaptive Clustering Hierarchy (LEACH), and Modified Low Energy Adaptive Clustering Hierarchy (MODLEACH) protocols. It intends to enumerate dead nodes, alive nodes, and packet-to-BS and packet-to-CH consumed by the entire network, and affected by its characteristics e.g. network area, probability, number of rounds, number of nodes, and energy of data aggregation. Different values of these characteristics produce different results of number dead nodes, alive nodes and packet-to-BS and packet-to-CH which effect network performance. Finally, a brief performance analysis of Low Energy Adaptive Clustering Hierarchy (LEACH) and Modified Low Energy Adaptive Clustering Hierarchy (MODLEACH) is carried out considering metrics of the previous characteristics of wireless sensor network.

Keywords: WSN, LEACH, MODLEACH, network area, probability, number of rounds, number of nodes and data aggregation energy.
Appl . Math. Inf . Sci . 13, No. 3, 361- 368 (2019)

Minutiae-Based Fing erprint Extraction: An EffectiveMethod Based on Harris Corner Detector

Samy Bakheet, Mahmoud A. Mofaddel, and Rehab Youssef
Computer Science Department, Faculty of Science, Sohag University, Sohag, Egypt

Abstract: Feature extraction is not only a crucial preprocessing step for fingerprint matching, but is also essentially involved as a core component of automated fingerprint identification (AFI) systems, which mainly aims at detecting singular as well as all other fingerprint minutiae points that impart individuality to each fingerprint and differentiate one fingerprint from another. The key question that constantly arises in fingerprint feature extraction is how to achieve high-accuracy minutiae with inherently varied-quality scanned fingerprints. In this paper, an effective method for minutiae-based fingerprint feature extraction is proposed, where high accuracy minutiae data are first obtained via preprocessing mechanisms, such as denoising, binarization, thinning, bifurcation, termination and ridge to valley area. Then, feature extraction is performed by employing the Harris corner detector that looks for large changes in local contrast to extract reliable minutiae points from a given fingerprint automatically and quickly. Experimental results indicate that the proposed method exhibit good performance in extracting valid minutiae points, even with low-quality fingerprint images.

Keywords: Biometrics, fingerprint, minutiae, bifurcation, Harris corner detector.
Appl. Math. Inf. Sci. 13, No. 6, 1079-1086 (2019)

A new memristive model with complex variables and its generalized complex synchronizations with time lag

Emad E.Mahmoud[1,2] Ohood A.Althagafi[3]
[1]Department of Mathematics, Faculty of Science, Taif University, Taif 888, Saudi Arabia
[2]Department of Mathematics, Faculty of Science, Sohag University, Sohag 82524, Egypt
[3]Department of Mathematics, Turabah College, Taif University, Turabah, Saudi Arabia

Abstract: The point of this paper is to display and explore a memristive complex hyperchaotic model with a flux-controlled memristor. The model's behavior is examined through numerical simulations by utilizing some tools of nonlinear theory, for example, generalized Hamiltonian, symmetry, dissipative, equilibria and their stability, bifurcation diagram, and Lyapunov exponents. Next, this paper centers around the complex function projective lag synchronization (CFPLS) for various-dimensional hyperchaotic models with complex variables and uncertain parameters. A simulation model displays the effectiveness of the obtained values. The effects of CFPLS were used to develop a precise application in secure correspondence. The digital outcomes were used to verify the adequacy and feasibility of the exhibited technique.

Keywords: Memristive Synchronization Lyapunov function Complex Scaling function matrix
Results in Physics Volume 15, December 2019, 102619

A New Nine-Dimensional Chaotic Lorenz System with Quaternion Variables: Complicated Dynamics, Electronic Circuit Design, Anti-Anticipating Synchronization, and Chaotic Masking Communication Application

Emad E. Mahmoud [1,2], M. Higazy [1,3] and Turkiah M. Al-Harthi [4]

[1]*Department of Mathematics, Faculty of Science, Taif University, Taif 888, Saudi Arabia*
[2]*Department of Mathematics, Faculty of Science, Sohag University, Sohag 82524, Egypt*
[3]*Department of Physics and Engineering Mathematics, Faculty of Electronic Engineering, Menoufia University, Menouf 32952, Egypt*
[4]*Department of Mathematics, Shaqra University, Shaqra 11921, Saudi Arabia*

Abstract: In this paper, a chaotic quaternion autonomous nonlinear structure is introduced and intends to be a contribution. It is the first nonlinear dynamical system with quaternion variables to be studied in the literature. With nine dimensions, the new system is a high-dimensional one. Several vital characteristics and features of this model are investigated, such as its Hamiltonian, symmetry, signal flow graph, dissipation, equilibriums and their stability, Lyapunov exponents, Lyapunov dimension, bifurcation diagrams, and chaotic behavior. A circuit implementation is designed to realize the new system, and a scheme is designed to achieve anti-anticipating synchronization (AAS) of two identical chaotic attractors with quaternion variables based on a Lyapunov function and active control. The concept of AAS is yet to be explored in the literature. A simulation experiment is designed and executed to illustrate the effectiveness of the acquired results. After synchronization, numerical outcomes are planned to explain the status variables and errors of these chaotic attractors to prove that AAS is achieved. The secure communication problem is studied based on the obtained events of the AAS of two identical nonlinear Lorenz systems with quaternion variables. AAS connecting the drive and response systems in chaotic systems with quaternion variables is the key to achieving communication. Signal encryption and restoration are simulated numerically.

Keywords: quaternion; chaotic; lyapunov function; anti-anticipating synchronization; secure communication
Mathematics 2019, 7(10),877; https://doi.org/10.3390/math7100877

Fuzzy ideal topological spaces

Ali N.A. Koam[a], Ismail Ibedou[b] and S.E. Abbas[c]

[a]Department of Mathematics, Faculty of Science, Jazan University, Jazan, Saudi Arabia
[b]Department of Mathematics, Faculty of Science, Benha University, Benha, Egypt
[c]Department of Mathematics, Faculty of Science, Sohag University, Sohag, Egypt

Abstract: In this paper, it is introduced the notion of r-fuzzy ideal separation axioms Ti, i = 0, 1, 2 based on a fuzzy ideal I on a fuzzy topological space (X, τ). An r-fuzzy ideal connectedness related to the fuzzy ideal I is introduced which has relations with a previous r-fuzzy connectedness. An r-fuzzy ideal compactness related to I is introduced which has also relations with many other types of fuzzy compactness.

Keywords: fuzzy ideal, fuzzy separation axioms, fuzzy compactness, fuzzy connectedness
Journal of Intelligent & Fuzzy Systems 36 (2019) 5919–5928

Complex anti-synchronization of two indistinguishable chaotic complex nonlinear models

Emad E Mahmoud[1], Madeha A Al-Adwani[2]
[1]Department of Mathematics, Faculty of Science, Taif University, Taif, Saudi Arabia
[2]Department of Mathematics, Faculty of Science, Sohag University, Sohag, Egypt

Abstract: The principal target of this work is to introduce and examine a novel kind of complex synchronization. This sort may be called complex anti-synchronization. There are surprising properties of complex anti-synchronization that do not exist in the writing, for example, (1) this sort of synchronization can dissect just for complex nonlinear frameworks. (2) The complex anti-synchronization contains or connects two sorts of synchronizations (anti-synchronization and complete synchronization). Anti-synchronization happens between the real part of main framework and the imaginary part of the slave framework, although complete synchronization accomplishes between the real part of slave framework and the imaginary part of the main framework. (3) In complex anti-synchronization, the attractors of the essential and slave structures are moving symmetrical to each other with a similar structure. (4) The state variable of the standard framework synchronizes with an other state variable of the slave structure. An explanation of complex anti-synchronization is presented for two indistinguishable chaotic complex nonlinear frameworks. In view of the Lyapunov function, a plan is intended to accomplish complex anti-synchronization of disordered or chaotic attractors of these frameworks. The effectiveness of the obtained results is outlined by a reenactment illustration. Numerical outcomes are plotted to show state variable, modulus errors, phase errors and the development of the attractors of these chaotic frameworks after synchronization to demonstrate that complex anti-synchronization is accomplished.

Keywords: Complex anti-synchronization, chaotic, Lyapunov function, complex
Measurement and Control 2019, Vol. 52(7-8) 922–928

Connectedness in Fuzzy Soft Topological Spaces

S. E. Abbas[1] · El-sayed El-sanowsy[2] · A. Atef[2]
[1] Department of Mathematics, Faculty of Science, Jazan University, Jizan, Saudi Arabia
[2] Department of Mathematics, Faculty of Science, Sohag 82524, Egypt

Abstract: In this paper, we define the fuzzy soft operator φ constructed from a fuzzy soft grill G E and a fuzzy soft topological space (X, τE). Also, we introduce and study the notion of connectedness to fuzzy soft topological spaces with fuzzy soft grills. Furthermore, we extend the notion of α-connectedness related to a fuzzy soft operator α on the set X.

Keywords: Fuzzy soft grill · Fuzzy soft operator · Fuzzy soft connectedness · Fuzzy soft component
Bull Braz Math Soc, New Series (2019) 50:587–601

A general formula of complex synchronizations with complex scaling diagonal matrix and time lag

Emad E.Mahmoud[ab] Fatimah S.Abood[c]

[a]Department of Mathematics, College of Science, Sohag University, Sohag 82524, Egypt
[b]Department of Mathematics, College of Science, Taif University, Taif 888, Saudi Arabia
[c]Department of Mathematics, College of Science, King Khalid University, Abha, Saudi Arabia

Abstract: In this paper, we show a novel sort of complex synchronization. We call this sort complex modified projective lag synchronization (CMPLS). CMPLS, which is a broader instance of synchronizations, is hardly studied or not mentioned till date. We study it to a framework, with certain or uncertain parameters, of two chaotic complexes n-dimensional owing to chaotic attractors with similar structure direct parts yet differing absolutely or mostly in nonlinear terms. In view of the Lyapunov work with lag in time an approach plans are intended to accomplish CMPLS for such matches of complex frameworks with certain or indeterminate parameters. Logical expressions for the complex control capacity are determined to utilize these plans to accomplish CMPLS. This kind of complex synchronization is considered as a speculation of many sorts of synchronizations and complex synchronizations that have shown up in the current writing. The frameworks in CMPLS can be synchronized using an unpredictable scale diagonal lattice. The viability of the obtained results is represented by concentrating two cases of such coupled chaotic attractors with certain or indeterminate parameters in the complex domain. We can plot the numerical results to clear errors frameworks, modulus errors and phase errors of chaotic attractors and that can be after synchronization to show that CMPLS is accomplished.

Keywords: Complex modified projective lag synchronization Chaotic Lyapunov function Certain and uncertain parameters Complex
Results in Physics Volume 12, March 2019, Pages 603-614

Department of Mathematics, Faculty of Science, Sohag 82524, Egypt

Abstract: In this paper, we introduce the notions of fuzzy soft interior spaces and fuzzy soft closure spaces. In particular, we prove the existence of initial fuzzy soft interior structures and initial fuzzy soft closure structures. From this fact, the category FSC is a topological category over SET.

Keywords: Initial fuzzy soft interior spaces, Initial fuzzy soft closure spaces, Fuzzy soft topological spaces.
Annals of Fuzzy Mathematics and Informatics Volume 17, No. 2, (April 2019) pp. 175{189

A phenomenal form of complex synchronization and chaotic masking communication between two identical chaotic complex nonlinear structures with unknown parameters

Emad E.Mahmoud[ab] Bushra H.AL-Harthi[c]

[a]*Department of Mathematics, Faculty of Science, Taif University, Taif 888, Saudi Arabia*
[b]*Department of Mathematics, Faculty of Science, Sohag University, Sohag 82524, Egypt*
[c]*Department of Mathematics, College of Science, Bisha University, Bisha, Saudi Arabia*

Abstract: In this paper, we review the complicated (or complex) lag (or slack) synchronization (CLS) of coupled complex chaotic nonlinear structures with unknown parameters. In spite of its unusual properties, the significance of CLS is yet to be fully demonstrated in the literature. Using a Lyapunov function, an adaptive (or versatile) controller is developed to synchronize coupled, generally unknown chaotic complex structures. This enables the uncertain parameters of the structures to be evaluated. The CLS of indistinguishable twin complex Lü structures is recognized as a simulation pattern. A number of results demonstrate the state characteristics, modulus errors, and phase errors for these chaotic attractors following the onset of CLS, thus verifying the theoretical derivations. CLS is an encouraging phenomenon, as the synchronization between the state characteristics of the principal structure and those of the slave structure enable excellent communication security. Numerical simulations of secure communications demonstrate the transmission of an encrypted message and an image signal.

Keywords: Complex lag synchronization Chaotic structures Unknown Secure communications Lyapunov function Complex
Results in Physics Volume 14, September 2019, 102452

Further Results on the Inverse Base of Axially Monogenic Polynomials

Mohamed Abdalla[1] · Mahmoud Abul-Ez[2] · Aida Al-Ahmadi[3]

[1]Department of Mathematics, Faculty of Science, South Valley University, Qena 83523, Egypt
[2]Department of Mathematics, Faculty of Science, Sohag University, Sohag 82524, Egypt
[3]Department of Mathematics, Faculty of Education for Girls, Tabuk University, Tabuk, Saudi Arabia

Abstract: The main goal of this paper is to investigate the convergence properties of the inverse base of axially monogenic polynomials. These convergence properties proceed from the investigation of the relation between the effectiveness in closed balls, open balls as well as effectiveness for integral functions. The obtained results are the natural generalization of the original ones in complex setting to higher dimensions. In the meantime our results cover some open questions concerning the Clifford inverse bases.

Keywords: Axially monogenic function · Bases of polynomials · Inverse base · Convergence properties
Bull. Malays. Math. Sci. Soc. (2019) 42:1369–1381

Effect of a magnetic field on the propagation of waves in a homogeneous isotropic thermoelastic half-space

AM Abd-Alla[1], SM Abo-Dahab[23], SM Ahmed[4], MM Rashid[1]

[1]Mathematical Department, Faculty of Science, Sohag University, 82524, Egypt

[2]Mathematical Department, Faculty of Science, South Valley University, Qena, Egypt

[3]Mathematical Department, Faculty of Science, Taif University, Taif, Saudi Arabia

[4]Mathematical Department, Faculty of Science, Al-Arish University, Egypt

Abstract: The prime objective of the present paper is to analyze the propagation of thermoelastic waves in a homogeneous isotropic elastic semi-infinite space that is exposed to a magnetic field at initial temperature T0 and whose boundary surface is subjected to the moving heat source and load moving with finite velocity. Temperature and stress distribution occurring due to heating or cooling have been determined using certain boundary conditions. Numerical results indicate that the effect of the magnetic field is very pronounced. Comparison is made with the results predicted by the theory of thermoelasticity in the absence of a magnetic field. Apart from geophysical applications, the consequences of the present study offer a better platform to design a surface wave sensor by means of its established results. The obtained results may be also used for acquiring a better performance in surface acoustic wave devices and waveguides ited films.

Keywords: moving heat source / moving load source / thermal stresses / thermoelasticity / wave propagation / magnetic field Физическая мезомеханика 22 (1) (2019) 81-91

Rayleigh surface wave propagation in an orthotropic rotating magneto-thermoelastic medium subjected to gravity and initial stress

AM Abd-Alla[1], SM Abo-Dahab[23], SM Ahmed[4], MM Rashid[1]

[1]Mathematical Department, Faculty of Science, Sohag University, 82524, Egypt

[2]Mathematical Department, Faculty of Science, South Valley University, Qena, Egypt

[3]Mathematical Department, Faculty of Science, Taif University, Taif, Saudi Arabia

[4]Mathematical Department, Faculty of Science, Al-Arish University, Al-Arish, Egypt

Abstract: The prime objective of the present article is to analyze the effects of rotation and initial stress on the propagation of Rayleigh surface waves in a homogeneous, orthotropic magneto-thermoelastic half space subjected to gravity field. The frequency equations in closed form are derived and the amplitude ratios of surface displacements, temperature change during the Rayleigh wave propagation on the surface of half space have been computed analytically. The highlights of this study are the effects of different parameters (rotation, magnetic field, initial stress, and gravity) on the velocity of Rayleigh waves. Variation in phase velocity of Rayleigh waves against a wave number is shown graphically. Some particular cases have been deduced. Also, the classical Rayleigh wave equation is obtained as a special case of the present study. Numerical example has been carried out and represented by the means of graphs. Impacts of various involved parameters appearing in the solutions are carefully analyzed. In fact, in the absence of various parameters, these equations are in agreement with the results for isotropic medium.

Keywords: Rayleigh waves, orthotropic medium, thermoelasticity, frequency equation, initial stress, gravity, magnetic field

Mechanics of Advanced Materials and Structures (2019) 1-12

A magneto–thermo-elastic problem for a half-space without energy dissipation subjected to rotation and gravity field

AM Abd-Alla[1], SM Abo-Dahab[23], SM Ahmed[4], MM Rashid[1]

[1]Mathematical Department, Faculty of Science, Sohag University, 82524, Egypt
[2]Mathematical Department, Faculty of Science, South Valley University, Qena, Egypt
[3]Mathematical Department, Faculty of Science, Taif University, Taif, Saudi Arabia
[4]Mathematical Department, Faculty of Science, Al-Arish University, Al-Arish, Egypt

Abstract: The prime objective of the present paper is to analyze the effects of the rotation, magnetic field and gravity in a thermo-elastic half-space containing heat source on the boundary of the half-space. The medium assumed under consideration is traction free, homogeneous, isotropic, as well as without energy dissipation. The normal mode analysis and eigenvalue approach technique are used to solve the resulting non-dimensional coupled equations. The comparisons for the physical quantities are established numerically and represented graphically in different cases with respect to the used effects. A comparative and remarkable study has been carried out through various graphs to deliberate the consequences of different parameter on the displacement components, stress components and temperature

Keywords: Green–Naghdi theory; Thermo-elasticity; Energy dissipation; Rotation; Magnetic field; Gravity field

Journal of Ocean Engineering and Science 4 (1), (2019) 55-63

Effect of magnetic field and three-phase-lag in a rotating micropolar thermo-viscoelastic half-space homogeneous isotropic material

SM Abo-Dahab[1, 2], AM Abd-Alla[1,3], SM Ahmed[4], MM Rashid[3]

[1]Mathematical Department, Faculty of Science, Taif University, Taif, Saudi Arabia
[2]Mathematical Department, Faculty of Science, South Valley University, Qena, Egypt
[3]Mathematical Department, Faculty of Science, Sohag University, 82524, Egypt
[4]Mathematical Department, Faculty of Science, Al-Arish University, Al-Arish, Egypt

Abstract: This paper is devoted to three-phase-lag theory of thermo-elasticity to study the effects of rotation, ramp parameter and magnetic field in a micropolar generalized thermo-viscoelastic medium. By employing normal mode analysis and Lame's potential theory, the analytical expressions for the displacement components, stresses components, couple stress and temperature field are obtained in the physical domain. Numerical examples are displayed to illustrate the effects of magnetic field, rotation and ramp parameter on the results. When there is no phase-lag effects, the results of the current paper are reduced to exactly the same results available in the literature. However, the magnetic field and rotation have no effect on the non-dimensional temperature. The results indicate that the effect of magnetic field, rotation, ramp parameter, viscous and Phase-lag on the micropolar thermo-viscoelastic medium are very pronounced.

Keywords: Magnetic field, three-phase-lag, micropolar, thermo-viscoelastic, rotation, ramp parameter, normal mode analysis

Waves in Random and Complex Media, (2019) 1-24

Solution of a problem of thermal stresses in a non-homogeneous thermoelastic infinite medium of isotropic material by finite difference method

A.M.Farhan[1, 2], AM Abd-Alla[3], MoaiadA.Khder[4]
[1]Physics Department,Facultyof Science,JazanUniversity,SaudiArabiab
[2] Physics Department, Faculty of Science, Zagzig University, Egypt
3 Mathematical Department, Faculty of Science, Sohag University, 82524, Egypt
[4] Department of Computer Science, Applied Science University, Bahrain

Abstract: The present work deals with a new problem of thermoelasticity for an infinitely long and isotropic circular cylinder of temperature dependent physical properties. The inner and outer curved surfaces of the cylinder are subjected to both the mechanical and thermal boundary conditions. A finite difference model is developed to derive the solution of the problem in which the governing equations are uncoupled linear partial differential equations. The transient solution at any time can be evaluated directly from the model. In order to demonstrate the efficiency of the present model we consider a suitable material and obtain the numerical solution of displacement, temperature, and stresses inside the cylinder for the homogeneous-dependent material properties of the medium. The results are analyzed with the help of different graphical plots.

Keywords Thermal stress, Thermoelasticity, Wave propagation, Finite difference Method, Non-homogeneous medium
Journal of Ocean Engineering and Science Volume 4, Issue 3, September 2019, Pages 256-262

Effects of rotation and gravity on an electro-magneto-thermoelastic medium with diffusion and voids by using the Lord-Shulman and dual-phase-lag models

SM Abo-Dahab[1,2], AM Abd-Alla[3], A. A. KILANY[3]
[1]Mathematical Department, Faculty of Science, Taif University, Taif, Saudi Arabia
2 Mathematical Department, Faculty of Science, South Valley University, Qena, Egypt
3 Mathematical Department, Faculty of Science, Sohag University, 82524, Egypt

Abstract: The effects of rotation and gravity on an electro-magneto-thermoelastic medium with diffusion and voids in a generalized thermoplastic half-space are studied by using the Lord-Shulman (L-S) model and the dual-phase-lag (DPL) model. The analytical solutions for the displacements, stresses, temperature, diffusion concentration, and volume fraction field with different values of the magnetic field, the rotation, the gravity, and the initial stress are obtained and portrayed graphically. The results indicate that the effects of gravity, rotation, voids, diffusion, initial stress, and electromagnetic field are very pronounced on the physical properties of the material.

Keywords: electromagnetic field gravity field rotation initial stress voids diffusion normal mode analysis Lord-Shulman (L-S) model dual-phase-lag (DPL) model
Appl. Math. Mech. -Engl. Ed., 40(8), 1135–1154 (2019)

Effect of rotation on wave propagation through a poroelastic wet bone with cavity

AM Abd-Alla[1], SM Abo-Dahab[2,3], Roqia Ateeq[3], MoaiadA.Khder[4]
[1]Mathematical Department, Faculty of Science, Sohag University, 82524, Egypt
[2]Mathematical Department, Faculty of Science, South Valley University, Qena, Egypt
[3]Mathematical Department, Faculty of Science, Taif University, Taif, Saudi Arabia
[4]Department of Computer Science, Applied Science University, Bahrain

Abstract Purpose The purpose of this paper is to investigate the wave propagation of wave in an infinite poroelastic cylindrical bone. The dynamic behavior of a wet long bone that has been modeled as a piezoelectric hollow cylinder of crystal class 6 is investigated.
Design/methodology/approach
An exact closed form solution is presented by employing an analytical procedure. The frequency equation for poroelastic bone is obtained when the boundaries are stress free and is examined numerically.
Findings
The study of wave propagation over a continuous medium is of practical importance in the field of engineering, medicine and bio-engineering. Application of the poroelastic materials in medicinal fields such as orthopedics, dental and cardiovascular is well known. In orthopedics, wave propagation over bone is used in monitoring the rate of fracture healing. There are two types of osseous tissue, such as cancellous or trabecular and compact or cortical bone, which are of different materials, with respect to their mechanical behavior.
Originality/value
The frequencies are calculated for poroelastic bone for various values for different values of rotation, angular velocity and density. In wet bone little velocity dispersion was observed, in contrast to the results of earlier studies on wet bone. Large values of attenuation were observed. Such a model would in particular be useful in large-scale parametric studies of bone mechanical response.

Keywords Rotation, Wave propagation, Natural frequency, Poroelastic, Wet bone
Multidiscipline Modeling in Materials and Structures (2019)

On problem of the stresses in a non-homogeneous composite of an infinite cylinder of orthotropic material

A.M.Farhan[1, 2], AM Abd-Alla[3], MoaiadA.Khder[4]
[1]Physics Department,Facultyof Science,JazanUniversity,SaudiArabiab
[2]Physics Department, Faculty of Science, Zagzig University, Egypt
[3]Mathematical Department, Faculty of Science, Sohag University, 82524, Egypt
[4]Department of Computer Science, Applied Science University, Bahrain

Abstract The prime objective of the present paper is to analyze the effect of inhomogeneity in an incompressible orthotropic elastic material in a cylinder. The dynamical problems of an orthotropic cylinder containing: (i) an isotropic core and (ii) a rigid core are considered. The radial displacement and stresses in different cases have been computed analytically. The numerical calculations arc carried out for the radial displacement and stresses of the composite elastic cylinder for various material inhomogeneity parameters are depicted graphically. The results indicate that the effect of inhomogeneity parameter on the components of displacement and the stresses is very pronounced. Several examples are considered. The approach is validated by comparing with previously known solutions. The MATHEMATICA software is applied to explicate the effect of these parameters graphically..

Keywords Elastodynamics, Wave stress, Non-homogeneous material, Homogeneous, Plane strains, Orthotropic material, Composite materials
Results in Applied Mathematics Volume 3, October 2019, 100014

Effect of heat laser pulse on wave propagation of generalized thermoelastic micropolar medium with energy dissipation

Mohamed I. A. Othman[1], Abo-el-nour N. Abd-alla[2], Elsayed M. Abd-Elaziz[3]
[1]*Department of Mathematics, Faculty of Science Zagazig University, Zagazig, Egypt*
[2] *Mathematical Department, Faculty of Science, Sohag University, 82524, Egypt*
[3] *Ministry of Higher Education, Zagazig Higher Institute of Engineering and Technology, Zagazig, Egypt*

Abstract The purpose of this paper is to introduce the Green–Naghdi theory of type III to study the influence of thermal loading due to laser pulse on the wave propagation of generalized micropolar thermoelasticity. The bounding plane surface is heated by a non-Gaussian laser beam with a pulse duration of 8 ps. The problem has been solved by using the normal mode analysis. The thermal shock problem is studied to obtain the exact expressions for the displacement components, force stresses, temperature, couple stresses and microrotation. The distributions of the considered variables are illustrated graphically. Comparisons are made with the results predicted by both types of Green–Naghdi theory for different values of time.

Keywords Heat laser pulse Micropolar, Thermoelasticity, Energy dissipation, Normal mode
Indian Journal of Physics pp 1–9

Shear horizontal waves in composite materials: Behavior under rotation and initial stress

Abo-el-nour N. Abd-alla[1,2], Mohamed I. A. Othman[3,4], NF Hasbullah[5]
[1]Department of Mathematics, Faculty of Science, Jazan University, Jazan, Saudi Arabia
[2]Mathematical Department, Faculty of Science, Sohag University, 82524, Egypt
[3]Mathematical Department, Faculty of Science, Taif University, Taif, Saudi Arabia
[4]Department of Mathematics, Faculty of Science Zagazig University, Zagazig, Egypt
[5]Department of Electrical and Computer Engineering, International Islamic University Malaysia, Kuala Lumpur, 53100, Malaysia.

Abstract The main scope of this paper is to present in a simple and concise way a mathematical model of composite materials able to describe the propagation of shear horizontal waves in the case where composite is rotating and subjected to an initial stress. This work is aimed at the relevant possibility to apply the obtained results for the establishment of highachievement applications of piezoelectric and semiconductor composites and surface acoustic waves devices. We conclude by analyzing numerical computations in which the influence of the rotation, initial stress and electromagnetic boundary conditions are graphically observed.

Keywords Shear horizontal waves, composite materials, piezoelectric materials, semiconductors
Mathematics and Mechanics of Solids 2019, Vol. 24(1) 85–97

Analytical solutions of fractional bioheat model in a spherical tissue

Aatef Hobiny[1] and Ibrahim Abbas[1,2]
[1]Nonlinear Analysis and Applied Mathematics Research Group (NAAM), Department of Mathematics, King Abdulaziz University, Jeddah, Saudi Arabia
[2]Mathematical Department, Faculty of Science, Sohag University, 82524, Egypt

Abstract In this paper, the bio-heat model with fractional derivative is established to study the variations of temperature and the thermal damage in spherical tissues during thermal therapy. Easily, the exact solution in the domain of Laplace are obtained. The effects of a fractional parameter, the blood perfusion and the laser exposure time on the temperature of living tissue and the resulting of thermal damages are studied. The results display that bio-heat model with the fractional derivative is reduced to parabolic and the hyperbolic bio-heat models when the thermal relaxation time is equal to zero and the fractional parameter is equivalent to one respectively. The numerical outcomes of thermal damage and temperatures are graphically introduced.

Keywords: Spherical tissues, thermal damages, fractional derivative, Laplace transforms
Mechanics Based Design of Structures and Machines 2019, pp 1–10

A GN model on photothermal interactions in a two-dimensions semiconductor half space

Aatef Hobiny[1] and Ibrahim Abbas[1,2]
[1]Nonlinear Analysis and Applied Mathematics Research Group (NAAM), Department of Mathematics, King Abdulaziz University, Jeddah, Saudi Arabia
[2] Mathematical Department, Faculty of Science, Sohag University, 82524, Egypt

Abstract The model of coupled plasma and thermo-elastic wave were used to investigate the wave propagation in a two-dimensional semiconducting half space by using eigenvalues approach. By using Fourier and Laplace transformations with the eigenvalues techniques methodology, the exact solution of all physical quantities is obtained. The boundary edge of the plane is due to a heat flux with a pulse that decays exponentially and is taken as free of tractions. A semiconductor media such as silicon has been studied. The outcomes have been verified numerically and are represented graphically.

Keywords: Photo-thermal waves, Laplace-fourier transforms, Eigenvalues approach
Results in Physics 2019, Vol. 15, p. 102588

Photo-thermo-elastic interactions without energy dissipation in a semiconductor half-space

Faris S. Alzahrani [1] and Ibrahim Abbas[1,2]
[1]Nonlinear Analysis and Applied Mathematics Research Group (NAAM), Department of Mathematics, King Abdulaziz University, Jeddah, Saudi Arabia
[2] Mathematical Department, Faculty of Science, Sohag University, 82524, Egypt

Abstract The photo-thermo-elastic analysis problem of a half space without energy dissipation are obtained in the context of Green–Naghdi's (GNII) theory. Closed-form analytical solutions to obtain the physical quantities subjected to a heat flux using the pulse that decays exponentially in the surface of semiconductor half-space are presented. Through the use of Laplace and Fourier transforms with the methodology of eigenvalues techniques, the analytical solutions of all variables are presented. The derived method is evaluated with numerical results which are applied to the semiconductor medium in simplified geometry. Suitable discussions and conclusions are presented.

Keywords: Photo-thermo-elastic waves, Laplace-Fourier transforms, Eigenvalues approach, Green–Naghdi's (GNII) theory ,
Results in Physics 2019, Vol. 15, p. 102805

Analytical solutions of thermal damage in living tissues due to laser irradiation

Faris S. Alzahrani [1] and Ibrahim Abbas[1,2]
[1]Nonlinear Analysis and Applied Mathematics Research Group (NAAM), Department of Mathematics, King Abdulaziz University, Jeddah, Saudi Arabia
[2]Mathematical Department, Faculty of Science, Sohag University, 82524, Egypt

Abstract In this article, the analytical solutions of dual-phase-lag (DPL) bioheat equation with various boundary conditions have been constructed for curative therapy of cancerous cells. The volumetric thermal source components in the model of DPL bioheat transfer, such as the metabolic heat generation and the rate of blood perfusion, are considered. The analytical solutions in the Laplace domain are obtained. The thermal injuries to the tissue are assessed by the denatured protein range, using the formulation of Arrhenius. Numerical outcomes for temperatures are graphically introduced. A parametric analysis is devoted to the identification of an appropriate procedure for selecting important design variables in order to predict more accurate to reach effective heating in hyperthermia treatment.

Keywords: Bioheat transfer, living tissue, thermal damage, dual-phase-lag model
Waves in Random and Complex Media 2019, pp. 1-14

Analytical estimations of temperature in a living tissue generated by laser irradiation using experimental data

Faris S. Alzahrani [1] and Ibrahim Abbas[1, 2]
[1]Nonlinear Analysis and Applied Mathematics Research Group (NAAM), Department of Mathematics, King Abdulaziz University, Jeddah, Saudi Arabia
[2]Mathematical Department, Faculty of Science, Sohag University, 82524, Egypt

Abstract This paper presents an analytical approach associated with Laplace transformation, experimental temperature data, and a sequential concept over time to obtain the thermal damage and the temperature in a living tissue due to laser irradiation. The analytical solutions in the Laplace domain are appreciably obtainable. The thermal damage to the tissue is completely assessed by the denatured protein range using the formulation of Arrhenius. Numerical outcomes for temperatures and the thermal damages are graphically introduced. Besides, the comparison between the numerical computations and the existing experimental study shows that a current mathematical model is an effective tool for evaluating the biological heat transfer in biological tissues.

Keywords: Bioheat transfers, Living tissue, Thermal damage, Laplace transform
Journal of Thermal Biology, Volume 85, 2019, 102421

Global properties of latent virus dynamics with B-cell impairment

A. M. Elaiw[1], S. F. Alshehaiween [1,2] , Aatef Hobiny[1] and Ibrahim Abbas[1,3]
[1]Nonlinear Analysis and Applied Mathematics Research Group (NAAM), Department of Mathematics, King Abdulaziz University, Jeddah, Saudi Arabia
[2]Department of Mathematics, Faculty of Science, Taibah University, P.O. Box 344, Medina 42353, Saudi Arabia
[3]Mathematical Department, Faculty of Science, Sohag University, 82524, Egypt

Abstract In this paper we construct virus dynamics models with impairment of B-cell functions. Two different forms of the incidence rate have been considered, bilinear and general. The latently infected cells have been incorporated into the models. The well-posedness of the models is justified. The models admits two equilibria which are determined by the basic reproduction number R0. The global stability of each equilibrium is proven by utilizing Lyapunov function and LaSalle's invariance principle. The theoretical results are illustrated by numerical simulations.

Keywords: Bioheat transfers, Living tissue, Thermal damage, Laplace transform
AIP Advances (2019) 9(9), 095035

An analytical solution of the bioheat model in a spherical tissue due to laser irradiation

Ibrahim Abbas[1,2] , Aatef Hobiny[1] and Faris S. Alzahrani [1]
[1]Nonlinear Analysis and Applied Mathematics Research Group (NAAM), Department of Mathematics, King Abdulaziz University, Jeddah, Saudi Arabia
[2]Mathematical Department, Faculty of Science, Sohag University, 82524, Egypt

Abstract This article studies an analytical approach associated with Laplace transform, experimental temperature data and a sequential concept over time to obtain the thermal damage and the temperature in living tissue due to laser irradiation. The effects of blood perfusion and the thermal relaxation time on the temperature of skin tissues and the resulting of thermal damage are investigated. The resulting of thermal damage to the tissue is assessed by the denatured protein range using the formulation of Arrhenius. The outcomes show that the hyperbolic bioheat model is reduced to the parabolic bioheat model when the relaxation time is close to zero. The numerical outcomes of thermal injuries and temperatures are graphically introduced. In conclusion, the comparison between the numerical computations and the existing experimental study displays that a current mathematical model is an effective tool for evaluating the biological heat transfer in biological tissues.

Keywords: Skin tissues, Thermal damages, Laser irradiation, Laplace transforms
Indian Journal of Physics (2019) pp 1–6

Two-Temperature Photothermal Interactions in a Semiconducting Material with a 3D Spherical Cavity

Aatef Hobiny[1] and Ibrahim Abbas[1,2]
[1]Nonlinear Analysis and Applied Mathematics Research Group (NAAM), Department of Mathematics, King Abdulaziz University, Jeddah, Saudi Arabia
[2]Mathematical Department, Faculty of Science, Sohag University, 82524, Egypt

Abstract In this paper, a two-temperatures photothermoelastic interactions in an infinite semiconductor medium with a spherical cavity were studied using mathematical methods. The cavity internal surface is traction free and the carrier density is photogenerated by boundary heat flux with an exponentially decaying pulse. Laplace transform techniques are used to obtain the exact solution of the problem in the transformed domain by the eigenvalue approach and the inversion of Laplace transforms has been carried numerically. Numerical computations have been also performed for a silicon-like semiconductor material.

Keywords: semiconductor material, two-temperatures , Laplace transforms, Spherical Cavity
Physical Mesomechanics (2019) volume 22, pages327–332

Fractional Order Thermoelastic Wave Assessment in a Nanoscale Beam Using the Eigenvalue Technique

Ibrahim Abbas[1,2] , Faris S. Alzahrani [2], Abo-el-nour N. Abd-alla[1], F. Berto[3]

[1]Mathematical Department, Faculty of Science, Sohag University, 82524, Egypt

[2]Nonlinear Analysis and Applied Mathematics Research Group (NAAM), Department of Mathematics, King Abdulaziz University, Jeddah, Saudi Arabia

[3]Department of Engineering Design and MaterialsNorwegian University of Science and Technology (NTNU), Trondheim, Norway

Abstract This paper presents an analytical approach associated with Laplace transforms and a sequential concept over time to obtain the increment of temperature in nanoscale beam with fractional order heat conduction clamped from both ends. The governing equations are written in the forms of differential equations of matrix-vector in the domain of the Laplace transforms and are then solved by the eigenvalue technique. The analytical solutions are obtained for the increment of temperature, displacement, lateral deflection, and stresses in the Laplace domain. Numerical simulations are provided for silicon-like nanoscale beam material, with graphical display of calculated results. The physical implications of distributions of physical variables considered in this article are discussed.

Keywords: Laplace transforms, nanoscale beam, fractional order, eigenvalues approach

Strength of Materials (2019), Volume 51, Issue 3, pp 427–438

An analytical study on the fractional transient heating within the skin tissue during the thermal therapy

Abdeljabbar Ghanmi [1],Ibrahim Abbas[2,3]

[1]Department of Mathematics, Faculty of Science, University of Jeddah, Jeddah, Saudi Arabia

[2]Mathematical Department, Faculty of Science, Sohag University, 82524, Egypt

[3]Nonlinear Analysis and Applied Mathematics Research Group (NAAM), Department of Mathematics, King Abdulaziz University, Jeddah, Saudi Arabia

Abstract In the present paper, the bioheat equation under fractional derivatives is used to study the thermal damage within the skin tissue during the thermal therapy. Basically, the analytical solutions in the Laplace domain are easily obtainable. The influences of the fractional derivative and moving heat source velocity on the temperature of skin tissues and the thermal injuries are precisely investigated. The outcomes show that the fractional bioheat model are reduced to the hyperbolic and parabolic bioheat models when the fractional order parameter is equal to one and the relaxation time is close to zero respectively. The thermal injuries to the tissue are assessed by the denatured protein range using the formulation of Arrhenius. The numerical outcomes of thermal injuries and temperatures are graphically introduced. In conclusion, a parametric analysis is devoted to the identification of an appropriate procedure for selecting important design variables to reach effective heating in hyperthermia treatment.

Keywords: Skin tissue, Thermal damage, Bioheat equation, Laplace transform, Fractional derivative

Journal of Thermal Biology Volume 82, May 2019, Pages 229-233

Solutions of Some Difference Equations Systems and Periodicity

Elsayed M Elsayed[1,2], Faris S. Alzahrani [1], Ibrahim Abbas[1], NH Alotaibi[1]

[1]Nonlinear Analysis and Applied Mathematics Research Group (NAAM), Department of Mathematics, King Abdulaziz University, Jeddah, Saudi Arabia

[2]Department of Mathematics, Faculty of Science, Mansoura University, Mansoura 35516, Egypt.

Abstract In this article, analysis and investigation have been conducted on the periodic nature as well as the type of the solutions of the subsequent schemes of rational difference equations

$x_{n+1}=\frac{1\pm z_n}{y_{n-1}}, y_{n+1}=\frac{1\pm x_n}{z_{n-1}}, z_{n+1}=\frac{1\pm y_n}{x_{n-1}}$

with a nonzero real numbers initial conditions.

Keywords: difference equation, periodic solutions, system of difference equations.
Journal of Advances in Mathematics Vol 16 (2019) ISSN: 2347-1921

Dynamical Behavior and Solution of Nonlinear Difference Equation Via Fibonacci Sequence

Elsayed M Elsayed[1,2], Faris S. Alzahrani[1], Ibrahim Abbas[1], NH Alotaibi[1]

[1]Nonlinear Analysis and Applied Mathematics Research Group (NAAM), Department of Mathematics, King Abdulaziz University, Jeddah, Saudi Arabia

[2]Department of Mathematics, Faculty of Science, Mansoura University, Mansoura 35516, Egypt.

Abstract In this paper we study the behavior of the difference equation x_{n+1}=ax_{n}+((bx_{n}x_{n-1})/(cx_{n-1}+dx_{n-2})),n=0,1, where the initial conditions are arbitrary positive real numbers and a,b,c,d are positive constants. Also, we give the solution of some special cases of this equation.

Keywords: stability, boundedness, solution of difference equations.
Journal of Applied Analysis and Computation (1) (2019)

Fractional Order GN Model on Photo-Thermal Interaction in a Semiconductor Plane

Aatef Hobiny[1] and Ibrahim Abbas[1,2]
[1]Nonlinear Analysis and Applied Mathematics Research Group (NAAM), Department of Mathematics, King Abdulaziz University, Jeddah, Saudi Arabia
[2] Mathematical Department, Faculty of Science, Sohag University, 82524, Egypt

Abstract A mathematical model of Green–Naghdi photothermal theory based on fractional-order of heat transfer is given to study the wave propagation in a two-dimensional semiconductor material. Closed-form analytical solutions to obtain the physical quantities subjected to a heat flux with a pulse that decays exponentially in the surface of semiconductor half-space are presented. Through the use of Laplace and Fourier transforms with the methodology of eigenvalues techniques, the analytical solutions of all physical quantities are obtained. A semiconductor medium such as silicon is studied. The derived method is evaluated with numerical results which are applied to the semiconductor medium in simplified geometry. The significant influence of time-fractional derivative parameters are discussed for all physical quantities. Suitable discussions and conclusions are presented.

Keywords: Laplace-Fourier transforms, Fractional GN model, Photo-thermal waves, Eigenvalues approach
Silicon (2019) pp1-8

Модель двухфазного сдвига фототермоупругих волн в двумерной полупроводниковой среде

Aatef Hobiny[1] and Ibrahim Abbas[1,2]
[1]Nonlinear Analysis and Applied Mathematics Research Group (NAAM), Department of Mathematics, King Abdulaziz University, Jeddah, Saudi Arabia
[2]Mathematical Department, Faculty of Science, Sohag University, 82524, Egypt

Abstract В статье с использованием обобщенной модели фототермической волны и модели двухфазного запаздывания проведены расчеты приращения температуры, компонент смещения, плотности носителей и компонент напряжений в двумерных полупроводниковых средах. С помощью преобразований Фурье и Лапласа в рамках подхода к определению собственных значений получены точные решения для всех физических величин. Исследование полупроводниковой среды проведено на примере кремния. С использованием полученных результатов проиллюстрирована разница между моделями динамической связи, Лорда–Шульмана и двухфазного сдвига.

Keywords: photothermal waves / dual phase lag model / eigenvalues approach
Физическая мезомеханика (22) 2 (2019) pp105-112

Analysis of photo-thermo-elastic response in a semiconductor media due to moving heat source

Faris S. Alzahrani [1] and Ibrahim Abbas[1, 2]
[1]Nonlinear Analysis and Applied Mathematics Research Group (NAAM), Department of Mathematics, King Abdulaziz University, Jeddah, Saudi Arabia
[2] Mathematical Department, Faculty of Science, Sohag University, 82524, Egypt

Abstract A mathematical model of Green-Naghdi photothermal theory is given to study the wave propagation in a two-dimensional semiconducting material due to moving heat source. By using the Fourier and Laplace transformations with the eigenvalues method, the physical quantities are obtained analytically. Initially, it is assumed that the medium is at rest and it is subject to a heat source in motion with a constant velocity, which is free of traction. A semiconductor media such as silicon has been studied. The derived method is evaluated with numerical results which are applied to the semiconductor medium in simplified geometry. The influences of the different values of moving heat source speed are discussed for all physical quantities.

Keywords: green-naghdi model / laplace-fourier transforms / photothermal waves / eigenvalues approach
Физическая мезомеханика (22) 5 (2019) pp105-112

Eigenvalue approach for generalized thermoelastic porous medium under the effect of thermal loading due to a laser pulse in DPL model

Mohamed IA Othman [1] and Ibrahim Abbas[2,3]
[1]Department of Mathematics, Faculty of Science Zagazig University, Zagazig, Egypt
[2]Nonlinear Analysis and Applied Mathematics Research Group (NAAM), Department of Mathematics, King Abdulaziz University, Jeddah, Saudi Arabia
[3] Mathematical Department, Faculty of Science, Sohag University, 82524, Egypt

Abstract The aim of the present study is concerned with the thermal loading due to laser pulse on thermoelastic porous medium under dual-phase-lag model DPL. The material is a homogeneous isotropic elastic half-space and heated by a non-Gaussian laser beam with the pulse duration of 8 ps. Eigenvalue approach is proposed to analyze the problem and obtain the analytical solutions of the displacement components, stresses, temperature distribution and change in the volume fraction field. The results of the physical quantities have been illustrated graphically by the comparison between the coupled theory, DPL model and Lord–Shulman theory of the certain value of time and distance. The results presented in this article should prove useful for researchers in material science (porous media), designers of new materials, physicists as well as for those working on the development of heat laser pulse practical situations as in geophysics, optics, acoustics and geomagnetic.

Keywords: Generalized thermoelastic, Laser pulse, Porous medium, DPL model, Eigenvalue approach
Indian Journal of Physics (2019) volume 93, pages1567–1578

A DPL model of photothermal interaction in a semiconductor material

Ibrahim Abbas[1,2] , Faris S. Alzahrani [2], Ahmed Elaiw[2]
[1] Mathematical Department, Faculty of Science, Sohag University, 82524, Egypt
[2]Nonlinear Analysis and Applied Mathematics Research Group (NAAM), Department of Mathematics, King Abdulaziz University, Jeddah, Saudi Arabia

Abstract The generalized model for plasma, thermal, and elastic waves under dual phase lag model have been applied to determine the carrier density, the displacement, the temperature, and the stresses in a semiconductor medium. Using Laplace transform and the eigenvalue approach methodology, the solutions of all variables have been obtained analytically. A semiconducting material like as silicon was considered. The results were graphically represented to show the different between the dual phase model, Lord and Shulman's theory and the classical dynamical coupled theory.
WAVES IN RANDOM AND COMPLEX MEDIA 2019, VOL. 29, NO. 2, 328–343

The Matrix of Matrices Exponential and Application

Z. Kishka[1], M. Saleem[1], A. Elrawy[2]
[1]Mathematical Department, Faculty of Science, Sohag University, 82524, Egypt
[2]Mathematical Department, Faculty of Science, South Valley University, Qena, Egypt

Abstract In this paper, we introduce a definition of an exponential function in the sense of the matrix of matrices (for short, MMs). After defining the eigenvalue and the eigenvector of MMs, we solve the system of a homogeneous linear matrix of first-order differential equations whose coefficients are constant matrices. Existence and uniqueness of a solution have been proven for that system. Finally, some examples are established.
Keywords: Matrix of matrices, Exponential function, System of a homogeneous linear matrix of first-order differential equations
International Journal of Mathematical Analysis Vol. 13, 2019, no. 2, 81 - 97

Quantum Fisher information of atomic system interacting with a single cavity mode in the presence of Kerr medium

N. Zidan[1,2], H. F. Abdel-Hameed[1,3], N. Metwally[4,5]
[1] Mathematical Department, Faculty of Science, Sohag University, 82524, Egypt
[2] Mathematics Department, College of Science, Jouf University, Sakaka, Saudi Arabia
[3]Mathematics Department, Khurma University College, Taif University, Al-Taif, Saudi Arabia
[4]Mathematics Department, College of Science, Bahrain University, Zallaq, Bahrain
[5]Mathematics Department, Faculty of Science, Aswan University, Aswan, Egypt

Abstract The quantum Fisher information of an atomic system interacting with a single cavity mode in the presence of Kerr medium is discussed. It is shown that quantum Fisher information for an initial separable atomic system is larger than that depicted for the initial entangled atomic system. For initial vacuum state of the cavity mode, the quantum Fisher information with respect to the Kerr medium and the phase decoherence parameter is larger than that displayed for the detuning parameter. Both phase decoherence and Kerr medium have the same efect on the decay of quantum Fisher information, while they have an opposite efect on its maximum values.

Scientific Reports | (2019) 9:2699

Dynamics of the entanglement and teleportation of thermal state of a spin chain with multiple interactions

Ahmad Redwan[1], Abdel-Haleem Abdel-Aty[3,4], Nour Zidan[1,2], Tarek El-Shahat
[1]Mathematical Department, Faculty of Science, Sohag University, 82524, Egypt
[2]Mathematics Department, College of Science, Jouf University, Sakaka, Saudi Arabia
[3]Department of Physics, College of Sciences, University of Bisha, Bisha 61922, P.O. Box 344, Saudi Arabia
[4]Physics Department, Faculty of Science, Al-Azhar University, 71524 Assiut, Egypt

Abstract We investigate the effect of Calogero-Moser (CM) type interactions on the thermal entanglement and teleportation in an anisotropic two-qubit Heisenberg XYZ system with Dzyaloshinskii-Moriya (D z) interaction in the presence of the external magnetic field. In this regard, the system is designed and analytically solved. The final state density of the system is obtained, and the impact of the system parameters is investigated. The negativity is used to quantify the entanglement dynamics over the system. The generated entangled channels are examined to exchange the information between the system qubits using the standard teleportation protocol; then, the fidelity of the transmitted information is quantified. The effect of the system parameters (Dzyaloshinskii-Moriya, Spin-orbit coupling, CM type interaction, and magnetic field) in the dynamics of the entanglement and state transfer is investigated

Chaos: An Interdisciplinary Journal of Nonlinear Science 29 (2019) pp. 013138

Entanglement, photon statistics and Wehrl entropy for a time-dependent qubit–field system in the presence of phase decoherence effect

S. Abdel-Khalek[1,2,3]
[1]Mathematical Department, Faculty of Science, Sohag University, 82524, Egypt
[2]Mathematics Department, Faculty of Science, Taif University, Taif, Saudi Arabia
[3]The Abdus Salam International Centre for Theoretical Physics, Strada Costiera 11, Miramare, Trieste, Italy

Abstract We investigate We investigate the effect of qubit motion in terms of speed and acceleration on the variation in dynamic behavior of Wehrl entropy, second order correlation function and qubit–field entanglement. We consider three different coherent states of low-power potential (CSLPP) through the value of its exponent, specifically, the infinite-square, triangular, and harmonic potential wells. The relationship between the photon statistics quantified by the second order correlation function and nonclassical correlation of the qubit–field system is explored as the system evolves. The results show that the proposed scheme is very sensitive to the value of the exponent for both a moving and a stationary qubit. A high correlation between the qubit and CSLPP field is achieved by a proper choice of exponent, qubit speed, and acceleration.

Keywords: Coherent states of low-power potential, Nonclassical correlation, Qubit speed, Entanglement, Wehrl entropy
Optik 10 December 2019, 163579

Quantum correlation and non-classical properties in semiconductor microcavities for multi-photon excitation

S. Abdel-Khalek[1,2,] K. Berrada3 and H. Eleuch[4,5]
[1]Mathematical Department, Faculty of Science, Sohag University, 82524, Egypt
[2]Mathematics Department, Faculty of Science, Taif University, Taif, Saudi Arabia
[3]Department of Physics, College of Science, Imam Mohammad Ibn Saud Islamic University (IMSIU), Riyadh, Saudi Arabia
[4]Institute for Quantum Science and Engineering, Texas AM University, College Station, Texas 77843, USA
[5]Department of Applied Sciences and Mathematics, College of Arts and Sciences, Abu Dhabi University, Abu Dhabi, UAE

Abstract We study how the interplay of weak excitation regime of quantum well confined in a semiconductor microcavity affects the dynamics of correlations and the statistical properties of photons. We discuss how the system parameters can impact the quantum entropy and Mandel's parameter, and illustrate our concerns with numerical simulations. We have found that the enhancement of the correlations and the control of the statistical properties of photons in semiconductor microcavities for multi-photon excitation highly benefits from the combination of the strength of the field, excitonic spontaneous emission rate, cavity dissipative rate, and the coupling between the exciton and photons. Our results may have important implications not only for those specially interested in quantum optics and information, but also for the general physics community.

Keywords: Coherent Semiconductor microcavities, four-photon excitation, correlations, statistical properties
International Journal of Quantum Information Vol. 17, No. 05, 1950047 (2019)

Optical tomography for excited coherent states associated to deformed oscillators

Abdullah M.Almarashi[1], Ali Algarni[1], Fahad M.Alaboud[1], S.Abdel-Khalek [2,3], K.Berrada[4]
[1]Statistics Department, Faculty of Science, King Abdulaziz University, Jeddah, Saudi Arabia
[2]Mathematical Department, Faculty of Science, Sohag University, 82524, Egypt
[3]Mathematics Department, Faculty of Science, Taif University, Taif, Saudi Arabia
[4]Department of Physics, College of Science, Imam Mohammad Ibn Saud Islamic University (IMSIU), Riyadh, Saudi Arabia

Abstract In this manuscript, we study the deformed optical tomography for excited coherent states associated to deformed Heisenberg algebra. By using the numerical solution of the recurrence relation, we evaluate the eigenstates of the deformed quadrature operator and give the exact analytical formula of the optical tomogram for the photon-added deformed coherent states (PA-DCSs) and photon-added deformed cat coherent states (PA-DCCSs). Finally, we display the variation of the excited coherent states in the terms of the different physical parameters defined in the coherent states and show how these parameters affect the shape of the optimal tomography.

Results in Physics Volume 14, September 2019, 102352

Interaction between two two-level atoms coupled to N-level quantum system

A.-S. F. Obada[1], Abdullah F. Al Naim[2], E. M. Khalil[1,3], S. Abdel-Khalek[3,4], H. Eleuch[5,6]
[1]Mathematics Department, Faculty of Science, Al-Azhar University, Nasr City, Cairo, 11884, Egypt
[2]Physics Department, King Faisal University, Alhasa, Hofuf, Saudi Arabia
[3] Mathematics Department, Faculty of Science, Taif University, Taif, Saudi Arabia
[4] Mathematics Department, Faculty of Science, Sohag University, Sohag, Egypt
[5]Department of Applied Science and Mathematics, College of Arts and Sciences, Abu Dhabi University, Abu Dhabi, UAE
[6]Institute for Quantum Science and Engineering, Texas A&M University, College Station, TX, 77843, USA

Abstract In this The interaction between two two-level atoms and N-level atoms (su(2) quantum system) in the non-resonance is investigated. The explicit mathematical form for the wave function is obtained. Statistical aspects, the population inversion, linear entropy, correlation function and the negativity are discussed. The influence of the number of levels and the detuning parameter on the population and atom–atom entanglement are studied. The results are shown that the entanglement depends crucially on the detuning.

Optical and Quantum Electronics volume 51, Article number: 259 (2019)

Quantum Fisher Information And Tomographic Entropy Of A Single Qubit In Excited Binomial And Negative Binomial Distributions

Abdullah M. Almarashi[1], Ali Algarni[1], S. Abdel-Khalek[2,3] and Hon Keung Tony Ng[4]
[1]Statistics Department, Faculty of Science King Abdulaziz University Jeddah, Saudi Arabia
[2]Mathematics Department, Faculty of Science, Sohag University, Sohag, Egypt
[3] Mathematics Department, Faculty of Science, Taif University, Taif, Saudi Arabia
[4]Department of Statistical Science Southern Methodist University Dallas, Texas, USA

Abstract We model the interaction between a qubit and optical radiation field (ORF) using an excited binomial distribution (EBD) and excited negative binomial distribution (ENBD). The explicit form of the density matrix of the qubit–ORF system is given in terms of the photon number distribution. The Mandel parameter is used to quantify the statistical properties of the ORF during the interaction. We derive the relation between the tomographic entropy and the quantum Fisher information of the estimators of model parameters in the EBD and ENBD. We also explore the properties and dynamics of these statistical quantities

Keywords: excited negative binomial distribution, Mandel parameter, quantum Fisher information, tomographic entropy
Journal of Russian Laser Research, Volume 40, Number 4, July, 2019

Entanglement and physical attributes of the interaction between two SC-qubits and thermal field in the presence of a magnetic field

Abdullah F.AlNaim[1], Javed Y.Khan[1], S.Abdel-Khalek[2,3], E.M.Khalil[3,4]
[1]Physics Department, King Faisal University, Alhasa, Hofuf, Saudi Arabia
[2]Mathematics Department, Faculty of Science, Sohag University, Sohag, Egypt
[3]Mathematics Department, Faculty of Science, Taif University, Taif, Saudi Arabia
[4]Mathematics Department, Faculty of Science, Al-Azher University, Cairo, Egypt

Abstract The interaction between two superconducting (SC) qubits and thermal field in the presence of a magnetic field, the qubit–qubit interaction and the Stark interaction are investigated. The wave function, and hence density matrix, that describe this system is obtained and the behavior of physical quantities that characterize it are evaluated. In particular, the von Neumann entropy and quantum concurrence as a measure of entanglement between parts of the system are discussed in detail. The effects of thermal and low temperature on the dynamical properties of the von Neumann entropy and nonclassical correlation are discussed. Also, the influences of the atomic coherence and magnetic field on the statistical properties of the physical quantities are examined. Moreover, some important physical phenomena during the time evolution of the interaction between the two SC-qubits, thermal field, and magnetic field are explored. The nonclassical correlation between the thermal field and the two SC-qubits is enhanced by increasing temperature whereas the SC qubit–qubit entanglement decreases. The magnetic field and Stark shifts play a central role in the dynamical and physical attributes of the two types of entanglement.

Keywords: Superconducting qubits, Entanglement, Thermal and magnetic field, Nonclassical properties
Microelectronics Journal Volume 86, April 2019, Pages 15-21

Nonclassical properties and field entropy squeezing of the dissipative two-photon JCM under Kerr like medium based on dispersive approximation

Haifa S.Alqannas[1,2], S.Abdel-Khalek[3,4]
[1]Physics Department, Faculty of Science, King Abdulaziz University, Jeddah, Saudi Arabia
[2]Physics Department, Faculty of Science, University of Jeddah, Jeddah, Saudi Arabia
[3]Mathematics Department, Faculty of Science, Sohag University, Sohag, Egypt
[4]Mathematics Department, Faculty of Science, Taif University, Taif, Saudi Arabia

Abstract The quantum state of a two-level atom and coherent field in Kerr medium under cavity damping effect is evaluated. The field density matrix of the system is given based on the dispersive approximation. The dynamical properties of Mandel parameter as a quantifier of the nonclassical properties for a radiation field during the interaction time are studied. The position and momentum components of entropy squeezing under Kerr like medium within dispersive approximation are investigated. The effect of initial field state consideration, Kerr medium, Stark shift terms and parameter of cavity damping on the time evolution of different quantities are examined. The results show that the entropy squeezing and non-classical properties are very sensitive to the Kerr medium and initial state of the field. The proposed system resists the damping when the field initially in statistical mixture of coherent state that the coherent state itself.

Keywords: Dispersive approximation, Jaynes-Cummings model, Kerr like medium, Field entropy squeezing, Mandel parameter, Cavity damping
Optics & Laser Technology Volume 111, April 2019, Pages 523-529

Entanglement, nonclassical properties, and geometric phase in circuit quantum electrodynamics with relativistic motion

S.Abdel-Khalek [1,2], K.Berrada[3,4]
[1]Mathematical Department, Faculty of Science, Sohag University, 82524, Egypt
[2]Mathematics Department, Faculty of Science, Taif University, Taif, Saudi Arabia
[3]Department of Physics, College of Science, Imam Mohammad Ibn Saud Islamic University (IMSIU), Riyadh, Saudi Arabia
[4]The Abdus Salam International Centre for Theoretical Physics, Strada Costiera 11, Miramare-Trieste, Italy

Abstract In this work, we study qualitatively the nonclassical properties, nonlocal correlation, and geometric phase in a superconducting qubit system connected to a transmission line resonator (TLR) within a circuit quantum electrodynamics setup, where the modulation of the coupling strength can imitate the harmonic motion of the superconducting system at relativistic speeds. We analyze the effects of the relativistic motion on these quantum quantifiers under the influence of the physical parameters implicated in the whole quantum system state. Furthermore, the relationship between the different quantifiers is explored. Our results may open new perspectives to understand and explore the relativistic phenomena on the comportment of the quantum quantifiers for new applications in superconducting quantum technologies.

Keywords: Solid state systems, Superconducting qubit system, Transmission line resonator, Circuit quantum electrodynamics, Nonclassical properties and correlation
Solid State Communications Volume 290, March 2019, Pages 31-36

Physical and nonclassical properties of the interaction between a four-level atom and field in coherent state of Morse potential

Haifa S.Alqannas[1,2], S.Abdel-Khalek[3,4]

[1]Physics Department, Faculty of Science, King Abdulaziz University, Jeddah, Saudi Arabia
[2]Physics Department, Faculty of Science, University of Jeddah, Jeddah, Saudi Arabia
[3]Mathematics Department, Faculty of Science, Sohag University, Sohag, Egypt
[4]Mathematics Department, Faculty of Science, Taif University, Taif, Saudi Arabia

Abstract The quantum system of the field initially defined by the k-photon-added Morse potential coherent states (MPCSs) of the radiation field interacting with a four-level atom (FLA) was studied. The physical and non-classical properties of the field defined by the MPCS system were quantified using the Mandel parameter. The effect of time-dependent coupling (TDC) on the atomic speed was examined. Moreover, the dynamic properties of the non-local correlation between the FLA and MPCS radiation field were studied and compared with those of the geometric phase. We also investigated the influence of the initial interaction conditions and different system parameters on the evolution of the non-local correlation, Mandel parameter, and geometric phase. The relationships between the geometric phase, Mandel parameter, and non-local correlation with TDC were explored.

Keywords: Mandel parameter · Geometric phase · Morse potential coherent states · Entanglement
Optical and Quantum Electronics volume 51, Article number: 50 (2019)

Effects of Kerr Medium and Stark Shift Parameter on Wehrl Entropy and the Field Purity for Two-Photon Jaynes–Cummings Model Under Dispersive Approximation

Abdullah F.AlNaim[1], Javed Y.Khan[1], S.Abdel-Khalek[2,3], E.M.Khalil[3,4]

[1]Physics Department, King Faisal University, Alhasa, Hofuf, Saudi Arabia
[2]Mathematics Department, Faculty of Science, Sohag University, Sohag, Egypt
[3]Mathematics Department, Faculty of Science, Taif University, Taif, Saudi Arabia
[4]Mathematics Department, Faculty of Science, Al-Azher University, Cairo, Egypt

Abstract We estimate the quantum state of a two-level atom and the coherent field in a Kerr medium subject to the cavity damping. The density matrix of the field is considered within the framework of the dispersive approximation. We study dynamical properties of the linear entropy, Wehrl entropy, and the Wehrl phase density during the time of interaction. The effects of the Kerr medium and cavity damping on the time evolution of different quantities are examined. The results refer to the sensitivity of these aspects to changes either in the decay parameter or in the Kerr-like medium and Stark-shift parameters. Linear entropy and nonclassical properties of the field quantified by the Wehrl entropy are also very sensitive to the Kerr medium and Stark-shift parameter.

Keywords: Dispersive approximation, Jaynes–Cummings model, Kerr-like medium, linear entropy, Wehrl entropy, cavity damping.
Journal of Russian Laser Research volume 40, pages20–29(2019)

Some features of the geometric phase and entanglement of three-level atom under cavity damping effects

S Abdel-Khalek[1,2], Y S El-Saman[3] , I Mechai[3] and M Abdel-Aty[1,4]
[1]Mathematics Department, Faculty of Science, Sohag University, Sohag, Egypt
[2]Mathematics Department, Faculty of Science, Taif University, Taif, Saudi Arabia
[3]Department of Mathematics, Faculty of Science, Jazan University, Jazan, Saudi Arabia
[4]Institute of Basic and Applied Sciences, Egypt-Japan University, E-JUST, Alexandria, Egypt

Abstract In this manuscript, we present a system consisting of a three-level atom interacting with optical field. We investigate qualitatively the entanglement and atomic (field) geometric phase under the effect of cavity damping. The atom–field entanglement is measured by the negativity. We show that these quantifiers depend strongly on the variations of the initial settings of the atom, and this exhibits substantial phenomena that depend on the cavity damping effect. Finally, we explore the link between the entanglement and atomic (field) geometric phase of different physical parameters within the presence and absence of the cavity damping effect.

Keywords: Entanglement; Geometric phase; Cavity damping; Negativity
Indian Journal of Physics (2019)

Some features of the nonlocal correlation and geometric phase of the quantum system in two-mode nondegenerate entangled states

S Abdel-Khalek[1,2], Sadah A. Alkhateeb[3,4]
[1]Mathematics Department, Faculty of Science, Sohag University, Sohag, Egypt
[2]Mathematics Department, Faculty of Science, Taif University, Taif, Saudi Arabia
[3]Mathematics Department, Faculty of ScienceKing Abdulaziz UniversityJeddahSaudi Arabia
[4]Mathematics Department, Faculty of ScienceUniversity of JeddahJeddahSaudi Arabia

Abstract We propose a quantum two-level system interacting with a two-mode nondegenerate entangled states (TMNESs). The dynamical properties of entropy squeezing component is investigated based on atomic density matrix in the absence and presence of classical field effect. Moreover, the dynamical properties of the nonlocal correlation between the atom and TMNESs are studied and compared with geometric phase. We examine the influence of the initial interaction conditions and classical field on the evolution of nonlocal correlation, linear entropy and geometric phase. Furthermore, we discuss the link between the geometric phase, field purity and nonlocal correlation during the time dynamics. Finally, the results clarified that a geometric phase and entanglement are strongly affected by the classical field and detuning parameter.

Keywords: Geometric phase Entropy squeezing Non-degenerate entangled state Field purity Entanglement
Journal of Mathematical Chemistry(2019) pp 1–11

Computing special smarandache curves according to darboux frame in euclidean 4-space

M. Khalifa Saad [1,2], M. A. Abd-Rabo[3]
[1]Department of Mathematics, Faculty of Science, Islamic University of Madinah, 170 Madinah, KSA
[2]Department of Mathematics, Faculty of Science, Sohag University, 82524 Sohag, Egypt
[3]School of Mathematics and Statistics, Zhengzhou University, 450001 Zhengzhou,

Abstract: In this paper, we study some special Smarandache curves and their differential geometric properties according to Darboux frame in Euclidean 4-space E^4. Also, we compute some of these curves which lie fully on a hypersurface in E^4. Moreover, we defray some computational examples in support our main results.

Keywords: and phrases. Smarandache curves; hypersurfaces; Darboux frame; Euclidean 4-space
International Journal of Analysis and Applications Volume 17, Number 4 (2019), 479-502

Estimation of Generalized Inverted Exponential Distribution based on Adaptive Type-II Progressive Censoring Data

Ahmed A. Soliman, Essam. A. Ahmed, Al-Wageh A. Farghal and Abdulgalil A. AL-Shibany
Department of Mathematics, Faculty of Science, Sohag University, Egypt

Abstract: In this paper, we consider generalized inverted exponential (GIE) model. Three issues represent the purpose of this paper. First, based on adaptive progressively Type-II censored data, we derive the maximum likelihood estimators (MLE) of the model parameters as well as the reliability and hazard rate functions. Next, the Bayes estimates are evaluated by applying Markov chain Monte Carlo method under the balanced squared error (BSEL) loss function and balanced linear exponential (BLINEX) loss function. Based on the asymptotic distributions of the MLEs and MCMC samples, we compute asymptotic confidence interval and symmetric credible interval along with the coverage probability. We analyze a real data set to illustrate the results derived. Simulation studies are conducted to compare the performances of the Bayes estimators with the maximum likelihood estimators. Finally, a numerical example is presented to illustrate the methods developed here.

Keywords: Generalized inverted exponential distribution; Adaptive type-II progressive censoring data ; Maximum likelihood estimation, Bayesian estimations; Markov chain Monte Carlo.
Journal of Statistics Applications & Probability, Pro. 7, 1-16 (2019)

A new chaotic system with line of equilibria: dynamics, passive control and circuit design

Aceng Sambas[1] , Mustafa Mamat[2] , Ayman Ali Arafa[3] Gamal M Mahmoud[4] , Mohamad Afendee Mohamed[5] , W. S. Mada Sanjaya[6]

[1]Department of Mechanical Engineering, Universitas Muhammadiyah Tasikmalaya, Indonesia
[2,5] Faculty of Informatics and Computing, Universiti Sultan Zainal Abidin, Kuala Terengganu, Malaysia
[3]Department of Mathematics, Faculty of Science, Sohag University, Egypt [4]Department of Mathematics, Faculty of Science, Assiut University, Egypt [6]Department of Physics, Universitas Islam Negeri Sunan Gunung Djati Bandung, Indonesia

Abstract: A new chaotic system with line equilibrium is introduced in this paper. This system consists of five terms with two transcendental nonlinearities and two quadratic nonlinearities. Various tools of dynamical system such as phase portraits, Lyapunov exponents, Kaplan-Yorke dimension, bifurcation diagram and Poincarè map are used. It is interesting that this system has a line of fixed points and can display chaotic attractors. Next, this paper discusses control using passive control method. One example is given to insure the theoretical analysis. Finally, for the new chaotic system, an electronic circuit for realizing the chaotic system has been implemented. The numerical simulation by using MATLAB 2010 and implementation of circuit simulations by using MultiSIM 10.0 have been performed in this study.

Keywords: Chaotic system Dynamical system Electronic circuit Line equilibrium Passive control

International Journal of Electrical and Computer Engineering (IJECE) Vol. 9, No. 4, August 2019, pp. 2365~2376

Thermomechanical response in a two-dimension porous medium subjected to thermal loading

Tareq Saeed[1], Ibrahim Abbas[2]

[1]Department of Mathematics, King Abdulaziz University Faculty of Sciences, Jeddah, Saudi Arabia,
[2]Mathematics Department, Faculty of Science, Sohag University, Egypt and Nonlinear Analysis and Applied Mathematics Research Group (NAAM), Mathematics Department, King Abdulaziz University, Jeddah, SA

Abstract: The purposes of this study, a mathematical model of generalized thermoelastic theory subjected to thermal loading is presented to study the wave propagation in a two-dimensional porous medium.

Keywords: Porous medium, Eigenvalues approach, Generalized thermoelastic theory, Laplace– Fourier transforms.

International Journal of Numerical Methods for Heat & Fluid Flow

Thermal response of cylindrical tissue induced by laser irradiation with experimental study

Aatef Hobiny[1] and Ibrahim Abbas[2]

[1]Department of Mathematics, Faculty of Sciences, King Abdulaziz University, Jeddah, Saudi Arabia,
[2]Department of Mathematics, Faculty of Science, Sohag University, Sohag, Egypt and Nonlinear Analysis and Applied Mathematics Research Group (NAAM), Department of Mathematics, King Abdulaziz University, Jeddah, Saudi Arabia

Abstract: The purpose of this paper is to provide a method for determining the numerical solutions of the thermal damage of cylindrical living tissues using hyperbolic bioheat model. Due to the complex governing equation, the finite element approach has been adopted to solve these problems. To approve the accuracy of the numerical solution, the numerical outcomes obtained by the finite element approach are compared with the existing experimental study. In addition, the comparisons between the numerical outcomes and the existing experimental data displays that the present mathematical models are efficient tools to evaluate the bioheat transfer in the cylindrical living tissue. Numerical computations for temperatures and thermal damage are presented graphically.

Keywords: Finite element method, Cylindrical living tissue, Hyperbolic bioheat model, Thermal damage, Hyperthermia, Biological tissue

International Journal of Numerical Methods for Heat & Fluid Flow

قسم الفيزياء
Physics Department

Physics

قسم الفيزياء
Physics Department

Optical, Electrical, and Thermoelectric Properties of Hydrothermally Synthesized Bi_2Te_3 Nanoflakes

Mohamed Abdullah Abdullah Mohamed, Hazem Mahmoud Ali, Eslam Mohamed Mohamed Ibrahim, and Moustafa Mohamed Wakkad

Physics Department, Faculty of Science, Sohag University, 82524 Sohag, Egypt

Abstract: Thermoelectric power generators are promising for clean energy production through converting the waste heat to electricity in environmentally friendly ways without any noise or pollutants. This work reports a facile method to synthesize Bi_2Te_3 nanoflakes with an investigation of their structural, optical, and thermoelectric properties. Various techniques such as X-ray diffraction, field emission scanning electron microscope, transmission electron microscope, and energy dispersive spectroscopy are used to characterize the synthesized compound. The results confirmed that the nanoflakes crystallize in a rhombohedral structure with an average diameter and thickness 31.2 and 27 nm, respectively. A narrow optical band gap of 0.43 eV is determined for the prepared nanoflakes confirming the potential of employing the nanoflakes in optoelectronic applications. The results of the thermoelectric measurements imply that the synthesized nanoflakes have high power factor values at high temperatures compared to those previously reported for the same compound by other research groups. The power factor values make the synthesized nanoflakes promising candidate for thermoelectric applications.

Keywords: Bi_2Te_3 nanoflakes; thermoelectric power*; x-ray diffraction;* field emission scanning electron microscope, *optical analysis.*

Phys. Status Solidi A 2019, 1800958

Optical and transport properties of few quintuple-layers of $Bi_{2-x}Sb_xSe_3$ nanoflakes synthesized by hydrothermal method

E.M.M. Ibrahim[a], M.A.A. Mohamed[a, b] , H. M. Ali[a] , Vyacheslav O. Khavrus[b], Silke Hampel[b] , M.M. Wakkad[a]

[a]Physics Department, Faculty of Science, Sohag University, 82524 Sohag, Egypt

[b]Leibniz Institute of Solid State and Material Research Dresden, Helmholtzstr. 20, D01069, Dresden, Germany

Abstract: Hydrothermal synthesis as a commonly bottom-up growth method has considerable advantages for manufacturing thermoelectric nanomaterials with advanced thermoelectric properties. However, the hydrothermally synthesized thermoelectric nanostructures often show a low thermoelectric performance due to their low power factor. In this work, we report on using a hydrothermal method for the growth of n-type Bi2-xSbxSe3 nanoflakes with a fixed thickness of ~16 quintuple-layers. The controlling of the stoichiometric composition, phase purity and crystallinity of the Bi2-xSbxSe3 nanoflakes are demonstrated by the X-ray diffraction, Raman spectroscopy, and high resolution transmission electron microscopy. We further prove that adding of antimony into Bi_2Se_3 compound mostly influences the in-plane vibration mode. The optical energy gap is sharply increased as the Sb content increases. The effect of the antimony incorporation on the electrical conductivity, Seebeck coefficient and power factor of Bi2-xSbxSe3 nanoflakes is systematically investigated. The $Bi_{1.92}Sb_{0.08}Se_3$ sample is found to have the highest power factor ~13.17 $\mu W/cm.K^2$ at 470 K which is much higher than those published for other various nanostructured or bulk Bi2Se3 compounds. The results propose a great prospect for further enhancing the thermoelectric power factor of the Bi2Se3 nanostructures synthesized by this hydrothermal method. Taking into consideration the progress in Bi–Se compounds, the results of this work advocate the promise of Bi–Se nanostructures towards producing high performance thermoelectric devices.

Keywords: $Bi_{2-x}Sb_xSe_3$, Bi_2Se_3,Thermoelectric nanostructures, Raman, Power factor

Journal of Alloys and Compounds, Volume 804, 2019, Pages 272-280

Structure, Optical, Corrosion, and Photocatalytic Properties of Thermally Evaporated Molybdenum Trioxide Thin Films deposited on different substrates

Sh. A. Elkot[1], W. S. Mohamed[1, 2], Mahmoud Elrouby[3], H. M. Ali[1], E. Kh. Shokr[1]

[1]Physics Department, Faculty of Science, Sohag University, 82524 Sohag, Egypt

[2]Physics Department, College of Science, Jouf University, Al-Jouf, Sakaka, P.O. Box 2014, Saudi Arabia

[3]Chemistry Department, Faculty of Science, Sohag University, 82524 Sohag, Egypt

Abstract: In this study, we report the physical properties of sub-stoichiometric Molybdenum trioxide (MoO_{3-x}) thin films synthesized by thermal evaporation technique for photocatalytic application. MoO_{3-x} thin films were deposited on glass and Fluorine doped Tin Oxide (FTO) coated glass substrates with different thicknesses (100 - 650 nm). Structure analysis by X-ray diffraction and field emission scanning electron microscope confirm the amorphous structure of MoO_{3-x} films deposited on FTO and glass substrates. The optical analysis by UV-Vis–near-infrared spectrophotometer showed that the optical band gap does not depend on the substrate type and takes values in the range from 3.6 to 3.31 eV. The Corrosion measurements for MoO_{3-x} films deposited on FTO coated glass substrates were performed using an electrochemical potentiostat in a neutral medium of NaCl solution. The corrosion studies demonstrate that the as deposited MoO_{3-x} film of thickness 650 nm exhibits the highest corrosion resistivity compared with other thicknesses. The methylene blue (MB) was employed as a representative dye pollutant to evaluate the photocatalytic activity of the current samples. The results show that the film thickness and substrate type play an important role in the enhancement of the photocatalytic properties of MoO_{3-x} films. We found that the deposited films on glass decompose MB more than the films deposited on FTO. In addition, the as deposited MoO_{3-x} film of thickness 100 nm exhibit the highest photocatalytic activity as compared with the other deposited films.

Keywords: MoO_{3-x} thin films; thermal evaporation; x-ray diffraction; optical analysis; corrosion; photocatalytic activity

International Journal of New Horizon in Physics, 2019

Study the effect of the sintering temperature on the microstructure and optical reflectance of the compacted bulk $CuAlS_2$ fabricated by powder metallurgy technique (p/m)

Elsayed A. Ahmed[1] , Moataz H. Ata[2] , Mahmoud El-Rouby Mohammed[3], Hazem M. Ali[4]

[1]Middle Valley Technological College, Production Engineering, Sohag, Egypt

[2]Mechanics Department, Faculty of Industrial Education, Sohag University, 82524-Sohag, Egypt

[3]Chemistry Department, Faculty of Science, Sohag University, 82524 Sohag, Egypt

[4]Physics Department, Faculty of Science, Sohag University, 82524 Sohag, Egypt

Abstract: In this work, the effect of the sintering temperature of the bulk compacted powder sample on the microstructure and reflectance of the bulk $CuAlS_2$, which fabricated by powder metallurgy [P/M] technique, has been studied. The bulk was produced by [P/M] at compacting pressure of 350 MP_a, sintering time 2 hr and different sintering temperature (100, 150, 200, 250 and 300°C). X-ray diffraction [XRD], scanning electron microscopy [SEM], energy dispersive analysis [EDS], and optical reflectance measurements were used for characterization of the prepared samples. The analysis of X-ray diffraction [XRD] indicated a formation of CuAlS2 phase with preferring orientations of [1 1 2], [2 0 0], [2 2 0] and [0 0 8]. The intensity of CuAlS2 phase continuously increases with increasing the sintering temperature. It has been observed that the crystallite size increases with increasing of the sintering temperature from 24.25 nm at 100°C to 31.33 nm at 300°C, giving an indication of enhancement in the crystallinity. The analysis of [SEM] indicated the treated surface morphology of the bulk $CuAlS_2$. An increase in crystallization and formation of the $CuAlS_2$ phase was observed with increasing the sintering temperature. The cluster size shows remarkable rise with the increase of sintering temperature which confirms improvement in grain growth. The optical data shows, that with increasing the sintering temperature the reflectance decreased to 15% at 200°C in the near of infrared region [NIR] and 10% at 200°C and 250°C in the visible region [VIS].

Keywords: $CuAlS_2$, Powder Metallurgy, Sintering Temperature, Optical Reflectance.

European Journal of Mechanical Engineering Research Vol.6, No.1, pp.44-52, April 2019

Near-Threshold Incoherent Pion Photoproduction on The Deuteron With Final-State Interaction Effects

E. M. Darwish[1,2], M. M. Almarashi[1], E. M. Mahrous[1], M. A. Hassanain[3,4], M. Saleh Yousef[1,5]

[1]Physics Department, Faculty of Science, Taibah University, Medinah 41477, Saudi Arabia

[2]Physics Department, Faculty of Science, Sohag University, Sohag 82524, Egypt

[3]Physics Department, Faculty of Science, King Khalid University, Abha, Saudi Arabia

[4]Physics Department, Faculty of Science, New-Valley University, New-Valley, Egypt

[5]Physics Department, Faculty of Science, Cairo University, Giza 12613, Egypt

Abstract: Incoherent pion photoproduction on the deuteron $\gamma d \rightarrow \pi NN$ is investigated in the energy region $E^{\gamma}_{thr} \leq E^{\gamma} \leq 160$ MeV. The model applied contains the amplitudes of the impulse approximation as well as the NN and πN rescattering in the final state. For the elementary $\gamma N \rightarrow \pi N$ amplitude, the unitary isobar MAID-2007 model is used. This model is parameterized in terms of invariant amplitudes and allows one to give a more reliable description of the threshold region. The half off-shell NN and πN scattering amplitudes are obtained from separable representations of realistic NN and πN interactions, respectively. For the first time, numerical results for the linear photon asymmetry Σ, vector T_{11} and tensor T_{2M} (M = 0, 1, 2) deuteron spin asymmetries for the reactions $\gamma d \rightarrow \pi^{-}pp$, $\gamma d \rightarrow \pi^{+}nn$, and $\gamma d \rightarrow \pi^{0}np$ are presented. In addition, results for the unpolarized differential and total cross sections are given. We found that the influence of NN rescattering is moderate in both charged-and neutral-pion production channels, whereas πN rescattering is almost negligible in the charged-pion production channels which is not the case in neutral-pion production since a noticeable contribution is obtained. The calculated results for unpolarized differential and total cross sections are compared with the available experimental data and other theoretical models, and a satisfactory agreement is obtained.

Keywords: Meson production; Photoproduction reactions; Polarization phenomena in reactions; Final-state interactions.

Annals of Physics (N.Y.), Vol. 411, (2019) 167990.

Analyzing Powers in Elastic e-d Scattering and Their Sensitivity to Nucleon Form Factors

E. M. Mahrous[1], E. M. Darwish[1,2], H. M. Abou-Elsebaa[1,2], A. Hemmdan[3]

[1]Physics Department, Faculty of Science, Taibah University, Medinah 41477, Saudi Arabia

[2]Physics Department, Faculty of Science, Sohag University, Sohag 82524, Egypt

[3]Physics Department, Faculty of Science, Aswan University, Aswan, Egypt

Abstract: Influence of nucleon structure on single tensor-deuteron and double beam-vector-deuteron analyzing powers in the elastic electron-deuteron scattering process is investigated. We report numerical results for the tensor-deuteron (T_{20}, T_{21}, and T_{22}), and beam-vector-deuteron (T_{10} and T_{11}) analyzing powers as functions of the four-momentum transfer square Q^2 and the electron scattering angle in the laboratory frame θ_e. This is made possible with the advent of recent polarization measurements with polarized electron beams and/or polarized deuteron targets at MIT-Bates, JLab, NIKHEF, VEPP-2, and VEPP-3. We found that the predicted results for T_{21}, T_{22}, T_{10}, and T_{11} are sensitive to the nucleon electromagnetic form factors. On the contrary, the T_{20} analyzing power is found to be almost independent on the actual nucleon form factors. The predicted analyzing powers are compared with the available experimental data and a satisfactory agreement is obtained.Bulgarian

Keywords: Elastic electron-deuteron scattering, Polarization phenomena in reactions; Deuteron; Polarized targets.

Journal of Physics, Vol. 46 (2), (2019) 134.

Analysis of Elastic $^{16}O + ^{40}Ca$ Refractive Scattering at 214 MeV

M. A. Hassanain[1,2,*], H. F. A. Alshrani[1], A. A. Ibraheem[1,3], M. Anwar[4], K. O. Behairy[4], Z. M. M. Mahmoud[1,2], E. M. Darwish[5,6]

[1]*Department of Physics, Faculty of Science, King Khalid University, Abha, Saudi Arabia*
[2]*Department of Physics, Faculty of Science, New-Valley University, El-Kharga, New-Valley, Egypt.*
[3]*Physics Department, Al-Azhar University, Assiut, Egypt.*
[4]*Physics Department, Faculty of Science, Aswan University, Aswan, Egypt*
[5]*Physics Department, Faculty of Science, Taibah University, Medinah 41477, Saudi Arabia*
[6]*Physics Department, Faculty of Science, Sohag University, Sohag 82524, Egypt*

Abstract: The elastic scattering of $^{16}O+^{40}Ca$ system at the incident energy 214 MeV has been analyzed within the optical model (OM) potential using the phenomenological Woods–Saxon (WS) and the real optical potentials calculated in two different versions of the folded model based upon the α–α effective interaction and CDM3Y6 effective nucleon–nucleon (*NN*) interaction. The new cluster Fermi three parameter (3PFC) density distribution has been extracted to calculate the DFC1 potential. The Airy oscillation observed recently in the elastic $^{16}O+^{40}Ca$ system at E_{lab} = 214 MeV is well reproduced by using the DFC1 potential without renormalization factor. The observed minimum around $\theta \approx 46^{\circ}$ in the angular distribution with DFC1 approach was shown to be an Airy minimum, probably of the third order (A3), which is in agreement with the previous study. The predicted volume integrals and total reaction cross section are consistent with the previous analyses. This reflects the success of our DFC1 potential to reproduce a nice description of the Airy structure for HI elastic scattering.

Keywords: Elastic $^{16}O+^{40}Ca$ scattering; Folding model; Woods-Saxon potential.
Physics of Atomic Nuclei, Vol. 82 (6), (2019) 615.

Influence of Nucleon Structure on Tensor and Vector Analyzing Powers in Elastic Electron–Deuteron Scattering

E. M. Mahrous[1], E. M. Darwish[1,2,*], H. M. Abou-Elsebaa[1,2], A. Hemmdan[3]

[1]*Physics Department, Faculty of Science, Taibah University, Medinah 41477, Saudi Arabia*
[2]*Physics Department, Faculty of Science, Sohag University, Sohag 82524, Egypt*
[3]*Physics Department, Faculty of Science, Aswan University, Aswan, Egypt*

Abstract: Influence of nucleon structure on single tensor-deuteron and double beam-vector-deuteron analyzing powers in the elastic electron-deuteron scattering process is investigated. We report numerical results for the tensor-deuteron (T_{20}, T_{21}, and T_{22}), and beam-vector-deuteron (T_{10} and T_{11}) analyzing powers as functions of the four-momentum transfer square Q^2 and the electron scattering angle in the laboratory frame θ_e. This is made possible with the advent of recent polarization measurements with polarized electron beams and/or polarized deuteron targets at MIT-Bates, JLab, NIKHEF, VEPP-2, and VEPP-3. We found that the predicted results for T_{21}, T_{22}, T_{10}, and T_{11} are sensitive to the nucleon electromagnetic form factors. On the contrary, the T_{20} analyzing power is found to be almost independent on the actual nucleon form factors. The predicted analyzing powers are compared with the available experimental data and a satisfactory agreement is obtained.

Keywords: Elastic electron scattering; deuteron; nucleon–nucleon interactions; spin observables.
Moscow University Physics Bulletin, Vol. 74 (4), (2019) 341.

Sensitivity of Beam-Target Polarized Response Functions in Elastic Electron–Deuteron Scattering to Nucleon Structure and Modern *NN* Potentials

E. M. Darwish[1,2,*], A. Hemmdan[3], K. O. Behairy[3], E. M. Mahrous[1], Kh. S. Alsadi[1], and M. A. Hassanain[4, 5]

[1]Physics Department, Faculty of Science, Taibah University, Medinah 41477, Saudi Arabia
[2]Physics Department, Faculty of Science, Sohag University, Sohag 82524, Egypt
[3]Physics Department, Faculty of Science, Aswan University, Aswan, Egypt
[4]Department of Physics, Faculty of Science, King Khalid University, Abha, Saudi Arabia
[5]Department of Physics, Faculty of Science, New-Valley University, El-Kharga, New-Valley, Egypt.

Abstract: Polarized response functions for beam and target polarization in the elastic electron-deuteron scattering process are investigated. We report numerical results for all the non-vanishing polarized response functions as functions of the four-momentum transfer square Q^2. The sensitivity of the predicted results to the nucleon form factors is investigated. For the neutron and proton form factors, the standard dipole fit, the modified dipole fit 1, the modified dipole fit 2, and the relativistic harmonic oscillator model are used. In addition, the dependence of the results on the deuteron wave functions obtained from different modern *NN* potentials is studied. For this purpose, the realistic and high-precision Argonne *v*18, chiral N3LO, Nijmegen-I, and CD-Bonn *NN* potentials are used. We found that all the non-vanishing polarized response functions are sensitive to the choices of nucleon form factors, whereas they are slightly dependent on the *NN* potential model adopted for the deuteron wave function. The results for all polarized response functions using the relativistic harmonic oscillator model for the nucleon form factors are found to be very small in comparison to the results of other models.

Keywords: Elastic e-d scattering; deuteron; nucleon–nucleon interactions; spin observables; structure functions.

Moscow University Physics Bulletin, Vol. 74 (4), (2019) 353.

Sensitivity of Tensor and Vector Analyzing Powers in Elastic e-d Scattering to Modern Local and Nonlocal NN Potentials

E. M. Darwish[1,2], H. M. Abou-Elsebaa[1,2], E. M. Mahrous[1], S. S. Al-Thoyaib[3]

[1]Physics Department, Faculty of Science, Taibah University, Medinah 41477, Saudi Arabia
[2]Physics Department, Faculty of Science, Sohag University, Sohag 82524, Egypt
[3]Physics Department, Faculty of Science, Qassim University, Buraydah 51452, Saudi Arabia

Abstract: In this study, the sensitivity of tensor-deuteron and beam-vector-deuteron analyzing powers in elastic e-d scattering to modern local and nonlocal NN potentials is investigated. We report numerical results for the tensor-deuteron (T_{20}, T_{21}, T_{22}) and beam-vector-deuteron (T_{10}, T_{11}) analyzing powers as functions of the four-momentum transfer square Q^2 and the electron scattering angle in the laboratory frame θ_e. This could be made possible with the advent of recent polarization measurements with polarized electron beams and polarized deuteron targets at MIT-Bates, JLab, NIKHEF, VEPP-2, and VEPP-3. We found that the estimated results for T_{20}, T_{21}, and T_{22} are slightly dependent on the local and nonlocal NN potential models adopted for the deuteron wave functions up to $Q^2 = 0.5$ (GeV/c) ^{2}. At $Q^2 > 0.5$ (GeV/c) ^{2}, the theoretical discrepancies among various local and nonlocal NN potential models were found. As for the beam-vectordeuteron analyzing powers T_{10} and T_{11}, we also found that they started to become model dependent when $Q^2 > 0.5$ (GeV/c)^2. The considerable dependence of T_{10} and T_{11} on the local and nonlocal NN potential models was observed at extremely forward electron angles. The T_{10} analyzing power was found to be smaller than T_{11}. Therefore, in addition to the single analyzing power T_{20}, the double beam-vector-deuteron analyzing power T_{11} can be used as another tool for extracting the three deuteron form factors, which provide an intuitive picture of the internal structure of the deuteron. The predicted results for analyzing powers are also compared with the available experimental data and a satisfactory agreement was obtained.

Keywords: Elastic e-d scattering; deuteron; nucleon–nucleon interactions; spin observables.

Indian Journal of Physics, (2019), DOI: https://doi.org/10.1007/s12648-019-01537-0

Coherent π^0-Photoproduction on The Deuteron Near Threshold and The Role of D-Wave Component of The Deuteron Wave Function

E. M. Darwish[1,2], M. Saleh-Yousef[1,3]

[1]Physics Department, Faculty of Science, Taibah University, Medinah 41477, Saudi Arabia
[2]Physics Department, Faculty of Science, Sohag University, Sohag 82524, Egypt
[3]Physics Department, Faculty of Science, Cairo University, Giza 12613, Egypt

Abstract: Near-threshold coherent photoproduction of π^0-meson on the deuteron is investigated. Numerical results for the unpolarized differential and total cross sections, the linear photon Σ-asymmetry, the vector T_{11} and tensor T_{2M} (M=0,1,2) deuteron spin asymmetries, and the spin asymmetry T_{20} of the total cross section are presented. The role of D-wave component of the deuteron wave function on these physical observables is studied. The calculations are based on the impulse approximation in which we use the realistic and high-precision Bonn NN potential (full model) for the deuteron wave function and the unitary isobar MAID-2007 model for the elementary γN→πN amplitude that describes well the threshold region. We have found that the D-wave component has a negligible effect on the unpolarized cross sections and the vector deuteron T_{11}-asymmetry at photon lab-energies close to threshold. On the contrary, we have obtained a significant role of the D-wave part of the deuteron wave function on the Σ, T_{2M}, and T_{20} spin asymmetries. The results for the unpolarized differential cross section are compared to the experimental data from TAPS and a satisfactory agreement within the uncertainties has been obtained at forward pion angles. At backward pion angles, our results underestimate the experimental data and a disagreement has been found.

Keywords: Meson production; Polarization phenomena in reactions; Polarized beams and targets.
Moscow University Physics Bulletin, Vol. 74 (5), (2019).

Study of Microstructural, Electrical and Dielectric Properties of $La_{0.9}Pb_{0.1}MnO_3$ and $La_{0.8}Y_{0.1}Pb_{0.1}MnO_3$ Ceramics

S. A. Saleh

Physics Department, Faculty of Science, Sohag University, Sohag 82524, Egypt
Physics Department, College of Science & Arts, Najran University, P. O. 1988 Najran, KSA.

Abstract: The present work studies the microstructural and electrical properties of $La_{0.9}Pb_{0.1}MnO_3$ and $La_{0.8}Y_{0.1}Pb_{0.1}MnO_3$ ceramics synthesized by solid-state route method. Microstructure and elemental analysis of both samples were carried out by field emission scanning electron microscope (FESEM) and energy dispersive spectroscopy (EDS) method, respectively. Phase analysis by X-ray diffraction (XRD) indicated formation of single phase distorted structure. The XRD data were further analyzed by Rietveld refinement technique. Raman analysis reveals that Y atom substitutes La site into the LPMO with shifting of phonon modes. The temperature variation of resistivity of undoped and Y-doped La0.9Pb0.1MnO3 samples have been investigated. The electrical resistivity as a function of temperature showed that all samples undergo a metal-insulator (M-I) transition having a peak at transition temperature TMI. Y doping increases the resistivity and the metal-insulator transition temperature (TMI) shifts to lower temperature. The temperature-dependent resistivity for temperatures less than metal-insulator transition is explained in terms the quadratic temperature dependence and for T > TMI, thermally activated conduction (TAC) is appropriate. Variation of frequency dispersion in permittivity and loss pattern due to La-site substitution in LPMO was observed in the dielectric response curve.

Keywords: Ceramics; Microstructure; Raman Scattering; Electrical resistivity; Dielectric constants.
Scientific Review ISSN(e): 2412-2599, ISSN(p): 2413-8835 Vol. 5, Issue. 2, pp: 33-44, 2019.

Enhancing the capability of plasma treated austenite stainless steels as thermal reactor materials

S U El-Kameesy[1], F M El-Hossary[2], M M Eissa[3], A A Abd El-Moula[2,4] and Samah A Al-Shelkamy[5]

Abstract: In this article, the influence of radio frequency plasma nitriding three different grades of austenite stainless steels as nuclear materials for thermal Reactors has been studied. The plasma nitriding process was performed for all samples at the same plasma nitriding environmental conditions, using (1:1) hydrogen and nitrogen gases at 500 W plasma power and 7.5×10^{-2} mbar gas pressure. The structure, surface microhadness, tribological, wettability and nuclear attenuation properties of samples were examined before and after the plasma nitriding process. The surface properties for all nitrided samples achieved remarkable improvement compared with untreated ones. The HMn10Ni sample showed the best surface microhardness, abrasive dry wear, sliding friction, wettability, absorption of slow neutrons while the gamma ray attenuation properties were comparable to the other investigated austenite stainless steel samples.

IOP Publishing Ltd, Materials Research Express, Volume 6, Number 12

Influence of Rf plasma carbonitriding on AISI304L, SSMn6Ni and SSMn10Ni for nuclear applications

F M El-Hossary[1], S U El-Kameesy[2], M M Eissa[3], A A Abd El-Moula[1], Samah A Al-Shelkamy[4]

Abstract: The present study aims to examine the effect of rf plasma surface carbonitriding on austenite stainless steel AISI304L, SSMn6Ni and SSMn10Ni for pressurized water reactors application. All samples were fabricated at Central Metallurgical Research & Devolopment Institute (CMRDI), Egypt. They were also carbonitrided by rf plasma in a mixture of nitrogen and acetylene gases (85% N_2 + 15% C_2H_2) at 500 W plasma power and 7.5×10^{-2} mbar total gas pressure. In addition, the mechanical, tribological and corrosion resistance of the treated steels revealed strenghthening in the surface properties compared with that of the untreated samples. Furthermore, nuclear properties were investigated using different radioactive sources of neutron and gamma rays at different energies. Gamma ray measurements compared between the experimental and theoretical (μ and σ) shielding parameters of all carbonitrided steel samples at various energies ranging between 300.63 and 2614.51 keV. Moreover, a slight increase occurred in the macroscopic cross section of the total slow neutrons of all carbonitrided samples.

IOP Publishing Ltd, Materials Research Express, Volume 6, Number 9

Mechanical and Gamma Ray Attenuation Properties of N316L Steel Treated by RF Plasma as a Nuclear Material

M. M. Eissa[1], F. M. El-Hossary[2], S. U. El-Kameesy[3], Aly Saeed[4]*, Al-Zahraa A. Abd Elmoula[5], Samah A. Al- Shelkamy[5]

[1]Steel Technology Department, Central Metallurgical Research and Development Institute (CMRDI), Helwan, Egypt

[2]Physics Department, Faculty of Science, Sohag University, Sohag, Egypt

[3]Physics Department, Faculty of Science, Ain-Shams University, Cairo, Egypt

[4]Nuclear Power Stations Department, Faculty of Engineering, Egyptian-Russian University, Cairo, Egypt

[5]Physics Department, Faculty of Science, Assiut University, New Valley, Egypt

The effects of plasma surface engineering on average surface roughness, wettability and gamma rayattenuation properties of AISI316L standard steel sample were investigated. The results showed an increase in surface roughness accompanied with an increase in the surface energy and a decrease in the contact angle of the N316L sample treated by plasma carbonitriding. The experimental measurements of gamma ray attenuation properties of the investigated stainless-steel alloys were carried out using gamma lines emitted from 232Th and 60Co gamma ray sources. The attenuation parameters such as linear and mass attenuation coefficients and half value layer were determined experimentally and theoretically. The obtained results indicate that the rf plasma surface treatment is an effective method for developing thesurface tribological properties of the treated stainless-steel alloy without any change in the gamma ray attenuation properties. The obtained results suggest the suitability of N316L for in-core applications of nuclear reactor systems.

Keywords: RF plasma, AISI316L, Roughness, Wettability, Gamma ray, Reactor materials

Arab J. Nucl. Sci. Appl., Vol. 52, 2, 7-12 (2019)

Optical, water splitting and wettability of titanium nitride/titanium oxynitride bilayer films for hydrogen generation and solar cells applications

S. H. Mohamed[ab] Huaping Zhao [a]Henry Romanus[c] F. M. El-Hossary[b] M. Abo EL Kassem[b] M. A. Awad[b] Mohamed Rabia[ad] Yong Lei[a]

Abstract: TiN/TiO_xN_y bilayer films with various TiN thicknesses were prepared using direct current (d.c.) reactive magnetron sputtering. The ratio of N/O in the bilayer films increased with increasing TiN top layer thickness. The observed crystalline peaks for the bilayer films, for different TiN layer thicknesses, were indexed to anatase TiO_2 with tetragonal structure. Only 0.31° peak shift, to lower 2θ angles was detected. FESEM indicated that the morphology of TiO_xN_y single layer is consisted of elongated nanocrystals with diameters in the range of 27.9–46.8 nm and the diameters of the nanocrystallites changed slightly with increasing the thickness of TiN layer. The transmittance, absorbance, reflectance spectra and the optical constants of the bilayer films were presented. The photoelectrochemical performance for water splitting of TiN/TiO_xN_y bilayer films was studied by examination both the continuous and chopped photocurrent density under light illumination. The photocurrent density increases with increasing TiN top layer up to a thickness of 9 nm, after which a reduction in photocurrent is observed. The wettability of TiN/TiO_xN_y bilayer films could be transformed by UV illumination from hydrophobic to hydrophilic.

Materials Science in Semiconductor Processing Volume 105, January 2020, 104704

Use of Magnetocaloric Material for Magnetic Refrigeration System: A Review

A. ABDEL-LATIF[1,2,3], MAHROUS R. AHMED[4]
1Physics Department, College of Science & Arts, Najran University, P. O. 1988 Najran, KSA
2Reactor Physics Department, NRC, Atomic Energy Authority, Abou Zabaal, P.O. 13759, Cairo, Egypt.
3Advanced Materials and Nano-Research Centre, Najran University, P.O. Box: 1988, Najran 11001, SA
4Physics Department, Faculty of Science, Sohag University, Sohag 82524, Egypt.

Abstract
Our daily need to cooling system is grown up. The used cooling systems are the source of the harmful changes in the global climate. And so, we need to search a new alternate cooling systems applying environmentally friendly technology that may help in decreasing the pollutions in our world. The progress in materials science allows to use some materials for cooling purposes. This new class of materials is so called "magnetic refrigerator". The basics of magnetic refrigeration depends on the magneto-caloric properties to reach low temperatures and obtain cooling system. The advantage of magnetic refrigerator (MR); First, the cooling efficiency is higher than conventional vapor refrigerator CVM where its cooling efficiency~30-60% while the cooling efficiency in CVM~5-10%. Second, MR can be more compactly built. Third, it is safe and an environmentally friendly cooling. In this work, we will highlight on the scientific efforts to find optimum properties to be applied as the magnetic refrigeration. In this review the highlights of the scientific efforts to seek for the best alternative materials to be used as a magnetic refrigeration applications. The low coast and small size of magnetic cooling is one the important advantage. This review consists of five sections; I. Introduction, II.Synthesis of MC materials, III. Crystal structure of MC materials and IV. Characterization and applications of MC materials, and V. Conclusions.

One-Dimensional Metallo-Superconductor Photonic Crystals as a Smart Window

Arafa H. Aly[1],Ayman A. Ameen[2], Hussein A. Elsayed[1], S. H. Mohamed[2],Mahi R. Singh[3]
[1]TH-PPM Group, Physics Department, Faculty of Science, Beni-Suef University, Beni-Suef, Egypt
[2]Physics Department, Faculty of Science, Sohag University, Sohag, Egypt
[3]Department of Physics and Astronomy, Western Ontario University, London, Canada

Abstract: A new structure to control the electromagnetic waves has been successfully designed for smart windows applications. Thepresent photonic crystals (PCs) smart window is designed from a unit cell of two different materials such as A (metal) and B(superconductor) of thicknesses that repeated for N periods. The numerical results are investigated based on the characteristicmatrix method. It was found that the angle of incidence has a significant effect on the transmission values. At 10^o angle ofincidence, we found more than 80% of the visible light and a near IR is transmitted whereas at 60^o angle of incidence, thephotonic band gap (PBG) begins to appear at wavelengths greater than 800 nm and the visible light transmittance remains morethan 80%. Also, the dependence of the transmittance values on the periodicity and thickness of the proposed design wasinvestigated. The proposed structure could be of potential use as a smart window in low-temperature applications and spaceindustry.

Journal of Superconductivity and Novel Magnetism 32 (2019) 2313–2318.

TiO_2/TiO_xN_Y hollow mushrooms-like nanocomposite photoanode for hydrogen electrogeneration

M. Rabia, S. H. Mohamed, H. Zhao, M. Shaban, Y. Lei, A. M. Ahmed

[1]Nanophotonics and Applications Lab, Physics Department,Faculty of Science, Beni-SuefUniversity, Beni-Suef 62514,Egypt

[2]Physics Department, Faculty of Science, Sohag University,Sohâg 82524, Egypt

[3]Institute of Physics & IMN Macronano®, Ilmenau Universityof Technology, 98693 Ilmenau, Germany

TiO_2/TiO_xN_y hollow mushrooms-like nanocomposite photocatalyst was prepared using atomic layer deposition (ALD) and reactive direct current magnetron sputtering, respectively. The preparation process depends on the aluminum oxide template (AOT) that was fabricated using the two-step anodization process after the Ni imprinting process. The chemical, morphological, and optical properties were recorded using different analyses such as XRD, SEM, EDX, and UV–Vis. From the SEM analyses, the AOT pore size increases from 177 to 305 nm after the pore widening process in H3PO4. The diameter of the TiO_2 in the upper part is 352 nm, while the diameter of the TiO_2/TiO_xN_y composite is 355 nm in the upper part. The estimated band gap values of TiO_2 and TiO_2/TiO_xN_y are 3.1 and 2.25 eV, respectively. From the values of band gaps, there is a clear enhancement in the optical absorption of the nanocomposite bilayers. The photoelectrochemical (PEC) behaviors of the TiO_2/TiO_xN_y electrodes supported in Au/Ni metal thin film was measured in 1 M NaOH as scarifying reagent. The thermodynamic parameters were calculated, in which ΔE, ΔH*, and ΔS* values are 16.75 kJ mol−1, 15.87 kJ mol−1 and − 115.65 kJ mol−1 K−1, respectively.

Journal of Porous Materials (2019) 1-7.

Study of the effects of both film thickness and annealing time on $Cu_xS_yO_z$thin films for the possibility of usage as solar control coatings

S. H. Mohamed[1], N. M. A. Hadia[1,2], M. A. Awad[1], Mohamed Ismail Hafez[1]

[1]Physics Department, Faculty of Science, Sohag University,Sohâg 82524, Egypt

[2]Department of Physics, College of Science, Jouf University,Jouf, Saudi Arabia

Abstract: $Cu_xS_yO_z$ thin films with various thicknesses were prepared by thermal evaporation. The structural, morphological, electrical and optical characteristics are examined for possible usage as solar control coatings on cars and architectural windows. The effect of thermal annealing on $Cu_xS_yO_z$ films was examined for the thick film of 734 nm at 550°C for various annealing times of 2, 4 and 6 h. Energy dispersive analysis of X-ray (EDAX) was used to evaluate the chemical composition of the as-prepared and annealed films. X-ray diffraction (XRD) elucidated the presence of hexagonal CuS and orthorhombic Cu_2S together with small contribution of, orthorhombic $CuSO_4$ phase for the thicker films (≥ 241 nm). With increasing the annealing time the hexagonal CuS and orthorhombic Cu_2S peaks disappeared. The morphology of the films is strongly dependent on both thickness and annealing time. By controlling the film thickness the transmission of the NIR region can be brought to zero whereas adequate transmission, 6-27%, in the visible spectral region was maintained. After annealing, the transmittance increased while the reflection decreased. The optical band gap and the optical constants of the annealed films were also studied. It was found that the values can differ depending on the annealing time. The as prepared $Cu_xS_yO_z$ films behaves as metallic materials. It is found that room temperature resistivity decreased as the film thickness increased while it increased with annealing.

Applied Physics A 125 (2019) 587 (10pp).

Effects of Thickness and Ag Layer Addition on the Properties of ZnS Thin Films

S.H. Mohamed[a], N.M.A. Hadiaa[b], M.A. Awad[a], Essam R. Shaaban[c]

[a]Physics Department, Faculty of Science, Sohag University, 82524 Sohag, Egypt

[b]Department of physics, College of Science, Jouf University, Jouf, Saudi Arabia

[c]Department of Physics, Faculty of Science, Al-Azahar University, Assiut, 71542, Egypt

Abstract: Zinc sulfide (ZnS) thin films, with different thicknesses and different silver (Ag) middle layer thickness, wereprepared on glass substrates using thermal evaporation. The structural and optical properties of ZnS thin films werecharacterized by X-ray diffraction and UV-VIS-NIR spectrophotometer. The X-ray diffraction analyses indicatedthat ZnS films have cubic structure with (111) preferential orientation, whereas the diffraction patterns sharpenwith the increase in the film thickness. The intensities of the Ag peaks increased strongly while the intensitiesof ZnS peaks decreased when the Ag layer increased to 86 nm. The optical band gap values decreased while therefractive index increased with the increase of the film thickness and Ag layer thickness. These results show thatZnS films are suitable for use as the buffer layer of the Cu(In, Ga)Se_2 solar cells.

ActaPhysicaPolonica 135 (2019) 420-425.

Experimental and theoretical studies of hybrid multifunctional *TiO_2*/ TiN / *TiO_2*

M. A. Awad[a], Arafa H. Aly[b]

[a]Physics Department, Faculty of Science, Sohag University, 82524 Sohag, Egypt

[b]Physics Department, Faculty of Science, Beni-Suef University, Egypt

Abstract: Triple layers of TiO_2/TiN/TiO_2 with different TiN thicknesses have been deposited using D.C. reactive magnetron sputtering on heated Si (100) and glass substrates. In this study, the effect of TiN thicknesses on different properties have been conducted. Analysis of XRD and SEM demonstrated the enhancement of the crystal structure and surface morphology with suitable TiN thickness. The optical studies elucidated the increase and the confinement of both reflectivity and refractive index with TiN thickness whilst the opposite was observed in the transparency and the optical band gap. The Essential Macleod software is used to design the optical coating hence predicting the extent of matching between theory and experiment. The self-cleaning tests demonstrated the quick transform from hydrophobic to superhydrophilic that is highly sensitive to the surface nature as well as the thickness of TiN layer. This newly designed system can be exploited as heat mirrors, dichroic filters and in self-cleaning applications.

Ceramics International 45 (2019) 19036-19043.

Simultaneous synthesis of various Sb_2S_3 nanostructures by vapor transport technique

N. M. A. Hadia[a,b], W.S.Mohamed[a,b], M.S.Abd El-sadek[c]

[a]Physics Department, Faculty of Science, Sohag University, 82524 Sohag, Egypt

[b]Department of physics, College of Science, Jouf University, Jouf, Saudi Arabia

[c]Physics Department, Faculty of Science, South Valley University, 83523Qena, Egypt

Abstract: In this study, we report the preparation of different Sb_2S_3 morphologies in the same experimental setup. We utilized the method of vapor phase transport with direct evaporation of high purity Sb_2S_3 powder on quartz and Si (100) substrates. The deposited Sb2S3 nanostructures showed different morphologies and crystallinities without using metal catalyst seed layers. The successfully formed Sb_2S_3 morphologies were nanowires, nanorods, nanodendrites and nanoparticles, as verified by the scanning electron microscopy and transmission electron microscopy analysis. We found that the physical characteristics of the final product are a function of the differential temperature inside the furnace tube. The X-ray diffraction analysis confirmed the formation of the orthorhombic pure phase of crystalline stibnite- Sb_2S_3. The energy-dispersive X-ray spectroscopy spectra validated the high purity of the synthesized products. Moreover, the relation of the morphology and the optical and electrical properties of Sb2S3 thin films have been studied by various techniques. The optical analysis by UV–vis–near-infrared (NIR) spectroscopy shows that the optical band gaps of the different synthesized films range from 1.64 to 1.92 eV. The refractive indices (n) of Sb_2S_3 thin films were found to be morphology dependent. The film with nanoparticles morphology has the highest n value of 2.1 and the film with nanowires morphology has the lowest n value of 1.97. In all prepared samples photoluminescence (PL) spectra exhibit a distinct emission peak at 615 nm (~ 2.02 eV) in terms of intensity and FWHM. The dc-electrical conductivity of various Sb_2S_3 nanostructures is thermally activated according to Arrhenius law with two types of conduction mechanisms. The conduction in the high temperature and lower temperature zones is due to the hopping conduction via localized states and the thermionic emission respectively. The study provides a framework for future research in semiconductor nanomaterials with controllable morphologies for applications of optoelectronics.Materials Chemistry and Physics235 (2019) 121750

Composition dependence of structural and linear and non-linear optical properties of $CdS_{1-x}Mn_x$ semiconducting thin films

Mansour Mohamed[1], A. M. Abdelraheem[1], M. I. Abd-Elrahman[1], N.M.A. Hadia[2,3] , E. R. Shaaban[4]

[1]Physics Department, Faculty of Science, Assiut University, Assiut 71516, Egypt Physics

[2]Department, College of Science, Jouf University, P.O. Box 2014, Al-Jouf, Sakaka, Saudi Arabia

[3]Physics Department, Faculty of Science, Sohag University, Sohag 82524, Egypt

[4]Physics Department, Faculty of Science, A1-Azhar University, Assiut 71542, Egyp

Abstract: This work reported the structure and optical investigations of $CdS_{1-x}Mn_x$ (x=0.00, 0.02, 0.04, 0.06, 0.08, 0.10) thin flms. The thin flms of $CdS_{1-x}Mn_x$ with diferent compositions were synthesized using electron beam evaporation method under high vacuum conditions at room temperature. X-ray difraction (XRD) analyses revealed the polycrystalline nature of the deposited flms. The observed difraction peaks were well ftted with a hexagonal crystal structure. In addition, the intensity of XRD peaks decreased by increasing the Mn concentration indicating a monotonical deterioration in the crystalline quality by the doping. The (101) plane is the preferential orientation for the crystal growth of the studied flms. The flm thickness as well as a refractive index were calculated by Swanepoel's method. The direct and indirect electronic transitions were found to be responsible for the high absorption process in the studied flms. Furthermore, both direct and indirect bandgaps decreased with increasing the Mn content. Other optical parameters such as optical conductivity, real and imaginary parts of dielectric constant, dispersion energy, and dissipation factor were determined and showed a strong dependence on the Mn content. These fndings were discussed in terms of the localized states.

Applied Physics A (2019) 125:483

Cross sectional complex structure analysis is a key issue of thin film research: A case study on the preferential orientation crossover in TiN thin films

P. B. Barna[a], D. Biro[b], M. F. Hasaneen,[a1], L. Székely[a], M. Menyhárd[a], A. Sulyok[a], Z. E. Horváth[a], P. Pekker[c,2], I. Dódony[c,d], G. Radnóczi[a]

[a]Centre for Energy Research of the Hungarian Academy of Sciences, Institute for Technical Physics and Materials Science, H1121 Budapest, Konkoly-Thege M. u. 29-33, Hungary, [b]Faculty of Technical and Human Sciences, Sapientia Hungarian University of Transylvania,540485 Târgu-Mures, Sighisoarei 1/C, Romania, [c]Bay Zoltán Nonprofit Ltd, H3510 Miskolc, Iglói u 2, Hungary d Eötvös Loránd University, Department of Mineralogy, H-1117 Budapest, Pázmány Péter Sétány 1/C, Hungary, [1]Physics Department, Faculty of Science, Sohag University, 82,524 Sohag, Egypt; Physics Department, College of Science, Jouf University, Al-Jouf, Sakaka, P.O. Box 2014, Saudi Arabia, [2]NANOLAB, Research Institute of Biomolecular and Chemical Engineering, University of Pannonia, Egyetem str. 10. Veszprém, H-8200, Hungary

Published results of the multitudinous experiments studying the relationships between the properties and process parameters of sputter deposited TiN films indicate a very complex problem. The complexity manifests itself preferentially in the sporadic formation of the <100> and <111>preferred orientation (PO) and in the sequential formation (crossover) of the <100> and <111> PO in thicker films, even when the deposition parameters are maintained constant during the deposition. The first problem has been clarified by dedicated experiments as well as theoretical works. These revealed that the selection between the development of the <100> and <111> PO is related to the condition of the impinging species, i.e. whether they are neutral or ionized, molecular or atomic Ti and N species, to the degree of ionization, to the ratio of the impinging rates of these species and to their energy as well. Understanding the cross-over formation between the <100> and <111> PO remained, however, an open question so far. As the driving force for this process, the operation of the proposed overall energy minimisation effect, the interplay of the surface and interface and the inner stress energy during thickness growth of the film has been queried. In the present work authors point out that the complex structural and micro-chemical analysis of the crosssectional specimens of TiN thin films with PO crossover could provide the fundamental information required to discover the possible phenomena governing the evolution of this particular structure and to reconstruct its pathway. That is demonstrated for the situation when the origin of the<100>to<111>PO crossover could be related to the contamination effect, caused by gas desorption at starting the deposition. In the discussed experiment the TiN film is doped by oxygen and the oxygen concentration changing from 18 to 11 at.% during the deposition.

Thin Solid Films 688 (2019) 137478

Investigating the structure and tribo-mechanical performance of PVD TiN onbearing TiN substrate constructed by rf plasma

M. Raaif

Physics Department, Faculty of Science, Sohag University, Sohag 82524, Egypt

Recent study was focused on conjoining rf plasma nitriding of titanium with TiN coating by rf plasma magnetron sputtering as a duplex treatment technique. To develop the tribo-mechanical characteristics and load bearing capacity of titanium substrate, rf plasma nitriding was engaged to predestine a bearing TiN layer on Ti base substrate. The PVD process was accomplished employing TiN target in argon plasma atmosphere. All PVD parameters were constant excluding the deposition time which was varied from 4 to 20 min with deposition rate of ~60–65 nm/min. The effect of PVD TiN film thickness which was varied from 240 to 1300 nm on structure,tribo-mechanical and electrochemical performance of TiN/TiN duplex coatings was investigated. It was found, the duplex treatment expressively increased the PVD TiN/TiN coatings hardness (max: 2600 ± 47 HV0.025) and constricted the substrate plastic deformation. An enhancement in the adhesion in the duplex TiN/TiN samples compared to TiN/Ti was observed. Moreover, the wear, friction (reduced to nearly 0.2) and the corrosion performance were markedly upgraded for the duplex treated samples compared with pure Ti and PVD TiN/Ti.

Materials Chemistry and Physics 224 (2019) 117–123

Impact of Co^{2+} Substitution on Microstructure and Magnetic Properties of $Co_xZn_{1-x}Fe_2O_4$ Nanoparticles

W. S. Mohamed [1,2,*], MeshalAlzaid[1] , Mohammed S. M. Abdelbaky[3], ZakariaeAmghouz[4],Santiago García-Granda[3], Ahmed M. Abu-Dief[5,6]

[1]Physics Department, College of Science, Jouf University, Al-Jouf, Sakaka P.O. Box 2014, Saudi Arabia; [2]Physics Department, Faculty of Science, Sohag University, 82524 Sohag, Egypt, [3]Departments of Physical and Analytical Chemistry, and Organic and Inorganic Chemistry, University of Oviedo-CINN, 33006 Oviedo, Spain, [4]Department of Materials Science and Metallurgical Engineering, University of Oviedo, Campus Universitario, 33203 Gijón, Spain, [5]Chemistry Department, Faculty of Science, Sohag University, 82524 Sohag, Egypt, [6]Chemistry Department, Faculty of Science, Taibah University, Madinah P.O. Box 344, Saudi Arabia

Abstract: In the present work, we synthesized $Co_xZn_{1-x}Fe_2O_4$ spinel ferrite nanoparticles (x= 0,0.1, 0.2, 0.3 and 0.4) via the precipitation and hydrothermal-joint method. Structural parameters were cross-verified using X-ray powder diraction (XRPD) and electron microscopy-based techniques. The magnetic parameters were determined by means of vibrating sample magnetometry. The as-synthesized $Co_xZn_{1-x}Fe_2O_4$ nanoparticles exhibit high phase purity with a single-phase cubic spinel-type structure of Zn-ferrite. The microstructural parameters of the samples were estimated by XRD line profile analysis using the Williamson–Hall approach. The calculated grain sizes from XRPD analysis for the synthesized samples ranged from 8.3 to 11.4 nm. The electron microscopy analysis revealed that the constituents of all powder samples are spherical nanoparticles with proportions highly dependent on the Co doping ratio. The $Co_xZn_{1-x}Fe_2O_4$ spinel ferrite system exhibits paramagnetic, superparamagnetic and weak ferromagnetic behavior at room temperature depending on the Co^{2+} doping ratio, while ferromagnetic ordering with a clear hysteresis loop is observed at low temperatures (5K).We concluded that replacing Zn^{2+} ions with Co^{2+} ions changes both the structural and magnetic properties of $ZnFe_2O_4$ nanoparticles.

Nanomaterials 2019, 9, 1602; doi:10.3390/nano9111602

Physical, Electrochemical and Biocompatibility Characteristics of Ti-Al-N Thin Film Synthesized by DC Pulsed Magnetron Sputtering

F. M. El-Hossary, A. M. Abd El-Rahman, M. Raaif, M. Abo El-Kassem
Physics Department, Faculty of Science, Sohag University, 82524-Sohag, Egypt

Abstract: Owing to the desired mechanical and biomedical characteristics of TiN-based coatings and the encourage features of pulsed magnetron sputtering, the current study was conducted to deposit Ti-Al-N thin film on AISI 316 using DC pulsed magnetron sputtering. All processing parameters were constant excluding the pulsed magnetron power which was varied from 100W to 175W. The effect of processing power on the structure, mechanical, electrochemical and biocompatibility characteristics of Ti-Al-N thin films were inspected. X-ray outlines the formation of (Ti, Al)N solid solution with (111) preferred orientation at high pulsed magnetron powers. The outcomes of this study demonstrated that the Vickers's microhardness of Ti-Al-N coatings increased with increasing the pulsed power to record a value of nearly 810 HV0.015 at 175W. Moreover, the wear characteristics and the friction coefficient of the coated AISI 316 with Ti-Al-N are ascendant as compared with the uncoated substrate. The wear rate of Ti-Al-N films deposited at pulsed power of 175W recorded a value of nearly $4.7x10^{-6}$ mm^3/Nm which is very low compared with that of stainless steel substrate ($3.2x10^{-4}$ mm^3/Nm). The biological peculiarities of Ti-Al-N films were examined by exploring the proliferation rate of MC3T3-E1 osteoblast cells on the film surface. The results reflected that the proliferation rate of the osteoblasts cells were enhanced on Ti-Al-N films deposited at pulsed powers of 150 and 175 W. The biological attitudes have been discussed according to the results of surface roughness, surface energy besides to the surface chemical compositions.

Journal of the Australian Ceramic Society, In Press

Thermoelectric properties of enhanced phonon scattering Hf-doped FeVSb Half-Heusleralloys

A. M. Adam[1,3], A. El-Khouly[2], A.P. Novitskii[1], E. M. M. Ibrahim[3], A. V. Kalugina[1], D. S. Pankratova[1], A. I. Taranova[1], A. A. Sakr[2], A. Trukhanov[1], M. M. Salem[1], V. Khovaylo[1,4]

[1]National University of Science and Technology MISIS, Moscow 119049, Russian Federation
[2]Physics Department, Damanhour University, Damanhour 22516, Egypt
[3]Physics Department, Sohag University, Sohag 82524, Egypt
[4]National Research South Ural State University, Chelyabinsk 454080, Russian Federation

Abstract: In the present work, the structural and thermoelectrical properties of Sb2-xBixTe3 samples prepared by the usual melting method were studied. The samples were milled, pressed and then annealed under vacuum for 3 h at 250 °C. Investigations of the microstructure and surface morphology were carried out using X-ray diffraction analysis, scanning electron microscopy and energy-dispersive X-ray spectroscopy. The Seebeck coefficient and electrical and thermal conductivities were measured from 300 to 473 K. Thermopower data indicated a p-type conduction in the samples. Structural defects were present in Sb2Te3 during Bi addition, acting as scattering centers and leading to a decrease in thermal conductivity, thus increasing the thermopower and power factor. The power factor showed its maximum value of around 24.7 μW/cm K2 for the sample containing the highest Bi content. High figure of merit of 1.14 was recorded for the same sample, indicating that the Bi-containing Sb2Te3 and the related alloys are promising materials for more efficient thermoelectric devices.

Keywords: Crystalline alloys; Electrical conductivity; Thermoelectric power; Figure of merit
Journal of Physics and Chemistry of Solids (In press 2019)

H_2 sensing characteristics in glass-removed amorphous $Co_{60.51}Fe_{3.99}Cr_{12.13}B_{13.53}Si_{9.84}$ microwires

S.A. El-Demrdash[a], A.M. Adam[b,*], L.V. Panina[c]

[a]Department of Physics, RMIT, GPO Box, 2476V, Melbourne 3001, Australia
[b]Physics Department, Faculty of Science, Sohag University, Sohag 82524, Egypt
[c]National University of Science and Technology, Moscow, Russia

Abstract

Hydrogen sensing is crucial to ensure safety in near-future zero-emission fuel cell powered vehicles and many otherareasofindustry.Inthiswork,wepresentanovelhydrogensensorbasedontheglassremovedmicrowires. Using microwire as Hydrogen gas sensor gives a promising result with high sensitivity, high response and ultralow power consumption. Microwires are tiny, very light and commercially available, hence, sensors based on microwires can widely be produced. In this manuscript, we report on sensitivities and response times of such sensors as a function of the change in hydrogen (H_2) concentration at standard conditions of room temperature and atmospheric pressure. It was found that the wire is able to detect H_2 of concentrations even lower than 0.05% within 1s at the onset of the diffusion using only a few amounts of power, matching the commercial requirements for H_2 safety sensors. Thermodynamic chemistry is used to explain the effect of hydrogen on the wire. Magnetic properties, in terms of, “hysteresis loop curves” of the wire are investigated. From hysteresis loops measurements, it was observed that there is no change occurring in the magnetic properties of the samples in response hydrogen exposure, a matter confirming and matching the data provided by thermodynamics. Asa direct result of the high response, simplicity of fabrication and time recovery, the proposed material is very promising for practical H_2 sensing applications.

Keywords: H_2sensing; Magnetic microwires; Electrical resistivity; Sensitivity
Materials Today Communications 20 (2019) 100601

Crossover effect of magnetotransport and magnetocaloric effect in $(La_{0.7}Ba_{0.3}MnO_3)1\text{-}x/(Al_2O_3)x$ composites

A.M. Ahmed, H.F. Mohamed⁎, A.K. Diab, Esraa Y. Omar
Physics Department, Faculty of Science, Sohag University, 82524 Sohag, Egypt

Abstract: Magnetotransport properties and magnetocaloric effect of $(La_{0.7}Ba_{0.3}MnO_3)_{1-x}/(Al_2O_3)_x$ composites have been investigated through their theoretical and experimental studies. The Al_2O_3 addition increases the resistivity, showing up a crossover from 3D Mott to the soft gap variable range hopping (*VRH*). The relative cooling power of LBMO matrix (~98.77 Jkg−1, *H*=2 T) is approximately 65 percentage of that of pure Gd (*RCP*=153 Jkg−1, *H*=2 T). It means to achieve an active magnetic refrigerator employing LBMO will need more than one and half times the volumes of a refrigerant unit consisting of pure Gd. A good concordance is observed as simulated both resistivity and magnetization curves.

Journal of Magnetism and Magnetic Materials 489 (2019) 165388

Tuning electrical conductivity of β-Ga_2O_3 single crystals by Ta doping

Huiyuan Cui[ab] H. F. Mohamed[bc] Changtai Xia[b] Qinglin Sai[b] Wei Zhou[b] Hongji Qi[b] Jingtai Zhao[a] Jiliang Si[b] Xiao li Ji[d]
[a]*School of Material Science and Engineering, Shanghai University, Shanghai 200444, China*
[b]*Key Laboratory of Materials for High Power Laser, Shanghai Institute of Optics and Fine Mechanics, Chinese Academy of Sciences, Shanghai 201800, China*
[c]*Physics Department, Faculty of Science, Sohag University, 82524, Sohag, Egypt*
[d]*College of Electronic Science and Engineering, Nanjing University, Nanjing 210093, China*

Abstract: Ta-doped β-Ga_2O_3 single crystals were grown to regulate the electrical properties of β-Ga_2O_3. The carrier concentration is intentionally controllable, and can be defined from 3.6×10^{16} cm^{-3} to 3.0×10^{19} cm^{-3}, by controlling Ta concentration. The optical transmittance of Ta-doped single crystals was as high as 70%–80% in the visible region. In addition, it distinguished by a decline trend in the IR region, which attributed to the increase of the carrier concentration with Ta doping. Raman spectra revealed that the intensity and the FWHM of GaO_6 octahedra peaks increased with increasing Ta content. DLTS showed only one deep level defect at 0.73 eV below the conduction band, and this defect had little contribution to the carrier concentration.

Keywords: β-Ga2O3; Electrical properties; Optical properties; Semiconductor; Defect.
Journal of Alloys and Compounds Volume 788, 5 June 2019, Pages 925-928

Growth and fundamentals of bulk β-Ga_2O_3 single crystals

H. F. Mohamed[1,2], Changtai Xia[1], Qinglin Sai[1], Huiyuan Cui[1], Mingyan Pan[1] Hongji Qi[1]

[1]Key Laboratory of Materials for High Power Laser, Shanghai Institute of Optics and Fine Mechanics, Chinese Academy of Sciences, Shanghai 201800, China

[2]Physics Department, Faculty of Science, Sohag University, 82524, Sohag, Egypt

Abstract: The rapid development of bulk β-Ga_2O_3 crystals has attracted much attention to their use as ultra-wide bandgap materials for next-generation power devices owing to its large bandgap (~ 4.9 eV) and large breakdown electric field of about 8 MV/cm. Low cost and high quality of large β-Ga_2O_3 single-crystal substrates can be attained by melting growth techniques widely used in the industry. In this paper, we first present an overview of the properties of β-Ga_2O_3 crystals in bulk form. We then describe the various methods for producing bulk β-Ga_2O_3 crystals and their applications. Finally, we will present a future perspective of the research in the area in the area of single crystal growth.

Keywords: β-Ga2O3 ; crystal structure; bulk crystal growth; applications

Journal of Semiconductors, Volume 40, Number 1

Crossover effect of magnetotransport and magnetocaloric effect in $(La_{0.7}Ba_{0.3}MnO_3)_{1-x}/(Al_2O_3)_x$ composites

A.M.AhmedH.F.MohamedA.K.DiabEsraa Y.Omar

Physics Department, Faculty of Science, Sohag University, 82524 Sohag, Egypt

Abstract: Magnetotransport properties and magnetocaloric effect of $(La_{0.7}Ba_{0.3}MnO_3)_{1-x}/(Al_2O_3)_x$ composites have been investigated through their theoretical and experimental studies. The Al_2O_3 addition increases the resistivity, showing up a crossover from 3D Mott to the soft gap variable range hopping (*VRH*). The relative cooling power of LBMO matrix (~98.77 Jkg^{-1}, $H = 2$ T) is approximately 65 percentage of that of pure Gd (*RCP* = 153 Jkg^{-1}, $H = 2$ T). It means to achieve an active magnetic refrigerator employing LBMO will need more than one and half times the volumes of a refrigerant unit consisting of pure Gd. A good concordance is observed as simulated both resistivity and magnetization curves.

Keywords: Electrical properties; Microstructure; Point defect; Physical properties ;Magnetic properties; Magnetocaloric effect.

Journal of Magnetism and Magnetic Materials, Volume 489, 1 November 2019, 165388

Impact of aluminum on the Seebeck coefficient and magnetic properties of $La_{0.7}Ba_{0.3}MnO_3$ manganites

H.F.Mohamed[ab] A.M.Ahmed[a] A.K.Diab[a] Esraa Y.Omar[a]

[a]Physics Department, Faculty of Science, Sohag University, 82524 Sohag, Egypt

[b]Key Laboratory of Materials for High Power Laser, Shanghai Institute of Optics and Fine Mechanics, Chinese Academy of Sciences, Shanghai 201800, China

Abstract: The effect of aluminum on $(La_{0.7}Ba_{0.3}MnO_3)_{1-x}/(Al_2O_3)_x$ composites is investigated based on their crystal structure, thermoelectric power and magnetic properties. The X-ray diffraction process reveals that the composite still exhibits a rhombohedral perovskite structure($R\bar{3}C$)of all composites. The thermoelectric power data satisfies the Magnon and Phonon-drag models in the low-temperature range, and the smaller Polaron conduction mechanism in the high-temperature range. The power factor values decrease with Al content and the $x = 0.025$ record the highest value. All composites undergo ferromagnetic to paramagnetic transition at a certain temperature T_C. The AC susceptibility values decrease with the increasing Al content.

Keywords: Composite materials; Solid-state reactions ; Crystal structure ;Thermoelectric ; Magnetization

Chemical Physics Letters Volume 726, July 2019, Pages 22-28

Modelling of high-efficiency substrate CIGS solar cells with ultra-thin absorber layer

A S Mohamed[1,2] H A Mohamed[3]

[1]Department of Physics, College of Sciences, King Saud University, Riyadh 11451, Saudi Arabia

[2]Physics Department, Faculty of Science, Al-Azhar University, Nasr City, Cairo, Egypt

[3]Physics Department, Faculty of Science, Sohag University, Sohaˆg 82524, Egypt

Abstract: Solar cells based on Cu(In,Ga)Se2 (CIGS) are very promising thin-film solar cells due to their high absorptioncoefficient and appropriate optical band gap. In this work, a model of substrate thin-film solar cell of structure ZnO:Al/CdS/CIGS/Mo/glass has been established to estimate the cell parameter of ultra-thin absorber layer. The quantitativeassessment of the optical losses due to reflection at interfaces and absorption in window layer (ZnO:Al) and buffer layer(CdS) as well as the recombination losses at front and rear surface of CIGS layer has been studied. The optical losses arecarried out based on the optical constants of the used materials, and the recombination losses are carried out in terms of theparameters of the absorber layer. The effect of antireflection coating and reflectivity from metal electrode on the shortcircuitcurrent density and hence on the cell efficiency has been studied. It has been shown that the optical losses can prevent 30% of the incident photons from reaching the absorber layer at 150 nm thickness for each of the ZnO:Al and CdSlayers. The antireflection coating of 100 nm thickness is capable of increasing JSC by 8%. High efficiency of 19.56% hasbeen obtained at 1 lm thickness of CIGS layer under certain parameters of the used materials, and this efficiency can reach20.22% at 100% reflectivity from the back contact.

Radioactivity Concentrations in Dust and Soil of Enhanced Naturally Occurring Radionuclides and their Transfer Factors to Urban Trees in Phosphate Polluted Areas

M. El-Zohry & M. H. El-Zayat
Physics Department, Faculty of Science, Sohag University, Sohag, Egypt

A survey was carried out to determine the activity concentration levels from the naturally occurring radionuclides (226Ra, 232Th, and 40K) in four different areas affected at various degrees by TE-NORM activity (Al-Nasr quarry for phosphate) using The High Purity Germanium Detector (HPGD) taking into account the background level. The average activity concentration levels due to radionuclides were measured for soil, dust and urban trees leaves (Eucalyptus globulus) samples collected from these areas. The transfer factors of radionuclides (226Ra, 232Th and 40K) from soil and dust to plant (Eucalyptus globulus) for these areas were measured. It was found that the activity concentration of 40K, 232Th, and 226Ra radionuclides varies according to the variations of the areas. Samples of area (4) showed lower 226Ra and 232Th concentrations than other areas. Area (1) which is close to the source of pollution showed the highest values for 226Ra activity concentration. Leaves of E. globulus exhibited different accumulation coefficients according to the distance from the quarry. The transfer factors of radionuclides (226Ra, 232Th and 40K) are given to make rough estimates of the two main mechanisms of radionuclide accumulation; atmospheric deposition and root uptake of the urban trees (Eucalyptus globulus). The relationship between radionuclides concentrations in leaf, deposited dust and soil samples was estimated using Pearson coefficients.

Keywords: Transfer factor / Radionuclide / Urban trees /Atmospheric deposition
Arab J. Nucl. Sci. Appl., Vol. 52, 4, 93-99 (2019)

The Annual Effective Dose of Natural Radioactivity Intake from Animal Products Consumption in Phosphate Polluted Area

Abdelmonem AM[1,2], El-Zohry M[3] El-Zayat MH[4]
[1]Department of Physics, Faculty of Science and Arts, University of Jouf, Post Office 207, Al-Jouf, Kingdom of Saudi
[3]Physics Department, Faculty of Science, Sohag University, Sohag, Egypt

Abstract: Due to the close correlation between environmental radiation protection and human health protection, the normal radiological activity of 226Ra, 232Th, and 40K were measured in samples of beef and milk as an animal products. The measurements were performed using a gamma spectrometer to measure those animal products collected from four different regions, namely Mahammid, Cap, Helal and Nesrab in Upper Egypt. The uptake of these radionuclides was estimated from animal food, clover, straw, and water. Results showed that the concentration of 226Ra, 232Th was lower than the permissible values. The total annual dose of natural radionuclides was estimated as a result of the consumption of the population in those areas contaminated with phosphates for animal products. The total effective annual dose of beef consumption was estimated are 1.868, 1.889, 1.644, 1.756 µSv/yr in the studied areas respectively. Since the concentration of radionuclides 226Ra, 232Th, 40K in milk is higher than in beef, the total annual effective dose of milk consumption was higher than beef consumption. The effective annual dose was less than the annual permissible dose for the public. The obtained results indicating that a safe consumption of an animal products in the area under investigation.

Keywords: Radioactivity; Concentration ratio; Animal products; Annual effective dose; Health risk
J Nucl Ene Sci Power Generat Technol 2019, 8:1

Inactivation by helium cold atmospheric pressure plasma for Escherichia coli and Staphylococcus aureus

Khaled Lotfy[1,2], Sayed Mohammed Khali l[3,4] , Hany Abd El-Raheem[5]
[1]Department of Biology, Faculty of Science, Branch of Tayma, Tabuk University, Tabuk, Saudi Arabia
[2]King Marriott Higher Institute of Engineering & Technology, Alexandria, Egypt
[3]Physics Department, Faculty of Science, Sohag University, 82524 Sohag, Egypt
[4]University College, Umm Al-Qura University, Alqunfadah, Saudi Arabia
[5]Center for Materials Science, Zewail City of Science and Technology, October Gardens, 6th of October City, Giza, Egypt

Abstract: A helium cold atmospheric pressure plasma jet (HCAPPJ) driven by a commercial neon power supply was designed and utilized for inactivation bacteria. The generated reactive spices by HCAPPJ were investigated by optical emission spectroscopy. The reactive species of OH, OI, OI, $N2^{1+}$, $N2^{1+}$ and He were identified in the UV–Vis wavelength region. The reactive species was not detected between 200 nm and 300 nm, as the flow rate of helium gas increased that led to the plasma temperature reducing to a value near to the room temperature. In this work, we studied the impact of HCAPPJ on Gram-positive and Gram-negative bacteria. The survival amounts of the two types of bacteria were decreased vastly when the rate flow rate was equal to 10 L/min.

Keywords: Cold plasma · Optical emission spectroscopy · Reactive species · Inactivation bacteria.
Journal of Theoretical and Applied Physics 2019, https://doi.org/10.1007/s40094-019-00362-4

Enhanced thermoelectric figure of merit in Bi-containing Sb_2Te_3 bulk crystalline alloys

M. Adam[1, 2], A. El-Khouly[1, 3], A. P. Novitskii[1], E.M.M. Ibrahim[2], A. V. Kalugina[1], D. S. Pankratova[2], A. I. Taranova[3], A. A. Sakr[3], A. Trukhanov[1], M. M. Salem[1], V. Khovaylo1[4],
[1]National University of Science and Technology, MISiS, Moscow 119049, Russian Federation
[2]Physics Department, Faculty of Science, Sohag University,82524 Sohag, Egypt
[3]Physics Department, Faculty of Science, Damanhour University, Damanhour, Egypt
[4]National Research South Ural State University, Chelyabinsk 454080, Russian Federation

Abstract: In the present work, the structural and thermoelectrical properties of $Sb_{2-x}Bi_xTe_3$ samples prepared by the usual melting method were studied. The samples were milled, pressed and then annealed under vacuum for 3 h at 250 °C. Investigations of the microstructure and surface morphology were carried out using X-ray diffraction analysis, scanning electron microscopy and energy-dispersive X-ray spectroscopy. The Seebeck coefficient and electrical and thermal conductivities were measured from 300 to 473 K. Thermopower data indicated a p-type conduction in the samples. Structural defects were present in Sb_2Te_3 during Bi addition, acting as scattering centers and leading to a decrease in thermal conductivity, thus increasing the thermopower and power factor. The power factor showed its maximum value of around 24.7 μW/cm K^2 for the sample containing the highest Bi content. High figure of merit of 1.14 was recorded for the same sample, indicating that the Bi-containing Sb_2Te_3 and the related alloys are promising materials for more efficient thermoelectric devices.

Journal of Physics and Chemistry of Solids, doi.org/10.1016/j.jpcs.2019.109262

Influence of nickel doping on the energy band gap, luminescence, and magnetic order of spray deposited nanostructured ZnO thin films

H. Ali[a], A.M. Alsmadi[b,c], B. Salameh[b, d], M. Mathai[b], M. Shatnawi[c], N.M.A. Hadia[a], E.M.M. Ibrahim[a]

[a]*Department of Physics, Sohag University, 82524, Sohag, Egypt*

[b]*Department of Physics, Kuwait University, 13060, Safat, Kuwait*

[c]*Department of Physics, The Hashemite University, Zarqa, 13115, Jordan*

[d]*Department of Applied Physics, Tafila Technical University, Tafila, Jordan*

Abstract: We synthesized Ni doped ZnO thin films, ZnxNi1-xO ($0.0 \leq x \leq 0.1$), using spray pyrolysis deposition and performed a systematic study on their crystal structure, electronic, photoluminescent properties, and magnetic order. X-ray diffraction analysis showed that all nanostructured films under investigation are crystalized in a single phase wurtzite structure (space group P63mc), with a preferred orientation along (002) plane. The phase purity and the successful incorporation of Ni dopants into the ZnO lattice were also confirmed by the x-ray photoelectron spectroscopy (XPS), Ultra Violet-Visible, and Energy Dispersive X-ray spectroscopy measurements. The XPS results indicated that Ni ions are in 2^+ oxidization state in all doped films. Photoluminescence (PL) spectroscopy showed strong emission peak in the UV region and multi-components emission peak in the visible luminescence, which is ascribed to deep-level emissions by different types of intrinsic defect states. Both XPS and PL spectroscopy clearly showed significant enhancement in the oxygen vacancy (V_O) concentration by increasing the Ni doping. The saturation magnetization and coercivity also increase with Ni doping, indicating a strong correlation between the concentration of V_O defects, and the observed magnetic order in the doped films. In addition, a red shift in the energy gap is found with Ni doping and is attributed to the sp-d exchange interaction, which is mediated by the V_O defects in the ZnO lattice.

Journal of Alloys and Compounds, doi.org/10.1016/j.jallcom.2019.152538

Magnetic Sm-BFO and Ce-BFO nanoflakes as protective coating layers for C-steel in acidic chloride environments

Mai M. Khalaf[a,b], Hany M. Abd El-Lateef [a,b], G. Farghal[c], E.M.M. Ibrahim[c]

[a]*Department of Chemistry, College of Science, King Faisal University, Al Hufuf, 31982 Al Hassa, KSA*

[b]*Chemistry Department, Faculty of Science, Sohag University, Sohag-82524, Egypt*

[c]*Physics Department, Faculty of Science, Sohag University, Sohag-82524, Egypt*

Abstract: This investigation suggests a straightforward method for the C-steel coating by two different doped $BiFeO_3$ (BFO) nanomaterials, specifically Ce and Sm doped BFO nanoflakes for protection against corrosion. The Ce and Sm doped BFO nanoflakes were prepared by sol–gel process and the C-steel was coated by the dip coating method. Influences of the number of layers and surfaces morphology of Ce-and Sm-BFO nanoflakes on the corrosion resistance of coated C-steel were studied. Different techniques such as FT-IR; X-ray diffraction and scanning electron microscopy were performed in order to describe the coatings structure. Moreover, the electrical and magnetic properties were also examined. Electrochemical impedance spectroscopy (EIS) and potentiodynamic measurements (PDP) were utilized to investigate the corrosion protection execution in HCl solution. Both samples are weak ferromagnetic ordering and have a semiconductor feature. It was found that the C-steel corrosion can be controlled by coating with Ce-and Sm-BFO nanoflakes. The corrosion protection results indicated that the efficiency of Sm-BFO nanoflakes as a corrosion protective material is very high compared to that of Ce-BFO nanoflakes due to the smooth surface of Sm-BFO and rough mesoporous surface of Ce-BFO as shown in SEM results.

Sonochemically synthesized Ni-doped ZnS nanoparticles: structural, optical, and photocatalytic properties

A. A. Othman[1], M. A. Osman[1], Manar A. Ali[1], W. S. Mohamed[2,3], . M. M. Ibrahim[2]

[1]Department of Physics, Faculty of Science, Assiut University, Assiut 71516, Egypt

[2]Physics 2Department, Faculty of Science, Sohag University, Sohâg 82524, Egypt PhysicsDepartment,

[3]College of Science, Jouf University, Al-Jouf, P.O. Box 2014, Sakaka, Saudi Arabia

Abstract: In the present work, we investigate the effect of Ni doping on the crystallite size (D_{hkl}), optical band gap (E_g^{opt}), Photoluminescence emission (PL) behavior, as well as the photocatalytic degradation efficiency of methylene blue (MB) by ZnS nanoparticles (NPs) catalyst. Undoped and Ni-doped ZnS NPs at Ni concentrations of 2, 4, 6, 8, and 10% are successfully synthesized with average D_{hkl} from 2.75 to 3.76 nm by the sonochemical technique. X-ray diffraction (XRD) patterns and high-resolution transmission electron microscope (HRTEM) images of all samples exhibit pure zinc-blende type of ZnS cubic structure. The increase in Ni content up to 4% results in an increase in the D_{hkl} and unit cell volume (V) accompanied by a decrease in E_g^{opt}. Meanwhile, a further increase in Ni content above 4% leads to a decrease in D_{hkl} and V and an increase in E_g^{opt}. The deconvoluted PL emission spectrum of the undoped sample at the excitation wavelength (λ_{ex}) of 325 nm reveals emission bands centered at 3.41, 3.16, 2.89, and 2.26 eV, which are red-shifted with increasing λ_{ex} to 370 nm. It is observed that the PL emission intensity is quenched with increasing Ni content without any noticeable change in the PL peak position. Ni-doped ZnS catalyst with 2% Ni exhibits maximum photo-degradation efficiency of 52.23% with a rate constant of 0.00396 min^{-1}. The obtained results demonstrate that Ni doping can tune the optical band gap and photocatalytic efficiency of ZnS NPs that make it applicable for many optoelectronic applications.

Journal of Materials Science: Materials in Electronics

Enhanced magnetic and DC electrical properties of Sm-doped $Bi_2Fe_4O_9$ nanoplates synthesized by a sol-gel method

E.M.M. Ibrahim[1*], G. Farghal[1], Mai M. Khalaf[2], Hany M. Abd El-Lateef[2]

[1]Physics Department, Faculty of Science, Sohag University, Sohag-82524, Egypt

[2]Chemistry Department, Faculty of Science, Sohag University, Sohag-82524, Egypt

Abstract: In this work, $Bi_{2-x}Sm_xFe_4O_9$ (x=0.0, 0.02, 0.06, 0.08, 0.1) nanoplates with an average thickness of 62-125 nm were synthesized using a sol-gel method. The samples were characterized by X-ray diffraction, Fourier transform infrared spectroscopy, and scanning electron microscopy. The magnetic measurements show that the nanoplates have weak ferromagnetic ordering. The saturation magnetization of the nanoplates increases as the Sm content increases. The DC electric transport properties were studied by measuring the temperature dependence of the resistivity in the temperature range 300 - 680 K. The materials show typical semiconductor features, and the conduction mechanisms are governed by electron and small polaron hopping in the low and high temperature measurement ranges, respectively. The Sm doping results in a significant enhancement in the electrical conductivity of the $Bi_2Fe_4O_9$ nanoplates.

NANO,

Linear and Non-linear Optical Parameters of Diluted Magnetic Semiconductor CdS0.9Mn0.1 Thin Film: Influence of the Film Thickness

A.M. ABDELRAHEEM,[1] M.I. ABD-ELRAHMAN,[1,6] MANSOUR MOHAMED,[1,2] N.M.A. HADIA,[3,4] E.R. SHAABAN[5]

[1]Physics Department, Faculty of Science, Assiut University, Assiut 71516, Egypt.
[2]Physics Department, Faculty of Science, University of Hail, Hail, Saudi Arabia.
[3]Physics Department, College of Science, Jouf University, P.O. Box 2014, Sakaka, Saudi Arabia.
[4]Physics Department, Faculty of Science, Sohag University, Sohaˆg 82524, Egypt.
[5]Physics Department, Faculty of Science, A1-Azhar University, Assiut 71542, Egypt.

The optical properties of CdS0.9Mn0.1 thin film with different thicknesses (d = 300, 450, 600, 750, 900 and 1000 nm) were explored. The Swanepoel method was employed to calculate the thickness of the studied films. Analyses of the absorption spectra indicated the existence of allowed indirect and direct transition mechanism in the CdS0.9Mn0.1 thin films. Both the absorption coefficient and optical band gap decreased while Urbach energy increased as the film thickness increased. The Wimple–DiDomenico single oscillator model was used to describe the dispersion of the refractive index. The film thickness dependence of the dispersion parameters was studied. The optical dielectric constants, optical conductivity, electrical susceptibility, and non-liner optical parameters such as the refractive index, first-order susceptibility (vð1Þ) and third-order susceptibility (vð3Þ) were determined. The present results show that the film thickness is an important factor which affected the optical parameters. Key words: Thin film, CdS0.9Mn0.1, optical constants, optical dielectric, Swanepool methods, nonlinear parameters

Journal of ELECTRONIC MATERIALS

Radiation shielding, mechanical and tribological properties of treated AISI304L using H2/N2 rf plasma

S U El-Kameesy , F M El-Hossary , M M Eissa , A A Abd El-Moula , Samah A Al-Shelkamy, A Saeed

Abstract: The electro-slag re-melting technique was used to produce locally two standard stainless steel samples, AISI304L and AISI316L. The shielding properties of both neutrons and gamma radiations were determined using He-3 and NaI(Tl) detectors. A mixture of hydrogen and nitrogen gases (1:1) was used to investigate the effect of rf plasma surface engineering on properties of austenite stainless steel AISI304L which is used in many parts of nuclear power plant. The X-ray diffraction technique was used for recognizing the structural phases on the studied austenite stainless steel samples. The rf plasma process was performed for half an hour at stable gas pressure and water cooling rate. As a result of the rf plasma surface engineering process, enormous enhancement was achieved in surface microhardness, tribological properties and remarkable increase in the absorption cross section for slow neutrons. Moreover, the gamma ray attenuation properties for the HN304L sample is to great extent comparable with those of AISI316L and AISI304L austenite stainless steel samples. As a consequence, the obtained results give a further support in favor of the rf plasma engineering in the nuclear domain.

Journal of Physics: Conference Series, Volume 1253, conference 1

Tuning the optical, electrical resistivity and structural properties of DC magnetron sputtered aluminum zinc oxide films by changing the oxygen flow rate

Mohammed S. Alqahtani[1], N. M. A. Hadia[2,3], S. H. Mohamed[3,4]
[1]Department of Physics and Astronomy, King SaudUniversity, Riyadh 11451, Saudi Arabia
[2]Department of Physics, College of Science, Jouf University,Jouf, Saudi Arabia
[3]Physics Department, Faculty of Science, Sohag University,Sohag 82524, Egypt
4Department of Physics, Faculty of Science, IslamicUniversity of Madinah, Medinah, Saudi Arabia

Abstract:
Thin films of aluminum zinc oxide (AZO) were fabricated by DC reactive magnetron sputtering from 50 wt% Al/Zn metallic target. The structure and optical constants of AZO films were controlled by changing the oxygen (O_2) flow rate. X-Ray diffraction revealed that the addition of oxygen transforms the crystalline nature of the metallic Al/Zn to completely amorphous film at 4.5 sccm. The film density, surface roughness and deposition rate were evaluated from X-ray reflectometry measurements and they were found to decrease strongly upon transformation from metallic to oxidic sputtering mode. The optical constants were extracted from the ellipsometry measurements. As O_2 flow increased from 4.5 to 30 sccm, the optical band gap increased from 4.74 to 5.33 eV whereas the refractive index decreased simultaneously. Low resistivity films were obtained as O_2 flow increased from 0 to 4 sccm whereas insulating films were obtained for O_2 flows above 4 sccm. The results indicated that by regulating the oxygen flow diverse ZAO films with diverse chemical stoichiometries and properties can be tuned.
Applied Physics A 125 (2019) 776.

Chemistry

A robust in vitro Anticancer, Antioxidant and Antimicrobial Agents Based on New Metal-Azomethine Chelates Incorporating Ag(I), Pd (II) and VO (II) Cations: Probing the Aspects of DNA Interaction

Ahmed M. Abu-Dief[a,b], Laila H. Abdel-Rahman[a], Azza A. Hassan Abdel-Mawgoud[a]

[a]*Chemistry Department, Faculty of Science, Sohag University, Sohag, 82524 Egypt*

[b]*Chemistry Department, Faculty of Science, Taibah University, Madinah, Saudi Arabia*

A novel azomethine ligand (HNAP) [HNAP = 1-(Pyridin-3-yliminomethyl)-naphthalen-2-ol] and its Ag(I), Pd (II) and VO (II) chelates have been synthesized and structurally inspected using a wide range of spectroscopic and analytical tools, including infra-red (IR), ultraviolet-visible (UV-Vis) and 1H NMR spectroscopy techniques, CHN analysis, molar conductance, magnetic susceptibility, and thermogravimetric analysis. The molar conductance measurements reveal that the chelates are non-electrolytes. The thermal behavior of the investigated metal chelates shows that the hydrated, coordinated water molecules and the anions are removed in successive steps followed immediately by decomposition of the ligand in the subsequent steps. The activation thermodynamic parameters are calculated from the TG curves and discussed. Complexes formation study via continuous variation m molar ratio has been investigated, and results were consistent to those found in the solid complexes with a ratio of (M:L) as (1:1) or 1:2 (M:L) molar ratio for all the monolithic and bi-valent metal complexes with square planar for Pd (II), and Ag(I) cations while, square pyramidal geometry for VO (II) cation. DFT calculations for the titled different metal-chelates have been studied and showed a good correlation with the experimental data. The prepared compounds had been checked In vitro towards numerous sorts of plant pathogenic fungi and bacteria to evaluate their antimicrobial properties and compared with some known antibiotics. Significantly, all the complexes show excellent antimicrobial activity against various strains of bacteria and fungi, including both Gram-negative and Gram-positive bacteria. Besides, the complexes exhibited high cytotoxicity against various carcinoma cell lines, including HCT-116, MCF-7, and HepG-2. Moreover, the effect of the new synthesized compounds as antioxidants was determined by reduction of 1,1-diphenyl-2-picryl hydrazyl (DPPH) and compared with that of Vitamin C. Furthermore, the binding interactions of the complexes with CT-DNA were explored using UV-Vis spectroscopy, viscosity and gel electrophoreses measurements. They cooperatively bind to DNA possibly through intercalations. The binding ability of the complexes was shown as HNAPAg > HNAPPd > HNAPVO complex.

Applied Organometallic Chemistry 2019, e5373

Kinetic study of humic acid adsorption onto smectite: The role of individual and blend background electrolyte

Laila H. Abdel-Rahman[1] ,Ahmed M. Abu-Dief[1] Badriah Saad Al-Farhan[2] Doaa Yousef[3] and Mohamed E.A. El-Sayed[3]

[1]*Chemistry Department, Faculty of Science, Sohag University, 82534 Sohag, Egypt*

[2]*Chemistry Department, Faculty of Girls for Science, King Khalid University, Abha, King Saudi Arabia*

[3]*Soils, Water, and Environmental Research Institute, Agriculture Research Center, El-Giza, Egypt*

Many factors can affect the natural organic matter adsorption on clay, such as pH and ionic strength. Blended background electrolyte could be causing better simulation to natural effects. Therefore, kinetic study of humic acid (HA) adsorption onto smectite has been studied under various conditions. Impact of pH and individual and blend background electrolyte with different ionic strength concentration on the rate of adsorption has been investigated. The rate and amount of adsorbed HA on smectite improved with raised background electrolyte concentration, declining pH, and in existence Ca^{2+}. The rate of adsorption order was in the presence of $CaCl_2$ > blend ($CaCl_2$ and KCl) > KCl. The adsorption isotherm was L-shap in the presence of $CaCl_2$ and KCl while was S-shap in presence blend ($CaCl_2$ and KCl). Moreover, the data revealed that the adsorption behavior of HA might be pronounced more obviously by Freundlich model than Langmuir. Two kinetic models were applied to assess the rate constants and kinetic data. The results clarified that HA adsorption on smectite was following to pseudo second order model under various conditions.

AIMS Materials Science, 6(6): 1176–1190.

Synthesis and characterization of new Cr(III), Fe(III) and Cu(II) complexes incorporating multi-substituted aryl imidazole ligand: Structural, DFT, DNA binding, and biological implications

Ahmed M.Abu-Dief[ab], Laila H.Abdel-Rahman[a], Antar A.Abdelhamid[a], Adel A. Marzouk[c], Mohamed R.Shehata[d], Mohamed AbdelaalBakheet[a], Omar A.Almaghrabi[e], AymanNafady[f]

[a]Department of Chemistry, Faculty of Science, Sohag University, 82524, Sohag, Egypt
[b]Chemistry Department, Faculty of Science, Taibah University, Madinah, Saudi Arabia
[c]Pharmaceutical Chemistry Department, Faculty of Pharmacy, Al Azhar University, Egypt
[d]Chemistry Department, Faculty of Science, Cairo University, Giza, Egypt
[e]University of Jeddah, Department of Biological Sciences, Faculty of Science, Jeddah, Saudi Arabia
[f]Department of Chemistry, College of Science, King Saud University, Riyadh, 11451, Saudi Arabia

Designing new metal-based molecular antibiotics is an efficient approach to overcome the growing threat of antimicrobial resistance. In this paper, novel Cr(III), Fe(III) and Cu(II) complexes comprising substituted aryl imidazole ligand (MSEB), namely (2-(1-(2-hydroxyethyl)-4,5-diphenyl-1H-imidazole-2-yl)(4-bromophenol)) have been synthesized and characterized using infra-red (IR), ultraviolet-visible (UV-Vis) and 1H, 13C NMR spectroscopic techniques, together with elemental (CHN) and thermogravimetric analyses, molar conductance, and magnetic susceptibility measurements. The combined results along with the DFT calculations revealed a 1:1 (M: L) stoichiometric ratio and the complexes adopted distorted-octahedral geometries to afford $[Cr(MSEB)Cl_2(H_2O)_2]$, $[Fe(MSEB)(NO_3)_2(H_2O)_2]$ and $[Cu(MSEB)Cl(H_2O)_3]$ respectively. Biological studies showed that all complexes exhibited powerful antimicrobial activity against various strains of bacteria and fungi, S. aureus (+ve), E. coli (-ve) and P. aeruginosa (-ve) bacteria and T. Rubrum, C. albicans, and A. flavus fungi. Moreover, the three metal-complexes showed high in vitro cytotoxicity against Colon (HCT-116), Breast (MCF-7), and hepatic cellular (HepG-2) carcinoma cell lines, with MSEBCu complex being the most cytotoxic one. Finally the binding interactions of the complexes with CT-DNA were explored using UV-Vis spectroscopy, viscosity and gel electrophoreses measurements.
Spectrochimica Acta Part A: Molecular and Biomolecular Spectroscopy, 2019, 117700

Impact of Co^{2+} Substitution on Microstructure and Magnetic Properties of $Co_xZn_{1-x}Fe_2O_4$ Nanoparticles

W. S. Mohamed[1,2], Meshal Alzaid[1], Mohammed S. M. Abdelbaky[3], Zakariae Amghouz[4], Santiago García-Granda[3] andAhmed M. Abu-Dief[5,6]

[1]Physics Department, College of Science, Jouf University, Al-Jouf, Sakaka P.O. Box 2014, Saudi Arabia
[2]Physics Department, Faculty of Science, Sohag University, 82524 Sohag, Egypt
[3]Departments of Physical and Analytical Chemistry, and Organic and Inorganic Chemistry, University of Oviedo-CINN, 33006 Oviedo, Spain
[4]Department of Materials Science and Metallurgical Engineering, University of Oviedo, Campus Universitario, 33203 Gijón, Spain
[5]Chemistry Department, Faculty of Science, Sohag University, 82524 Sohag, Egypt
[6]Chemistry Department, Faculty of Science, Taibah University, Madinah P.O. Box 344, Saudi Arabia

In the present work, we synthesized $Co_xZn_{1-x}Fe_2O_4$ spinel ferrite nanoparticles (x= 0, 0.1, 0.2, 0.3 and 0.4) via the precipitation and hydrothermal-joint method. Structural parameters were cross-verified using X-ray powder diffraction (XRPD) and electron microscopy-based techniques. The magnetic parameters were determined by means of vibrating sample magnetometry. The as-synthesized $Co_xZn_{1-x}Fe_2O_4$ nanoparticles exhibit high phase purity with a single-phase cubic spinel-type structure of Zn-ferrite. The microstructural parameters of the samples were estimated by XRD line profile analysis using the Williamson–Hall approach. The calculated grain sizes from XRPD analysis for the synthesized samples ranged from 8.3 to 11.4 nm. The electron microscopy analysis revealed that the constituents of all powder samples are spherical nanoparticles with proportions highly dependent on the Co doping ratio. The $Co_xZn_{1-x}Fe_2O_4$ spinel ferrite system exhibits paramagnetic, superparamagnetic and weak ferromagnetic behavior at room temperature depending on the Co^{2+} doping ratio, while ferromagnetic ordering with a clear hysteresis loop is observed at low temperatures (5K). We concluded that replacing Zn^{2+} ions with Co^{2+} ions changes both the structural and magnetic properties of $ZnFe_2O_4$ nanoparticles
Nanomaterials 2019, 9(11), 1602.

Novel Di- and Tri-azomethine Compounds as Chemo Sensors for the Detection of Various Metal Ions

Ahmed M. Abu-Dief and Azza A. Hassan Abdel-Mawgoud Laila H. Abdel-Rahman
Department of Chemistry, Faculty of Science, Sohag University, 82524, Sohag, Egypt

In this study, HNA imine compound was synthesized by a simple one-pot condensation of 2-hydroxy-1-naphthaldhide with 2-amino benzoic acid in 1: 1 ratio and HNAP imine compound derived from 2-hydroxynaphthaldhide and 3-amino pyridine. Results of the newly synthesized compounds established by elemental analyses, FT-IR, 1H-NMR, 13C-NMR and electronic spectral studies experiments were consistent with their chemical structures. The theoretical DFT calculations were applied to verify the molecular geometry of the investigated chemosensors. The sensor properties of all prepared imines were examined upon addition of the metal ions, such as Cr (III), Fe (II), Co (II), Ni (II), Zn (II), Cu (II), Mn (II), VO (II) and Pd (II). The interactions between receptors and ions are easily monitored by UV-visible spectroscopy. The HNA receptor showed color changes from yellow to intense deep orange color for Pd (II), a brown color for Fe (II) and different colors for other ions. Where the HNAP receptor showed color changes from pale yellow to intense deep green color for Co (II), and different colors for other ions.

Int. J. Nano. Chem. 5, No. 1, 1-17 (2019)

A Simple and Reliable Synthesis of Superparamagnetic Magnetite Nanoparticles by Thermal Decomposition of $Fe(acac)_3$

C. Toyos-Rodríguez,[1,2] J. Calleja-García,[1] L. Torres-Sánchez,[1,2] A. López,[1] Ahmed M. Abu-Dief,[3] A. Costa,[4] L. Elbaile,[2] R. D. Crespo,[2] J. S. Garitaonandia,[5] E. Lastra,[1] J. A. García,[2] and F. J. García-Alonso[1]
[1]Departamento de Química Orgánica e Inorgánica, c/ Julián Clavería, 8, 33006 Oviedo, Spain
[2]Departamento de Física, Universidad de Oviedo, c/ Calvo Sotelo s/n, 33007 Oviedo, Spain
[3]Chemistry Department, Faculty of Science, Sohag University, 82524-Sohag, Egypt
[4]Departamento de Química Analítica y Química Física, c/ Julián Clavería, 8, 33006 Oviedo, Spain
[5]Fisika Aplicatua II Saila, Euskal Erriko Universitatea, Alameda Urquijo s/n 48013 Bilbao, Spain

Magnetic nanoparticles have been largely proposed as means of technological tools due to its value in different fields, especially in biomedicine. Herein, we present a robust, highly reproducible and low-cost method to obtain superparamagnetic magnetite nanoparticles (MNP-II) of about diameter by thermal decomposition of $[Fe(acac)_3]$ in a one-pot, two-step method. In the first step, magnetite nanoparticles (MNP-I) of lower size, with a saturation magnetization (M_S) of 65 emu/g and a coercive field () of 1 Oe are obtained. In the second step, those particles MNP-I act as seeds for the final MNP-II which presents a saturation magnetization of 70 emu/g and a coercive field of 12 Oe

Journal of Nanomaterials, Volume 2019, Article ID 2464010, 10 pages, 2019

Synthesis, catalysis, antimicrobial activity, and DNA interactions of new Cu(II)-Schiff base complexes

Mohamed Shaker S. Adam, Laila H. Abdel-Rahman,Ahmed M. Abu-Dief, Nahla A. Hashem
Chemistry Department, Faculty of Science, Sohag University-82524, Egypt

Structural features and catalytic activities of five ternary copper (II)-Schiff base complexes are investigated. The ligands are derived from 3-methoxysalicylaldehyde (MS) or 4-diethylaminosalicylaldehyde (DS) and amino acids {L-phenylalanine (Phe), L histidine (His) or DL-tryptophan (Trp)}, as primary ligands, and 2,4′-bipyridyl (DP) as a secondary ligand. Cu(II)-complexes are characterized by various physicochemical tools. The catalytic efficiency of Cu(II)-complexes is studied in the oxidation of benzyl alcohol by an aqueous H2O2 in different reaction conditions. Temperature and catalyst features are involved in order to obtain the optimized catalytic oxidation conditions of benzaldehyde production. The Schiff base ligands and their ternary complexes are screened for their antimicrobial activities in various types of fungi and bacteria. The interaction between Cu(II)-complexes and (CT-DNA) was examined by employing various techniques, including viscosity, spectral and gel electrophoreses studies.
Inorganic and Nano-Metal Chemistry, 2019

Catalytic Potential of Mononuclear Cr(III)-Imine Complexes for Selective Oxidation of Benzyl Alcohol by Aqueous H_2O_2

Laila H. Abdel-Rahman,[1] Mohamed Shaker S. Adam,[1,2] Ahmed M. Abu-Dief,[1] and Azza A. H. Abdel-Mawgoud[1]
[1]Chemistry Department, Faculty of Science, Sohag University, 82534 Sohag, Egypt
[2]Department of Chemistry, College of Science, King Faisal University, P.O. Box 380, 31982 Al-Ahsa, KSA

Chromium(III) complexes were derived, as tri- and tetradentate imine chelates, from 2-hydroxy-1-napthaldehyde or 3-ethoxysalicylaldehyde with 2-aminophenol or 1,2-phenylenediamine. The catalytic potentials of Cr(III)-imine chelates were probed and tested in the chemoselective benzyl alcohol oxidation to benzaldehyde (BA) within an eco-friendly terminal oxidant (i.e., H_2O_2). The effect of various applicable parameters in the catalytic systems (e.g., solvents, temperature, and catalyst molar ratios) was studied. From the obtained results, it is found that the most favored and suitable solvent applied is acetonitrile at best reaction conditions; temperature 80 ℃ after 4 h. The mechanistic aspects of the Cr(III)-catalyzed oxidation were tentatively described and discussed based on electron and oxygen transfer processes.
Journal of Transition Metal Complexes, 2 (2019), art236077

Novel azomethine Pd (II)- and VO (II)-based metallo-pharmaceuticals as anticancer, antimicrobial, and antioxidant agents: Design, structural inspection, DFT investigation, and DNA interaction

Ahmed M. Abu-Dief[a], Laila H. Abdel-Rahman[a], Mohamed R. Shehata[b], Azza A. Hassan Abdel-Mawgoud[a]

[a]*Chemistry Department, Faculty of Science, Sohag University-82524, Egypt*
[b]Chemistry Department, Faculty of Science, Cairo University, Giza, Egypt

The new NO bidentate imine ligand, namely, (2-[(3-nitro-benzylidene)-amino]-benzoic acid) (NBA) imine ligand (L), and its Pd (II) and VO (II) complexes have been synthesized and characterized by utilizing different physiochemical methods including elemental analyses, Fourier transform infrared (FT-IR), nuclear magnetic resonance (NMR), molar conductance, and magnetic susceptibility measurements. The stability constant of these complexes has also been determined. In studies of these complexes, they were found to have [M(L)] composition where the ligand acts as a bidentate and coordinates with the various metal ions through azomethine and one oxygen atom. Moreover, the suggested geometrical structure of Pd (II) and VO (II) complexes is square planar and a distorted square pyramid, respectively. Density functional theory (DFT) calculations for the different metal complexes were studied and show a good agreement with the experiment data. The minimum inhibitory concentration method has been applied to evaluate the in vitro antimicrobial activity. Furthermore, the interaction of calf thymus DNA with the metal-imine chelates has been assessed, and Pd (II) complex showed the strongest interaction with DNA for a binding constant value of (9.72 × 104 kcal mol−1). The cytotoxic activity of the new metal chelates has been evaluated against three human cancer cell lines (hepatic carcinoma HepG2 cells, breast carcinoma cells MCF-7, and colon carcinoma cells HCT-116). It has found that NBAPd complex exhibited a significant decrease in the time and dose of the cell viability than did the reference drug vinblastine. The antioxidant activity of the tested compounds was determined and compared with that of vitamin C as a standard drug. It has been found that the metal complexes exhibit higher activity than the free ligand. The finding from this investigation revealed that the new compounds are considered to be prospective antibiotic and anticancer agents.

Journal of physical organic chemistry, 32, 12, 2019, e4009

Design, synthesis and structural inspection of some novel di- and tri-azomethene compounds as chemo sensors for the detection of various metal ions

Laila H. Abdel-Rahman, Ahmed M. Abu-Dief, Azza A. Hassan Abdel-Mawgoud

Chemistry Department, Faculty of Science, Sohag University-82524, Egypt

In this study, NBA imine compound was synthesized *via* an easy one-pot condensation of 3-nitro-benzaldyhide with 2-amino benzoic acid in 1:1 ratio and DAPH imine compound derived from 2,6-diacetyl pyridine and phenyl hydrazine hydrochloride . Consequences of the newly synthesized compounds hooked up with the aid of FT-IR, elemental analyses, ^{13}C-NMR,1H-NMR and digital spectral research. Experiments had been consistent with their chemical structures. Theoretical DFT calculations had been implemented to confirm the molecular geometry of the investigated chemosensors. The sensor property of all organized imines had been tested upon addition of the metal ions, consisting of Cr(III), Fe(II), Co(II), Ni(II), Cu(II), Zn(II), Mn(II), VO(II) and Pd(II). The interactions among receptors and ions are effortlessly monitored with the aid of UV-visible spectroscopy.DAPH receptor confirmed colour modification from blood red to excessive deep green color to Co(II), a yellow color to Cu(II) and different colors to different ions. Where the NBA receptor showed color modification from light yellow to excessive deep orange color to Fe(II), pale orange to Pd(II) and different colors for other ions.

Ann. Chem. Sci. Res. 1(4).ACSR.000518.2019.

Some new Ag(I), VO(II) and Pd(II) chelates incorporating tridentate imine ligand: Design, synthesis, structure elucidation, density functional theory calculations for DNA interaction, antimicrobial and anticancer activities and molecular docking studies

Laila H. Abdel-Rahman Ahmed M. Abu-Dief, Mohamed R. Shehata, Faten M. Atlam, Azza A. Hassan Abdel-Mawgoud

[a]*Chemistry Department, Faculty of Science, Sohag University, 82524 Egypt*
[b]*Chemistry Department, Faculty of Science, Cairo University, Giza, Egypt*
[c]*Department of Chemistry, Faculty of Science, Tanta University, Tanta, Egypt*

Some new complexes derived from VO(II), Ag(I) and Pd(II) metal ions and HNA imine ligand (L), i.e. (2-((6-allylidene-2-hydroxycyclohexa-1,3-dienylmethylene)amino)benzoic acid), have been prepared and their structures elucidated via molar conductance measurements, elemental analyses, infrared, NMR and electronic spectra and magnetic susceptibility estimations. Moreover, stability constants of the synthesized complexes were evaluated utilizing a spectrophotometric technique. On the basis of molar conductance and elemental analyses, the metal imine chelates have structure [M(L)], where M = Pd(II), VO(II) and Ag(I). The results indicate that the prepared HNA imine ligand acts as a tridentate moiety via nitrogen atom of azomethine group and two oxygen atoms of phenolic and carboxylic groups. All the complexes are found to be monomeric with 1:1 stoichiometry with square planar geometry for Pd(II), tetrahedral geometry for Ag(I) and distorted square pyramidal for VO(II). Theoretical density functional theory calculations were applied to verify the molecular geometry of the chelators and their metal chelates. The geometry optimization results are in agreement with experimental observations. The antimicrobial properties of the prepared HNA imine ligand and its metal chelates were evaluated against numerous plant pathogenic fungi and bacteria. The results of these studies indicate that the metal complexes exhibit a stronger antibacterial and antifungal effect compared to the imine ligand. In addition, the interaction of the metal imine chelates with calf thymus DNA was observed by way of viscosity, gel electrophoreses and spectral studies. Absorption titration studies reveal that each of the complexes is an avid binder to calf thymus DNA. Also, there are appreciable changes in the relative viscosity of DNA, which are consistent with enhanced hydrophobic interaction of the aromatic rings and intercalation mode of binding. Additionally, the cytotoxic activity of the investigated compounds against various cancer cell lines shows promising results which makes them prospective compounds for antibiotic and anticancer medicament studies. Furthermore, docking studies of the prepared compounds were conducted for confirming the biological results.

Applied organometallic chemistry, 33, 4, 2019, e4699

Azomethine Metal Chelates as an Efficient Catalyst for Oxidation of Organic Compounds

Ahmed M. Abu-Dief

Chemistry Department, Faculty of Science, Sohag University, Sohag 82524, Egypt.

Azomethine ligands and their metal chelates are flexible compounds synthesized from the condensation of an amino compound with carbonyl compounds and extensively used for industrial purposes and also show a broad range of biological efficiencies including antibacterial, antifungal, antiviral, antimalarial, antiproliferative, anti-inflammatory, anticancer, anti-HIV, anthelminthic and antipyretic properties. Azomethine metal chelates show excellent catalytic activity in diversity reactions. Over the past few years, there have been many reports on their applications in homogeneous and heterogeneous catalysis. The high thermal and moisture stabilities of many azomethine metal chelates were useful attributes for their application as catalysts in reactions involving at high temperatures. Recent researches in oxidation catalysis have focused on how to employ the metal-catalyzed oxidation of organic substrates. This review concerns with the current developments for the oxidations of organic compounds.

Ann Chem Sci Res. 1(3) ACSR.000515.2019.

Antimicrobial and anticancer activities of cobalt (III)-hydrazone complexes: Solubilities and chemical potentials of transfer in different organic co-solvent-water mixtures

Ahmad Desoky M. Mohamad[1,2], M. J. A. Abualreish[1,3] and Ahmed M. Abu-Dief[2]
[1]*Chemistry Department, Faculty of Science, Northern Border University, Arar, KSA.*
[2]*Chemistry Department, Faculty of Science, Sohag University, Sohag 82524, Egypt.*
[3]*Department of Chemistry, Faculty of Science and Technology, Omdurman Islamic University, Sudan*

The present study focused on the measurement of the solubilities and the calculation of the chemical potentials of transfer of Co(III)-hydrazone complexes in mixtures of water and ethyl alcohol (EtOH), isopropyl alcohol (*i*-PrOH), or *tert*-butyl alcohol (*t*-BuOH) at 298 K, using the assumption that $\delta_m \mu^\theta Ph_4As^+ = \delta_m \mu^\theta BPh_4^-$ (TATB). A comparison between the chemical potentials of transfer of Co(III)-hydrazone complex ions with each other and with single ions is described. The change in solubility and chemical potentials of the transfer of the Co(III)- hydrazone complex ions are explained with respect to the nature of the ligand and organic solvents. The titled hydrazone ligands and their Co(III) chelates are tested for their biological antimicrobial activity against different types of bacteria (Gram-negative bacteria: *Serratia Marcescence* and *Escherichia coli*; Gram-positive bacteria: *Micrococcus Luteus*) and fungi (*Aspergillus flavus, Fusarium oxysporum* and *Getrichm candidum*). Both hydrazone ligands and their Co(III) complexes exhibit antibacterial and antifungal activities, but the Co(III)-hydrazone complexes act as more potent bactericidal agents than the hydrazone ligands and metal salt. The anticancer properties of these compounds are also tested against colon carcinoma cells and breast carcinoma cells. The Co(III)-hydrazone complexes display more significant cytotoxic activities against these cells than those of the hydrazone ligands.

Journal of Molecular Liquids, 290, 2019, 111162

Green synthesis of TiO_2 nanoparticles as an efficient heterogeneous catalyst with high reusability for synthesis of 1, 2-dihydroquinoline derivatives

Mahmoud Abd El Aleem Ali Ali El-Remaily, Ahmed M. Abu-Dief, O.M Elhady
Chemistry Department, Faculty of Science, Sohag University, Sohag 82524, Egypt.

Nano materials find wide applications due to their behavior at nano scale. TiO_2 nanoparticles (TiO_2 NPs) was synthesized using Neem leaf extract. This is simple, rapid, eco-friendly, cheaper and green tools for TiO_2 NPs synthesis using agricultural waste at lower applied temperature. Characterization of the extracted TiO_2 NPs was confirmed by XRD, SEM, EDAX, TEM, HR-TEM, SAED, and FT-IR, respectively. The catalytic activity of TiO_2 NPs was investigated in synthesis of 1,2-dihydroquinoline derivatives with excellent yields and low cost. Purification of the synthesized 1,2-dihydroquinoline derivatives carried out by easy work-up of non-chromatographic methods.

Applied organometallic chemistry, 33, 8, 2019, e5005

Iron (III)-porphyrin Complex FeTSPP as an efficient catalyst for synthesis of tetrazole derivatives via [2 + 3]cycloaddition reaction in aqueous medium

El-Remaily, M.A.E.A.A.A.,Elhady, O.M.
Department of Chemistry, Faculty of Science, Sohag University, Sohag, 82524, Egypt

The metal complex (5,10,15,20-tetrakis-(4-sulfonatophenyl)-porphyrin-iron (III) chloride (FeTSPP) was new employed in an environmentally benign protocol as an efficient catalyst for a "click" chemistry approach for the synthesis of tetrazole and guanindinyltetrazole derivatives via [2 + 3] cycloaddition reaction of nitriles and azide derivatives in aqueous medium. The synthesized compounds were obtained in excellent yield, short reaction times and a recoverable catalyst.

Applied Organometallic ChemistryVolume 33, Issue 8, August 2019, Article number e4989

Development of DNA Nanotechnology for Cancer Therapy

Ahmed M. Abu- Dief
Chemistry Department, Faculty of Science, Sohag University, Sohag 82524, Egypt.

Cancer is one of the main causes of worldwide mortality, due to the absence of precise diagnostic tools for the cancer early stages. Thus, early diagnosis, which supplies important information for therapy of cancer timely, is of great prominence for propagation of cancer cells, controlling the growth of the disease, and improving of patients survival rates. To attain the goals of early diagnosis and cancer therapy timely, nanotechnology of DNA can be effective, since it has protruded as a suitable technique for the fabrication of different nanoscale devices and structures. The eventual DNA-based nanoscale devices and structures show wonderful performance in diagnosis of cancer, owing to their small sizes, structures, high programmability and biocompatibility. In particular, the quick development of DNA nanotechnologies, like molecular association technologies, confers DNA-based nanomaterials with more intellectualization and functionalization. In DNA nanotechnology, Watson-Crick DNA molecules are arranged into variety of nanostructures in the range of 10-100nm size under special physical conditions due to electrostatic attraction between free electrons of base nitrogen and phosphate oxygen and sugar. Here, i summarize recent advances made in the development of DNA nanotechnology for the fabrication of intelligent and functional nanomaterials and highlight the potentials of this technology in diagnosis and therapy of cancer.

Determinations anomed Nanotechnol. 1(4). DNN.000517.2019.

Development, structural investigation, DNA binding, antimicrobial screening and anticancer activities of two novel quari-dentate VO (II) and Mn (II) mononuclear complexes

Laila H Abdel-Rahman, Ahmed M Abu-Dief, Azza A Hassan Abdel-Mawgoud
Chemistry Department, Faculty of Science, Sohag University, Sohag 82524, Egypt

Two novel VO(II) and Mn(II) imine chelates derived from the condensation of o-phenylenediamine (PN) with 3-ethoxysalicylaldehyde(ES) were synthesized. The prepared ESPN imine ligand and its chelates were investigated *via* different analytical and physicochemical tools. Correlation between all the obtained results, the parent ligand behaves as tetra-dentate ONNO ligand and coordinates to Mn(II) and VO(II), in octahedral and square pyramidal geometry, respectively. Also, the prepared compounds were screened for their antimicrobial activities on different pathogenic bacteria and fungi. The results show that the complexes have a stronger antimicrobial activity in comparison with its ligand. Moreover, the interaction of the prepared metal chelates with CT-DNA was detected utilizing spectral studies, viscosity and gel electrophoreses measurements. The obtained results clearly demonstrate that, the binding affinity with CT-DNA for ESPN > ESPNV complex. Furthermore, the cytotoxic activity of the tested compounds on human colon carcinoma cells, hepatic cellular carcinoma cells and breast carcinoma cells has been examined. From these results it was found that the investigated complexes have effective cytotoxicity against growth of carcinoma cells with respect of its imine ligand.

Journal of King Saud University - Science, 31, 1, 2019, 52-60

Fabrication, spectroscopic characterization, calf thymus DNA binding investigation, antioxidant and anticancer activities of some antibiotic azomethine Cu(II), Pd(II), Zn(II) and Cr(III) complexes

Ahmed M. Abu-Dief[a], Hussein M. El-Sagher[a], Mohamed R. Shehata[b]
[a]Chemistry Department, Faculty of Science, Sohag University, Sohag 82524, Egypt.
[b]Chemistry Department, Faculty of Science, Cairo University, Giza, Egypt

This study was conducted to prepare novel azomethine chelates of Cu(II), Pd(II), Zn(II) and Cr(III) with tridentate dianionic azomethine OVAP ligand 2-[(2-hydroxyphenylimino)methyl]-6-methoxyphenol. The prepared compounds were characterized using elemental analyses and spectral, conductivity, magnetic and thermal measurements. The spectroscopic data suggest that the parent azomethine ligand binds to the investigated metal ions through both deprotonated phenol oxygen and azomethine nitrogen atoms, and adopts distorted octahedral geometry in the case of Cr(III) and Cu(II) ions while tetrahedral and square planar geometries for Zn(II) and Pd(II) ions, respectively. In order to confirm the molecular geometry of the investigated azomethine chelator and its complexes, theoretical density functional theory calculations were employed. Correlation between experimental observations and theoretical calculations of geometry optimization results are in a good agreement. Absorption titration was used to explore the interaction of the investigated azomethine metal chelates with calf thymus DNA, and the binding constant as well as Gibbs free energy were evaluated. Viscosity measurements and gel electrophoresis studies suggest intercalative and replacement binding modes of the azomethine metal chelates with calf thymus DNA. Additionally, the antimicrobial activity of the complexes was screened against some pathogenic bacteria and fungi. This biological study shows that the complexes exhibit a marked inhibitory effect compared to the corresponding ligand and standard drug**s.** Furthermore, the effect of the novel compounds as antioxidants was determined by reduction of 1,1-diphenyl-2-picrylhydrazyl and compared with that of vitamin C. Finally, *in vitro* cell proliferation via MTT assay was investigated against colon carcinoma cells (HCT-116), hepatic cellular carcinoma cells (HepG-2(and breast carcinoma cells (MCF-7) to calculate the cytotoxicity of the prepared compounds. Cell proliferation is inhibited for all compounds and in a dose-dependent manner in the sequence of OVAPPd > OVAPCu > OVAPZn > OVAPCr > OVAP azomethine ligand.

Applied organometallic chemistry, 33, 8, 2019, e4943

Electrochemical methods for fabrication of polymers/calcium phosphates nanocomposites as hard tissue implants

Hany M. Abd El-Lateef[a], Ahmed H. Touny[b], Mohamed M. Saleh[c], Mahmoud M. Saleh[d]
[a]Faculty of Science, Chemistry Department, Sohag University, Sohag, Egypt
[b]Department of Chemistry, Faculty of Science, Helwan University, Helwan, Egypt
[c]Wake Forest Institute for Regenerative Medicine, Winston Salem, North Carolina 27103, USA
[d]Department of Chemistry, Faculty of Science, Cairo University, Cairo, Egypt

Developing and manipulating new biomaterials is an ongoing topic for their needs in medical uses. The evolution and development of new biomaterials, in both the academic and industrial sectors, have been encouraged due to the dramatic improvement in medicine and medical-related technologies. Due to the drawbacks associated with natural biomaterials, the use of synthetic biomaterials is preferential due to basic and applied aspects. Various techniques are involved in fabricating biomaterials. Among them are the electrochemical-based methods, which include electrodeposition and electrophoretic methods. Although electrospinning and electrospraying are not typical electrochemical methods, they are also reviewed in this article due to their importance. Many remarkable features can be acquired from this technique. Electrodeposition and electrophoretic deposition are exceptional and valuable processes for fabricating thin or thick coated films on a surface of metallic implants. Electrodeposition and electrophoretic deposition have some common positive features. They can be used at low temperatures, do not affect the structure of the implant, and can be applied to complex shapes, and they can produce superior properties, such as quick and uniform coating. Furthermore, they can possibly control the thickness and chemical composition of the coatings. Electrospinning is a potentially emerging and efficient process for producing materials with nanofibrous structures, which have exceptional characteristics such as mechanical properties, pore size, and superior surface area. These specialized characteristics induce these nanostructured materials to be used in different technologies.

Applied Physics Reviews 6, 021303 (2019)- IF= 12.894

Comparative study of synergistic inhibition of mild steel and pure iron by 1- hexadecylpyridinium chloride and bromide ions

Hany M. Abd El-Lateef[a], M.M. Saleh [c], Manal G. Mahmoud[b]
[a]Chemistry Department, Faculty of Science, Sohag University, Sohag 82524, Egypt
[b]Marine Chemistry Lab., Marine Environment Division, National Institute of Oceanography and Fisheries, Alexandria Branch, Alexandria, Egypt
[c]Department of Chemistry, Faculty of Science, Cairo University, Giza, Egyp

The comparison of the corrosion behavior of mild steel (MS) and pure iron (PI), and synergistic action of 1-Hexadecylpyridinium chloride (HDPCl) and Br − ion are studied in 0.5M sulphuric acid solution. The study was carried out using open-circuit potential, potentiodynamic polarization, and electrochemical impedance spectroscopy measurements. In absence of inhibitor (blank), the corrosion rate of mild steel is greater than that of pure iron. In presence of HDPCl only, the inhibition efficiency for MS corrosion in H 2 SO 4 is higher than that of PI and attributedto the different surface charges on both MS and PI in H2SO4 solution. The obtained results indicate that the inhibition efficiency (η i %) of HDPCl is significantly increased in the presence of Br − ions for both MS and PI. In the presence of the Br − ions, the η i increases significantly at relatively low concentrations of HDPCl ([HDPCl] = 8× 10 -6 M), i.e, η i is 96 and 99% for MS and PI, respectively. The synergism factor (Sθ) is found to be more than unity suggesting greater η i due to the addition of Br − ions to the HDPCl with a co-operative adsorption action. Chemisorption is postulated as the mode of adsorption based on extracted thermodynamic parameters.

Corrosion Science 154 (2019) 70–79- IF= 6.32

Solvent-free synthesis and corrosion inhibition performance of Ethyl 2-(1,2,3,6-tetrahydro-6-oxo-2-thioxopyrimidin-4-yl)ethanoate on carbon steel in pickling acids: Experimental, quantum chemical and Monte Carlo simulation studies

Hany M.Abd El-Lateef[a], Zeinab A.Abdallah[b], Mohamed S.Mohamed Ahmed[b]
[a]Chemistry Department, Faculty of Science, Sohag University, Sohag 82524, Egypt [b]Department of Chemistry, Faculty of Science, Cairo University, Giza, Egypt

Ethyl 2-(1,2,3,6-tetrahydro-6-oxo-2-thioxopyrimidin-4-yl)ethanoate (EOTPE) was synthesized by a facile and cost-effective method. The structure confirmation of the synthesized EOTPE was performed by different spectroscopic methods. The corrosion inhibition action of EOTPE in pickling acids (1.0 N HCl and1.0 N H2SO4) at different temperatures (30–60 °C) was tested by various surface and corrosion methods, including open circuit potential (EOCP-t), potentiodynamic polarization (PDP), electrochemical impedance spectroscopy (EIS), Fourier-transform infrared spectroscopy (FTIR), Field emission scanning electron microscopy (FE-SEM) and energy-dispersive X-ray spectroscopy (EDX). The inhibition capacity of EOTPE was found to 92.1% and 97.0% in the case of H2SO4 and HCl, respectively at the optimum dose of $1 \times 10{-}3$ M. The PDP method demonstrated that EOTPE compound acted as a mixed-type inhibitor in both studied acids. Moreover, adsorption of EOTPE inhibitor on the steel surface conforms to the model of Langmuir isotherm. Additionally, the thermodynamic parameters for the inhibitor adsorption were estimated and interpreted. FE-SEM/EDX and FTIR investigations confirmed the formation of a defensive film on the electrode surface. The findings obtained from the above methods are in good agreement and are fully supported by Monte Carlo (MC) simulations and density functional theory (DFT) calculations.

Journal of Molecular Liquids 296, 2019, 111800- IF= 4.561

Sulfonated salicylidene thiadiazole complexes with Co (II) and Ni (II) ions as sustainable corrosion inhibitors and catalysts for cross coupling reaction

Hany M. Abd El-Lateef[1], Abdelwahed R. Sayed[2], Mohamed Shaker S. Adam[1]
[1]Chemistry Department, Faculty of Science, Sohag University, 82524 Sohag, Egypt
[2]Department of Chemistry, Faculty of Science, University of Beni Suef, Egypt

Condensation of 2,5-dihydrazinyl thiadiazole with 5-sodium sulfonate salicylaldehyde afforded dibasic tetradentate pincer N,O,O,N-salicyldiene thiadiazole ligand (H 2Sanp). The novel dipolar ligand formed para-magnetic pincer complexes within Co (II) and Ni (II) ions (Co-Sanp and Ni-Sanp) under sustainable conditions. The water-soluble ligand and its metal-complexes were estimated by mass, IR and UV–Visible spectroscopy, EA (elemental analyses), TGA (Thermogravimetric analyses), magnetic susceptibility, and conductivity measurements. The catalytic reactivity of Co-Sanpand Ni-Sanp were evaluated in the Suzuki and Buchwald-Hartwig cross coupling reaction in aqueous- methanol binary mixtures. Both reactions of boronic acid or aryl amines with aryl halides gave high chemoselective yield ofC—CorC—N product. The inhi- bition characteristics of H 2Sanp and its Ni- and Co-complexes were performed for the C-steel corrosion in 1.0 M HCl using electrochemical measurements and surface analysis methods. These methods indicated that the synthesized compounds have served as efficient mixed-type corrosion inhibitors and their adsorption on the steel surface obeyed isotherm model of Langmuir. Co-Sanp inhibitor displays the best corrosion inhibition efficiency, and the capacity is up to 97.11% at of 250 mg L^{-1} . Surface analysis confirms formation of protec- tive layer on the C-steel surface.

Appl Organometal Chem. 2019;33:e4987 – IF=3.2

Magnetic Fe_3O_4 nanocubes coated by SiO_2 and TiO_2 layers as nanocomposites for Cr (VI) up taking from wastewater

Mai M. Khalaf [a],,Kawther Al-Amer [b], Hany M. Abd El-lateef [a]

[a]Chemistry Department, Faculty of Science, Sohag University, 82524 Sohag, Egypt

[b]Department of Chemistry, Faculty of Science, King Faisal University, Alahsa, 31982, Saudi Arabia

Magnetic Fe_3O_4 (FO) nanocubes coated by SiO_2 (FO–S) and TiO_2 (FO-T) layers with perfect adsorption char- acteristics were successfully fabricated by a simple technique, and characterized by Fourier-transform infrared spectroscopy (FTIR), Field emission-scanning electron microscopy (FE-SEM), energy dispersive X-ray spectro- meter (EDS), X-ray diffraction (XRD), High resolution transmission electron microscopy (HR-TEM), dynamic light scattering (DLS) and Brunauer-Emmett-Teller (BET) specific surface area. HR-TEM analysis confirms the susccess of Fe_3O_4 coating with TiO_2 and SiO_2 with a shell thickness ranged from 24 to 33 nm and 12–16nm, respectively. Cr (VI) elimination from wastewater by the fabricated materials was carried out using a batch adsorption method at varying initial [Cr(VI)] (10–200ppm), initial pH (1–8), shaking speed (200–400 rpm), temperature (293–333 K), contact time (0–180 min) and adsorbent dose (0.1–0.5g). The point of zero charges (PZC) for adsorbents was estimated. The equilibrium findings of Cr (VI) ions removal were illustrated by Freundlich and Langmuir isotherm models and their kinetic results of ions were followed the pseudo-second- order sorption. The maximum adsorption capacity of Cr (VI) onto FO, FO-T, and FO-S were estimated to be 25.3, 28.7 and 32.6 mg/g, respectively. Further, the utilized adsorbents can be readily renovated and the adsorption capacity was still excellent after six sorption-regeneration cycles.

Ceramics International 45 (2019) 23548–23560- IF= 3.4

Novel dispersed Tl_2O_3-SiO_2/polyaniline nanocomposites: in-situ polymerization, characterization and enforcement as a corrosion protective layer for carbon-steel in acidic chloride medium

Hany M. Abd El-Lateef, MaiM. Khalaf

Chemistry Department, Faculty of Science, Sohag University, Sohag 82524, Egypt

The current approach discussed a synthesis and characterization of polyaniline (PANI) and two modified loading of 5, 10% Tl2O3-SiO2/ PANI, in which Tl2O3-SiO2 nanoparticles (NPs) were modified with PANI forming nanocomposites. The composite formation and structure were confirmed by X-ray diffraction (XRD), UV–vis absorption spectra (UV–vis), Fourier transform infrared spectroscopy (FTIR), scanning electron microscopy (SEM) with energy dispersive X-ray spectroscopy (EDX), High resolution transmission electron microscopy (HR-TEM), and dynamic light scattering (DLS) technique. The prepared polymer (PANI) and its nanocomposites (Tl2O3-SiO2/PANI) were examined as a corrosion protective layer for carbon steel in 2.0 N HCl at different temperature (30–60 °C) by different electrochemical methods including potentiodynamic polarization (PDP) and electrochemical impedance spectroscopy (EIS) measurements. PANI inhibited the corrosion of carbon steel, yielding maximum protection capacity of 89%, which were further increased to 96% by the modification with Tl2O3-SiO2 nanocomposites. The SEM/EDX investigations confirmed the presence of Tl2O3-SiO2/ PANI nanocomposites film covering the metal surface.

Colloids and Surfaces A 573 (2019) 95–111- IF=3.3

Removal of cationic surfactants from dilute solutions using nanoporous nickel phosphate: A structural, kinetic and thermodynamic study

Hany M. Abd El-Lateef[a], M.M. Saleh [c], Ahmed H. Touny[c]
[a]Chemistry Department, Faculty of Science, Sohag University, Sohag 82524, Egypt
[b]Chemistry Department, Faculty of Science, Helwan University, Helwan, Egypt
[c]Department of Chemistry, Faculty of Science, Cairo University, Giza, Egyp

The removal of cetylpyridinium chloride (CPC)(as a cationic surfactant) on nanoporous nickel phosphate (nano- NiPOx)particles is studied for the first time. The structure and morphology of the material are investigated using X-ray diffraction (XRD), scanning electron microscopy (SEM), energy dispersive X-ray analysis (EDAX), trans- mission electron microscopy (TEM) and BET surface area determination. Various operating parameters, such as the initial CPC concentration, amount of NiPOx, shaking speed, pH and temperature, are investigated. The point of zero charge (PZC) for NiPOx in 0.1 M KCl solution is found to be 6.5. The adsorption of the CPC on the NiPOx follows pseudo-first-order kinetics. Furthermore, the experimental data follow the modified Frumkin ad- sorption isotherm. Important thermodynamic parameters, such as the free energy of adsorption at different temperatures, are extracted by fitting the experimental data with the isotherm model. The parameters obtained above suggest that there is a strong extent of adsorption of the CPC on the NiPOx surface.

Journal of Molecular Liquids 283 (2019) 30–38- IF= 4.561

Efficient route synthesis of new polythiazoles and their inhibition characteristics of mild-steel corrosion in acidic chloride medium

Hany M. Abd El-Lateef[a], Abdelwahed R. Sayed[b], Mahmoud M. Saleh[c,] Mohammed A. Al-Omair[d]
[a]Chemistry Department, Faculty of Science, Sohag University, Sohag 82524, Egypt
[b]Department of Chemistry, Faculty of Science, Beni-Suef university, Beni-suef, 32514, Egypt
[c]Department of Chemistry, Faculty of Science, Cairo University, Cairo, Egypt
[d]Department of Chemistry, College of Science, King Faisal University, P.O. Box 380 Al Hufuf, 31982 Al Hassa, Saudi Arabia

In this work, an expedient and good yielding prepared tactic for production of polythiazoles offered through treatment of bis-hydrazonoyl halides with bis (hydrazinecarbothioamide). The description scheme for the final polymers is proposed and discussed. Organic substances of the final products were clarified by spectral data. The prepared polythiazoles compounds were examined as corrosion inhibitors for M-steel in 2.0N HCl solutions. The corrosion inhibition performance was determined by electro- chemical techniques including open circuit potential (OCP), electrochemical impedance spectroscopy (EIS) and potentiodynamic polarization (PDP) measurements. The obtained outcomes showed that such two polymer inhibitors could effectively inhibit the corrosion of M-steel of in the studied media, espe- cially at their low concentrations; the inhibition capacity was increased from 55.8% in the presence of 10ppme98.8% in the presence of 100 ppm. Moreover, para-substituted polymer showed higher inhibi- tion capacity than the corresponding meta-substituted polymer. SEM observations demonstrated the formation of a protective inhibitor layer on the M-steel surface. Additionally, the adsorption of the polymer molecules on the surface of M-steel was found to obey the Langmuir isotherm model

Journal of Molecular Structure 1184 (2019) 452-461 - IF= 2.2

Synthesis of crystalline and amorphous iron phosphate nanoparticles by simple low-temperature method

Hany M. Abd El-Lateef[a], M.M. Saleh[b], Ahmed H. Touny[c]
[a]Chemistry Department, Faculty of Science, Sohag University, Sohag 82524, Egypt
[b]Chemistry Department, Faculty of Science, Helwan University, Helwan, Egypt
[c]Department of Chemistry, Faculty of Science, Cairo University, Giza, Egyp

A simple and well-designed route for controlled synthesis of crystalline iron phosphate ($FePh_{cry}$) and amorphous iron phosphate ($FePh_{amph}$) with simple reflux-based method at 90 °C is introduced. The method allows for mass production at low cost. The crystalline is formed at initial pH of 0.38 to final pH = 1.0 and the amorphous form is obtained at initial pH of 1.3 to final pH (after completed reflux) of 8.0. Characterization techniques such as FT-IR spectroscopy, energy dispersive x-ray analysis (EDS), field-emission scanning electron microscopy (FE-SEM), transmission electron microscopy (TEM), x-ray diffraction (XRD) and BET surface area determination are used for the investigation of the phase structure and morphological properties of the $FePh_{cry}$ and $FePh_{amph}$ nanomaterials. The average values of particle size are ~50–100 nm and ~5–15 nm with surface area of 16.013 $m^2 g^{-1}$ and 154 $m^2 g^{-1}$ for $FePh_{cry}$ and $FePh_{amph}$, respectively. Based on the XRD pattern, the obtained phase structure of the $FePh_{cry}$ is $FePO_4.2H_2O$ (80%) and $Fe_{12}(OH)_{7.3}(PO_4)_8.4.7H_2O$ (20%) with a monoclinic and orthorhombic crystallographic form, respectively. For the $FePh_{amph}$ sample the phase structure is completely amorphous with chemical structure of $FePO_4$.

Mater. Res. Express 6(2019) 035030

Magnetic Sm-BFO and Ce-BFO nanoflakes as protective coating layers for C-steel in acidic chloride environments

Mai M. Khalaf [a], Hany M. Abd El-Lateef [b,] G. Farghal [b], E.M.M. Ibrahim[b]
[a]Chemistry Department, Faculty of Science, Sohag University, Sohag 82524, Egypt
[b]Physics Department, Faculty of Science, Sohag University, Sohag-82524, Egypt

This investigation suggests a straightforward method for the C-steel coating by two different doped BiFeO 3 (BFO) nanomaterials, specifically Ce and Sm doped BFO nanoflakes for protection against corro- sion. The Ce and Sm doped BFO nanoflakes were prepared by sol–gel process and the C-steel was coated by the dip coating method. Influences of the number of layers and surfaces morphology of Ce-and Sm-BFO nanoflakes on the corrosion resistance of coated C-steel were studied. Different techniques such as FT-IR; X-ray diffraction and scanning electron microscopy were performed in order to describe the coatings structure. Moreover, the electrical and magnetic properties were also examined. Electrochemical impedance spectroscopy (EIS) and potentiodynamic measurements (PDP) were utilized to investigate the corrosion protection execution in HCl solution. Both samples are weak ferromagnetic ordering and have a semiconductor feature. It was found that the C-steel corrosion can be controlled by coating with Ce-and Sm-BFO nanoflakes. The corrosion protection results indicated that the efficiency of Sm-BFO nanoflakes as a corrosion protective material is very high compared to that of Ce-BFO nano- flakes due to the smooth surface of Sm-BFO and rough mesoporous surface of Ce-BFO as shown in SEM results.

Measurement 132 (2019) 99–108- IF= 2.791

Electrodeposited Pt nanorods on a novel flowered-like nanostructured Ni e Co alloy as an electrocatalyst for methanol oxidation

Mahmoud Elrouby, Hany M. Abd El-Lateef, Mansour Sadek
[a]*Chemistry Department, Faculty of Science, Sohag University, Sohag 82524, Egypt*

For the first time, a novel system of Pt nanorods supported on nano flowered-like structure NiCo alloy has been successfully electro-synthesized onto a glassy carbon electrode for the electrocatalytic oxidation of methanol. The electrodeposited system has been character- ized using scanning electron microscope (SEM), energy dispersive X-ray spectroscopy (EDX), and X-ray diffraction (XRD). The electrocatalytic efficiency of the electro-fabricated system of Pt/NiCo/GCE have been confirmed by cyclic voltammetric (CV) and current-time methods. It is discovered that the electrodeposited nano flowered NiCo alloy substrate has a great effect on the electrocatalytic properties of the electrodeposited Pt nanorods. The electrocatalytic efficiency of the new system for methanol oxidation reaction (MOR) is found to be 174 A/g Pt . The effect of electrodeposition time for NiCo alloy has been studied. Also, the effect of pH, temperature, and concentration for the electrodeposition of Pt catalyst on the electrocatalytic properties of the Pt/NiCo/GCE have been studied for detection the optimum conditions. The mechanism of the electrocatalytic oxidation of methanol has been discussed. Furthermore, the stability and the corrosion resistance test of the Pt/NiCo/GCE system have been investigated by electrochemical impedance spec- troscopy (EIS), Tafel plot and current-time methods.

International journal of hydrogen energy 44 (2019) 13820-13834- IF= 4.1

Antimicrobial activities of mesoporous nickel phosphate synthesized with low-temperature method

Mai M.Khalaf[a], Mohammed A.Al-Omair [b], A.H.Touny [c], H.Elsawy [d], M.M.Saleh[e]
[a]*Chemistry Department, Faculty of Science, Sohag University, Sohag 82524, Egypt*
[b]*Chemistry Department, College of Science, King Faisal University, Al-Hasa, P.B. Box 380, Hofuf, KSA*
[c]*Chemistry Department-Faculty of Science, Tanta University, Tanta, Egypt*
[d]*Department of Chemistry, Faculty of Science, Sohag University, Sohag, Egypt*
[e]*Department of Chemistry, Faculty of Science, Helwan University, Helwan, Egypt*

Mesoporous crystalline phase of nickel phosphate (m-NP) have been synthesized by a simple low-temperature hydrothermal approach. For the first time, the antimicrobial activities of m-NP are studied using different microbial media. The chemical structure and crystallinity of the m-NP are studied by XRD pattern and is confirmed by FT-IR results. The morphology is verified by scanning electron microscopy (SEM) and transmission electron micrographs (TEM). According to BET studies, the total pore volume is found to have an average value of 0.074 cc/g with surface area of 29.0 m2/g. m-NP particles are screened for antimicrobial activities against one G-positive bacteria, three G-negative bacteria and C. albicans fungal pathogen. The results show that the m-NP exhibits good antimicrobial activities against both G-positive and G-negative bacteria and against C. albicans with good selectivity against G-negative bacteria.

Microchemical Journal, 145, 2019, 113-118- IF= 3.3

Experimental Design Modeling of the Effect of Hexagonal Wurtzite—ZnO Synthesis Conditions on Its Characteristics and Performance as a Cationic and Anionic Adsorbent

Mai M.Khalaf[1], Enshirah Da'na[2],Kawther Al-Amer[2] and Manal Hessien[2]
[1]Chemistry Department, Faculty of Science, Sohag University, Sohag 82524, Egypt
[2]Chemistry Department, College of Science, King Faisal University, Al-Hasa, P.B. Box 380, Hofuf, KSA

Surface composite design was used to study the effect of the ZnO synthesis conditions on its adsorption of methyl orange (MO) and methylene blue (MB). The ZnO was prepared via hydrothermal treatment under different conditions including temperature (T), precursor concentration (C), pH, and reaction time (t). Models were built using four Design expert-11 software-based responses: the point of zero charge (pHzc), MO and MB removal efficiencies (R_{MO}, R_{MB}), MO and MB adsorption capacities (q_{MO}, q_{MB}), and hydrodynamic diameter of ZnO particles (D_h). ZnO was characterized by X-ray diffraction (XRD), Fourier-transform infrared (FTIR) spectroscopy, UV/VIS spectroscopy, thermal gravimetric analysis (TGA), and dynamic light scattering (DLS). The formation of ZnO was confirmed by the XRD, UV, and FTIR spectra. Results showed a very high efficiency for most of the samples for adsorption of MB, and more than 90% removal efficiency was achieved by 8 samples among 33 samples. For MO, more than 90% removal efficiency was achieved by 2 samples among 33 samples. Overall, 26 of 31 samples showed higher MB adsorption capacity than that of MO. R_{MB} was found to depend only on the synthesis temperature while R_{MO} depends on temperature, pH, and reaction time. pHzc was found to be affected by the synthesis pH only while D_h depends on the synthesis pH and precursor concentration.

Molecules 2019, 24(21), 3884- IF= 3.06

Sustainable dipolar homo-dicopper (II) dihydrazone complex as a catalyst for Sonogashira cross couplings

Mohamed Shaker S. Adam
Chemistry Department, Faculty of Science, Sohag University, Sohag 82524, Egypt

A novel dicopper (II) complex, Cu_2L, was prepared form the complexation of the new polydentate ligand (H_4L), bis(sodium 3-formyl-4-hydroxybenzenesulfonate) succinylhydrazone, with copper acetate. The novel homobinuclear complex was quite characterized by various physico-chemical tools and employed as a homogeneous and efficient-green catalyst for Sonogashira cross-couplings of phenylacetylene with halobenzenes under sustainable conditions. Cu_2L exhibited very good catalytic performance with excellent chemoselectivity. The catalytic efficiency of Cu_2L was improved by using ionic liquids–aqueous media (1: 1, binary mixture). A mechanistic pathway was also proposed for Cu(II)-catalyzed Sonogashira cross-coupling reactions for the reported finding. DFT for H_4L and Cu_2L were studied. Electronic configurations, energy of HOMO and LUMO orbitals, energy gap between orbitals (ΔE), electronegativity, hardness and softness were also calculated and compared with the applicable catalytic findings of Cu_2L, which are in good conformity.

Journal of Organometallic Chemistry Volume 903, 15 December 2019,

Chemical design and bioefficacy screening of new insect growth regulators as potential insecticidal agents against Spodoptera littoralis (Boisd.)

Abdelhamid A. A.[a], Elwassimy M. M[a] Aref, S. A.[b], Gad M. A.[b]
[a]Department of Chemistry, Faculty of Science, Sohag University, Sohag, 82524, Egypt
[b]Research Institute of Plant Protection, Agriculture Research Center, Giza, 12112, Egypt

The 13 new compounds were chemically synthesized and their spectroscopic analysis was done to determine their chemical structure. All the compounds were screened for their insecticidal potential against Spodoptera littoralis (Boisd.). Among the tested compounds, the compound 13 was found to be the most potent. It displayed one fold more activity than a reported insect growth regulator, fenoxycarb. The other target compounds demonstrated weak to strong toxicological activities against Spodoptera littoralis (Boisd.).
Biotechnology Reports Open AccessVolume 24, December 2019, Article number e00394

Biocatalysis explained: From pharmaceutical to bulk chemical production(Review)

Abdelraheem E. M. M.[a,b], Busch H.[a],Hanefeld U.[a], Tonin F.[a]
[a]Department of Biotechnology, Delft University of Technology, Van der Maasweg 9, Delft, 2629 HZ, Netherlands
[b]Chemistry Department, Faculty of Science, Sohag University, Sohag, 82524, Egypt

Biocatalysis is one of the most promising technologies for the sustainable synthesis of molecules for pharmaceutical, biotechnological and industrial purposes. From the gram to the ton scale, biocatalysis is employed with success. This is underpinned by the fact that the global enzyme market is predicted to increase from $7 billion to $10 billion by 2024. This review concentrates on showing the strong benefits that biocatalysis and the use of enzymes can provide to synthetic chemistry. Several examples of successful implementations of enzymes are discussed highlighting not only high-value pharmaceutical processes but also low-cost bulk products. Thus, biocatalytic methods make the chemistry more environmentally friendly and product specific.
Reaction Chemistry and Engineering, Volume 4, Issue 11, November 2019, Pages 1878-1894

Novel Cr (III), Fe (III) and Ru (III) Vanillin Based Metallo-Pharmaceuticals for Cancer and Inflammation Treatment: Experimental and Theoretical Studies

Abdel-Rahman L.H.[a], El-Khatib R.M.[a], Abdel-Fatah S. M.[a], Moustafa H.[b], Alsalme A. M.[c], Nafady, A.[c]
[a]Chemistry Department, Faculty of Science, Sohag University, Sohag, 82534, Egypt
[b]Chemistry Department, Faculty of Science, Cairo University, Giza, Egypt
[c]Chemistry Department, College of Science, King Saud University, Riyadh, Saudi Arabia

In this study, three novel complexes comprising trivalent Cr (III), Fe (III) and Ru (III) with imine ligand derived from 2-amino-3-hydroxypyridine and o-vanillin (H_2L) have been synthesized and characterized via wide range of spectroscopic and analytical tools such as ^1H NMR and ^{13}C NMR, infrared (IR) and UV–Vis spectrophotometry, conductivity and magnetic measurements. The obtained results along with DFT data confirmed a 1:1 (metal: ligand) stoichiometry with non-planner geometries for the three complexes. The binding action and the docking study of the prepared metal-complexes to calf thymus DNA was also studied by absorption spectra and viscosity technique, which revealed that the three complexes interact strongly with DNA through intercalative binding mode. Significantly, these metal-imine complexes showed strong and efficient anti-inflammatory and antimicrobial activities against various gram-positive (Microccus luteus), gram-negative (Escherichia coli and Serratia marcescence) bacteria, and three strains of fungus. Moreover, all complexes exhibited more potent cytotoxicity effect on the outgrowth of different types of carcinoma cells, including human colon (HCT-116 cell line), breast (MCF-7 cell line), and hepatic cellular (HepG-2), than the clinically-proven Vinblastine standard.

Applied Organometallic Chemistry, Volume 33, Issue 11, 1 November 2019, Article number e5177

Biogenic silver nanoparticles for trace colorimetric sensing of enzyme disrupter fungicide vinclozolin

Hussain, M.[a],Nafady, A.[b,c]Email Author,Sirajuddin[d], Avcı, A.[e],Pehlivan, E.[f],Nisar, J.[g],Sherazi, S.T.H.[a],Balouch, A.[a],Shah, M.R.[d],Almaghrabi, O.A.[h],Ul-Haq, M.A.[d]
[a]National Centre of Excellence in Analytical Chemistry, University of Sindh, Jamshoro, 76080, Pakistan
[b]Department of Chemistry, College of Science, King Saud University, Riyadh, 11451, Saudi Arabia
[c]Chemistry Department, Faculty of Science, Sohag University, Sohag, 82524, Egypt
[d]HEJ Research Institute of Chemistry, International Center for Chemical and Biological Center, University of Karachi, Karachi, 75270, Pakistan
[e]Department of Mechanical Engineering, Selcuk University, Konya, 42079, Turkey
[f]Department of Chemical Engineering, Selcuk University, Konya, 42079, Turkey
[g]National Centre of Excellence in Physical Chemistry, University of Peshawar, Peshawar, 25120, Pakistan
[h]Department of Biological Sciences, Faculty of Science, University of Jeddah, Jeddah, 21959, Saudi Arabia

We report a novel, simple, efficient, and green protocol for biogenic synthesis of silver nanoparticles (AgNPs) in aqueous solution using clove (Syzygium aromaticum) extract as a reducing and protecting agent. Ultraviolet-visible (UV-Vis) spectroscopy was employed to monitor the localized surface plasmon resonance (LSPR) band of clove extract-derived AgNPs prepared under various conditions. Fourier-transform infrared (FTIR) spectroscopy analysis provided information about the surface interaction of the clove extract with the AgNPs. Ultrahigh-resolution transmission electron microscopy (UHRTEM) results confirmed the formation of spherical, uniformly distributed clove extract-capped AgNPs with sizes in the range of 2–20 nm (average size: 14.4 ± 2 nm). Powder X-ray diffractometry analysis (PXRD) illustrated the formation of pure crystalline AgNPs. These AgNPs were tested as a colorimetric sensor to detect trace amounts of vinclozolin (VIN) by UV-Vis spectroscopy for the first time. The AgNP-based sensor demonstrated very sensitive and selective colorimetric detection of VIN, in the range of 2–16 μM (R^2 = 0.997). The developed sensor was green, simple, sensitive, selective, economical, and novel, and could detect trace amounts of VIN with limit of detection (LOD) = 21 nM. Importantly, the sensor was successfully employed for the determination of VIN in real water samples collected from various areas in Turkey.

Nanomaterials Volume 9, Issue 11, November 2019, Article number 1604

An efficient synthesis of benzylidene-2-alkoxy-4-aryl-2,3-cycloalkenopyridine-3-carbonitrile derivatives

Albayati M. R.[a], Moustafa A. H[b], Abdelhamed A. A[b]
[a]*Department of Chemistry, College of Education, Kirkuk University, Kirkuk, Iraq*
[b]*Department of Chemistry, Faculty of Science, Sohag University, Sohag, Egypt*

An efficient procedure for the synthesis of a novel class of benzylidene-2-alkoxy-4-aryl-6,7-dihydro-5H-cyclopenta[b]pyridine-, -5,6,7,8-tetrahydroquinoline and/or -6,7,8,9-tetrahydro-5H-cyclohepta[b]pyridine-3-carbonitrile was introduced through the one-pot multi-component reaction of cyclopentanone, cyclohexanone, and/or cycloheptanone with different aromatic aldehydes and malononitrile. The same products were also produced by classical route by the two-component reaction of dibenzylidine cyclopentanone, cyclohexanone, and/or cycloheptanone derivatives with malononitrile. The reactions were achieved using sodium alkoxide solution as catalyst and reagent.
Synthetic CommunicationsVolume 49, Issue 19, 2 October 2019, Pages 2546-2553

Iridium complex immobilization on covalent organic framework for effective C - H borylation

Vardhan, H.[a],Pan, Y.[b],Yang, Z.[b],Verma, G.[a],Nafady, A.[c,d],Al-Enizi, A.M.[c],Alotaibi, T.M.[e],Almaghrabi, O.A.[f],Ma, S.[a]
[a]*Department of Chemistry, University of South Florida, 4202 East Fowler Avenue, Tampa, FL 33620, US*
[b]*Department of Chemistry and Biochemistry, North Dakota State University, 1231 Albrecht Blvd., Fargo, ND 58108, United States*
[c]*Chemistry Department, College of Science, King Saud University, Riyadh, 11451, Saudi Arabia*
[d]*Chemistry Department, Faculty of Science, Sohag University, Sohag, 82534, Egypt*
[e]*King Abdullah City for Atomic and Renewable Energy, Riyadh, 11451, Saudi Arabia*
[f]*Faculty of Science, University of Jeddah, Jeddah, 21959, Saudi Arabia*

The strong coordination between metal ions and binding moieties in functional porous materials is central to the design and advancement of heterogeneous catalysis. In this study, we have successfully immobilized catalytically active iridium ions on a two-dimensional covalent organic framework (COF) having bipyridine moieties using a programmed synthetic procedure. The iridium immobilized framework, Ir_{cod}(I)@Py-2,2′-BPyPh COF, had high porosity, good stability, and exhibited excellent catalytic activity for C - H borylation, as compared with the pristine framework. Additionally, Ir_{cod}(I)@Py-2,2′-BPyPh COF was found to be an efficient catalyst for a series of electronically and sterically substituted substrates. The immobilized COF possessed excellent reusability, recyclability, and retention of crystallinity. This report highlights the role of porous materials as an ideal decorating platform for conducting a wide range of potent chemical conversions.
APL Materials Volume 7, Issue 10, 1 October 2019, Article number 101111

A regioselective and convenient one-pot multicomponent synthesis of polyfunctionalized 4-aryl-2-cyanoimino-3,4-dihydro-1H-pyrido[2,3-d] pyrimidines

Hussein B. R. M., Moustafa A. H.
Department of Chemistry, Faculty of Science, Sohag University, Sohag, 82524, Egypt

A novel series of 5,7-diamino-4-aryl-6-cyano-2-cyanoimino-3,4-dihydro-1H-pyrido[2,3-d]pyrimidines (aryl-CIDHPPMs) 3a–i was prepared via the one-pot four-component reaction of cyanoguanidine with aromatic aldehydes and malononitrile with molar ratio (1:1:2) using sodium methoxide as catalyst. These new polyfunctionlized aryl-CIDHPPMs were also synthesized by a classical route via reaction of cyanoguanidine with the respective arylidenes of malononitrile dimer under the same condition. In the same manner, the reaction of cyanoguanidine with isatinylidene of malononitrile dimer afforded the new spiro-pyrido[2,3-d]pyrimidines 7. While using aromatic aldehydes having electron donating groups (hydroxyl or dimethylamino groups) gave 4-Amino-2-aryl-6-methoxypyridine-3,5-dicarbonitrile 5a,b.

Synthetic Communications Volume 49, Issue 18, 17 September 2019, Pages 2401-2410

Theoretical insight into the structure-property relationship of mixed transition metal oxides nanofibers doped in activated carbon and 3D graphene for capacitive deionization

Yasin A. S.[a], Mohamed A. Y.[b], Mohamed I. M. A.[a,d], Cho D.-Y.[b], Park C.H.[a,c], Kim C.S.[a,c]
[a]Department of Bionanosystem Engineering, Chonbuk National University, Jeonju, Jeonbuk 561-756, SK
[b]IPIT & Department of Physics, Chonbuk National University, Jeonju, 54896, South Korea
[c]Division of Mechanical Design Engineering, Chonbuk National University, Jeonju, Jeonbuk 561-756, SK
[d]Department of Chemistry, Faculty of Science, Sohag University, Sohag, 82524, Egypt

Over the last two decades, the capacitive deionization (CDI) technique has been developed into a high performance, low-cost, and environmental-friendly desalination technology. The development of novel advanced nanostructures via the hybridization of diverse carbon materials to improve the performance of CDI technology has attracted considerable attention. In this study, the combination of graphene hydrogel and ZrO_2-doped TiO_2 nanofibers as efficient dopants into activated carbon (AC), has been achieved through a simple electrospinning technique followed by a post annealing process. The strong interactions between the graphene hydrogel, nanofibers and AC were found to enhance the wettability as well as the electrical conductivity of the AC. The morphology and electrochemical performance of the as-synthesized composite were characterized by field-emission scanning electron microscopy (FE-SEM), Transmission electron microscopy (TEM), cyclic voltammetry (CV) and electrochemical impedance spectroscopy (EIS). What's more, the X-ray diffraction (XRD), X-ray photoelectron spectroscopy (XPS) and synchrotron X-ray absorption structures (XAS) are performed to investigate the atomic and electronic structure of titania and zirconia in order to understand their phase stability. We observed the appearance of anatase structure of titania and cubic structure of zirconia after doping the AC and graphene hydrogel with the nanofibers. The water contact angle of the composite was examined and found to be less than 3°. The introduced nanocomposite showed high electrosorption capacity of 9.34 mg g^{-1} at the initial solution conductivity of ~100 μS cm^{-1}, which is much higher compared to the other surveyed materials; these results should be attributed to its significant hydrophilicity, high specific capacitance, and reduced charge transfer resistance.

Chemical Engineering JournalVolume 371, 1 September 2019, Pages 166-181

Catalytic comparison of various polar Zn(II)-Schiff base complexes and VO(II)-Schiff base complexes in (ep)oxidation processes of 1,2-cyclohexene and cyclohexane

Adam M. S. S.[a,b], Al-Omair M. A.[a], Ullah F.[c]

[a]Department of Chemistry, College of Science, King Faisal University, P.O. Box 380, Al Hufuf, Al Hassa 31982, Saudi Arabia

[b]Chemistry Department, Faculty of Science, Sohag University, Sohâg, 82534, Egypt

[c]Department of Chemistry, Winnipeg University, 515 Portage Avenue, Winnipeg, MB R3B 2E9, Canada

The reactivity of Zn^{2+} and VO^{2+} ions towards pyridinyl Schiff bases, in the absence or presence of a p-sodium sulfonate group (HPSNa and HPS, respectively), provided polar and less polar catalyst complexes, which were characterized by various measurements. Stability constants of Zn-complexes [$Zn(PS)_2$ and $Zn(PSNa)_2$], and VO-complexes [$VO(PS)_2$ and $VO(PSNa)_2$] were measured spectrophotometrically. A typical (ep)oxidation processes of 1,2-cyclohexene or cyclohexane using 30% aqueous H_2O_2 catalyzed by our synthesized catalyst system, were tested. VO-complexes were found to be more effective catalysts than Zn-chelates. The polarity of Zn- and VO-complexes, i.e. the presence of p-SO_3Na, displayed an observable influence on their catalytic performance chemoselectively. The polar catalyst system, $Zn(PSNa)_2$ and $VO(PSNa)_2$, in polar solvents such as H_2O, MeOH, acetonitrile and acetone exhibited higher catalytic activity towards the (ep)oxidation processes than the less polar catalysts, $Zn(PS)_2$ and $VO(PS)_2$. In a less polar solvent such as $CHCl_3$, polar catalysts showed higher conversion, but low chemoselectively, whereas the less polar catalysts showed relatively higher conversion and chemoselectivity. Under solvent-free conditions, less polar complexes were found to be more efficient catalysts than the polar chelates.

Research on Chemical IntermediatesVolume 45, Issue 9, 15 September 2019, Pages 4653-4675

Near UV-Irradiation of CuO_x-Impregnated TiO_2 Providing Active Species for H_2 Production Through Methanol Photoreforming

Vitiello G.[a,b], Clarizia L.[a], Abdelraheem W.[c,d], Esposito S.[e], Bonelli B.[e], Ditaranto N.[f], Vergara A.[g], Nadagouda M.[h], Dionysiou D. D.[c], Andreozzi R.[a], Luciani G.[a], Marotta R.[a]

[a]Department of Chemical, Materials and Production Engineering (DICMaPI), University of Naples Federico II, p.le Tecchio 80, Naples, 80125, Italy

[b]CSGI – Center for Colloids and Surface Science, University of Florence, via della Lastruccia 3, Sesto Fiorentino, Italy

[c]Environmental Engineering and Science Program, Department of Chemical and Environmental Engineering 705 Engineering Research Center, University of Cincinnati, Cincinnati, OH 45221-0012, US

[d]Department of Chemistry, Faculty of Science, Sohag University, Sohag, 82524, Egypt

[e]Department of Applied Science and Technology and INSTM Unit of Turin-Polytechnic, Polytechnic of Turin, C.so Duca degli Abruzzi 24, Turin, I-10129, Italy

[f]Department of Chemistry, University of Bari Aldo Moro, via Orabona 4, Bari, 70125, Italy

[g]Dep. Chemical Sciences, University of Naples Federico II, Complesso di Monte S. Angelo, Naples, Italy

[h]Department of Mechanical and Materials Engineering, Wright State University, Dayton, OH 45324, US

Copper doped-TiO_2 (P25) nanomaterials have been intensively studied as promising catalysts for H_2 production by photo-reforming of selected organic compounds. However, the role of copper oxidation states on the improvement of photocatalytic activity is still debated. In this work, CuO_x-impregnated P25-TiO_2 catalysts were used for photocatalytic production of hydrogen from methanol. Copper species/oxidation states both in the as-prepared catalysts and after the photocatalytic process were investigated. To this purpose, H_2 production rates were correlated to physico-chemical properties of the samples, both before and after photocatalytic process, by means of Raman, X-Ray Diffraction, Electron Paramagnetic Resonance spectroscopy, X-Ray Photoelectron Spectroscopy, Temperature-Programmed Reduction and High Resolution Transmission Electron Microscope techniques. Results revealed the presence of both Cu_2O and CuO deposits on the samples surface after calcination. Notably, under near-UV irradiation, the fraction of highly dispersed CuO particles undergo a partial dissolution process, followed by reduction to metallic copper $Cu_{(s)}$ by photogenerated electrons, boosting H_2 production rate. Our findings indicate that both Cu_2O and $Cu_{(s)}$ act as co-catalysts for H_2 generation, yet by different mechanisms. Overall this study, provides the basis to enhance catalytic performance of red-ox active systems through UV-irradiation approach.

Chem Cat Chem Volume 11, Issue 17, 5 September 2019, Pages 4314-4326

Synthesis of electrospun 1D-photoanode nanocomposite based on electrospinning followed by hydrothermal treatment for highly efficient liquid-junction photovoltaic devices

Mohamed, I. M. A.[a,b,c], Dao V.-D.[d,e], Liu, C.[a,b], Barakat, N.A.M.[f], Choi, H.-S.[g]

[a]College of Chemistry and Environmental Engineering, Shenzhen University, Shenzhen, 518060, China

[b]Shenzhen Key Laboratory of Environmental Chemistry and Ecological Remediation, Shenzhen University, Shenzhen, 518060, China

[c]Department of Chemistry, Faculty of Science, Sohag University, Sohag, 82524, Egypt

Electrospinning has received much interest as a versatile fabrication technique for 1D (one-dimension) nanomaterials. This study introduces a novel 1D nanomaterial, N&GO@Zr/TiO_2, which was synthesized through electrospinning followed by hydrothermal methods and applied as a photoanode in low-cost dye-sensitized solar cells (DSCs). The prepared material was characterized via FESEM, EDX mapping, XRD, and XPS analyses. After the hydrothermal step, there was an enhancement in the crystallinity, which is attributed to the high growth rate of the anatase crystallites. Then, the performance of DSCs incorporating the photoanodes was investigated by J–V curves, IPCE, dye loading, and EIS, and a high photoresponse efficiency of 5.3% was obtained, which is higher than the efficiencies for cells based on nitrogen-doped Zr/TiO_2 nanofibers (NFs) (5.0%) and GO@Zr/TiO_2 NFs (5.1%). Besides the crystallinity enhancement, Zr doping can affect the electronic properties of the pristine TiO_2 via the replacement of Ti^{4+} by Zr^{4+}, which has different size and electronegativity. Hence, this composite was used as a substrate for the photoanode after GO&N doping. GO can improve the electron transport via increasing the photoanode conductivity, which is demonstrated via impedance studies, and N can increase the current produced via the enhancement of dye loading, which is studied through UV–visible spectroscopy. This study introduces the preparation of the novel nanocomposites toward highly efficient low-cost liquid-junction photovoltaics. [Figure not available: see fulltext.].

Journal of Sol-Gel Science and TechnologyVolume 91, Issue 2, 15 August 2019, Pages 342-352

Electrospun carbon nanofiber-encapsulated NiS nanoparticles as an efficient catalyst for hydrogen production from hydrolysis of sodium borohydride

Al-Enizi A. M.[a], Nafady A.[a,b], El-Halwany M. M.[c], Brooks R. M.[d], Abutaleb A.[e], Yousef A.[e,f]

[a]Department of Chemistry, College of Science, King Saud University, Riyadh, 11451, Saudi Arabia

[b]Department of Chemistry, Faculty of Science, Sohag University, Sohag, 82524, Egypt

[c]Engineering Mathematics and Physics Department, Faculty of Engineering, Mansoura University, El-Mansoura, Egypt

Carbon nanofibers (CNFs) incorporating NiS nanoparticles (NPs), namely NiS@CNFs were prepared by one-step electrospinning and successfully employed as a catalyst for hydrogen production from hydrolytic dehydrogenation of sodium borohydride (SBH). As-prepared NiS@CNFs, composed of polyacrylonitrile (PAN), nickel acetate, and ammonium sulfide, was calcined at 900 °C in argon atmosphere, and characterized using standard surface science techniques. The combined results revealed the growth of NiS NPs inside the CNFs, hence confirmed the presence of elemental Ni, S, and C. The as-prepared NiS@CNFs catalyst has a significantly higher surface area (650.92 m^2/g) than the reported value of 376 m^2/g. Importantly, this catalyst exhibited a much higher catalytic performance, for H_2 production from SBH, than that of Ni@CNFs, as evidenced by its low activation energy (~25.11576 kJ/mol) and their R_{max} values of 2962 vs. 1770 mL/g·min. Recyclability tests on using NiS@CNFs catalyst showed quantitatively production (~100% conversion) of H_2 from SBH and retained up to 70% of its initial catalytic activity after five successive cycles. The low cost and high catalytic performance of the designed NiS@CNFs catalyst enable facile H_2 production from readily available hydrogen storage materials.

International Journal of Hydrogen Energy, Volume 44, Issue 39, 13 August 2019, Pages 21716-21725

Facile synthesis, characterizations, and impedance spectroscopic features of Zn(II)-bis Schiff base complex films towards photoelectronic applications

Shehata M. M.[a], Adam M. S. S.[b,c], Abdelhady K.[a], Makhlouf M. M.[d,e]
[a]Physics Department, Faculty of Science, Minia University, Minia, 61519, Egypt
[b]Department of Chemistry, College of Science, King Faisal University, Al Hassa, 31982, Saudi Arabia
[c]Chemistry Department, Faculty of Science, Sohag University, Sohag, 82534, Egypt

Complexation of Zn^{2+} with pyridyl Schiff base (ZnL_2) was synthesized. The ZnL_2 was examined and characterized using the elemental analysis, NMR, IR, UV-Vis, and mass spectra. ZnL_2 was formed within 1:2 molar ratios of metal ion to ligand, respectively, which is proven by continuous variation method. The thin films of ZnL_2 are grown on the quartz substrates for optical measurements using thermal evaporation method. The absorbance, transmittance, and reflectance were measured using a spectrophotometric technique, from which many optical parameters were determined. The indirect allowed transition is the most probable transition and the optical energy gap is found to be 2.41 eV. Additionally, the ZnL_2 was tested as a photosensitizer material in the thin film form grown onto single crystal of p-Si wafer to form a hybrid organic-inorganic Au/ZnL_2/p-Si/Al heterostructure device for the first time. Many electrical aspects were studied for such device including impedance spectroscopic, dielectric constant, electric modulus, and electrical conductivity at various frequencies and under different illumination intensities. The high photosensitivity of Au/ZnL_2/p-Si/Al heterojunction for low and high power intensity of light confirmed that the ZnL_2 material is a promising candidate photosensitizer for photovoltaic applications.

Journal of Solid State Electrochemistry, Volume 23, Issue 8, 1 August 2019, Pages 2519-2531

Mechanistic Investigations of Photoelectrochemical Water and Methanol Oxidation on Well-Defined TiO_2 Anatase (101) and Rutile (110) Surfaces

Ahmed A. Y.[a], Kandiel T. A.[b,c], Oekermann T.[d], Günnemann C.[e], Bahnemann D.[e,f]
[a]Department of Chemistry, Faculty of Science, Sohag University, Sohag, 82524, Egypt
[b]Department of Chemistry, King Fahd University of Petroleum and Minerals (KFUPM), Dhahran, SA
[c]Researcher at K.A. CARE Energy Research and Innovation Center at Dhahran, Dhahran, 31261, SA

The mechanisms of photoelectrochemical water and methanol oxidation on TiO_2 anatase (101) and rutile (110) surfaces have been studied using the intensity modulated photocurrent spectroscopy (IMPS) technique. The phenomenological rate constants for the photogenerated charge carriers transfer and recombination have been determined at different band bending values in the presence and absence of methanol as well as at different methanol concentrations. The obtained results have been analyzed based on the IMPS theory for a bulk semiconductor surface together with a model to define the nature of the surface-bound intermediates. The results of the analysis indicated that (i) water oxidation proceeds via coupling of two $>OH^{\bullet}_{br}$ radicals on both surfaces and the coupling of $>OH^{\bullet}_{br}$ radicals is about 1 order of magnitude faster on the anatase (101) surface than that on the rutile (110) surface; (ii) the rate constant of surface recombination at the flatband potential on anatase (101) surface is much lower than that on rutile (110) surface; and (iii) in the presence of methanol, the coupling of the $>OH^{\bullet}_{br}$ radicals on the anatase (101) surface is still the dominating reaction whereas on the rutile (110) surface the photogenerated $>OH^{\bullet}_{br}$ reacts rapidly with methanol, faster by a factor of 18 times than on anatase (101) surface so that the $>OH^{\bullet}_{br}$ coupling is less dominant. On the basis of those findings, it is concluded that the coupling of the $>OH^{\bullet}_{br}$ radicals is an essential step to trap the photogenerated holes and reduce the surface recombination on anatase (101) surface in the absence and presence of methanol. The faster reaction of methanol with the $>OH^{\bullet}_{br}$ on rutile (110) compared with that on anatase (101), while the former usually exhibits lower photocatalytic activity, indicates that the charge separation (not the charge transfer) is the rate controlling step in the photocatalytic process.

ACS Applied Energy Materials, Volume 2, Issue 7, 22 July 2019, Pages 5308-5318

Sub-ppt level voltammetric sensor for Hg^{2+} detection based on nafion stabilized l-cysteine-capped Au@Ag core-shell nanoparticles

Siddiqui S.[a], Nafady A.[b,c], El-Sagher H. M.[c], Al-Saeedi S. I.[d], Alsalme A. M.[b], Sirajuddin[a,e], Talpur F. N.[a], Sherazi S. T. H.[a], Kalhoro M. S.[f], Shah M. R.[e], Shaikh T.[a], Arain M.[g], Bhargava S. K.[h]

[a]National Center of Excellence in Analytical Chemistry, University of Sindh, Jamshoro, Sindh 76080, Pakistan

[b]Department of Chemistry, College of Science, King Saud University, Riyadh, Saudi Arabia

[c]Chemistry Department, Faculty of Science, Sohag University, Sohag, 82524, Egypt

Bimetallic nanoparticles (BMNPs) have received considerable attention due to their distinctive properties when compared to the corresponding monometallic NPs and their bulk counterpart. In this report, the formation of gold@silver core-shell nanoparticles (Au@AgCSNPs) was achieved via a one-pot synthetic approach after mixing 1:1 M solutions of Au and Ag ions. L-cysteine was used as reducing as well as capping agent for preparing Au@AgCSNPs. Ultraviolet-visible (UV-Vis) spectroscopy was employed for surface plasmon study while Fourier-transform infrared (FTIR) spectroscopy gave insights for interaction of NPs with specific functionality of the capping material. Surface morphology of the fabricated Au@AgCSNPs, probed by atomic force microscopy (AFM), indicated an average height of nanoparticles around 43 ± 3 nm and their crystallinity were confirmed via powder X-ray diffraction (PXRD) study. Significantly, the as synthesized Au@AgCSBMNPs were fabricated onto the conductive surface of glassy carbon electrode (GCE), stabilized with nafion, and then utilized as an extremely sensitive/greatly selective sensor for voltammetric detection of Hg^{2+}. The developed sensor responded linearly to Hg^{2+} between 0.001 and 19 ppb with limit of detection (LOD) as low as 0.0001 ppb (0.1 ppt). Finally, the sensor was effectively applied for Hg^{2+} detection in different groundwater samples and is workable at concentrations undetectable by several sensing tools. [Figure not available: see fulltext.].

Journal of Solid State ElectrochemistryVolume 23, Issue 7, 19 July 2019, Pages 2073-2083

Efficient Aerobic Oxidation of trans-2-Hexen-1-ol using the Aryl Alcohol Oxidase from Pleurotus eryngii

de Almeida T. P.[a], van Schie M. M. C. H.[a], Ma A.[a],Tieves, F.[a],Younes, S.H.H.[a,d], Fernández-Fueyo E.[a], Arends I. W. C. E.[b], Riul A. Jr.[c], Hollmann F.[a]

[a]Department of Biotechnology, Delft University of Technology, Netherlands

[b]Faculty of Science, University of Utrecht, Netherlands

[c]Department of Applied Physics, "Gleb Wataghin" Institute of Physics (IFGW), University of Campinas (UNICAMP), SP, Brazil

[d]Department of Chemistry, Faculty of Science, Sohag University, Sohag, 82524, Egypt

The selective oxidation of trans-2-hexen-1-ol to the corresponding aldehyde using a recombinant aryl alcohol oxidase from Pleurotus eryngii (PeAAOx) is reported. Especially using the two liquid phase system to overcome solubility and product inhibition issues enabled to achieve more than 2.200.000 catalytic turnovers for the production enzyme as well as molar product concentrations, pointing towards an economic feasible reaction.

Advanced Synthesis and Catalysis, Volume 361, Issue 11, 6 June 2019, Pages 2668-2672

Formate Oxidase (FOx) from Aspergillus oryzae: One Catalyst Enables Diverse H_2O_2-Dependent Biocatalytic Oxidation Reactions

Tieves F.[a], Willot S. J.-P.[a], van Schie M. M. C. H.[a], Rauch M. C. R.[a], Younes S. H. H.[a,b], Zhang W.[a], Dong J.[a], Gomez de Santos P.[c], Robbins J. M.[d], Bommarius B.[d], Alcalde M.[c], Bommarius A. S.[d,e], Hollmann F.[a]

[a]Department of Biotechnology, University of Technology Delft, van der Massweg 9, Delft, 2629HZ, Netherlands

[b]Chemistry Department, Faculty of Science, Sohag University, Sohag, 82524, Egypt

[c]Department of Biocatalysis, Institute of Catalysis, CSIC, Madrid, 28049, Spain

[d]School of Chemical and Biomolecular Engineering, Georgia Institute of Technology, 311 Ferst Drive, N.W., Atlanta, GA 30332, United States

[e]School of Chemistry and Biochemistry, Georgia Institute of Technology, 901 Atlantic Drive, N.W., Atlanta, GA 30332, United States

An increasing number of biocatalytic oxidation reactions rely on H_2O_2 as a clean oxidant. The poor robustness of most enzymes towards H_2O_2, however, necessitates more efficient systems for in situ H_2O_2 generation. In analogy to the well-known formate dehydrogenase to promote NADH-dependent reactions, we here propose employing formate oxidase (FOx) to promote H_2O_2-dependent enzymatic oxidation reactions. Even under non-optimised conditions, high turnover numbers for coupled FOx/peroxygenase catalysis were achieved.

Angewandte Chemie - International Edition, Volume 58, Issue 23, 3 June 2019, Pages 7873-7877

Electrochemical determination of antihypertensive drugs by employing costless and portable unmodified screen-printed electrodes

Khorshed A. A.[a], Khairy M.[b], Banks C. E.[c]

[a]Department of Pharmaceutical Analytical Chemistry, Faculty of pharmacy, Sohag University, Sohag, 82524, Egypt

[b]Department of Chemistry, Faculty of Science, Sohag University, Sohag, 82524, Egypt

[c]Faculty of Science and Engineering, Manchester Metropolitan University, Chester Street, Manchester, M1 5GD, United Kingdom

Hypertension increases the risk of heart disease and stroke, is commonly known as a silent killer disease and considered as one of the key risk factor for premature death and disability over the world. Herein, we report for the first time a sensitive, costless and reproducible voltammetric method for individual determination of five antihypertensive drugs namely, propranolol (PRO), timolol (TIM), amlodipine (AML), amiloride (AMI) and triamterene (TRI) using differential pulse voltammetry at bare/unmodified screen-printed carbon electrodes (SPEs) in presence of sodium dodecyl sulfate (SDS). Each drug exhibits an electrochemical signal in aqueous media which is significantly enhanced in presence of optimized concentration of SDS due to accumulation of the protonated drug molecules and electrostatically interaction with negatively charged micellar structures. As a result, the spherical micellar orientation of SDS onto the graphitic surface of SPEs offered the analytically sensitive determination of the target drugs over a wide linear concentration range with nano-molar detection limits possible negating the need for any complicated surface modifications. Finally, the proposed voltammetric method was successfully utilized in the individual determination of the target antihypertensive drugs in pharmaceutical formulations and human urine samples

Talanta, Volume 198, 1 June 2019, Pages 447-456

Multi-component Reactions, Solvent-free Synthesis of Substituted Pyrano-pyridopyrimidine under Different Conditions Using ZnO Nanoparticles

Mahmoud, N.F.H.[a], El-Saghier, A.M.[b]
[a]*Chemistry Department, Faculty of Science, Ain Shams University, Abbassia, Cairo, 11566, Egypt*
[b]*Chemistry Department, Faculty of Science, Sohag University, Sohag, Egypt*

2-Amino-4-(4-substitutedphenyl)-5-oxo-4H,5H-pyrano[2,3-d]pyrido[1,2-a]pyrimidine -3-carbonitrile-derivatives 2–12 were synthesized via multi-component condensation reactions of different aromatic aldehydes, 3H-pyrido[1,2-a]pyrimidine-2,4-dione 1, and malononitrile by using ZnO nanoparticles as green chemistry, environmentally friendly catalyst under solvent-free conditions. The present work creates a variety of biologically active heterocyclic compounds in excellent yield and a short time. The structures of all synthesized compounds were elucidated with the elemental analyses, IR, ^{1}H NMR, and mass spectral data.

Journal of Heterocyclic Chemistry, Volume 56, Issue 6, June 2019, Pages 1820-1824

Nano ZnO (hexagonal wurtzite) of different shapes under various conditions: Fabrication and characterization

Hessien M.[a], Da'Na E.[a], Al-Amer K.[a], Khalaf M. M.[a,b]
[a]*Department of Chemistry, Faculty of Science, King Faisal University, Alahsa, 31982, Saudi Arabia*
[b]*Chemistry Department, Faculty of Science, Sohag University, Sohag, 82524, Egypt*

One-dimensional nanorods, two-dimensional nanoflakes or nanoplates ZnO had been effectively prepared by a promising hydrothermal process. The growth of the synthesized ZnO morphology has readily affected by the four synthesis key parameters of Zn concentration, pH, temperature, and growth time together as a compatible study. All the series of the synthesized specimens were analyzed using diverse characterization techniques including, Fourier transform infrared spectroscopy (FTIR), x-ray diffraction analysis (XRD), and scanning electron microscopy (SEM). The results discussed the action of all synthetic parameters in a good quality of the formed wurtzite phase by enhancing the ZnO growth and its order. Likewise, the aspect ratio data showed that the well-crystalline hexagonal nanorods were successfully obtained under the following synthesis conditions: precursor Zn concentration less than 0.4 M, pH = 7-9, 250 °C and 2.5 h of the growth time.

Materials Research Express, Volume 6, Issue 8, 17 May 2019, Article number 085057

Synthesis, structural characterization, DFT calculations, biological investigation, molecular docking and DNA binding of Co(II), Ni(II) and Cu(II) nanosized Schiff base complexes bearing pyrimidine moiety

Basha M. T.[a,b], Alghanmi R. M.[a,b], Shehata M. R.[c], Abdel-Rahman, L. H.[d]
[a]*Chemistry Department, Faculty of Science, King Abdulaziz University, Jeddah, Saudi Arabia*
[b]*Chemistry Department, Faculty of Science, University of Jeddah, Jeddah, Saudi Arabia*
[c]*Chemistry Department, Faculty of Science, Cairo University, Giza, Egypt*
[d]*Chemistry Department, Faculty of Science, Sohag University, Sohag, 82534, Egypt*

Three new NNO tridentate Schiff bases derived from 5-bromosalicylaldehyde with 2-amino-4,6-dimethylpyrimidine, 2-amino-4-methoxy-6-methylpyrimidine and 2-amino-4-chloro-6-methylpyrimidine (HL_1, HL_2 and HL_3, respectively) and their complexes with Co(II), Ni(II) and Cu(II) have been prepared. These complexes were characterized by elemental analysis, ^{1}H NMR, IR and electronic spectra, and with the aid of magnetic moment, molar conductivity and mass spectrometry. We further determined some of their size on the nanoscale. The results indicated that Schiff bases behaved as a tridentate NNO chelator that coordinates to the metal ions by azomethine nitrogen, pyrimidine nitrogen and phenolic oxygen, demonstrating 1 to 1 (metal to ligand) ratio. The measurements of conductivity revealed a nonelectrolytic nature of the complexes. Electronic absorption and viscosity were used to explore the ability of investigated complexes to bind to DNA, and the results indicated that binding occurred through intercalation. The antimicrobial activities of the considered complexes were evaluated against some types of fungi and bacteria. Metal complexes exhibited more antimicrobial activity as compared to their ligands. Interestingly, the CuL_3 showed the highest antimicrobial activity. The anticancer activity of the chelators and their metal complexes were investigated on hepatic cellular and human colon carcinoma cells (HepG-2 cell line) and (HCT-116 cell line), respectively. The metal complexes have shown promising results in preclinical testing and they have enhanced anti-proliferative activity against growth of cancer cells compared to their ligand. Moreover, the docking study of the HL_1 HL_2 HL_3 and their Co(II), Ni(II) and Cu(II) was reported. The theoretical DFT calculations were applied to verify the molecular geometry of chelators and their complexes. The geometry optimization results are in agreement with experimental observations.

Journal of Molecular Structure, Volume 1183, 5 May 2019, Pages 298-312

Piperidinium Hydrogen Sulfate (PHS) as an Efficient Ionic Liquid Catalyst for the Synthesis of Imidazole Derivative under Solvent-Free Condition

Albayati M. R.[a], Marzouk A. A.[b], Abdelhamid A. A.[c]
[a]*College of Education, Department of Chemistry, Kirkuk University, Kirkuk, Iraq*
[b]*Pharmaceutical Chemistry Department, Faculty of Pharmacy, Al Azhar University, Cairo, Egypt*
[c]*Department of Chemistry, Faculty of Science, Sohag University, Sohag, 82524, Egypt*

Piperidinium hydrogen sulfate is used as a very important new catalyst for the synthesis of the biologically active compounds from a series of multi-substituted imidazole components by the simple reaction of benzyl with different aromatic aldehydes, ammonium acetate, and phenethylamine or butylamine as amine derivatives. The key merits of this method are very shorter reaction times, excellent yield, and ease of stabilization. Furthermore, the produced products can be purified by a non-chromatographic technique, and the catalyst is reusable. All of these new synthesized components have been characterized and checked from spectral data: IR, ^{1}H-NMR, and ^{13}C-NMR spectra and elemental analyses.

Journal of Heterocyclic Chemistry, Volume 56, Issue 5, May 2019, Pages 1514-1519

Chemical design of novel electrospun CoNi/Cr nanoparticles encapsulated in C-nanofibers as highly efficient material for urea oxidation in alkaline media

Mohamed, I.M.A.[a,b,c],Liu, C.[a,b]

[a]*College of Chemistry and Environmental Engineering, Shenzhen University, Shenzhen, 518060, China*
[b]*Shenzhen Key Laboratory of Environmental Chemistry and Ecological Remediation, Shenzhen University, Shenzhen, 518060, China*
[c]*Department of Chemistry, Faculty of Science, Sohag University, Sohag, 82524, Egypt*

A novel nonprecious material was designed via electrospinning and carbonization to fabricate metallic (CoNi/Cr) nanoparticles (NPs)-encapsulated carbon nanofibers (NFs). The as-fabricated NFs were investigated in terms of morphology, crystallinity and surface chemistry through FESEM, TEM, EDX, XRD and XPS measurements. These analyses confirmed that the designed material owned metallic NPs encapsulated in carbon NFs. The introduced material had a rich carbon content on the surface which was due to the use of polyvinyl alcohol as a precursor polymer. Cyclic voltammetry (CV), chronoamperometry (CA) and impedance (EIS) analyses were applied in a three-electrode system to study the efficiency of the fabricated NFs for urea electrooxidation. The synthesized NFs showed superior catalytic behavior in the alkaline medium towards urea oxidation. The high efficiency was found to be at 0.5 M of urea according to the influence of urea and applied potential studies. This superior activity can be due to the assembly of trimetallic system CoNi/Cr encapsulated C-NFs which has rarely been studied before. This study presents the preparation of a novel cheap material to facilitate the urea fuel cell commercialization

Applied Surface Science, Volume 475, 1 May 2019, Pages 532-541

Photochemical treatment of tyrosol, a model phenolic compound present in olive mill wastewater, by hydroxyl and sulfate radical-based advanced oxidation processes (AOPs)

Kilic M. Y.[a], Abdelraheem W. H.[b,c], He X.[b], Kestioglu K.[a], Dionysiou D. D.[b]

[a]*Department of Environmental Engineering, Faculty of Engineering, Bursa Uludag University, Nilufer, Bursa 16059, Turkey*
[b]*Environmental Engineering and Science Program, Department of Chemical and Environmental Engineering (ChEE), University of Cincinnati, Cincinnati, OH 45221-0071, United States*
[c]*Chemistry Department, Faculty of Science, Sohag University, Sohag, 82524, Egypt*

The photochemical degradation and mineralization of tyrosol (TSL), a model phenolic compound present in olive mill wastewater, were studied by UV-254 nm irradiated peroxymonosulfate (PMS), hydrogen peroxide (H_2O_2) and persulfate (PS). Effects of initial TSL concentration, UV fluence, pH, phosphate buffer and presence of inorganic anions (i.e., Cl^-, SO_4^{2-} and NO_3^-) were also investigated. Sulfate and hydroxyl radicals were demonstrated to be responsible for TSL degradation and mineralization. Regardless of the treatment conditions, pseudo-first-order kinetics could be obtained, with the efficiencies following UV/PS > UV/H_2O_2 > UV/PMS. The better removal of TSL by UV/PS correlated with the quantum yield and concentration of sulfate radical in the system. Albeit acidic condition slightly enhanced the performance of the AOPs, complete oxidation of TSL was achieved at pH 6.8 by both UV/PS and UV/H_2O_2. Though, inorganic anions or different concentrations of phosphate buffer did not affect TSL degradation kinetics, presence of inorganic ions decreased significantly the TOC removal for both UV/PMS and UV/H_2O_2 processes. Meanwhile, UV/PS process was the least influenced by inorganic ions and showed the highest TOC removal of ~35%. Overall, UV/PS process was the most effective for TSL degradation and mineralization in the presence or absence of common water constituents.

Journal of Hazardous Materials, 5 April 2019, Pages 734-742

Multicomponent Reaction for Synthesis of Novel 2-Tosyloxyphenylpyridines

Hussein B. R. M., Ali A. M.
Chemistry Department, Faculty of Science, Sohag University, Sohag, 82524, Egypt

2-Tosyloxybenzaldehyde 1 was reacted with some active methylene compounds as 1:1 or 1:2 molar ratio under different basic conditions to afford the corresponding 2-tosyloxyarylidenes 2–4 and/or 2-tosyloxyphenylpyridine 5, respectively. Multicomponent reaction of 2-tosyloxyarylidene 2 and $AcONH_4$ with active methylene compounds namely: malononitrile, ethyl acetoacetate, ethyl benzoylacetate, 1,3-benzothiazol-2-ylacetonitrile, acetophenones or 3-acetylheterocycle derivatives in methanol gave 2-tosyloxyphenylpyridine derivatives 8–17, respectively. The structures of new compounds were elucidated by elemental and spectral analysis.

Journal of Heterocyclic Chemistry, Volume 56, Issue 4, April 2019, Pages 1420-1425

Novel aryl carboximidamide and 3-aryl-1,2,4-oxadiazole analogues of naproxen as dual selective COX-2/15-LOX inhibitors: Design, synthesis and docking studies

Youssif B. G. M.[a,b], Mohamed M. F. A.[c], Al-Sanea M. M.[b], Moustafa A. H.[d], Abdelhamid A. A.[d], Gomaa H. A. M.[e,f]
[a]*Pharmaceutical Organic Chemistry Department, Faculty of Pharmacy, Assiut University, Assiut, Assiut 71526, Egypt*
[b]*Pharmaceutical Chemistry Department, College of Pharmacy, Jouf University, Sakaka, Aljouf 2014, SA*
[c]*Department of Pharmaceutical Chemistry, Faculty of Pharmacy, Sohag University, Sohag, 82524, Egypt*

A series of novel naproxen analogues containing 3-aryl-1,2,4-oxadiazoles moiety (4b-g) and their reaction intermediates aryl carboximidamides moiety (3b-g) was synthesized and evaluated in vitro as dual COXs/15-LOX inhibitors. Compounds 3b-g exhibited superior inhibitory activity than celecoxib as COX-2 inhibitors. Compounds 3b-d and 3g were the most potent COX-2 inhibitors with IC_{50} range of 6.4 – 8.13 nM and higher selectivity indexes (3b, SI = 26.19; 3c, SI = 13.73; 3d, SI = 29.27; 3g, SI = 18.00) comparing to celecoxib (IC_{50} = 42.60 nM, SI = 8.05). Regarding 15-LOX inhibitory activity, compounds belonging to aryl carboximidamide backbone 3b-e and 3g were the most potent with IC_{50} range of 1.77–4.91 nM comparing to meclofenamate sodium (IC_{50} = 5.64 μM). Data revealed that The levels of NO released by aryl carboximidamides 3b-g were more higher than 3-aryl-1,2,4-oxadiazole derivatives 4b-g, which correlated well with their COX-2 inhibitory activities.

Bioorganic Chemistry, Volume 85, April 2019, Pages 577-584

Novel adsorbents derived from recycled waste polystyrene via cross-linking reaction for enhanced adsorption capacity and separation selectivity of CO_2

Fu Z.[a,b,c], Mohamed I. M. A.[a,b,d], Li J.[e], Liu C.[a,b]

[a]College of Chemistry and Environmental Engineering, Shenzhen University, Shenzhen, 518060, China
[b]Shenzhen Key Laboratory of Environmental Chemistry and Ecological Remediation, Shenzhen University, Shenzhen, 518060, China
[c]Shenzhen Changlong Technology Co. Ltd., Shenzhen, 518060, China
[d]Department of Chemistry, Faculty of Science, Sohag University, Sohag, 82524, Egypt
[e]School of Chemistry and Chemical Engineering, Chongqing University, Chongqing, 400044, China

Design of novel non-precious polymers towards separation science is a fast-growing research point because of the need for high potential applications such as CO_2 capture. Herein, we use four external cross-linkers (carbon tetrachloride, formaldehyde dimethyl acetal, α,α′-dichloro-p-xylene, 4,4′-bis(chloromethyl)-1,1′-biphenyl) to enhance the porosity of the polymeric adsorbents derived from the waste polystyrene. The best CO_2 adsorption capacity and separation selectivity was achieved by the prepared adsorbents using carbon tetrachloride as the external cross-linkers (HCP-A). The CO_2 adsorption capacity (2.521 mmol/g) at 1.0 bar and 273 K was achieved via the HCP-A adsorbents, which is 31.1% higher than the that of the adsorbents without using external cross-linkers (HCP-0). The BET surface area of HCP-A was 777 m^2/g, which is 82.8% higher than that of HCP-0. In addition, the ideal separation selectivity (CO_2/N_2) was increased from 16.7 to 37.8 for the adsorbents after the introduction of the external cross-linkers.

Journal of the Taiwan Institute of Chemical Engineers, Volume 97, April 2019, Pages 381-388

Structure-Activity Relationships of Hierarchical Three-Dimensional Electrodes with Photosystem II for Semiartificial Photosynthesis

Fang, X.[a],Sokol, K.P.[a],Heidary, N.[a],Kandiel, T.A.[a,b],Zhang, J.Z.[a],Reisner, E.[a]

[a]Department of Chemistry, University of Cambridge, Cambridge, CB2 1EW, United Kingdom
[b]Department of Chemistry, Faculty of Science, Sohag University, Sohag, 82524, Egypt

Semiartificial photosynthesis integrates photosynthetic enzymes with artificial electronics, which is an emerging approach to reroute the natural photoelectrogenetic pathways for sustainable fuel and chemical synthesis. However, the reduced catalytic activity of enzymes in bioelectrodes limits the overall performance and further applications in fuel production. Here, we show new insights into factors that affect the photoelectrogenesis in a model system consisting of photosystem II and three-dimensional indium tin oxide and graphene electrodes. Confocal fluorescence microscopy and in situ surface-sensitive infrared spectroscopy are employed to probe the enzyme distribution and penetration within electrode scaffolds of different structures, which is further correlated with protein film-photoelectrochemistry to establish relationships between the electrode architecture and enzyme activity. We find that the hierarchical structure of electrodes mainly influences the protein loading but not the enzyme activity. Photoactivity is more limited by light intensity and electronic communication at the biointerface. This study provides guidelines for maximizing the performance of semiartificial photosynthesis and also presents a set of methodologies to probe the photoactive biofilms in three-dimensional electrodes.

Nano Letters, Volume 19, Issue 3, 13 March 2019, Pages 1844-1850

Design and Synthesis of Some New Analgesic Azole Derivatives Containing Tramadol Moiety

Khodairy A.[a], Ahmed E. A.[a], Ismael M.[a], Mohamed K. M.[b], Thabet S. A.[c]
[a]Chemistry Department, Faculty of Science, Sohag University, Sohag, 82524, Egypt
[b]Assuit Chemical Laboratory, Medical legal Department, Ministry of Justice, Assuit, 71511, Egypt
[c]Central Research Laboratory, Faculty of Medicine, Sohag University, Sohag, 82524, Egypt

Some new triazole, thiadiazole, oxadiazole, thiazole, oxazole, and imidazole derivatives have been synthesized via the reaction of tramadol bearing a hydrazide, hydrazine carbodithioate, and/or acetic acid group with certain reagents. Molecular docking study had been carried out to demonstrate the reactivity of these synthetic compounds for interaction with Cytochrome P450 2D6 (CYP2D6).
Journal of Heterocyclic Chemistry, Volume 56, Issue 3, March 2019, Pages 1055-1062

Green synthesis, antileishmanial activity evaluation, and in silico studies of new amino acid-coupled 1,2,4-triazoles

El-Saghier A. M.[a], Mohamed M. A.[a], Abd-Allah O. A.[a], Kadry A. M.[a], Ibrahim T. M.[b], Bekhit A. A.[c,d]
[a]Chemistry Department, Faculty of Science, Sohag University, Sohag, 82524, Egypt
[b]Pharmaceutical Chemistry Department, Faculty of Pharmacy, Kafrelsheikh University, Kafr El-Sheikh, 33516, Egypt
[c]Pharmaceutical Chemistry Department, Faculty of Pharmacy, Alexandria University, Alexandria, 21521, Egypt

Candidates of triazole-containing amino acid derivatives 5a−k were prepared under green chemistry conditions via multicomponent reaction using lemon juice as an acidic catalyst. All compounds were characterized by different spectral and elemental analyses. They were evaluated for their in vitro antileishmanial activity against miltefosine and amphotericin B deoxycholate as reference drugs. Compounds 5c, 5d, 5e and 5f showed superior potencies to miltefosine by 200 folds. These compounds are well tolerated by experimental animals orally up to 250 mg/kg and parenterally up to 100 mg/kg. Reverse docking approach against validated leishmanial targets pinpointed mitogen-activated protein kinase (MAPK) as a possible putative antileishmanial target. In addition, in silico predictions revealed that these compounds exhibited promising drug-likeness and pharmacokinetics profile.
Medicinal Chemistry Research, Volume 28, Issue 2, 15 February 2019, Pages 169-181

Surface activation of wood plastic composites (WPC) for enhanced adhesion with epoxy coating

Mohamed M. R.[a], Naguib H. M.[b,c,d], El-Ghazawy R.A.[b,c], Shaker N. O.[b,c], Amer A. A.[a], Soliman A. M.[a], Kandil U. F.[b,e]

[a]*Department of Chemistry, Faculty of Science, Sohag University, Sohag, 82524, Egypt*
[b]*Polymer Nanocomposite Center (PNC), Egyptian Petroleum Research Institute (EPRI), 1 Ahmed El-Zomor St., Nasr City, Cairo 11727, Egypt*
[c]*Department of Petroleum Applications, Egyptian Petroleum Research Institute (EPRI), Nasr City, Cairo 11727, Egypt*

This work aims to improve the adhesive force of epoxy coating with a wood-plastic composite (WPC) surface. First, WPC was formulated using the extrusion technique through different percentages of wood flour (WF) with virgin polyethylene (PE) in the presence of a coupling agent. Dynamic mechanical analysis and water percentage gain (WPG%) were performed to find the optimized WF/PE mixing ratio. The optimized formula was subjected to surface treatment by different methods, including chromic acid oxidation, ultraviolet irradiation, and flame and heat treatment. Then the treated surface of WPC was coated with nano-modified epoxy resin using carboxylated carbon nanotube, organically modified nanoclay (Cloisite-30B), and reactive rubber nanoparticles. The surface treatment of the WPC was characterized with contact angle measurement and Fourier Transform Infrared (FTIR), while the interaction between the WPC and epoxy coat was investigated by attenuated total reflection FTIR microscopy analysis. The adhesion strength of the nano-modified epoxy showed significant enhancement when investigated by pull-off method and cross-cut test. Nano-scratching was utilized in exploring the effect of different surface treatments on enhancing adhesion to epoxy. The interfacial morphological behavior of epoxy coating on the WPC surface was investigated by Scanning Electron Microscope. The results indicated that chemical treatments helped for the functionalization of the WPC surface, leading to stronger adhesion with epoxy. These epoxy-coated WPC composites recorded enhanced mechanical properties because of the chemical reaction between the WPC surface and epoxy.

Materials Performance and Characterization, Volume 8, Issue 1, 2019-02-08, Pages 34-52

New Route for the Synthesis of Hetaryl-1,5-benzodiazepines: Part 2

Ahmed, A.M., Abdel-Ghany, H.,Moustafa, H.M., Khodairy, A.
Chemistry Department, Faculty of Science, Sohag University, Sohag, Egypt

1,2,4-Triazin-3-ylthio-, 1,2,4-triazepin-3-ylthio-, 1,2,4-triazol-3-ylthio-, and 1,2,4,3-triazaphosphol-5-ylthio-1,5-benzodiazepines 4–20 were prepared via the reaction of 2-oxo-4-phenyl-2,3-dihydro-1H-1,5-benzodiazepin-3-ylhydrazonothiocarbamate (2) with halocompounds, dicarbonyl compounds, enaminones, 4-chlorobenzaldehyde, 4-chlorobenzylidenemalononitriles, N,N-dimethylformamide dimethylacetal, carbon disulfide, and 2,4-bis(4-methoxyphenyl)-1,3,2,4-dithiadiphosphetane-2,4-disulfide (Lawesson's reagent).

Journal of Heterocyclic Chemistry, Volume 56, Issue 2, February 2019, Pages 464-469

Hydrothermal synthesis of photoactive nitrogen- and boron- codoped TiO_2 nanoparticles for the treatment of bisphenol A in wastewater: Synthesis, photocatalytic activity, degradation byproducts and reaction pathways

Abdelraheem W. H. M.[a,b], Patil M. K.[a,c], Nadagouda M. N.[d], Dionysiou D. D.[a]
[a]*Environmental Engineering and Science Program, Department of Chemical and Environmental Engineering (ChEE), University of Cincinnati, Cincinnati, OH 45221-0012, United States*
[b]*Chemistry Department, Faculty of Science, Sohag University, Sohag, 82524, Egypt*
[c]*Department of Chemistry, Dr. Babasaheb Ambedkar Marathwada University, Sub-Campus Osmanabad, 413501, India*

Hydrothermal technique was employed for the synthesis of N- and B-codoped TiO_2 at different atomic percentages and calcination temperatures (350 and 400 °C). Borane tert-butylamine complex was used as a novel precursor for the dopant atoms. The photocatalytic activities of catalysts were evaluated for destruction of bisphenol A (BPA) spiked in clean water and in secondary treated wastewater influent (SWI) collected from the Groundwater Replenishment System GWRS (Orange County, CA, USA), the world's largest water purification system for indirect potable reuse. Results of X-ray photoelectron spectroscopy (XPS) revealed the incorporation of N and B atoms onto TiO_2 lattice via substitution of O and/or Ti, and interstitial incorporation mechanisms. Carbon doping (graphite-like carbon; O-C = O) was also evidenced from XPS spectra. X-ray diffraction (XRD) and high-resolution transmission electron microscopy (HR-TEM) revealed pristine TiO_2 and all doped TiO_2 existed in anatase structure. The anatase phase of catalysts was further confirmed by simulation of selected area electron diffraction (SAED) of the catalysts and reported anatase TiO_2 using the simulation software CrysTBox (v 1.10). Among all prepared catalysts, 2.0NBT-350 (N + B = 2.0%, calcination = 350 °C) possessed the smallest particle size (12.9 nm), largest BET surface area (108.5 m^2/g) and highest visible-light absorption (i.e., $\lambda > 400$ nm). Simulated solar light/2.0NBT-350 system exhibited the maximum removal of BPA (0.1 μM) at the optimum catalyst dose of 0.8 g/L in clean water, over three consecutive degradation reuse cycles without any noticeable decrease in its photocatalytic activity. BPA was also successfully removed in SWI water, however with slower kinetics due to hydroxyl radical quenching effect of dissolved organic and inorganic species present in the SWI matrix. Degradation byproducts were identified by LC/Q-TOF-ESI-MS analysis. Six byproducts were found in the reaction mixture, with two compounds were newly identified in the current study. BPA oxidation routes comprised successive BPA hydroxylation, elimination of aromatic ring, ring opening, and cyclization of aliphatic compounds. This study is a promising demonstration for controlled design and synthesis of photocatalysts useful for environmental applications, especially for the treatment of BPA in wastewater effluents.

Applied Catalysis B: Environmental, Volume 241, February 2019, Pages 598-611

Synthesis, characterization of novel p-tert-butylthiacalix[4]arene derivatives and its application for extraction of alkali and transition elements

Ahmad Desoky M. Mohamad · Omran A. Omran
Department of Chemistry, Department Faculty of Science, Sohag University, Egypt

Formation of novel lower rim derivatives of p-tert-butylthiacalix[4]arene through direct refux between p-tert-butylthiacalix[4]arene tetrahydrazides (cone, partial cone and 1,3-alternate conformers) and N-methylisatin in absolute ethanol. The study is clearly showed a facile synthesis of di- and tetrasubstituted p-tert-butylthiacalix[4]arene derivatives (2, 3 and 4) with excellent yields (up to 95%). The novel products were investigated by using the state-of-the-art techniques such as FT-IR, 1 H-NMR and 13C-NMR spectroscopies. Moreover, the potential applications of these derivatives were screened for their ability to detect and remove alkali and transition metals (Li+, Na+, K+, Cs+, Pb2+, Cd2+, Hg2+, Ni2+, Co2+, Cu2+, Ag+) using the liquid–liquid extraction method with promising results.

Journal of the Iranian Chemical Society, Accepted: 9 May 2019

Incorporating zirconia nanoparticles into activated carbon as electrode material for capacitive deionization

Yasin A. S.[a], Mohamed I. M. A.[a,d], Amen M. T.[a], Barakat N. A. M.[a,c], Park, C.H.[a,b], Kim C. S.[a,b]
[a]Department of Bionanosystem Engineering, Chonbuk National University, Jeonju, Jeonbuk 561-756, SK
[b]Division of Mechanical Design Engineering, Chonbuk National University, Jeonju, Jeonbuk 561-756, SK
[c]Chemical Engineering Department, Faculty of Engineering, El-Minia University, El-Minia, Egypt
[d]Department of Chemistry, Faculty of Science, Sohag University, Sohag, 82524, Egypt

In recent years, capacitive deionization (CDI) has attracted intensive research due to its environmentally-friendly nature and low power requirement. Although the characteristics of titania (TiO_2) and zirconia (ZrO_2) are almost the same, ZrO_2 has not attracted the same attention since the characteristics of the carbonaceous material need to be modified to enhance its performance as an electrode in CDI cells. In this study, the wettability and electrochemical behavior of activated carbon (AC), as a widely used, effective, and inexpensive material, was distinctively improved by doping with zirconia nanoparticles. The introduced AC/ZrO_2 nanocomposite was fabricated using the alkaline hydrothermal method. Investigation of the surface morphology, phase and crystallinity by SEM, TEM, XPS, and XRD demonstrated the successful doping of AC by zirconia nanoparticles. Interestingly, the wettability measurement showed excellent enhancement, since the water contact angles of pristine and doped AC are 45° and 148°, respectively. The electrochemical experiments demonstrated that the synthesized composite (AC/ZrO_2) has a specific capacitance of 282.8 F g^{-1}, which is higher than that for AC (207.5 F g^{-1}). Due to the significant improvement in wettability and specific capacitance, the desalination performance and the salt ion electrosorption capacity were also enhanced: 40.4% and 68.5%, and 2.82 and 4.79 mg/g for AC and AC/ZrO_2, respectively. Moreover, the introduced AC/ZrO_2 revealed 99% remaining desalination retention suggesting high stability. Overall, this study demonstrates ZrO_2 is an effective, stable, and environmentally safe material for improving the performance of carbonaceous CDI electrodes.

Journal of Alloys and Compounds, Volume 772, 25 January 2019, Pages 1079-1087

Disposable screen-printed electrodes modified with uniform iron oxide nanocubes for the simple electrochemical determination of meclizine, an antihistamine drug

Khorshed A. A.[a], Khairy M.[b], Elsafty S. A.[c], Banks C. E.[d]
[a]Department of Pharmaceutical Analytical Chemistry, Faculty of Pharmacy, Sohag University, Sohag, 82524, Egypt
[b]Chemistry Department, Faculty of Science, Sohag University, Sohag, 82524, Egypt
[c]Research Centre for Functional Materials, National Institute for Materials Science (NIMS), 1-2-1 Sengen, Tsukuba-shi Ibaraki-ken, 305-0047, Japan

Meclizine (MEC) is an antihistamine drug with long action and moderate sedative effects. It is commonly used in management of nausea, motion sickness and vomiting. Herein, a disposable screen-printed carbon electrode modified with uniform iron oxide nanocubes (Fe_2O_3 NCs-SPEs) was explored for simple electrochemical determination of MEC. The influence of the supporting electrolyte on the voltammetric signal of MEC was studied by using cyclic voltammetry. A sharp irreversible oxidation wave was observed at +1.5 V (vs. pseudo Ag/AgCl). The Fe_2O_3 NCs-SPEs showed an enhanced voltammetric signal of MEC in 0.05 M H_2SO_4, which significantly increased in the presence of sodium dodecyl sulfate (SDS). The optimum experimental parameters for differential pulse voltammetry (DPV) were studied. It was found that MEC can be easily determined in an aqueous 0.05 M H_2SO_4 solution over a wide linear range of 6.66-196.08 μM with a detection limit of 1.69 μM based on a 3.3 S/N ratio. The analysis of MEC in pharmaceutical formulations and human urine samples with satisfactory recoveries revealed the potential applicability of Fe_2O_3 NCs-SPEs for on-site analysis.

Analytical Methods, Volume 11, Issue 3, 21 January 2019, Pages 282-287

Green Synthesis of new Trizole Based Heterocyclic Amino Acids Ligands and their Transition Metal Complexes. Characterization, Kinetics, Antimicrobial and Docking Studies

El-Saghier A. M.[a], Abd El-Halim H. F.[b], Abdel-Rahman L. H.[a], Kadry A.[a]
[a]*Chemistry Department, Faculty of Science, Sohag University, Sohag, 82534, Egypt*
[b]*Pharmaceutical Chemistry Department, Faculty of Pharmacy, Misr International University, Cairo, Egypt*

Two novel amino acids imine ligands (H_2L_1 and H_2L_2) have been synthesized using green condensation reaction from 2-[3-Amino-5-(2-hydroxy-phenyl)-5-methyl-1,5-dihydro-[1, 2, 4]triazol-4-yl]-3-(1H-indol-3-yl)-propionic acid with benzaldehyde/p-flouro benzaldehyde (1:1 molar ratio) in the presence of lemon juice as a natural acidic catalyst in aqueous medium. Their transition metal complexes have been prepared in a molar ratio (1:1). Characterization of the ligands and complexes using elemental analysis, spectroscopic studies, ^{1}HNMR, ^{13}CNMR, and thermal analysis has been reported. E*, ΔH*, ΔS* and ΔG* thermodynamic parameters, were calculated to throw more light on the nature of changes accompanying the thermal decomposition process of these complexes. The molar conductance measurement of metal complexes showed nonelectrolyte behavior. The metal complexes of the two ligands have tetrahedral geometry with a general molecular structure $[M(H_2L)X_n]$, where [(M = Mn (II), Co (II), Cu (II) and Zn (II), X = Cl, n = 2]; M = VO (II), X = SO_4, n = 1] for H_2L_1. [M = Co (II), Cu (II), Zn (II)] for H_2L_2. Antibacterial activity of the complexes against (Bacillis subtilis, Micrococcus luteus, Escherichia coli), also antifungal activity against (Aspergillus niger, Candida Glabarta, Saccharomyces cerevisiae) have been screened. The results showed that all complexes have antimicrobial activity higher than free ligands. Molecular docking studies results showed that, all the synthesized compounds having minimum binding energy and have good affinity toward the active pocket, thus, they may be considered as good inhibitor of targeting PDB code: 1SC7 (Human DNA Topo-isomerase I).

Applied Organometallic Chemistry, Volume 33, Issue 1, January 2019, Article number e4641

Biological and catalytic potential of sustainable low and high valent metal-Schiff base sulfonate salicylidene pincer complexes

Adam M. S. S.[a,b], El-Hady O. M.[b], Ullah F.[c]
[a]*Department of Chemistry, College of Science, King Faisal University, P. O. Box 380, Al Hofuf Al Ahsa, 31982, Saudi Arabia*
[b]*Chemistry Department, Faculty of Science, Sohag University, Sohag, 82534, Egypt*
[c]*Department of Chemistry, Winnipeg University, 515 Portage Avenue, Winnipeg, MB, Canada*

ONO-Pincer Schiff base salicylidene (HSaln ligand) complexes with VO^{2+}, UO_2^{2+}, MoO_2^{2+} and Mn^{2+} ions (MSaln complexes = VOSaln, UO_2Saln, MoO_2Saln and MnSaln, respectively) were synthesized and fully characterized by different physico-chemical tools. The VOSaln complex was further treated with 1,10-phenanthroline which afforded a new VO-complex (VOSaln-Ph). All complexes and their ligands, as eco-friendly reagents, were explored for their biological potential as antibacterial and antifungal agents. Reactivity of MSaln complexes against the tested pathogen strains exhibited a remarkable inhibitory effect compared to the coordinated ligand (HSaln) and applicable standard drugs. Moreover, the MSaln complex-DNA interaction was investigated by ultraviolet-visible spectroscopy, viscosity and gel electrophoresis techniques affording binding strengths in the order: UO_2Saln > MnSaln > MoO_2Saln > VOSaln-Ph > VOSaln. Additionally, the biological potential of the investigated compounds was further explored by molecular docking to illustrate the nature of the drug-DNA interactions. All MSaln complexes show respectable anti-proliferative potential as anticancer agents against selected human carcinoma cell lines. Aside from the biological activities these complexes (MSaln complexes) were also investigated for catalytic efficiency in the Suzuki-Miyaura cross-coupling system of phenylboronic acid with 2-bromopyridine in water, sustainably. The results indicated that the MnSaln catalyst performed well with high yield. The catalytic potential of MnSaln was compared in water, water-ionic liquid mixtures and ionic liquids.

RSC Advances, Volume 9, Issue 59, 2019, Pages 34311-34329

Investigation of the anticancer activity of coordination-driven self-assembledtwo-dimensional ruthenium metalla-rectangle

Vardhan H.[a], Nafady A.[b,c], Al-Enizi A. M.[b], Khandke K.[a], El-Sagher, H.M.[c],Verma, G.[a],Acevedo-Duncan, M.[a],Alotaibi, T.M.[d],Ma, S.[a]

[a]*Department of Chemistry, University of South Florida, 4202 East Fowler Avenue, Tampa, FL 33620, United States*

[b]*Department of Chemistry, College of Science, King Saud University, Riyadh, 11451, Saudi Arabia*

[c]*Chemistry Department, Faculty of Science, Sohag University, Sohag, 82524, Egypt*

Coordination-driven self-assembly is an effective synthetic tool for the construction of spatially and electronically tunable supramolecular coordination complexes (SCCs), which are useful in various applications. Herein, we report the synthesis of a two-dimensional discrete metalla-rectangle [(η^6-p-cymene)$_4$Ru$_4$($C_6H_2O_4$)$_2$(2)$_2$] (CF_3SO_3)$_4$ (3) by the reaction of a dinuclear half-sandwich ruthenium (II) complex [Ru$_2$(η^6-p-cymene)$_2$($C_6H_2O_4$)Cl_2] (1) and bis-pyridyl amide linker (2) in the presence of AgO_3SCF_3. This cationic ruthenium metalla-rectangle (3) has been isolated as its triflate salt and characterized by analytical techniques including elemental analysis, Fourier-transform infrared spectroscopy (FT-IR), proton nuclear magnetic resonance spectroscopy (^{1}H-NMR), carbon nuclear magnetic resonance spectroscopy (^{13}C-NMR), ^{1}H-^{1}H correlation spectroscopy (COSY), ^{1}H-^{1}H nuclear Overhauser effect spectroscopy (NOESY), diffusion ordered spectroscopy (DOSY), and high-resolution electrospray ionization mass spectrometry (HR-ESI-MS). Significantly, the 2D cationic ruthenium metalla-rectangle showed better anticancer activity towards three different cell lines (A549, Caki-1 and Lovo) as compared with the parent ruthenium complex (1) and the commercially used drug, cisplatin.

Molecules, Volume 24, Issue 12, 2019, Article number 2284

Investigation of the electrochemical reduction process of the molybdate ions in the tartaric electrolytes

Majidzade V. A.[a], Aliyev A. S.[a], Babanly D. M.[a,c], Elrouby M.[b], Tagiyev D. B.[a]

[a]*Institute of Catalysis and Inorganic Chemistry named after acad.M.Nagiyev, Azerbaijan National Academy of Sciences, H. Javid ave., 113, AZ, Baku, 1143, Azerbaijan*

[b]*Chemistry Department, Faculty of Science, Sohag University, Sohag, 82524, Egypt*

[c]*Azerbaijan State Oil and Industry University (Ufaz), Baku, Azerbaijan*

The electrochemical reduction of molybdate ions in tartaric electrolyte has been investigated in this work. Kinetics and mechanism of the electrochemical process have been studied by cyclic and linear voltammetric polarization methods. The effect of the temperature, the rate of potential-scanning and the concentration of the molybdate ions on the electrochemical process has been also studied. By estimating the effective activation energy, it was revealed that the electroreduction process is accompanied by mixing kinetics control.

Acta Chimica Slovenica, Volume 66, Issue 1, 2019, Pages 155-162

Pore environment engineering in metal-organic frameworks for efficient ethane/ethylene separation

Wang X.[a,b], Niu Z.[b], Al-Enizi A. M.[c], Nafady A.[c,d], Wu Y.[a], Aguila B.[b], Verma G.[b], Wojtas L.[b], Chen Y.-S.[e], Li Z.[a], Ma S.[b]

[a]*School of Chemistry and Chemical Engineering, South China University of Technology, Guangzhou, 510640, China*

[b]*Department of Chemistry, University of South Florida, 4202 East Fowler Avenue, Tampa, FL 33620, US*

[c]*Department of Chemistry, College of Science, King Saud University, Riyadh, 11451, Saudi Arabia*

[d]*Chemistry Department, Faculty of Science, Sohag University, Sohag, 82524, Egypt*

[e]*ChemMatCARS, Center for Advanced Radiation Sources, University of Chicago, 9700 South Cass Avenue, Argonne, IL 60439, United States*

Selective adsorption of trace amounts of C_2H_6 from bulk C_2H_4 is a significantly important and extremely challenging task in industry, which requires an adsorbent with specific pore properties. Herein, we describe a strategy for adjusting the pore environment of metal-organic frameworks (MOFs) by introducing different amounts of methyl groups in the channel to enhance the guest-host interaction between C_2H_6 and the framework. To prove this concept, 2,3,5,6-tetramethylterephthalic acid (TMBDC) was deliberately added to a microporous MOF, $Ni(BDC)(DABCO)_{0.5}$, affording a series of mixed-ligand materials, $Ni(BDC)_{1-x}(TMBDC)_x(DABCO)_{0.5}$ (x = 0, 0.2, 0.45, 0.71, 1), having different pore environments. Significantly, these mixed-ligand materials demonstrated improved performance in terms of the adsorption capacity of C_2H_6 and C_2H_4 with an unprecedented C_2H_6 uptake of 2.21 mmol g^{-1} for $Ni(TMBDC)(DABCO)_{0.5}$ at 0.0625 bar and 298 K. With the best theoretical C_2H_6/C_2H_4 selectivity predicted by IAST, $Ni(TMBDC)(DABCO)_{0.5}$ exhibited effective separation of C_2H_6/C_2H_4 (1/15, v/v) and great recyclability in five consecutive adsorption/desorption cycles throughout the breakthrough experiment.

Journal of Materials Chemistry A, Volume 7, Issue 22, 2019, Pages 13585-13590

Antibacterial and photocatalytic activities of controllable (anatase/rutile) mixed phase TiO_2 nanophotocatalysts synthesized: Via a microwave-assisted sol-gel method

Almashhori, K.[a], Ali T. T.[b,c], Saeed A.[a,d], Alwafi R.[a], Aly M.[e], Al-Hazmi, F.E.[a]

[a]Department of Physics, Faculty of Science, King Abdulaziz University, Jeddah, 21589, Saudi Arabia

[b]Department of Chemistry, Faculty of Science, Sohag University, P.O. Box 82524, Sohag, Egypt

[c]Department of Chemistry, Faculty of Science, King Abdulaziz University, Jeddah, 80203, Saudi Arabia

TiO_2 samples with different ratios of anatase/rutile phases were synthesized via a microwave assisted sol-gel method and by applying particular concentrations of titanium(iv) isopropoxide as a single source precursor (SSP) with a constant concentration of nitric acid, which was used as the structure directing agent. The effect of the TiO_2 composition ratio of anatase to rutile on the physicochemical and photocatalytic properties was studied. The structural, morphological, and optical properties of the as-prepared samples were studied via X-ray diffraction (XRD), high-resolution transmission electron microscopy (HRTEM), and UV-Vis diffuse reflectance spectroscopy (DRS), respectively. In addition, the functional groups were determined via Fourier transform infrared (FTIR) spectroscopy. The characterization results showed that the crystallite sizes were in the range of 30-70 nm and also revealed the different crystalline phase ratios of anatase and rutile depending on the concentrations of the Ti precursor. The photocatalytic degradation of the as-synthesized samples was evaluated with crystal violet (CV) and methylene blue (MB) solutions under UV light irradiation. The results confirmed that the TiO_2 sample containing 81.65 wt% anatase exhibited a high photoactivity of organic dye degradation. The inhibitory effects of the as-synthesized samples of TiO_2 nanoparticles were determined against different multidrug resistant Gram-positive and negative bacterial pathogens. The most active sample was the one with the highest ratio of anatase to rutile.

New Journal of Chemistry, Volume 44, Issue 2, 2019, Pages 562-570

Ranolazine-functionalized copper nanoparticles as a colorimetric sensor for trace level detection of As^{3+}

Laghari G.N.[a], Nafady A.[b,c], Al-Saeedi S. I.[d], Sirajuddin[a], Sherazi S. T. H., Nisar J.[e], Shah M. R.[f], Abro, M. I.[g], Arain M.[h], Bhargava S. K.[i]

[a]National Centre of Excellence in Analytical Chemistry, University of Sindh, Jamshoro, 76080, Pakistan
[b]Department of Chemistry, College of Science, King Saud University, Riyadh, 11451, Saudi Arabia
[c]Department of Chemistry, Faculty of Science, Sohag University, Sohag, 82524, Egypt

This study involves environmentally friendly synthesis of copper nanoparticles in aqueous medium without inert gas protection, using ranolazine as a capping material. UV-Visible (UV-Vis) spectrometry showed that ranolazine-derived copper nanoparticles (Rano-Cu NPs) demonstrate a localized surface plasmon resonance (LSPR) band at 573 nm with brick-red color under optimized parameters, including pH, reaction time, and concentrations of copper salt, hydrazine hydrate, and ranolazine. The coating of ranolazine on the surface of Cu NPs was studied via Fourier transform infrared (FTIR) spectroscopy. Scanning electron microscopy (SEM) revealed that Rano-Cu NPs consist of spherical particles. X-ray diffraction (XRD) verified that Rano-Cu NPs are crystalline in nature. Atomic force microscopy (AFM) showed that the average size of Rano-Cu NPs was 40 ± 2 nm in the range of 22–95 nm. Rano-Cu NPs proved to be highly sensitive as a selective colorimetric sensor for As^{3+} via color change from brick red to dark green, in the linear range of 3.0×10^{-7} to 8.3×10^{-6} M, with an R^2 value of 0.9979. The developed sensor is simple, cost effective, highly sensitive, and extremely selective for As^{3+} detection, showing a low detection limit (LDL) of 1.6×10^{-8} M. The developed sensor was effectively tested for detection of As^{3+} in some water samples.

Nanomaterials, Volume 9, Issue 1, 1 January 2019, Article number 83

Copper (I) Nicotinate complex Abrogates Acrylamide Induced Hepatotoxicity in Male Rats: Biochemical and Histological Studies

Nagwa M. Elsawi[1], Wejdan, A. Aldajani[2], Mounir A. A. Mohamed[1], Ahmed. M. Ali[3], Gamal S. A.[4], Soad Shaker Ali[5], Sabra A. Abd El lah[1]

[1]Department of Chemistry, Department Faculty of Science, Sohag University, Egypt
[2]Department of Biochemistry, Department Faculty of Science, Sohag University, Egypt
[3]Department of Chemistry, Department Faculty of Science, Al-Azhar University, Assiut Branch, Egypt
[4]Department of Zoology, Department Faculty of Science, Sohag University, Egypt
[5]Department of Medical Biology, Department Faculty of Medicine, King Abdulaziz University, Jeddah, SA

This study was conducted as a trail to abrogates acrylamide induced hepatotoxicity in male rats by administration of copper (I) nicotinic acid complex. Animals were divided into 4 groups ;GI: control kept on balanced diet and tap water, GII :Acrylamide group received acrylamide in drinking water (7.5 mg/kg b.w.)for 30 days .GIII: treated with copper (I)-nicotinate complex (400 µg/kg b.w.) after acrylamide intoxication for 30 days and GIV the complex then acrylamide (prophylactic). Results showed significant increase in serum levels of AST, ALT,ALP,GGT and total antioxidant capacity (TAC) in acrylamide group. Moreover a significant increase in tumer markers AFU and TNF-Alpha. while Levels of each of S. total protein and S. albumin were significantly decreased in ACR group compared with control. Histological study showed congestion of central vein in liver section and vacuolation of hepatocytes in ACR group. Anticancer activity using in-vitro cytotoxic assay of Cu(I) Nicotinate complex ;proves the anticancer properties of it comparing with doxorubicin .Treatment with Copper (I)-Nicotinate Complex restored tissue and serological indices concomitantly towards normal levels. These results revealed that Copper (I)-Nicotinate Complex is able to significantly alleviate the hepatotoxicity induced by AA in rats and could be utilized as a potent food additives.

International Journal of Food and Nutritional Science, DOI: 10.15436/2377-0619.19.2416

Biochemical Analysis of C-X-C Motif Chemokine Ligand 10 (CXCL10) as a Biomarker in Patients with Rheumatoid Arthritis

Amal M. Imam[1], Amany M. Hamed[2], Samah I. Nasef[3], Amany M. Hassan[4], Hanan H. Omar[4]
[1]Department of Chemistry, Faculty of Science and Arts in Qurayat, Jouf University, KSA
[2]Department of Chemistry, Faculty of Science, Sohag University, Sohag Egypt
[3]Department of Physical Medicine and Rheumatology & Rehabilitation, Faculty of Medicine, Suez Canal University, Suez Canal, Egypt
[4]Department of Clinical Pathology, Faculty of Medicine, Suez Canal University, Suez Canal, Egypt.

Rheumatoid arthritis (RA) is characterized by chronic inflammation and synovial hyperplasia that eventually leads to the destruction of the joints. CXCL10 has been originally identified as a proinflammatory chemokine that mediate leukocyte trafficking and modulate innate and adaptive immune responses. It plays a critical role in the inflammatory response and is involved in several biological processes. The aim of the study was to assess the diagnostic efficacy of serum CXCL10 levels in early RA patients. Patients and methods: The study included 60 RA patients; 30 of them were early diagnosed, and 30 longstanding RA and 30 healthy controls. Clinical examination was done for all patients. Measurement of serum CXCL10 level was done by ELISA, while assessment of disease activity in patients was done using disease activity score (DAS-28). Serum levels of CXCL10 were significantly higher in RA patients than controls (P< 0.001), and was more elevated in early diagnosed than longstanding RA patients, with a a significant positive correlation with DAS-28 ESR (r=0.361, P=0.005), number of tender joint (r=0.319, P=0.013), and number of swollen joint (r=0.280, P=0.030). A cutoff at 470.0 pg/ml was able to recognize longstanding RA with a sensitivity of 88.3% and a specificity of 90%, while a cutoff of 793 pg/ml was able to diagnose early RA with 65% sensitivity and 77% specificity (p=0.009). in conclusion, serum CXCL10 may be a useful biomarker for diagnosis of early RA and determination of disease activity.

THE EGYPTIAN JOURNAL OF IMMUNOLOGY Vol. 26 (2), 2019 Page: 79-86

Structure, Optical, Corrosion, and Photocatalytic Properties of Thermally Evaporated Molybdenum Trioxide Thin Films Deposited on Different Substrates

Sh. A. Elkot[1], W. S. Mohamed[1, 2], Mahmoud Elrouby[3], H. M. Ali[1], E. Kh. Shokr[1]
[1]Physics Department, Faculty of Science, Sohag University, 82524 Sohag, Egypt.
[2]Physics Department, College of Science, Jouf University, Al-Jouf, Sakaka, P.O. Box 2014, Saudi Arabia.
[3]Chemistry Department, Faculty of Science, Sohag University, 82524 Sohag, Egypt.

Abstract: In this study, we report the physical properties of sub-stoichiometric Molybdenum trioxide (MoO_{3-x}) thin films synthesized by thermal evaporation technique for photocatalytic application. MoO_{3-x} thin films were deposited on glass and Fluorine doped Tin Oxide (FTO) coated glass substrates with different thicknesses (100 - 650 nm). Structure analysis by X-ray diffraction and field emission scanning electron microscope confirm the amorphous structure of MoO_{3-x} films deposited on FTO and glass substrates. The optical analysis by UV-Vis–near-infrared spectrophotometer showed that the optical band gap does not depend on the substrate type and takes values in the range from 3.6 to 3.31 eV. The Corrosion measurements for MoO_{3-x} films deposited on FTO coated glass substrates were performed using an electrochemical potentiostat in a neutral medium of NaCl solution. The corrosion studies demonstrate that the as deposited MoO_{3-x} film of thickness 650 nm exhibits the highest corrosion resistivity compared with other thicknesses. The methylene blue (MB) was employed as a representative dye pollutant to evaluate the photocatalytic activity of the current samples. The results show that the film thickness and substrate type play an important role in the enhancement of the photocatalytic properties of MoO_{3-x} films. We found that the deposited films on glass decompose MB more than the films deposited on FTO. In addition, the as deposited MoO_{3-x} film of thickness 100 nm exhibit the highest photocatalytic activity as compared with the other deposited films. Keywords: MoO_{3-x} thin films; thermal evaporation; x-ray diffraction; optical analysis; corrosion; photocatalytic activity.

Keywords: MoO_{3-x} thin films; thermal evaporation; x-ray diffraction; optical analysis; corrosion; photocatalytic activity.

Int. J. New. Hor. Phys. 7(1), 7 -17 (2019)

Study the Effect of the Sintering Temperature on the Microstructure and Optical Reflectance of the Compacted Bulk $CuAlS_2$ Fabricated by Powder Metallurgy Technique (P/M)

Elsayed Abd Ellatif Ahmed[a], Moataz H. Ata[b], Mahmoud Elrouby[c], Hazem M. Ali[d]

[a]Lecturer at Middle Valley Technological College, Production Engineering, Ministry of Higher Education, Al Kawthar District, Sohag, Egypt

[b]Mechanics Department, Faculty of Industrial nn, Sohag University, 82524-Sohag, Egypt

[c]Chemistry Department, Faculty of Science, Sohag University, 82524-Sohag, Egypt

[d]Physics Department, Faculty of Science, Sohag University, 82524-Sohag, Egypt

Abstract: In this work, the effect of the sintering temperature of the bulk compacted powder sample on the microstructure and reflectance of the bulk $CuAlS_2$, which fabricated by powder metallurgy (P/M) technique, has been studied. The bulk was produced by (P/M) at compacting pressure of 350 MPa, sintering time 2 hr and different sintering temperature (100, 150, 200, 250 and 300°C). X-ray diffraction (XRD), scanning electron microscopy [SEM], energy dispersive analysis (EDS), and optical reflectance measurements were used for characterization of the prepared samples. The analysis of X-ray diffraction (XRD) indicated a formation of $CuAlS_2$ phase with preferring orientations of (1 1 2), (2 0 0), (2 2 0) and (0 0 8). The intensity of $CuAlS_2$ phase continuously increases with increasing the sintering temperature. It has been observed that the crystallite size increases with increasing of the sintering temperature from 24.25 nm at 100°C to 31.33 nm at 300°C, giving an indication of enhancement in the crystallinity. The analysis of (SEM) indicated the treated surface morphology of the bulk $CuAlS_2$. An increase in crystallization and formation of the $CuAlS_2$ phase was observed with increasing the sintering temperature. The cluster size shows remarkable rise with the increase of sintering temperature which confirms improvement in grain growth. The optical data shows, that with increasing the sintering temperature the reflectance decreased to 15% at 200°C in the near of infrared region (NIR) and 10% at 200°C and 250°C in the visible region (VIS).

European Journal of Mechanical Engineering Research, 6(1), (2019) 44-52.

g

Simultaneous Voltammetric Determination of Gallic and Protocatechuic Acids in Mango Juice Using a Reduced Graphene Oxide-Based Electrochemical Sensor

Refat Abdel-Hamid[1], Ahmed Bakr[1], Emad F. Newair[1], François Garcia[2]

[1]Unit of Electrochemistry Applications (UEA), Department of Chemistry, Faculty of Science, Sohag University, Sohag 82524, Egypt

[2]SPO, INRA, Montpellier Supagro, Montpellier University, UMR 1083, F-34060 Montpellier, France

Abstract: A simple and sensitive reduced graphene oxide-modified glassy carbon electrode-based electrochemical sensor was used for the concomitant determination of gallic acid (GA) and protocatechuic (PA) acid. The prepared sensor showed a significant enhancement in synergetic electro-catalytic performance towards GA and PA oxidation. A good resolution of the voltammetry peaks was obtained and a method of square wave voltammetry was developed for detection. The modified electrode was characterized by electrochemical techniques. The optimal experimental parameters were considered. GA and PA exhibited a linear increase in the peak currents with their concentrations in the range from 20 to 144 μmol·L−1 for GA and from 20 to 166 μmol·L−1 for PA, with limits of detection (S/N = 3) of 30.8 μmol·L−1 for GA and 10.2 μmol·L−1 for PA. The sensor applicability was simultaneously tested for the analytical determination of GA and PA in mango juice and exhibited a robust functionality.

Keywords: voltammetry; reduced graphene oxide; electrochemical sensor; phenolic acids; mango juice

Beverages 2019, 5, 17

Template Assisted Microwave Synthesis of rGO-ZrO_2 Composites: Efficient Photocatalysts Under Visible Light

Tarek T. Ali[1], Katabathini Narasimharao[2], Sulaiman N. Basahel[2], Mohamed Mokhtar[2], Edreese H. Alsharaeh[3], Hatem A. Mahmoud[1]

[1]*Chemistry Department, Faculty of Science, Sohag University, Sohag. 82524, Egypt*

[2]*Chemistry Department, Faculty of Science, King Abdulaziz University, Jeddah, KSA*

[3]*Chemistry Department, Colleage of Science and General Studies, Alfaisal University, Riyadh, KSA*

In this research, cetyltetraethyl ammonium bromide template assisted microwave procedure was utilized to synthesize reduced graphene oxide-zirconia (rGO-ZrO_2 nanocomposites by varying the rGO composition (1, 2, 5 and 10 wt%). The physico-chemical characteristics of the nanocomposites were studied using X-ray diffraction (XRD), Raman, differential scanning calorimetry (DSC), scanning electron microscopy (SEM), diffusive reflectance ultraviolet-visible (DRUV-vis), X-ray photoelectron spectroscopy (XPS) and N_2-physisorption techniques. The results from XRD, Raman and DSC studies indicate that the increase in rGO concentration resulted in the delay in ZrO2 crystallization temperature and alteration of ZrO_2 phase from monoclinic to tetragonal due to an effective incorporation of rGO nanosheets in ZrO_2 structure. The rGO loading also have an influence in the morphology of nanocomposites, as sample with 10 wt% rGO possessed unique monolith like morphology with macro pores. All the nanocomposites were utilized as photocatalysts for degradation of crystal violet dye in visible light irradiation. The rGO-ZrO_2 nanocomposites showed high reaction rates; the nanocomposite with 5 wt% rGO showed the superior photocatalytic performance as this sample possessed low band gap energy, high surface area, pore volume and presence of surface rGO-ZrO_2 interactive species as well as the reactive –OH groups. In addition, the synthesized nanocomposites exhibited excellent recyclability for photocatalytic degradation.

Keywords: rGO-ZrO_2, Nanocomposite, Microwave Synthesis, Photocatalytic Degradation, Crystal Violet, Visible Light.

Journal of Nanoscience and Nanotechnology, Vol. 19, 1–12, 2019

Morphology, Histology, and Chemistry of the wings of Tribolium castanaeum and Tribolium confusum (Coleoptera: Tenebrionidae)

Nasra M. H. Zohry[1], Ahmed Mohamed El-Sayed[2]

[1]Departement of zoology, Faculty of science, Sohag University

[2]Departement of Chemistry, Faculty of science, Sohag University

Abstract: Insect wings are excessively diverse structures which have fascinated scientist for centuries. Coleoptera is the largest in insect group and the most successful animal on earth (Nature communications 9(205): 1-11, 2018). In order to adapt to change in the environments, they developed strategies to cope up with different factors. The most distinctive feature of beetles is that the forewings are sclerotized into elytra; from this they get their formal name (Koleos=sheath, pteron=wing). The elytra play an important role in protecting the delicate hindwings and the dorsal surface of the abdomen. Besides its influence on protective the hindwing during flight the forewings are open enough to allow the hindwings to unfold and function.The structural and mechanical properties in living organisms may improve the understanding of natural solutions and advance the design of novel artificial materials. In this paper, the morphology and histological structure of the wings of two species of beetles, Tribolium castanaeum and Tribolium confusum, has been investigating using scanning electron microscopy (SEM). The organic chemical function groups of the wings were detected using Fourier-Transformed infrared spectroscopy (FTIR). Both Tribolium sp. have considerable variations regarding the total thickness, and width of the haemolymph space within the elytra. The elytra of both species bear conspicuous field of trichoid sensillae from dorsal side and numerous gland openings with a pit. The michrotrichia found on the ventral side may have an important role in wing folding. The presence of C-H stretching bands with the prevalence of methylene bands may indicate the presence of long chain aliphatic acids in surface waxes in T.castanaeum. The height of spikes of the hindwings was remarkable by hydrogen-bonded O-H and N-H amide stretching vibration and was correlated to the thickness of the wing.Insect wings are a core example of histological and morphological novelty. This study illustrates the morphological and histological structure of both the forewing and hindwing of Tribolium castaneum and Tribolium confusum which were the most destructive pest stored products.

The Journal of Basic and Applied Zoology (2019), Volume 80:16

Botany Department
قسم النبات

Botany

Botany Department
قسم النبات

Additions to the genus *Savoryella* (*Savoryellaceae*), with the asexual morphs *Savoryella nypae comb. nov.* and *S. sarushimana sp. nov.*

Sheng-Nan Zhang, Mohamed A. Abdel-Wahab, E.B. Gareth Jones, Kevin D. Hyde, Jian-Kui (Jack) Liu

Abstract:
Two asexual trichocladium-like species were recorded from coastlines in Japan and Thailand. Phylogenetic analysis of multi-gene sequence data placed them in *Savoryella* (*Savoryellaceae*), grouping with an unidentified strain isolated from submerged wood in a saline environment, but distinct from other *Savoryella* species. In this paper, we propose a new combination as *Savoryella nypae* based on *Trichocladium nypae* and a new species *Savoryella sarushimana*. *Savoryella sarushimana* differs from *S. nypae* in having larger conidial dimensions, with a rough to spiny surface and the proliferation of conidia. Detail morphological features coupled with sporulation in culture of the new taxa are illustrated. Notes on the phylogenetic placement of the discussed taxa and emendation of the genus *Savoryella* are provided.

Keywords: 1 new species, Mangrove habitat, Palm fungi, Phylogeny, Sordariomycetes, Taxonomy, Fungi
Phytotaxa 408(3):195-207. 2019

Natural products of *Alternaria* sp., an endophytic fungus isolated from *Salvadora persica* from Saudi Arabia

Abdallah M.Elgorban, Ali H.Bahkali, Dunia A.Al Farraj, Mohamed A.Abdel-Wahab

Abstract:
This study is to evaluate the potential of endophytic fungi of *Salvadora persica* for the production of bioactive compounds against pathogenic bacteria and fungi. Forty-two fungal isolates were obtained from 135 young and old stem and 125 root segments. Those 42 isolates representing ten fungi include: *Trichoderma* sp. (the most common), two species of *Alternaria*, *Rhizopus* arrhizus and 6 sterile mycelia. The ten fungi were grown in liquid culture and their crude extracts were tested against pathogenic bacteria and fungi. Nine crude extracts gave positive reactions against pathogenic bacteria of which *Alternaria* sp. (A8) was chosen further study. The fungal isolate was growing as sterile mycelium and was identified by phylogenetic analyses based on LSU rDNA sequence data and it might represent undescribed species of *Alternaria*. Sixty-two bioactive chemical compounds were identified from the ethyl acetate crude extracts of *Alternaria* sp., of which the following were recorded as major compounds in the active sub-fractions. These compounds showed strong antibacterial activity in combination.

Keywords: Arabian Peninsula, Antibacterial, Pleosporaceae, Molecular phylogeny
Saudi Journal of Biological Sciences Volume 26, Issue 5, July 2019, Pages 1068-1077

Saturnispora mangrovi f.a., sp. nov. from Syhat mangrove, Saudi Arabia

Abd El-Rahim M. A. El-Samawaty[1,2], Teun Boekhout[3], Mohamed A. Yassin[1,2], Mohamed A. Abdel-Wahab[1,4]

Abstract:
Strain SY-07 was isolated from decaying leaves of *Avicennia marina* collected from Syhat mangroves, Dammam city, Arabian Gulf, Saudi Arabia. Phylogenetic analyses of three genes [D1/D2 region of the LSU and SSU rRNA genes and internal transcribed spacer (ITS) region] showed that strain SY-07 represents a novel species of the genus *Saturnispora* distinct from closely related species. *Saturnispora mendoncae* was the most closely related species with an LSU gene sequence similarity of 89.3% (58 nucleotide substitutions and four indels out of 578 nt), 97% similarity for the SSU gene (42 nucleotide substitutions and 10 indels out of 1614 nt) and 88% similarity for the ITS region (15 nucleotide substitutions and eight indels out of 430 nt). In addition, strain SY-07 differed from *S. mendoncae* by its ability to assimilate D-galactose (weak), D-xylose (weak), meso-erythritol (delayed), glucono-δ-lactone, citrate (delayed) and ethylamine. *S. mendoncae* produced persistent asci that contain two to four spherical ascospores and lacked pseudohyphae, while sexual reproduction was not observed in strain SY-07 and extensive and pseudohyphae were present. Strain SY-07 was able to grow at between 25 and 40 °C, while *S. mendoncae* did not grow at 37 °C. The name *Saturnispora mangrovi* f.a., sp. nov. is proposed for strain SY-07. The holotype is CBS 15874, with the ex-type culture AUMC 12005. The MycoBank number for *Saturnispora mangrovi* f.a., sp. nov. is MB 827036.

Keyword(s): Arabian Gulf , yeast , *Avicennia marina*, Pichiaceae and Saccharomycetales
International journal of systematic and evolutionary microbiology (2019)

Nia lenicarpa sp. nov. (Niaceae, Agaricales) from Red Sea mangroves in Saudi Arabia with comments on *Nia vibrissa*

Mohamed A. Abdel-Wahab, E. B. Gareth Jones, Faten A. Abdel-Aziz, Ali H. Bahkali

Abstract
An undescribed *Nia* species was recorded from intertidal decayed wood of *Avicennia marina* collected from Red Sea mangroves in Saudi Arabia. *Nia lenicarpa sp. nov.* is characterized by smooth basidiomes, growing singly or in groups of 2 to 10 confluent basidiomes, with a three-layered, thick peridium and 4-spored basidia. *Nia lenicarpa* differs from *N. vibrissa* by having smaller basidiomes without peridial hairs but with thick peridia, larger basidia and basidiospores. Phylogenetic analyses of SSU and LSU rDNA placed *N. lenicarpa* in a monophyletic clade with two *N. vibrissa* clades. There are no molecular data available for the other two *Nia* species; *N. epidermoidea* and *N. globispora*. The morphology of *N. vibrissa* from driftwood collected from a beach in Japan is illustrated. Vertical sections of basidiomes of the Japanese material showed the presence of an outer peridium that is formed by the tips of the peridial hairs which was not reported before. This supports the presence of several cryptic species in the *N. vibrissa* complex.

Keywords: lignicolous manglicolous fungi, marine fungi, Middle East, molecular phylogeny, systematics, Fungi
Phytotaxa 406.3 (2019): 157-168.

An online resource for marine fungi

E. B. Gareth Jones • Ka-Lai Pang • Mohamed A. Abdel-Wahab et al.,

Abstract

Index Fungorum, Species Fungorum and MycoBank are the key fungal nomenclature and taxonomic databases that can be sourced to find taxonomic details concerning fungi, while DNA sequence data can be sourced from the NCBI, EBI and UNITE databases. Nomenclature and ecological data on freshwater fungi can be accessed on http://fungi.life.illinois.edu/, while http://www.marinespecies.org/provides a comprehensive list of names of marine organisms, including information on their synonymy. Previous websites however have little information on marine fungi and their ecology, beside articles that deal with marine fungi, especially those published in the nineteenth and early twentieth centuries may not be accessible to those working in third world countries. To address this problem, a new website www.marinefungi.org was set up and is introduced in this paper. This website provides a search facility to genera of marine fungi, full species descriptions, key to species and illustrations, an up to date classification of all recorded marine fungi which includes all fungal groups (Ascomycota, Basidiomycota, Blastocladiomycota, Chytridiomycota, Mucoromycota and fungus-like organisms e.g. Thraustochytriales), and listing recent publications. Currently, 1257 species are listed in the marine fungi website (www. marinefungi.org), in 539 genera, 74 orders, 168 families, 20 classes and five phyla, with new taxa continuing to be described. The website has curators with specialist mycological expertise who help to provide update data on the classification of marine fungi. This article also reviews knowledge of marine fungi covering a wide range of topics: their higher classification, ecology and world distribution, role in energy transfer in the oceans, origin and new chemical structures. An updated classification of marine fungi is also included. We would like to invite all mycologists to contribute to this innovative website.

Keywords: Fungal classification marine fungi website High-throughput sequencing techniques. Fungal diversity Origin of marine fungi

Fungal Diversity (2019) 96:347–433

Phylogeny of new marine Dothideomycetes and Sordariomycetes from mangroves and deep-sea sediments

Evan Benjamin Gareth Jones, Bandarupalli Devadatha, Mohamed A. Abdelwahab, Monika C. Dayarathne, Sheng-Nan Zhang, Kevin D. Hyde, Jian-Kui Liu, Ali Hassan Bahkali, V. Venkateswara Sarma, Sanja Tibell, Leif Tibell, Meng-meng Wang, Fang Liu, Lei Ca

Abstract

This paper documents six new saprobic marine fungi and one new genus based on morphology and multi-gene phylogenies. Three Dothideomycetes, and members of the Pleosporales, are introduced: *Pseudomassariosphaeria triseptata* sp. nov. was recognized as a mangrove species in Amniculicolaceae, and *Salsuginea phoenicis* sp. nov. was discovered as a second member of Salsugineaceae. A new genus *Raghukumaria* with *Raghukumaria keshaphalae* sp. nov., recovered from mangroves, is phylogenetically sister to *Halomassarina* and nests in the Trematosphaeriaceae. Three new species are referred to the Sordariomycetes: *Coniochaeta marina* (Coniochaetales, Coniochaetaceae) on driftwood; *Fusicolla bharatavarshae* (Hypocreales, Nectriaceae) is introduced with asexual and sexual morphs, on decayed mangrove wood of *Avicennia marina*; and *Fusarium sedimenticola* (Hypocreales, Nectriaceae) is new to the *Fusarium solani* species complex (FSSC) from deep-sea sediment.

Keywords: Coniochaetales; deep sea; estuarine palm; Hypocreales; Pleosporales

Botanica Marina. 2019

Phaeonectriella alba sp. nov. from the River Nile, Egypt

Ahmed E. Abdel-Aziz, Sabah S. Mohamed, Ahmed M. Abdel-Raheem†, Mohamed A. Abdel-Wahab

Abstract

A new species, *Phaeonectriella alba*, collected from the River Nile, Aswan Governorate, Egypt, is described and illustrated. Phylogenetic analyses of LSU rDNA sequences placed the new species with *P. lignicola* (the type species) in a highly supported clade. *Phaeonectriella alba* is characterized by conical, superficial, hyaline, membranous ascomata; 4- or 8-spored asci that are persistent, clavate, with a truncate apical thickening and a simple pore and cytoplasmic retraction below apex; early deliquescing catenophyses; and ascospores that are ellipsoid to broad ellipsoid, thin-walled, 1–3 septate, hyaline when young, becoming brown at maturity, with an apical germ pore in each cell and without appendages.

Key words: freshwater fungi, *Halosphaeriaceae*, *Microascales*, Middle East, subtropical Fungi

Mycotaxon (2019) Volume 133, pp. 597–605

Marine fungi from Red Sea mangroves in Saudi Arabia with Fulvocentrum rubrum sp. nov. (Torpedosporales, Ascomycota)

Abdel-Wahab, Mohamed A.; Jones, E. B. Gareth; Bahkali, Ali H. A.; El-Gorban, Abdallah M.

Abstract

Twelve fungi (ten ascomycetes, one asexual fungus, and one basidiomycete) were recorded from 833 samples of intertidal decayed wood of *Avicennia marina* collected from three mangrove sites at the Red Sea coast of Al-Leith city, Saudi Arabia. Common fungi were: *Nia* sp. (10%), *Sammeyersia grandispora* (8.5%), *Fulvocentrum rubrum* sp. nov. (5.8%), *Marinosphaera mangrovei* (4.2%) and *Okeanomyces cucullatus* (4.2%). Among the recorded fungi, six taxa are potentially new to science, of which *Fulvocentrum rubrum* sp. nov. is described in this article based on morphology and LSU rDNA sequence analysis. Phylogenetic analyses positioned the new species within the family Juncigenaceae, Torpedosporales. *Fulvocentrum rubrum* is characterized by erumpent to superficial, membraneous ascomata with long and wide necks; asci with apical ring and 3–5-septate ascospores that are larger than those recorded in the two previously described *Fulvocentrum* species. *Fulvocentrum rubrum* differs from F. *aegyptiacum* and *F. clavatisporum* by having longer and wider ascospores that are surrounded by a gelatinous sheath and an apical ring in the ascus.

Keywords: Hypocreomycetidae • manglicolous fungi • Middle East • molecular phylogeny • tropical fungi

Nova Hedwigia 108.3-4 (2019): 365-377

Biosynthesis of cadmium selenide quantum dots by *Providencia vermicola*
Abou-Assy, Rawan S., Bahig A. El-Deeb, Abdullah D. Al-Talhi, Nasser Y. Mostafa.

Abstract:
Cadmium selenide quantum dots (CdSe QDs) were synthesized by using Providencia vermicola BGRW, which has discriminatory ability to resist many metals such as Selenium, Cadmium, Silver, Zinc, Copper, Lead, Nickel, Cobalt and Bismuth metals. BGRW was able to grow in the presence of 6 mM of CdCl2. The best conditions for extra/intracellular CdSe QDs synthesis were 0.1 mM SeO2: 0.9 mM CdCl2, 37°C, pH 9 within 24 h. The biosynthesis of CdSe QDs was monitored by UV–Visible spectrum that showed surface plasmon resonance (SPR) peaks at 388 nm. Depending on fluorescence property of quantum dots, photoluminescence characteristics of the biogenic CdSe QDs were at 385 nm. Further characterization of synthesized CdSe QDs was carried out using the X-ray Diffraction (XRD), Transmission Electron Microscope (TEM) and Fourier Transform Infrared (FTIR) spectroscopy. TEM and XRD analysis revealed that CdSe QDs was cubic in shape with a size range of ~2 to 4 nm. EDS analysis confirmed the composition of QDs from cadmium and selenium ions. FTIR spectroscopy confirmed the presence of proteins as the stabilizing agent surrounding the quantum dots. Key words: Quantum dots, cadmium selenide quantum dots, capping agent, transmission electron microscope, fluorescence spectroscopy, X-ray and FTIR analysis.

African Journal of Microbiology Research (2019)

Potassium Synergize the Positive Effect of Ascorbic Acid on some Morpho-physiological Parameters of Salt Stressed Faba Bean Cultivars
Naglaa Loutfy, M. M. Azooz, A. M. Hassanein, A. Bassiony

Abstaract:
THIS WORK was undertaken to evaluate the effect of ascorbic acid (AsA) and potassium (K) on some morpho-physiological parameters of two *Vicia faba* L cultivars (Giza 843 and Giza 716) grown in nutrient solutions containing different concentrations of NaCl (50, 100 and 150mM NaCl) and K (5, 10 and 15mM) for two weeks. In general, under saline conditions, significant reduction in plant biomass and chlorophylls was detected. Seed presoaking in AsA solution resulted in massive increase in growth parameters and chlorophyll contents in both genotypes of stressed and non-stressed plants, but it depended on K concentration, 15mM K was the best. The positive effect of AsA on growth of salt stressed plants was not manifested when K concentration was low (5mM). In both genotypes, carbohydrate and protein contents increased as NaCl increased. Further significant-increase in their contents was detected when seeds were soaked in AsA and plants were cultured under salt stress; it depended on K concentration in the nutrient solution, 15mM K was the best. This type of synergizing between AsA and K on carbohydrate and protein contents was absent under low concentration of K. Sodium increased but K, Mg and Ca contents decreased in both cultivars under salt stress especially when K concentration was low (5mM). Under stressed or unstressed conditions, significant decrease in Na but significant increase in K, Ca and Mg contents due to AsA was detected and it was proportional to K concentration, 15mM K was the best.

Keywords: Ascorbic acid, Organic solutes, Potassium, *Vicia faba*.
Egypt. J.Bot. Vol. 59, No.3, pp. 735-751 (2019)

Oxidative stress caused by Basagran® herbicide is altered by salicylic acid treatments in peanut plants

DEM Radwan, AK Mohamed, KA Fayez, AM Abdelrahman

Abstract:

The present work was to study a protective role of salicylic acid (SA) on oxidative stress caused by Basagran®herbicide application. Two peanut cultivars (Arachis hypogaeacv. Giza 5 and Giza 6) with different sensitivities tothe herbicide were monitored for their antioxidant responses to Basagran®and/or SA treatments. Two weeks aftertreatment, Basagran®lowered leaf pigments (Chlorophyll a, Chlorophyll b and total Carotenoids) but increasedhydrogen peroxide (H2O2) and malondialdehyde (MDA) contents indicating occurrence of lipid peroxidation andoxidative stress. Salicylic acid applied prior to low dose Basagran®lowered H2O2and MDA contents in both G5and G6. Except for SOD which is highly stimulated, POD, CAT and APX activities showed slight changes comparedto control in leaves treated with Basagran®SA. The extracts tested by DPPH showed increase in total antiox-idant activity by 4%–7% in SAþBasagran®treated leaves compared to control. The increased total antioxidantactivity was related to the accumulation of amounts of phenolics as a protective action stimulated by SA. Al-terations of antioxidant enzymatic system, accumulation of phenolics, increasing the total antioxidant activity by SA provide an evidence of protective action of SA in Basagran®detoxification

Keyword: Agriculture

Heliyon 5.5 (2019): e01791.

Isolation and Characterization Of Novel Egyptian Regulatory Gene Tri 10 From *Fusarium fujikuroi* (MG211161)

Samia El-Rabbat, Osman El-Maghraby, Samah El-Debaiky, Ashraf Haider

Abstract:

The Egyptian isolate *Fusarium fujikuroi* (MG211161) has been previously isolated and showed high accumulation of T-2 toxin. In the present study, Tri10 gene fragment was isolated and characterized from *Fusarium fujikuroi*. A regulatory gene that control the pathway of cluster genes (Tri 3, Tri 5, Tri 4, Tri 8, Tri 6 and Tri 7) to produce T-2 toxin. The gene fragment was PCR amplified using nested primer. Nucleotide sequence analysis indicated 522 base pair fragment, that showed 98% similarity with the gene isolated from *F. fujikuroi* (HF679024.1). Amplified sequence was submitted to the gene bank and registered with the accession number (MG674224).

Keywords: *Fusarium*, Tri 10 gene, Nested PCR

GSJ: Volume 7, Issue 4, April 2019

Floristic Diversity and Phytogeography of Mil steppe-Azerbaijan

Gurbanov E. M., Naglaa Y. Abdallah, Mammadova Z. J., Asadova K. A. Ahmed Elkordy

Abstract:
Chorology and Phytogeography of Mil steppe and environs were studied. The results show that; 926 species belonging to 457 genera and 91 families were recorded. Five families: Poaceae, Asteraceae, Fabaceae, Brassicaceae and Chenopodiaceae contribute 42.51 % of the total plant species recorded in this study. Poaceae is represented by 59 genera (12.83 %) of the total observed plant species. Asteraceae carry 54 genera (11.83 %), while Brassicaceae, Fabaceae and Chenopodiaceae carry 39, 22 and 21 genera (8.48 %, 4.79 %, and 4.57 %) respectively. 40 endemic species belonging to 31 genera and 20 families were listed. Among them, 25 species are endemic to Caucasus, 11 species are endemic to Azerbaijan and 4 species are subendemics. The majority of the listed species in this study are annual represented by 440 species (47 %), the second most recorded life span was the perennial, which are represented by 404 species (44 %). Five life forms are observed in the current study. Therophytes are the most frequent life form with 475 species (51%), followed by hemicryptophytes with 314 species (34 %), Cryptophytes with 76 species (8 %), Phanerophytes with 26 species (4 %) and Chamephytes with 38 species (3 %). Chorological analysis revealed that the Mediterranean -Irano-Turanian is the most dominant phytochorion represented by 151 species (13.1 %), followed by Palearctic and Mediterranean phytochoria represented by 115 species (12.5 %) and 113 species (12.3 %) respectively.

Keywords: Chorology, Floristic composition, Kura-Araks lowland, Mil steppe, phytogeographical elements.
J. Eco. Heal. Env. 7, No. 1, 21-30 (2019)

Bioaccumulation of heavy metals air pollutants by Urban trees

Ahmed Ali El-Khatib, Nasser A. Barakat, Naglaa A. Youssef & Nesrin A. Samir

Abstract:
Leaf and bark of trees are tools for assessing the effects of the heavy metals pollution and monitoring the environmental air quality. In this study, the possibility of using leaves and bark of two urban trees, namely, *Ficus nitida* and *Eucalyptus globulus* as a bioindicator of atmospheric pollution was evaluated by determining the composition of heavy elements in the tree leaves, bark, soil, and the atmospheric dust. Two common tree species, namely, *F. nitida* and *E. globulus* were selected in the heavily industrial zone of surrounding Minya governorate, Upper Egypt. Two urban areas with heavy traffic load (sites 1 and 2), three industrial zones (sites 3, 4, and 5) and an uncontaminated area as a control were selected (site 6). Sampling from leaf, bark, soil, deposited dust of trees was carried out in winter and summer seasons (from November 2016 to March 2017). The concentrations of heavy metals in dust, soil, leaves, and bark possess the same trend: Pb>Cu>Cd. The highest concentration of cadmium, lead, and copper was found in the leaf of *F. nitida* and *E. globulus* higher than bark samples of the studied species, supporting the idea suggesting that tree leaves can be used as a good indicator of heavy metals accumulation. A high and statistically significant correlation ($p<.05$) was found between Pb concentrations in the atmospheric dust and those in the leaves of both species throughout the two growing seasons, confirming that the main source of incorporated Pb is the atmospheric dust. Otherwise, the obtained results showed that F. nitida tree does not seem to be a good accumulator of Cu. According to the obtained results, F. nitida and *E. globulus* trees are more likely to capture cadmium and lead from air, so planting these trees in industrial areas with such atmospheric pollutants would be beneficial.

Keywords: Bark; bioaccumulation; heavy metals; leaf; monitoring; urban trees
International Journal of Phytoremediation (2019)

Fine-template synthetic process of mesoporous TiO_2 using ionic/nonionic surfactants as potential remediation of Pb(II) from contaminated soil

M. M. Khalaf · N. Y. Abdallah · H. M. Abd El-Lateef

Abstract:
This trend of research deals with preparation of mesoporous TiO_2 by a simple approach using sol–gel method by various surfactant templates. The designed nano-adsorbents TiO_2 were featured by various characterization methods of Fourier transform infrared, X-ray diffraction, surface area analysis (Brunauer–Emmett–Teller), transmission electron microscope, and scanning electron microscope. These obtained nano-adsorbents are examined as functional adsorbents for lead ions up taking from contaminated soil specimens. The results presented the effect of ionic and nonionic surfactant templates on the texture of the three types of mesoporous TiO_2 nano-adsorbents. The effects of the temperature, pH, and amount of nanoadsorbents TiO_2 on the adsorption process were studied. The optimum conditions of 25 °C, 5, and 0.1 g were obtained for temperature, pH, and amount of adsorbents, respectively. The obtained results revealed that about 97.6, 99.1, and 95.3% of total adsorptive capacity were obtained for Ti C, Ti S, and Ti P, respectively, at 100 mg L−1 of Pb(II) ions in soil solutions during 120 min. The adsorption isotherm and the thermodynamic parameters were further illustrated. These findings recommended these nano-adsorbent TiO_2 as adequate adsorbents in remediation process of Pb-enriched soil.

International Journal of Environmental Science and Technology (2019) 16:1933–1944

Floristic diversity and vegetation analysis of riparian and aquatic plants of the canals in the Sohag Governorate, Egypt

Ahmed Elkordy, Omer Elshikh & Naglaa Abdallah

Abstract.
This paper analyzes the five elements of vegetation: floristic composition, lifespan, life form, chorology, and species distribution of the riparian and aquatic flora of canals in the Sohag Governorate of Egypt. The riparian vegetation included 126 taxa belonging to 35 families and 95 genera. Poaceae, Fabaceae and Asteraceae were the dominant plant families (50.00 % of the total number of the plant taxa). Annuals claimed 57.94 % of all plant taxa, and 40.48 % were perennials. Therophytes and hemicryptophytes were the predominant life forms of riparian taxa. Monoregional and pleuriregional taxa dominated the vegetation along the canals of the Sohag Governorate, both with 29 species or 23.02 % of all identified taxa. Biregional taxa accounted for 20.63 % of all taxa. There were 11.11 % of cosmopolitan and 11.91 % of indigenous taxa to the tropical areas worldwide. Plants from the Palaeotropical Kingdom constituted 8.73 % of the riparian plant taxa. Plants originally distributed over the Mediterranean floristic region dominated in the canal riparian areas of the studied area, with 61 taxa or 48.41 %. Furthermore, this study identified 41 taxa of aquatic plants from 21 genera and 16 families that were free-floating, rooted and floating, or submerged plants.

Keywords: Aquatic, biogeography, canal banks, chorology, diversity,flora, life form, riparian vegetation
PHYTOLOGIA BALCANICA 25(1): 81–95, Sofia, 2019

Detection of free and bound microcystins in tilapia fish from Egyptian fishpond farms and its related public health risk assessment

Zakaria Mohamed, • Zeinab Ahmed, • Asmaa Bakr, • Mohamed Hashem, • Saad Alamri

Abstract

Microcystins (MCs), the most common cyanobacterial toxins in freshwaters, can accumulate in aquatic animals in free and bound forms. MCs therefore pose a risk to human health upon consumption of contaminated fish tissues, as they cause severe liver damage and death with potential carcinogenic effects. While there have been extensive studies on free MC contents in fish tissues, the detection of bound MCs in fish is largely unexplored. In the present study, both free and bound MCs were monthly monitored in tilapia fish from three tropical fishponds in Egypt for one year. Fishpond waters contained high concentrations of MCs (18–44 lg/l). Free MCs were estimated in tilapia fish organs at levels up to 11.8 ng/g in intestines, 8.3 ng/g in livers and 0.38 ng/g in edible tissues. Concentrations of bound MCs in edible tissues as determined by Lemieux oxidation technique (15,000–19,000 ng/g fresh weight, FW) were several-folds higher than free MCs. The estimated daily intake (EDI) for free MCs (0.0006–0.002 lg/kg/day MCs) in edible tissues was lower than the WHO limit (0.04 lg/kg/day), while EDI of bound MCs exceeded this limit by a factor of 77–2396. Therefore, both free and bound MCs in fish tissues should be considered when fish are monitored for human consumption.

Keywords: Accumulation _ Bound microcystins _ Cyanobacteria _ Fish _ Human health

Journal of Consumer Protection and Food Safety. 2019

Direct transesterification of fatty acids produced by *Fusarium solani* for biodiesel production: Effect of carbon and nitrogen on lipid accumulation in the fungal biomass

Abdel-Hamied M. Rasmey, Mostafa A. Tawfik, Marwa M. Abdel-Kareem

Abstract:

The present work aims to explore a new oleaginous *Fusarium* isolate potential to accumulate lipids in its biomass from inexpensive substrates. In addition, impacts of crabon and nitrogen sourses and their ratios on lipid production by the interested fungal isolate were also conducted.

Journal of Applied Microbiology (2019)

Assessment of phytoplankton species in gut and feces of cultured tilapia fish in Egyptian fishponds: Implications for feeding and bloom control

Zakaria Mohamed, Zeinab Ahmed and Asmaa Bakr

Abstract: Aim: This study was carried out to determine which phytoplankton species, as a natural food, can be ingested and digested by Nile tilapia (*Oreochromis niloticus* L.). **Methods:** During this study, phytoplankton in the gut contents of Nile tilapia collected from three fishponds in southern Egypt were investigated during the period Oct. 2012-Sep. 2013. Samples of tilapia fish were grown in aquarium containing filtered pond water to detect undigested phytoplankton species in the feces. **Results:** The majority of the phytoplankton found in the gut of Nile tilapia was Cyanobacteria (36-50%) and Chlorophyta (27-38%). Other groups such Diatoms, Euglenophyta and Dinophyta were also found but with lower percentages (<19%). The most important and dominant phytoplankton species found in Tilapia gut were the potentially toxic cyanobacteria, *Anabaena*, *Anabaenopsis*, *Cylindrospermopsis*, *Microcystis* and *Planktothrix*. Only diatoms were recorded in the feces, indicating the ability of Tilapia to digest all phytoplankton except diatoms. **Conclusions:** The data of this study could be useful for biomanipulation of nuisance phytoplankton blooms in eutrophic aquacultures.

Keywords: cyanobacteria; diatoms; digestion; ingestion; tilapia.
Acta Limnologica Brasiliensia, 2019, vol. 31, e27

Exogenous application of zinc mitigates the deleterious effects in eggplant grown under salinity stress

Abdelnasser Galal

Abstract:
The present study was conducted to investigate the effects of Zn application to salt stressed eggplant (*Solanum melongena* L.) seedlings grown in vitro and whether it can alleviate the deleterious effects of salinity or not. Zinc (0, 5, 10 and 20 mg/L) and sodium chloride (NaCl) at different concentrations (0, 50, 100 and 150 mM) were added to solidified half strength MS medium placed in 250 mL glass jars. The treatments were arranged in a 4×4 factorial experiment in a completely randomized design with four replications. Application of Zn to growing seedlings at different concentrations (5, 10 or 20 mg/L) increased the length of shoot and root and their dry weights, as well as enhanced the photosynthetic pigment contents and leaf relative water content compared to control. However, the application of NaCl to growing seedlings at different concentrations (50, 100 and 150 mM) significantly reduced the above mentioned attributes compared to control and those of Zn treatments alone. Treatment of seedlings with either Zn (5, 0 or 20 mg/L) or NaCl (50, 100 or 150 mM) significantly increased the proline content and the antioxidant enzyme activities of superoxide dismutase (SOD), peroxidase (POX) and ascorbate peroxidase (APX) in growing seedlings. However, the application of Zn to salt stressed seedlings mitigated the deleterious effects of salt stress in growing seedlings and increased the tolerance of seedlings to its deleterious effects.

Keywords: eggplant, antioxidant enzymes, electrolyte leakage, lipid peroxidation, salt stress
JOURNAL OF PLANT NUTRITION 2019, VOL. 42, NO. 8, 915–927

Some important aspects in Moringa oleifera Lam. micropropagation
Ahmed Hassanein, Jehan Salem, Fayza Faheed, Abdullah El-Nagish

ABSTRACT
Type and source of explant as well as the type of cytokinin were important factors for successful moringa micropropagation. Explants obtained from in vitro grown plant materials were better than others obtained from soil growing seedlings. In addition, nodal segments were better than shoot cuttings in terms of number of shoots/ explants, frequency of shoot formation and number of nodes/shoot. While callus formation on the base of nodal segment on BAP containing media were higher than those of KIN, especially under the influence of high concentration as an aspect of vitrification, BAP was better than KIN in moringa multiplication. Low nutrient medium (half strength MS) supplemented with 0.5 mg l-1 IAA was essential for successful root formation. The suitable conditions for moringa micropropagation on full strength MS or SH may exert low stress and low need to raise the expression of SOD and POX. On the other side, stress due to over increase of chemical components of double MS medium or low nutrient content of half strength MS, B5 or WPM expressed the highest number and staining intensity of SOD and POX bands, vice versa was detected in case of CAT .

Key words: medium type; shoot multiplication; cytokinins; gene expression; isoenzymes; micropropagation; antioxidant enzymes; type of explant
Acta agriculturae Slovenica 113.1 (2019): 13-27.

The action mechanism and biocontrol potentiality of novel isolates of Saccharomyces cerevisiae against the aflatoxigenic *Aspergillus flavus*
M. Marwa Abdel-Kareem[1], A.M. Rasmey[2], A.A. Zohri[3]

Abstract
Inhibition of Aspergillus flavus growth and its aflatoxins production using the biocontrol agent Saccharomyces cerevisiae as well as to explore its mode of action was studied. Eight strains of S. cerevisiae strains were able to suppress the growth of A. flavus Z103. The maximum growth inhibition of A. flavus Z103 was obtained by living cells of S. cerevisiae EBF101 and *S. cerevisiae* 117 with 85 and 83%, respectively. The sporulation inhibition and hyphae deterioration of A. flavus Z103 by *S. cerevisiae* cells adhesion were observed under SEM; up to 99_8% inhibition of aflatoxins biosynthesis by *A. flavus* Z103 was resulted when the fungus was treated by autoclaved extracellular crude of S. cerevisiae. Also, the tested strains are potential to produce exochitinase which could be suggested as another mode of action for its antifungal activity. GC-MS analysis of S. cerevisiae 117 extracellular secondary metabolites revealed the existence of 4-Hydroxyphenethyl alcohol (46.32%), 4, 4-Dimethyloxazole (9.14%) and 1,2-Benzenedicarboxylic acid dioctyl ester (2.8%).

Keywords: Aflatoxin, antagonism, chitinase, detoxification, GC-MS analysis, *S. cerevisiae.*
Letters in Applied Microbiology (2018). 68, 104--111

Metabolic profiling of endophytic *Bacillus subtilis* US2 isolated from *Rosmarinus officinalis* leaves with potential antimicrobial activity

Magdy A. Abu-Gharbia, Rehab M. Mohamed and Mohamed A. Awad

Abstract:

Twelve isolates of endophytic bacteria from *Rosmarinus officinalis* (Rosemary) have been screened for their potential in preventing growth of pathogens (*Bacillus subtilis, Staphylococcus epidermidis, Serratia marcescens, Proteus vulgaris, Bacillus cereus, Staphylococcus aureus, Pseudomonas aeruginosa, Klebsiella pneumonia, Fusarium oxysporum, Acremonium solani, Aspergillus flavus* and *Penicillium griseofulvum*) in addition to non-pathogenic *Aspergillus columnaris* and *Aspergillus ochraceus*. Endophytic bacterial isolates displayed considerable antimicrobial activity. The mean zones of inhibition produced by the different bacterial endophytes fluctuated between one and 49 mm. The most active endophyte inhibited growth of *Staphylococcus epidermidis* (28.67mm), *Serratia marcescens* (48.67mm) and *Bacillus cereus* (10mm). 16S rRNA sequence has been deposited in the NCBI GenBank database under accession number: MH093646 (*Bacillus subtilis*). Metabolic profiling analysis by GC-MS revealed that five compounds were major constituents of the crude extract obtained from endophytic *Bacillus subtilis* MH093646; (Cyclo-hexanone / 2-butoxy-Ethanol / Acetic acid, butyl ester / Propanoic acid, ethyl ester and 2-Butoxyethyl acetate). Twelve chemical constituents were identified from the crude extract of *Rosmarinus officinalis*. Alpha-Pinene / Camphene / 3-Carene / p-Cymene / D-Limonene / Bornyl acetate and Caryophyllene compounds had antimicrobial properties. Data indicated that antimicrobial activity of *Rosmarinus officinalis* is not related to the activity of the endophytic bacteria.

Key words: Endophyte; *Rosmarinus officinalis*; *Bacillus subtilis;* 16s rRNA; Antimicrobial activity**;** GC-MS

Journal of Pharmaceutical and Applied Chemistry, Vol. 6, No. 1, PP: 9-20

Zoology

Induction of hyperpigmentation and heat shock protein 70 response to the toxicity of methomyl insecticide during the organ development of the Arabian toad, Bufo arabicus (Heyden,1827)

Amin Abdou Seleem

Methomyl (MET) is a carbamate insecticide which is used as a substitute for organophosphorus compounds to protect crops against insects. The present study aims to evaluate the cytoprotection response of pigment cells and heat shock protein 70 (HSP70) after exposure to MET during the tadpole developmental stages of the Arabian toad, Bufo arabicus. Three developmental larval stages of the toad were selected and divided into two groups; Control and MET-exposed (MET-EX) tadpoles (10ppm). MET-EX tadpoles showed an increased number of pigment cells in the liver, kidney, anterior eye chamber, and skin tissues as compared to the control. The glycogen content in the developing liver and muscles (myotomes) of MET-EX tadpoles was decreased as compared to the control. In the MET-EX tadpoles, immunohistochemical staining showed an increase of HSP70 expression in the liver hepatocytes, the nucleated red blood cells (nRBC) in kidney glomeruli, the iridocorneal angle of anterior eye chamber, and the skin as compared to the control. The current study concluded that pigment cells and HSP70 represented a cytoprotecting response against MET insecticide during the organ development of B. arabicas tadpoles. Therefore, MET use should be regularly monitored in the environment to protect animals and human from exposure to this insecticide.

Keywords: Bufo arabicus, hyperpigmnetation, heat shock protein 70, methomylinsecticide, toxicity

Journal of Histotechnology, Volume 42, 2019 - Issue 3

Teratogenicity and neurotoxicity effects induced by methomyl insecticide on the developmental stages of Bufo arabicus

Amin A. Seleem

Abstract: Methomyl (MET) is a carbamate insecticide that has been widely used to protect the crop against insects as an alternative for organophosphorus insecticide. Thus the present study aims to evaluate the potential toxic effects of MET on the developmental stages of Bufo arabicus. Tadpoles were classified into three stages (25, 37, 40). Every stage was divided into two groups, control and MET-treated group (10 ppm for two weeks) after LC50 determination in acute toxicity test for 96 h. Control and MET-treated larvae were examined at the level of morphological, histological, skeleton deformities and immunohistochemical labeling of alpha-synuclein in the spinal cord and dorsal root ganglion. MET-exposed larvae showed hyperactivity, extreme agitation, abnormal swimming and kinking tail as compared to control. Alizarin Red S-Alcian blue staining showed scoliosis in MET-treated tadpoles at 25 and 37 stages; kyphosis, retarded tail regression and reduced ossification of the phalanges of digits for both fore-and hind limbs were noted in MET-exposed tadpoles at 40 stage as compared to control. Histopathological changes in myotomes, notochord and spinal cord were shown in MET-exposed tadpoles as compared to control. Immunohistochemical examination showed an over expression of alpha-synuclein either in the neurons of the spinal cord or in the dorsal root ganglion of MET-exposed tadpoles at stage 40 as compared to control. The present study concluded that MET insecticide induces malformation and teratogenicity effects which were accompanied by neurodegenerative effects for the neurons either in the spinal cord or in the dorsal root ganglion.

Keywords: Bufo arabicus; Alpha-synuclein; Methomyl insecticide; Teratology; Neurotoxicity

Neurotoxicology and Teratology, Volume 72, 2019, Pages 1-9

Evaluation of Leiurus quinquestriatus scorpion venom anticancer potential against Prostate Cancer Cell Lines (PC3)

Tito N. Habib*,Hemely A. Hassan, Fayza M. Ali, Nadia S. Mahrous

*Molecular Genetics' Lab, Zoology Dept., Faculty of science, Sohag University

Cytogenetic Lab, Zoology Dept., Faculty of Science, (Qena) South Valley University, Egypt

Abstract: Several recent studies by others have demonstrated the preventive and therapeutic efficacy of scorpion venom in different animal tumor models and cell culture systems including prostate, breast, colon and skin cancers. Polypeptide extracted from the Egyptian scorpion venom (Leiurus quinquestriatus), is being studied for both prevention and treatment of prostate cancer. We proposed that there are alterations in pattern of cell cycle in prostate cancer cell line (PC3) post incubation with scorpion venom (1mg/ml) for 24 h in vitro. The results are supported by comparing the percentage of cells in each phase of cell cycle It showed an increasing of apoptotic rate as 26.33% for pre G1; 71.2 % for G1/G0; 20.4% for S, and 8.4 % for G2/M phases, compared with cell control recording 66.4 % for G1/G0, 25.9% for S, and 7.7 % G2/M phases, respectively. Data recorded that scorpion venom induced Pre-G1 phase PC3 cell arrest for enhancing and providing the chance for the role DNA repair system. The present results providing strong rationale for further studies, to evaluate prevention and intervention strategies for L. quinquestriatus venom in pre-clinical prostate cancer models.

Keywords: Prostate cancer, L. quinquestriatus, DNA content, PC3, cell cycle, apoptosis.

Journal of Environmental Studies [JES] 2019. 19: 7-137

Marine Pollution of Chemicals Detergents Contamination Induced Apoptosis and Necrosis in Fish Liver (Sardine aurita) by Flow Cytometry DNA Measurements

Tito N. Habib* Mohamed F. El-Sayed, Fathi M. Ali, Tawfiq M. Almsatar

Abstract: Background: Presently, there are wide uses of detergents, which discharged to marine environment (Mediterrean sea). Detergents are organic chemical compounds, consisting of fatty acids, and different components of Alkyl Benzene, Sulphonates, Polyphosphates, Cellulose, Sucrinic acid, and Sodium Lauryl Sulfates. Further, even if at low concentrations, the synthetic detergents are considered to be toxic to marine biodiversity. Since, these surfactants are not completely degraded by waste water treatment. It has ability to damage the DNA and accumulated on fish and other marine organisms. Methods: Flow cytometry technique was applied, because it's accuracy for analysis of DNA contents. Hence, the present study evaluated the impact of sodium lauryl sulfate as synthetic detergent on the DNA of sardine fish as a marine biological indicator. Sardinella aurita was collected from clean and SLScontaminated sites. The flow cytometry technique was employed to assess levels of active (apoptosis) and passive (necrosis) cell death in both exposed and unexposed fishes to SLS. Result: Chemical detergent contains 120 ml (i.e., 20mg/L) of sodium lauryl sulfates. The result shows more distinct and significant differences of the early and late apoptosis/ necrosis of Sardine fish liver, compared with unexposed fish samples from cleaned reference site. Conclusions: The present data indicate that SLS was able to cause toxicity to fish. Data recorded revealed that toxicity as a significant accumulation of hepatic tissue cellular DNA during the G0-G1 in a significant way ($P<0.05$), compared with that of unexposed liver tissue. In the same way, there was an insignificant accumulation of hepatic cell's DNA in the S phase but not during the G2/M phase, finally there was a significant arrest / DNA accumulation during the PreG1- phase ($P<0.05$). In the meantime, accompanies of apoptotic profile of cells exposed to SLS showed a significant total apoptotic form significantly elevated compared with reference site.

Keywords: Detergents; Apoptosis; Necrosis; Flow cytometry; DNA content; Histopathology.

Journal of Biotechnology Research, Vol. 5, Issue. 11, pp: 113-122, 2019

RAPD-Contaminant Indicative Bands Induced by Sodium Lauryl Sulfate of Economic Fish (Sardine Aurita) from Libyan Coasts

Tito N. Habib* , Mohamed F. El-Sayed, Fathi M. Ali ,Tawfiq M. Almsatar

Abstract

The presence of sodium Lauryl sulfates (SLS) as synthetic detergents, in marine environment arises mainly from its presence in complex domestic and industrial effluents as well as its release directly from some applications (e.g., oil dispersants and pesticides). It has been reported that SLS is toxic and affects survival of aquatic animals such as fishes, microbes like yeasts and bacteria. It is also toxic to mammals like mice and humans but to a lesser extent. Many studies have shown that the direct discharge of untreated wastewater into aquatic environment containing anionic surfactants causes significant damage to the aquatic environment due to the growth of algae that consume oxygen needed for the life of aquatic organisms. These damages in the aquatic environment are caused not only by the presence of anionic surfactants (SLS), but also by their interaction with other pollutants in the aquatic environment, which increases their toxic effect on aquatic organisms. Such detergents, however, became a public nuisance because they were neither soluble nor biodegradable. The present study intended to evaluate the fate of SLS as synthetic detergents on Tripoli coastal site of Libya, and quantifying their impacts on fish (Sardine aurita) DNA mutation, compared with other species through literature review. Our results provide functional evidence for genome toxicity of fish, of the DNA mutation caused by detergents effluents. This study provides the rationale for a simple genetic test to identify the impacts of detergents on aquatic ecosystem of Libyan coastal region.

Keywords: Polymorphism; Contaminants' indicative bands; RAPD marker; SLS; Sardine aurita.

Journal of Biotechnology Research, Vol. 5, Issue. 8, pp: 69-76, 2019

Toxic impacts of the neem biopesticide (Triology®) on the histological structure of gills and intestine in the Grass Carp " Ctenopharyngodon idella".

Hamdy M.A. Hassanein, El-Sabry Abu_Amra, Faiza M. Soliman, Hanan A. Okail

Zoology Department, Faculty of Science, Sohag Uni., Egypt.

Abstract: The present study was planned to investigate the impact of neem biopesticide (Triology®) on the histological pictures of gills and intestine in the fresh water fish, grass carp " Ctenopharyngodon idella". Fish were divided into 3 fish groups, the first group was kept in pesticide free water and served as control, the second group was exposed to 1/10 LC_{50} (11.2 mg/L) of the pesticide for 15 days, throughout the period fish sampled after intervals of 5, 10 and 15 days post exposure followed by 10 days recovery, then sampled after the intervals of 5 and 10 days. The third group was exposed to 1/2 LC_{50} (56 mg/L) of neem pesticide for 6 days, then they were sampled after successive intervals of 2, 4 and 6 days of exposure followed by 6 days recovery where fish were sampled after the intervals of 3 and 6 days. The results showed that gills and intestine have exhibited severe and time-dependent histopathological lesions after exposure to both two concentrations of the used pesticide. However, a gradual recovery in the histological pictures was noticed after cessation of the treatment with the pesticide.

Key words: Neem- Azadirachta indica- Triology®- gills – intestine - grass carp "Ctenopharyngodon idella- histopathology.

Cypris polygoniae n. sp. (Ostracoda: Cyprididae) collected from wastewater of sewage station, Sohag, Egypt

Somaia A. Ramadan, Ebtesam A. Yousef, Amal M. Mohamed

Zoology Department, Faculty of Science, Sohag University, 82524 Sohag, Egypt.

Abstract: A new species of freshwater Ostracoda Cypris polygoniae collected from El-cola wastewater of the sewage station at Sohag, Upper Egypt was described and identified. Among the specific characters, carapace ornamentation is divided into three areas (Thimble-like depression, polygonal reticulation, Smooth area). The first antenna bears 3 rows of fine hairs pseudochaetae on the first segment, one spine on the third segment and γ seta on the sixth segment. Second antenna has three rod-like processes, two swimming setae and rows of fine pseudochaetae hairs on its segments. Mandibula has number of weak teeth, rod-like processes, rows of fine pseudochaetae hairs and a pair of strong setae with small setules on its different regions. Maxillula has two rows of fine pseudochaetae hairs on the second segment of maxillular palp and two claws with 11 teeth on the endite. There are several numbers of rows of fine pseudochaetae hairs of the three thoracopods. Additionally, there are fan-like setae on the fourth segment and one chelated process on the fifth one of third thoracopod. Furca has two rows of fine spines on each uropodal ramus.

Key words: Freshwater- Ostracoda- Cyprididae- Cypris.

Studies on the cuticle and musculature of freshwater mite, Unionicola aegyptiaca

Somaia A. Ramadan, Tarek G. Ismail, Asmaa N. Mustafa

Zoology Department, Faculty of Science, Sohag University

Abstract

Background: The aquatic Acari are known as water mites and occupy a wide range of habitats. The freshwater mite, Unionicola aegyptiaca were collected from the freshwater mussel, Caelatura aegyptiaca, River Nile, Sohag, Egypt. The present paper focuses on the structure of the cuticle and musculature of freshwater mite, U. aegyptiaca.

Results: Histologically, the cuticle consists of two main layers; epicuticle and procuticle. The latter divided into two sublayers, exocuticle (exo) and endocuticle (en). The musculature of the present species, U. aegyptiaca is divided into three regions; gnathosoma, idiosoma and legs. The muscles of the body are classified according to their position and function.

Conclusion: Details of muscles of gnathosoma, coxal epimerae, genital field and legs were all described and discussed. The cuticle and musculature of U. aegyptiaca were studied by using the light microscope and the drawings were down with the help of a camera Lucida. It is likely to note that, the cuticle and musculature of freshwater mite, U. aegyptiaca were described and discussed for the first time in Egypt.

Keywords: Water mites, Unionicola, cuticle, musculature.

Ameliorative effect of Spirulina platensis against lead nitrate–induced cytotoxicity and genotoxicity in catfish Clarias gariepinus

Mohamed Hamed, Hamdy A. M. Soliman, Alaa El-Din H. Sayed

Abstract

The present study was designed to investigate the protective role of dietary supplementation of Spirulina platensis (SP) against cytotoxic and genotoxic effects of lead nitrate in Clarias gariepinus. Four groups of fishes were used: first group as control which fed on basal diet, second group fed on basal diet and exposed to (1 mg/L of lead nitrate), third group fed on diet containing 0.25% SP and exposed to (1 mg/L of lead nitrate), and fourth group fed on diet containing 0.5%SP and exposed to (1 mg/L of lead nitrate). Fish samples were taken at 2nd and 4th week of exposure. The hematological indices of lead nitrate–exposed group were decreased significantly compared to the control group at 2nd and 4th week of exposure. Lead nitrate caused a significant increase in the percentage of poikilocytosis, micronuclei, and apoptotic cells as well as comet tail length and olive tail moment compared

with the control group at 2nd and 4th week of exposure. The highest level of damage was found on 4th week of exposure with all parameters. Dietary inclusion of SP ameliorated these cytotoxic and genetic changes, as well as this amelioration was concentration and time dependent. Consequently, the present study proposed that the addition of SP to the fish diet can be used as a promising protective agent to oppose cytotoxic and genotoxic effects of lead nitrate in aquaculture.

Environmental Science and Pollution Research

Assessment the effect of exposure to microplastics in Nile Tilapia (Oreochromis niloticus) early juvenile: I. blood biomarkers

Mohamed Hamed, Hamdy A.M. Soliman, Alaa G.M. Osman, Alaa El-Din H. Sayed

Abstract: There is a scarcity of knowledge about the impacts of microplastics (MPs) on the early juvenile stage of freshwater fish. The current study aims to inspect the exposure and post-exposure recovery of microplastics (MPs) on accumulation and blood biomarkers of Nile Tilapia (Oreochromis niloticus) early juvenile. Four groups of fishes were used; the first group was the control group, the second group was exposed to (1mg/L of MPs), the third group was exposed to (10 mg/L of MPs), and the fourth group was exposed to (100mg/L of MPs) for 15 days and 15 days of recovery. The results showed that significantly higher numbers of microplastics were observed in microplastics-exposed groups compared to control group. Biochemical parameters (creatinine, uric acid, AST, ALT, ALP, glucose, cholesterol, total protein, albumin, globulin, and A/G ratio) showed significant increment after exposure to microplastics for 15 days compared to control group in dose dependent manner. The hematological indices (RBC's count, Hb, Ht, MCHC, Platelets, WBC's count, and monocytes) showed a significant decline after exposure to microplastics for 15 days compared to control group, while MCV and MCH showed a significant increase after exposure to microplastics for 15 days. After the recovery period, microplastics accumulations, hemato-biochemical alterations were still detected in microplastics exposed groups compared to the control group except for WBC's count and MCV which return to normal levels. MPs caused anemia andperturbations in hemato-biochemical parameters which may cause mortality of tilapia early juvenile and should be considered in a program for monitoring hazard materials in the ecosystem.

Chemosphere 228 (2019) 345e350

Protective effects of a novel pyrazolecarboxamide derivative against lead nitrate induced oxidative stress and DNA damage in Clarias gariepinus

Hamdy A.M. Soliman , Mohamed Hamed , Jae-Seong Lee, Alaa El-Din H. Sayed

Abstract: Pyrazole derivatives display diverse biological and pharmacological activities. The aim of this study is to investigate the antioxidant properties of a novel pyrazolecarboxamide derivative (4-amino-N-[(4-chlorophenyl)]-3-methyl-1-phenyl-1H-thieno [2, 3-c] pyrazole-5-carboxamide) in African catfish, Clarias gariepinus, exposed to 1 mg/L PbNO3. Fish were intramuscularly injected with pyrazole-5-carboxamidederivative according to the following groupings: Group 1 (control), Group 2 (1 mg/L lead nitrate), Group 3 (1 mg/L lead nitrate 5 mg pyrazole derivative/kg body weight), and Group 4 (1 mg/L lead nitrate 10 mg pyrazole derivative/kg body weight) for two weeks and four weeks. Lead nitrate (1 mg/L) caused significant elevation of serum aspartate aminotransferase (AST), alanine aminotransferase (ALT), creatinine, uric acid, cholesterol, and glucose-6-phosphate dehydrogenase (G6PDH) compared to the control group after two and four weeks of exposure, while serum total lipids, alkaline phosphatase (ALP), and lactate dehydrogenase (LDH) were significantly reduced compared to the control group. Furthermore, levels of antioxidant enzymes superoxide dismutase (SOD) and catalase (CAT) and total antioxidant capacity (TAC) were reduced in group 2 compared to the control group. However, in group 2, hepatic lipid peroxidation (LPO) and DNA fragmentation percentage were significantly increased compared to the control group. Histopathological changes in the liver of lead-exposed groups included marked disturbance of hepatic tissue organization, degeneration of hepatocytes, dilation of blood sinusoids and the central vein as well as necrosis. Injection of pyrazole derivative for two weeks and four weeks reversed alterations in biochemical parameters, antioxidant biomarkers, lipid peroxidation, hepatic DNA damage, and histopathological changes in liver tissue induced by 1 mg/L lead nitrate. This amelioration was higher in response to high-dose pyrazole derivative (10 mg) at the fourth week of exposure, showing concentration-and time-dependency. Overall, the sensitized derivative pyrazolecarboxamide is likely a useful tool to minimize the effects of lead toxicity due to its potent antioxidant activity.

Environmental Pollution 247 (2019) 678e684

Recent progress in biomedical applications of chitosan and its nanocomposites in aquaculture: A review

Fatma Ahmed, Faiza M.Solim, Mohamed A. Adly, Hamdy A.M.Solim, Mansour El-Matboulia, Mona Saleha

Abstract: Chitosan nanoparticles (CSNPs) are the nanostructures of chitosan biopolymer which is derived from chitin polysaccharide, the main component of crustacean shells. Chitosan is a biocompatible, nontoxic and biodegradable polymer soluble in acidic solutions and easily excreted from kidneys. It is widely used in medical and pharmaceutical applications including artificial matrices for tissue engineering, drug transport, targeted drug delivery and protein or gene delivery. The antimicrobial activities of chitosan and CSNPS against different bacterial, fungal and viral pathogens made them valuable for several biological applications including food preservation purposes. In addition, they have immunomodulatory effects on fish and crustaceans providing direct positive impact on aquaculture and fish farming industry. Sustained release of some bioactive ingredients such as hormones, vitamins, nutrients and antioxidants has improved the biological activities of fish. Furthermore, CSNPs have recently been employed to diagnose fish diseases. In this review, we present the medical and biological applications of chitosan and CSNPs on aquatics to provide an update on recent advances and the potential for further advanced applications for aquaculture in the future.

Research in Veterinary Science, Volume 126, October 2019, Pages 68-82

Toxic and Genotoxic Effects of Silver Nanoparticles in Drosophila.

Alaraby M[1,2], Romero S[1], Hernández A[1,3], Marcos R[1,3].

[1]Grup de Mutagènesi, Departament de Genètica i de Microbiologia, Facultat de Biociències, Universitat Autònoma de Barcelona, Cerdanyola del Vallès, Barcelona, Spain.

[2]Zoology Department, Faculty of Sciences, Sohag University, Sohag, Egypt.

[3]CIBER Epidemiología y Salud Pública, ISCIII, Madrid, Spain.

Abstract

The in vivo model Drosophila melanogaster was used here to determine the detrimental effects induced by silver nanoparticles (AgNPs) exposure. The main aim was to explore its interaction with the intestinal barrier and the genotoxic effects induced in hemocytes. The observed effects were compared with those obtained by silver nitrate, as an agent acting via the release of silver ions. Larvae were fed in food media containing both forms of silver. Results indicated that silver nitrate was more toxic than AgNPs when the viability "egg-to-adult" was determined. Depigmentation was observed in adults including those exposed to nontoxic concentrations, as indicative of exposure action. Interestingly, AgNPs were able to cross the intestinal barrier affecting hemocytes that show significant increases in the levels of intracellular reactive oxygen species. Additionally, significant levels of genotoxic damage, as determined by the comet assay, were also induced. When the expression of different stress-response genes was determined, for both AgNPs and silver nitrate, significant upregulation of Sod2 and p53 genes was observed. Our results confirm for the first time that in an in vivo model as Drosophila, AgNPs are able to cross the intestinal barriers and produce primary DNA damage (comet assay) via oxidative stress induction. In general, the effects induced by silver nitrate were more pronounced than those induced by AgNPs what would emphasize the role of silver ions in the observed effects. Environ. Mol. Mutagen. 60:277-285, 2019.

Keywords: Drosophila melanogaster; comet assay; genotoxicity; reactive oxygen species; silver nanoparticles

Environ Mol Mutagen. 2019 Apr;60(3):277-285. doi: 10.1002/em.22262. Epub 2018 Nov 29.

Ultrastructural studies on the sensilla of the mouth parts and antennae of the pre-adult stages of sitophilus granarius (coleoptera: curculionidae)

Nasra M. H. Zohry

Department of Zoology, Faculty of Science, Sohag University,Sohag, Egypt

Abstract: The granary weevil S. granarius is one of the most important stored product pests on the world, because of its damage. This pest is the main reason of the post harvest losses in world production; as a result of adults and larvae infesting and feeding on stored grains. The morphology and ultrstructure of the mouth parts and antennae of the pre-adult stage of S. granarius was investigated using scanning electron microscopy. The antennae and mouth parts of the granary weevil larvae and pre-pupal stage have a number of very interesting sensillae. The antennae have one large sensillum with different morphological appearance. Pores have been noticed on both sides. This one is known as sensilla basiconica. The pores may have an auditory function. The 2nd, 4th, and prepupal stages have a very strong mandibles each of them have two long sensillae. On the lateral view of the distal part of maxillary palp there was a digitiform sensillum. The digitiform organ is considered as a hygrothermo-receptor and was located on the lateral surface of the last segment of the larval maxillary palp. Another type of sensillae have been present and called chaetica sensillae, sensillae like a peg (sensilla twig basiconica) and campaniform sensilla which are located on the upper surface of the antennae of the 2nd, 4th larval instar and prepupal stages.

Keywords: Sitophilus; Sensillae; SEM; Thermohygroreceptors; Olfactory receptors.

Morphology, Histology, and Chemistry of the wings of Tribolium castanaeum and Tribolium confusum (Coleoptera: Tenebrionidae)

Nasra M. H. Zohry[1], Ahmed Mohamed El-Sayed[2]

[1]Departement of zoology, Faculty of science, Sohag University

[2]Departement of Chemistry, Faculty of science, Sohag University

Abstract

Insect wings are excessively diverse structures which have fascinated scientist for centuries. Coleoptera is the largest in insect group and the most successful animal on earth (Nature communications 9(205): 1-11, 2018). In order to adapt to change in the environments, they developed strategies to cope up with different factors. The most distinctive feature of beetles is that the forewings are sclerotized into elytra; from this they get their formal name (Koleos=sheath, pteron=wing). The elytra play an important role in protecting the delicate hindwings and the dorsal surface of the abdomen. Besides its influence on protective the hindwing during flight the forewings are open enough to allow the hindwings to unfold and function.The structural and mechanical properties in living organisms may improve the understanding of natural solutions and advance the design of novel artificial materials. In this paper, the morphology and histological structure of the wings of two species of beetles, Tribolium castanaeum and Tribolium confusum, has been investigating using scanning electron microscopy (SEM). The organic chemical function groups of the wings were detected using Fourier-Transformed infrared spectroscopy (FTIR). Both Tribolium sp. have considerable variations regarding the total thickness, and width of the haemolymph space within the elytra. The elytra of both species bear conspicuous field of trichoid sensillae from dorsal side and numerous gland openings with a pit. The michrotrichia found on the ventral side may have an important role in wing folding. The presence of C-H stretching bands with the prevalence of methylene bands may indicate the presence of long chain aliphatic acids in surface waxes in T.castanaeum. The height of spikes of the hindwings was remarkable by hydrogen-bonded O-H and N-H amide stretching vibration and was correlated to the thickness of the wing.Insect wings are a core example of histological and morphological novelty. This study illustrates the morphological and histological structure of both the forewing and hindwing of Tribolium castaneum and Tribolium confusum which were the most destructive pest stored products.

The Journal of Basic and Applied Zoology (2019), Volume 80:16

Carcinoembryonic Cell Adhesion-Related Molecule 2 Regulates Insulin Secretion and Energy Balance

Salaheldeen Elsaid, Alexa Jaume and Sonia Michael Najjar

[1]Department of Biomedical Sciences, Heritage College of Osteopathic Medicine, Ohio University, Athens, OH 45701-2979, USA

[2]Department of Zoology, Faculty of Science, Sohag University, Sohag 82524, Egypt

[3]Diabetes Institute, Heritage College of Osteopathic Medicine, Ohio University, Athens, OH 45701-2979, USA

Abstract: The Carcinoembryonic Antigen-Related Cell Adhesion Molecule (CEACAM) family of proteins plays a significant role in regulating peripheral insulin action by participating in the regulation of insulin metabolism and energy balance. In light of their di_erential expression, CEACAM1 regulates chiefly insulin extraction, whereas CEACAM2 appears to play a more important role in regulating insulin secretion and overall energy balance, including food intake, energy expenditure and spontaneous physical activity. We will focus this review on the role of CEACAM2 in regulating insulin metabolism and energy balance with an overarching goal to emphasize the importance of the coordinated regulatory e_ect of these related plasma membrane glycoproteins on insulin metabolism and action.

Keywords: hyperinsulinemia; insulin clearance; insulin resistance; hyperphagia; energy balance

Protective Effects of Melatonin and Thymoquinone on Hematological Parameters, Hepatic and Renal Activities against Lithium-Chloride Toxicity in Male Albino Rats.

Mohamed F. El-Sayed[1], Sary Kh. Abd El-ghaffar[2], Aziz Awaad[1] and Mohamed M. Mahmoud[1]

[1]Zoology Department, Faculty of Science, Sohag University, Sohag, Egypt.

[2]Clinical Pathology Department, Assuit University, Faculty of Veterinary medicine, Assuit, Egypt.

Abstract: Lithium is a toxic alkaline metal that occur in the environment as industrial pollution and therapeutic use. Lithium is widely used in medicine in the treatment of mania and mood disordered, however its administration causes many side effects. The present study aimed to evaluate the protective effect of melatonin and thymoquinone as antioxidants against lithium toxicity. The study is designed five groups of male albino rats (6 for each group): I (Control)- treated with drinking water and food, II (Li)-treated with lithium chloride (LiCl), III-treated with LiCl and melatonin, IV-treated with LiCl and thymoquinone, and V-treated with LiCl combined with melatonin and thymoquinone. The following parameters were determined: red blood cells, hemoglobin, haematocrit, mean corpuscular volume, mean corpuscular heamoglobinconcentration, platelets, white blood cells, neutrophils, eosinophils, basophiles, monocytes and lymphocytes. Also, biochemical analysis such as glucose, total proteins, albumin and activities of alkaline phosphatase, aspartate aminotransferase and alanine aminotransferase in plasma as well as urea, uric acid, creatinine, cholesterol and triglycerides were determined. Results showed that oral administration of lithium chloride caused a non-significant decrease in RBCs , whereas it caused a significant decrease in hemoglobin (Hb) concentration, haematocrit(Ht), mean corpuscular volume(MCV), mean corpuscular hemoglobin concentration(MCH), eosinophils ,monocytes and lymphocytes, respectively. But, it caused a significant increase in the WBCs , the platelets and neutrophils, relative to the control group. Lithium significantly decreased serum glucose, total protein, albumin, whereas it significantly increased activities of alkaline phosphatase, aspartate aminotransferase and alanine aminotransferase, respectively, relative to the control. On the other hand, it caused a significant increase in the plasma levels of urea, uric acid, creatinine, cholesterol and triglycerides, respectively, relative to that of control. Administration of lithium chloride combined with either melatonin or thymoquinone, or both of them removed the toxic effects of lithium chloride on the above parameters via decreasing and increasing their values. These findings demonstrate that melatonin and thymoquinone may attenuate the toxic effects of lithium on the blood parameters, hepatic and renal functions in the experimental animals.

Keywords: Lithium chloride, Melatonin, Thymoquinone, Toxicity.

Molecular Method vs. Traditional Methods for Estimating the Prevalence of Larval Trematode Infections in Some Red Sea Snails

Muslimah, N. ALsulami[1, 2]*, Sabah M. Hassan[2, 3], Amaal Hassan[2, 4]

[1] Biology Department, Faculty of Science, University of Jeddah, Jeddah, Saudi Arabia

[2]Biology Department, Science College, King Abdulaziz University, Jeddah, Saudi Arabia

[3]Department of Genetics, Faculty of Agriculture, Ain Shams University, Cairo, Egypt

[4]Zoology Department, Faculty of Science, Sohag University, Sohag, Egypt.

Abstract

The importance of marine snails in the transfer of cercariae to fish as a provenance of zoonoses should be considered. Parasitic studies in marine snails have been uncommon in Saudi Arabia. In the present study, 550 Nerita genus of marine snails were monthly and randomly collected from January to December 2016 from Obhor bay, Saudi Arabia. The snails were subjected to light. They were crushed to evaluate the presence of larval trematodes. PCR technique was performed using the internal transcribed spacer region of ribosomal DNA (ITS-rDNA) which has been a specific primer to detect the extent of larval trematode infection in some snails infected as positive control samples and all non-infected snails to assess if they were infected or not. PCR technique showed a high prevalence of infection (55.82%) than the classical methods (21.45%). These studies can help in collecting data on the ecological importance of the distribution of disease in sympathetic fish, and the transmission of digenean trematodes disease through snails. Moreover, they can be useful in preventing and control of fish and human diseases.

Keywords: Marine snails, Prevalence, Trematode larvae, Cercaria, Molecular.

Corynebacterium tuberculostearicum, a human skin colonizer, induces the canonical nuclear factor kappa B inflammatory signaling pathway in human skin cells

Altonsy Mohammed Omar, Kurwa, Habib A.

University of Calgary, medicine Lauzon, Gilles; University of Calgary, Medicine Amrein, Matthias; University of Calgary, Cell Biology and Anatomy Gerber, Anthony; National Jewish Health, Medicine Almishri, Wagdi; University of Calgary, Medicine Mydlarski , P. Régine; University of Calgary, Medicine

Abstract

Introduction: Corynebacterium tuberculostearicum (C. t.) is a ubiquitous bacterium that colonizes human skin. In contrast to other members of the genus Corynebacterium, such as toxigenic Corynebacterium diphtheriae (C. d.) or the opportunistic pathogen Corynebacterium jeikeium (C. j.), several studies suggest that C. t. may play a role in skin health and disease. However, the mechanisms underlying these effects remain poorly understood. Methods To investigate whether C. t. induces inflammatory pathways in primary human epidermal keratinocytes (HEKs) and human cutaneous squamous carcinoma (SCC) cells, Cell culture, RT39 PCR, ELISA, immunofluorescence microscopy, Western blot, ChIP-PCR, siRNA knockdown and luciferase reporter expression system were used. Results Herein, we demonstrate that C. t. upregulates the mRNA and protein levels of inflammatory mediators in two human skin cell lines, HEKs and SCCs. We further show activation of the canonical nuclear factor kappa-B (NF-κB) pathway in response to C. t. infection, including phosphorylation of the inhibitor of kappa-B (IκB), the nuclear translocation of NF-κB subunit (NF-κB-P65) and the recruitment of NF-κB-P65 and RNA polymerase (RNA-Pol-II) to the NF-κB response elements at the promoter region of the inflammatory genes. The data further confirm that C. t.-induced TNF mRNA expression in HEKs is TLR2 dependent.

Conclusion: Our results offer a mechanistic model for C. t.-induced inflammation in human keratinocytes via TLR2 and activation of IκB kinase (IKK) and downstream signaling through the canonical NF-κB Immunity, Inflammation and Disease Page 4 of 48 For Review Only 4 pathway. Relevance to chronic inflammatory diseases of skin and cutaneous oncology are discussed.

Keywords: Corynebacterium tuberculostearicum, NF-kappa B, IKK, keratinocytes, cutaneous squamous 56 carcinoma cells, inflammation.

Immunity, Inflammation and Disease, IID3-2019-09-0062.R1

Copper (I) Nicotinate complex Abrogates Acrylamide Induced Hepatotoxicity in Male Rats: Biochemical and Histological Studies

Nagwa M. Elsawi[1], Wejdan, A. Aldajani[2], Mounir A. A. Mohamed[1], Ahmed. M. Ali[3], Gamal S. A.[4], Soad Shaker Ali[5], Sabra A. Abd El lah[1]

[1]Department of Chemistry, Department Faculty of Science, Sohag University, Egypt

[2]Department of Biochemistry, Department Faculty of Science, Sohag University, Egypt

[3]Department of Chemistry, Department Faculty of Science, Al-Azhar University, Assiut Branch, Egypt

[4]Department of Zoology, Department Faculty of Science, Sohag University, Egypt

[5]Department of Medical Biology, Department Faculty of Medicine, King Abdulaziz University, Jeddah, SA

This study was conducted as a trail to abrogates acrylamide induced hepatotoxicity in male rats by administration of copper (I) nicotinic acid complex. Animals were divided into 4 groups ;GI: control kept on balanced diet and tap water, GII :Acrylamide group received acrylamide in drinking water (7.5 mg/kg b.w.)for 30 days .GIII: treated with copper (I)-nicotinate complex (400 µg/kg b.w.) after acrylamide intoxication for 30 days and GIV the complex then acrylamide (prophylactic). Results showed significant increase in serum levels of AST, ALT,ALP,GGT and total antioxidant capacity (TAC) in acrylamide group. Moreover a significant increase in tumer markers AFU and TNF-Alpha. while Levels of each of S. total protein and S. albumin were significantly decreased in ACR group compared with control. Histological study showed congestion of central vein in liver section and vacuolation of hepatocytes in ACR group. Anticancer activity using in-vitro cytotoxic assay of Cu(I) Nicotinate complex ;proves the anticancer properties of it comparing with doxorubicin .Treatment with Copper (I)-Nicotinate Complex restored tissue and serological indices concomitantly towards normal levels. These results revealed that Copper (I)-Nicotinate Complex is able to significantly alleviate the hepatotoxicity induced by AA in rats and could be utilized as a potent food additives.

International Journal of Food and Nutritional Science, DOI: 10.15436/2377-0619.19.2416

Geology

Expansive potentiality of sabkha soils of Rabigh Lagoon, Saudi Arabia: a case study

Bader A. Hakami[1], El-Sayed Sedek Abu Seif[1,2]

[1]Faculty of Earth Sciences, King Abdulaziz University, P.O. Box 80206, Jeddah, Saudi Arabia

[2]Geology Department, Faculty of Science, Sohag University, P.O. Box 82524, Sohag, Egypt

Abstract: The geotechnical assessment of expansiveness potentiality of sabkha soils, Saudi Arabia has been achieved on subsurface clayey soil samples collected in Rabigh sabkha along the Red Sea throughout a variety of physical, chemical, mineralogical, and mechanical tests. The obtained results show that the studied Rabigh sabkha clays were deposited in restricted supra-tidal marine conditions. These sabkha clayey soils consist of silts (53.4 to 69.1%), clays (20.1 to 35.7%), and sands (5.457 to 9.93%) and are classified into high plasticity clays (CH) and high inorganic silts (MH). The clay mineral species (montmorillonite, illite, kaolinite, chlorite, and palygorskite) are of detrital origin except palygorskite that was formed authigentically. Based upon the activity (A), these sabkha soils are classified into active soil type. The swelling potentiality of Rabigh sabkha clays ranges from moderate to critical swell potentiality.

Keywords: Sabkha soils, Mineralogy, Expansiveness potentiality, Rabigh, Saudi Arabia.

Arabian Journal of Geosciences, Volume 12, Issue 4, 1 February 2019, Article niumber 107

Derivation of empirical relationships between geotechnical parameters and resistivity using electrical resistivity tomography (ERT) and borehole data at Sohag University site, Upper Egypt

Mohammed, M.A.[1], Sensoy, M.M.[2]and Abudeif, A.M.[1]

[1]Sohag University, Faculty of Science, Geology department, Egypt

[2]Assiut University, Faculty of Science, Geology Department, Egypt

Abstract: The new site is located in desert region of rugged topography. Quaternary boulders, gravels, sands and clays intercalation are the main rock types in the area. Geophysical evaluation of the subsurface lithology and structures using 2D and 3D electrical resistivity tomography (ERT) of the proposed site for construction was the main target of the present study, in addition finding empirical relationships between rock's electrical resistivity and some geotechnical parameters are also another target. Four geoelectrical resistivity layers were discriminated after the 2D inversion. Inspection of all 2D inverted profiles and 3D electrical resistivity depth slices showed rapid lateral and vertical variations in electrical resistivity values indicating heterogeneity in soil section. Clayey gravels or clayey sands and clays facies are predominant and hence swelling actions of the foundation beds is highly expected. The results of electrical resistivity tomography (ERT) were correlated with that inferred from the boreholes within the investigated area. The geotechnical parameters: liquid limit L.L%, plastic limit P.L%, free swelling F.S% and density Qu were calculated for representative samples collected from drilled boreholes. All samples showed considerably high L.L%, low to moderate P.L% with high F.S% which characterizes clayey soil.

A trial for finding empirical relationships between the geotechnical properties and the rock electrical resistivity (L.L%, P.L%, F.S% and Qu) were carried out. These relations revealed that there is a considerable correlation between them when the rock has a resistivity more than 400 Ω.m and poor correlation when the electrical resistivity is less than 400 Ω.m. Accordingly, inferring applicable empirical equations between rock electrical resistivity and geotechnical parameters can be strong in the dry successions with a limited clays content, but in the wet or clayey soil materials the correlation will be weak and risky in application. From all obtained results and relationships, highly engineering awareness should be taken into account during establishing any construction in this site.

Keywords: 2D Electrical Resistivity tomography (ERT), Geotechnical properties, Rock resistivity and geotechnical parameters relationships, New Sohag University.

Journal of African Earth Sciences, Volume 158, October 2019, Article number 103563

Geotechnical performance of sandy bricks made with fine aggregates of sand dunes, Saudi Arabia

El-Sayed Sedek Abu Seif[1,2], Abdullah Rashed Sonbul[1]

[1]Faculty of Earth Sciences, King Abdulaziz University, Jeddah, Saudi Arabia

[2]Geology Department, Faculty of Science, Sohag University, P.O. Box 82524, Sohag, Egypt

Abstract: The utilization of eolian sands as construction fine aggregates in bricks and mortar production has been achieved on dune sands collected from Jeddah-Al-Lith area (Saudi Arabia). These dune sands had been mixed with well-graded crushed fine aggregates at a variety mixing ratio fluctuated between 10 and 100% of the total volume of sand at constant ratio 1:2:3 (cement/water/sand). By comparing the physical characteristics (grain size, specific gravity, texture) mineral composition, workability and compressive strength features of the study materials, it is found that similarity with the most of the dune sands characteristics which reported in pervious literatures. The obtained results show that except for the gradational and textural features, these materials are fitting as construction fine aggregates when the mixing ratio not exceed than 50% of the total quantity of sands. Up to 50%, the compressive strength will be abruptly decreased owing to internal failure as a result of bleeding and segregation of raw mixtures before consolidation processes that due to increasing of surface area of well-rounded and high sphericity of dune grains.

Keywords: Sand dunes, Sandy bricks, Workability and strength, South Jeddah, Saudi Arabia.
Arabian Journal of Geosciences, Volume 12, Issue 5, 1 March 2019, Article number 166

Pleistocene aquifer sediments at sohag region, nile valley, egypt: a statistical approach

Shaymaa Rezk , Ahmed.A.Abdel Moneim, Abdallah M. Hassan, Mohamed H. Ali

Geology department Faculty of Science, Sohag University

Abstract: Well representative detrital sandy samples from the Quaternary aquifer system of the Nile River basin at Sohag area, Egypt, were collected for the geochemical and heavy minerals investigations. Multivariate statistical techniques were applied to the obtained data. Although the heavy mineral analysis is useful in determining the provenance of the siliciclastic sediments, yet the interpretation of the data is greatly improved by determining the chemical composition of the enclosed sediments. The present study revealed that many heavy mineral species show significant variations in their distribution which may be related to their provenance. Thus, as giving greater confidence in minerals identification, but geochemical analysis of the Pleistocene sediments adds precision to the evaluation of the relative contributions of the potential source ideologies. Furthermore, multivariate statistical analyses of the geochemical and heavy minerals data from the investigated wells were used to clarify the relationships between heavy metals content and heavy minerals distribution. The results revealed significant positive correlation between the well depth and the sediment contents of opaques ($p<0.001$), epidote ($p<0.001$), garnet ($p<0.05$), Ti ($p<0.01$) and Cr ($p<0.01$). Opaque minerals show positive significant relationship with Ti and S and to some extent Cr and OM (organic matter). Integration of multivariate statistical techniques and mineralogical analysis discriminate the studied sediments into two distinct groups. The first group consists of the older sediments of Kom Ombo and Qena formations which extended from depths of 39 to 54m and from 55 to 89m bgl (below ground level), respectively. The second group stated as younger sediments (from 5m to 38 m in depth) whish ascribed to El Ghawanim Formation. The older sediments have higher content of opaques, amphiboles, epidotes and garnet minerals as well as a higher concentration of OM, S, Mn, Fe, Ti, Cr than the younger sediments. This work considered as an introductory to study the impact of the geochemical and mineral composition of the Quaternary aquifer sediments on the quality of drinking water extracted from similar wells in the study area.

Keywords: Geochemical, Heavy minerals, Multivariate statistical, Quaternary aquifer, Pleistocene sediments
Annals of the Geological Survey of Egypt, 36 no. ISSN 1110-0435, (2019)

Rockfall hazards assessment along the Aswan–Cairo highway, Sohag Governorate, Upper Egypt

Abu Seif, E.-S.S. [a,b], Bahabri, A.A. [a]

[a]*Faculty of Earth Sciences, King Abdulaziz University, Jeddah, Saudi Arabia*

[b]*Geology Department, Faculty of Science, Sohag University, Sohag, Egypt*

Abstract: The geotechnical evaluation of rockfall hazards along the Aswan–Cairo highway, Sohag Governorate, Upper Egypt has been achieved throughout a variety of field investigations and lab tests on the slopes and rock cut faces of Lower Eocene Plateau limestone. The studied Aswan–Cairo highway is located in a mountainous area and surrounded on both sides by highly sheared limestone plateau possesses steep slopes and swelling clayey hosted bands. The clayey bands are characterized by highly swelling potentiality that considered as instability and weakness planes along which the limestone blocks will be downward fallen. Based on slope height and angle, the studied slopes are mostly considered instable. Kinematically, the Lower Eocene limestone blocks have planer and wedge failure modes.

According to the estimated values of the coverage distance and rebound amplitude, ditches must be dug (2 m width and 1.5 m depth) to reduce the rebound amplitude height of falling blocks and catch these blocks to avoid them to reach the highway toe. Ditches can be filled with sands to will absorb the falling blocks kinetic energy as well as rockfall barrier must be constructed at the most hazards sites to retain the falling blocks away from the road toe.

Keywords: Rockfalls, Aswan–Cairo highway, Sohag Governorate, Upper Egypt.

Natural Hazards, Volume 99, Issue 2, 1 November 2019, Pages 991-1005

Characterization and environmental impact assessment of gold mine tailings in arid regions: A case study of Barramiya gold mine area, Eastern Desert, Egypt

Mostafa Redwan[a], and Abdullah O. Bamousa[b]

[a]*Geology Dept., Faculty of Science, Sohag Univ, 82524, Sohag, Egypt*

[b]*Geology Dept., Faculty of Science, Taibah Univ, Al Madinah, P.O. box 30002, 41477, Saudi Arabia*

Abstract: Geochemical and mineralogical characterization and environmental impact assessment were performed on Barramiya gold mine tailings, Eastern Desert, Egypt. The Barramiya gold mine is situated within ophiolitedecorated Nugrus suture zone, which composed of dismembered sequence of highly deformed and metamorphosed mafic to ultramafic rocks and their hydrothermal alteration products (carbonate rocks), interbedded with meta-volcano clastic rocks of the Nubian Shield. Morphometric parameters were quantified using ArcGIS 10.0 with Shuttle Radar Topography Mission (SRTM) maps. A total of four tailings samples were gathered and analysed by XRF, XRD, ICP-OES/MS and ESEM. Tailings are characterized by homogeneous silty fine sand, high carbonates in the form of dolomite and ankerite, and low sulfides content in the form of arsenopyrite and pyrite relics. High concentration averages of heavy elements are found for As (2936 mg/kg), Cr (237 mg/kg), Sr (219 mg/kg), Ni (150 mg/kg), V (131 mg/kg), Zn (64 mg/kg), Cu (51 mg/kg), Co (19 mg/kg) and Pb (12 mg/kg). They reflect mafic and ultramafic rocks, graphite schists, and quartz veins of the study area. Gypsum is present as secondary phase, identified in the shrinkage crack fillings. Morphometric drainage basin parameters for wadi Barramiya basin show rectangular to subdendritic drainage pattern with a moderate hazard degree. This study recommends designing multiple-layered dry cover, overlain by plant cover at uppermost part for treatment of the gold mine tailings; otherwise, wind and water erosion can easily remove all dissolved and unconsolidated material that absorb heavy elements and would create a potential risk to the surrounding ecosystem.

Keywords: Heavy elements, Tailings, Contamination, Morphometric, drainage basin, Gold mine, Barramiya, Egypt

Journal of African Earth Sciences, Volume 160, December 2019, 103644

Chemical characteristics and assessment of groundwater quality in Halayieb area, southeastern part of the Eastern Desert, Egypt

Sameh R. Zaki[1], Mostafa Redwan[2], Ahmed M. Masoud[2], Ahmed A. Abdel Moneim[2]

[1]The Egyptian Mineral Resources Authority, 11517 Cairo, Egypt

[2]Geology Department, Faculty of Science, Sohag University, 82524 Sohag, Egypt

Abstract: Halayieb area is located at the southeastern corner on the border between Egypt and Sudan. The area has very important strategic aspects to Egypt. Groundwater is the only source of fresh water in the area. The hydrogeochemical characterizations of groundwater in the area were carried out, to assess the quality of groundwater for its suitability for drinking and irrigation purposes. Geologically the Precambrian rocks underlain the Mesozoic sandstone and Tertiary marine sediments. The groundwater of the area is recorded at the Miocene sedimentary succession and the fractured basement aquifers with a maximum water depth of 26.5 m from the ground surface. Groundwater quality is mostly saline caused by the sources of geogenic, anthropogenic, and marine origin of the water bearing formations. The resulting groundwater is characterized by Na+ > Ca^{2+} > Mg^{2+}/Cl^{-}> HCO^{3-} > SO_4^{2-}: Na^{+} > Ca^{2+} > K^{+}/SO_4^{2-} > Cl^{-} > HCO^{3-} facies, following the topographical and water flow-path conditions. The hydrochemical facies in this area fall in the field of NaCl type and the hydrogeochemical signatures indicated active hydrolysis and dissolution process of Ca-bearing minerals of the basement rocks and some sodium is lost, most probably through reverse ion exchange. Enrichment of Mn+ in some wells is regarded to the mining activity for manganese ores in the area. Groundwater quality is mostly not suitable for drinking purposes. For irrigation, the groundwater is mostly suitable in regard to the residual sodium carbonate and the magnesium hazard. According to the water quality assessment using United States salinity laboratory (USLL) diagram, most water samples located in category C3–S2, C3–S3, C3–S4, C4–S2 highlighting high to very high salinity hazard and medium to very high sodium content class. Most of the groundwater samples that are located away from the shoreline are suitable for livestock and poultry consumption. High salinity contents in the study area create severe problems for using water supplies and for future exploitation.

Keywords: groundwater characterization, groundwater quality, Halayieb, Egypt, salinity, suitability.

Geosciences Journal, Volume 23, Issue 1, 1 February 2019, Pages 149-164

Tracking the transition from subduction-related to post-collisional magmatism in the north Arabian–Nubian Shield: A case study from the Homrit Waggat area of the Eastern Desert of Egypt

Mokhles K. Azer[1], Khaled M. Abdelfadil[2], Paul D. Asimow[3], Ahmed E. Khalil[1]

[1]Geological Sciences Department, National Research Centre, Cairo, Egypt

[2]Geology Department, Faculty of Science, Sohag University, Sohag, Egypt

[3]Division of Geological and Planetary Sciences, California Institute of Technology, Pasadena, California

Abstract: Field and geochemical observations of the granitoids of the Homrit Waggat area in the central Eastern Desert of Egypt reveal two magmatic phases. The early phase of weakly deformed subduction-related calc-alkaline rocks includes tonalite and granodiorite. We name the later phase the Homrit Waggat Pluton (HWP); it includes undeformed syenogranite, alkali feldspar granite, and minor albitized granite. The tonalite and granodiorite have distinct negative Nb–Ta anomalies and lower alkalis, REE, Nb, Zr, and Hf than the HWP. The early magmatic pulse is a subduction-related suite, likely generated by underplating of mantle-derived magmas that triggered partial melting of mafic lower crust; mixing of these melts led to intermediate magma that further fractionated to tonalite and granodiorite. The HWP granites of the late magmatic pulse are transitional from a subduction-related to an anorogenic within-plate environment, plausibly generated by post-collisional lithosphere delamination. Although the parent magma of the HWP was I-type, extensive fractional crystallization produced residual liquids with A2-type character. Albitized granites are found only along the outer margin of the HWP, and contacts with the alkali feldspar granite are gradational, suggesting fluid interactions at a late stage of crystallization. The original textures of the albitized granites are preserved, but their bulk composition was modified by the production of Na-rich minerals and the removal of K, REE, and some trace elements by fluids.

Keywords: albitization, allanite, Arabian-Nubian Shield, delamination, Eastern Desert, post-collisional

Geological Journal, 18 November, https://doi.org/10.1002/gj.3643; p: 1–27

Geochemistry and Petrogenesis of Late Ediacaran Rare-Metal Albite Granite of the Nubian Shield: Case Study of Nuweibi Intrusion, Eastern Desert, Egypt

Azer, M.K.[a], Abdelfadil, K.M.[b], Ramadan, A.A.[c]

[a]Geological Sciences Department, National Research Centre, Dokki, Cairo, 12622, Egypt
[b]Geology Department, Faculty of Science, Sohag University, Sohag, Egypt
[c]Geology Department, Faculty of Science, Mansoura University, Mansoura, Egypt

Abstract: The Nuweibi albite granite (NAG) is a postcollisional intrusion emplaced as a high-level magmatic cupola into metamorphic and syntectonic calc-alkaline country rocks. It consists of two cogenetic intrusive bodies: the western, nonporphyritic, albite granite was emplaced deeper than the eastern, fine-grained, porphyritic, albite granite. In places the nonporphyritic phase crosscuts the earlier porphyritic phase, but the occurrence of gradational contacts between the phases implies a near coincidence in time, with the nonporphyritic phase emplaced before crystallization of the porphyritic phase was complete. The steeply dipping slope of the western contact of the Nuweibi pluton against country rocks, in contrast to the gently dipping contacts above the eastern and northeastern parts, indicates the probable location of the cupola apex in the eastern part of the pluton. The NAG intrusion is highly evolved meta- to peraluminous leucocratic rare-metal albite granite. The NAG intrusion is chemically zoned, with upward increases of Al2O3, Na2O, Sr, Ga, and Ta concentrations, alongside upward decreases in SiO2, K2O, Rb, Nb, Zn, Zr, Th, Sn, and rare earth element concentrations. These trends are interrupted by a compositional gap with discontinuities in evolutionary trends of both compatible and incompatible elements, suggesting multiple pulses of intrusion.
The NAG was generated via partial melting of a juvenile crust that had undergone extensive fractional crystallization combined with late-magmatic fluid overprint. Accumulation of residual volatile-rich melt and exsolved fluids in the apical part of the magmatic cupola produced stockscheider pegmatite, greisen, and quartz veins that cut the peripheries of the NAG pluton. Metasomatic activity by late- to postmagmatic fluids drove changes in the bulk composition of the cupola, removing K and driving the alkali feldspars toward pure albite.

Keywords: albite, country rock, Ediacaran, emplacement, granite, igneous geochemistry, igneous intrusion, magma, petrogenesis, rare earth element.
Journal of Geology, Volume 127, Issue 6, 1 November 2019, Pages 665-690

Electrical resistivity tomography applications for the construction an educational building in New Sohag University at Al Kawamil area, Sohag, Upper Egypt

Mohammed Atef Elsayed[1], Abdelbaset Mohamed Abudeif[1]

[1]Faculty of Science, Sohag University, Sohag, Egypt

Abstract: Electrical resistivity tomography is one of the most effectively methods to get a detailed picture of subsurface conditions without digging and it is become an important tool in solving civil engineering problems because of high resolution, low cost, time saving and relatively accurate technique. So the site investigation by using two-dimensional and three-dimensional electrical resistivity imaging has become a fundamental step before any successful design of the constructions at the University of Sohag. At this study, two- and three-dimensional electrical resistivity tomography has been used at two predefined sites to choose an ideal location between them for the construction an educational building. The obtained results show that, the study area consists of four geoelectric layers are the boulders of gravels intercalation with a percentage of sand and reddish clay, the fine crushed calcareous gravels and sands with intercalation clayey clay, the dry sand and clayey sand, and the clay, respectively. The results were confirmed using boreholes drilling technique at the two predefined sites. According to evaluation of the abundance of shale and sand contents within the two proposed sites and presence of cracks, fissures and faults, it is concluded that the second site is more suitable than the first one for constructions.

Journal of National Research Tomsk Polytechnic University, Russia

Single and multi-channel passive source methods for calculating the shallow S-wave velocity structure and site effect parameters at 15th May City, Egypt

A.M. Abudeif[a,*], M.A. Mohammed[a], A.K. Abd el-aal[b,c], Kh.A. Omar[b]

[a]*Sohag University, Faculty of Science, Geology Department, Sohag, Egypt*

[b]*National Research Institute of Astronomy and Geophysics (NRIAG), Helwan, Cairo, Egypt*

[c]*Kuwait Institute for Scientific Research, Safat, Kuwait*

Abstract: In this work, two passive seismic techniques were utilized for recording noise data at 57 sites to estimate nearsurface soil response in 15th May city. Single seismic station of microtremor data was used to investigate the study area utilizing Nakamura method of Horizontal to Vertical Spectral Ratio (HVSR) to determine the structure in terms of the predominant frequency. At each point of microtremor measurement, the natural frequency and amplification factor were estimated. Velocities of transverse waves (VS) of the upper part section of the sedimentary succession are estimated using microtremor observations technique. The spatial autocorrelation (SPAC) method was employed for estimation dispersion curves, VS structure was resulting by genomic algorithm.

The results demonstrate that, the fundamental resonance frequency is varying from 1.36 Hz to 1.607 Hz at the majority of the study area, amplification values ranges between 1.09 and 3.61 and the thickness of unconsolidated sediments were determined. The retrieved shear-wave velocity models were characterized by significant impedance contrasts for array site № 1 at 7 m, 13 m, and 36m depths corresponding to velocities 142, 636 and 1047 m/s, array site № 2 at 2 m, 6 m, and 16m depths corresponding to velocities 253, 614 and 942 m/s and array site № 3 at 2 m, 6 m, and 20m depths corresponding to velocities 242 m/s, 608 m/s and 1027 m/s respectively. Value results of Fo were used in the calculation of bedrock depth at the measured sites. The parameters obtained in this study are matching well with the site geology. Based on the average shear wave velocity values for the top 30m (VS30) for each array location, the site classes were estimated. The sites Ar_1 and Ar_2 belong to class C (very dense soil and soft rock), while Ar_3 fit in class B (rock).

Keywords: Array measurement, Rayleigh waves, Genetic algorithm, Microtremor, Spatial autocorrelation, Fundamental frequency, Site effect, S-Wave velocity.

Journal of African Earth Sciences, Volume 159, November 2019, Article number 103579

Geotechnical aspects and associated problems of Al-Shuaiba Lagoon soil, Red Sea coast, Saudi Arabia

Bader A. Hakami[1] and El-Sayed Sedek Abu Seif[1,2]

[1]Faculty of Earth Sciences, King Abdulaziz University, Jeddah, Saudi Arabia

[2]Geology Department, Faculty of Science, Sohag University, P.O. Box 82524, Sohag, Egypt

Abstract: Al-Shuaiba Lagoon area locates along the eastern Red Sea coast, south of Jeddah city, Saudi Arabia. Its soil profile consists mainly of coarse-grained saline sabkha soil. Based on the vertical variations of grain size, the studied Al-Shuaiba Lagoon soil profile was subdivide into three zones A: saline sandy gravels, B: calcareous sandy silts and C: well-graded sands.

According to the SPT-N60 values, these soil zones were classified into stiff, medium stiff and very stiff soil-type. The soil zone B has CC values vary from 0.234 to 0.279 thus it classifies into loose and very high compressible soil. Consequently, based on the exchangeable sodium percentages vs. cation exchange capacity (CEC) classification chart, the soil zone B was classified into medium dispersive potential soil-type. The studied soil samples contain a relatively higher TDS values and high concentration of calcium carbonates, sulfates, and chlorides. Thus, these salts can play an essential harmful effectiveness on the durability of concrete when reacted with cement alkalis.

Keywords: Al-Shuaiba Lagoon, Saline soils, Red Sea coastal sabkha, Jeddah, Saudi Arabia.

Environmental Earth Sciences, Volume 78, Issue 6, 1 March 2019, Article number 203

Geotechnical engineering evaluation of soil utilizing 2D Multichannel Analysis of Surface Waves (MASW) technique in New Akhmim City, Sohag, Upper Egypt

A.M. Abudeif[1], R. E. Fat-Helbary[2], H.M. Alkhashab[1], M.A. Mohammed[1], M. M. Masoud[1]

[1]Geology Department, Faculty of Science, Sohag University, (Sohag), Egypt

[2]Aswan Earthquake Research Center, P.O. Box 152 Aswan, Egypt

Abstract: New Akhmim is one of the recent cities in Sohag Governorate which was proposed by Egyptian Urban Communities Authority (EUCA) to build new communities overcoming overpopulation problems. The main goals of this research are delineating the shallow subsurface structures and lithology of the engineering layers and their geotechnical characteristics**.** Site engineering characterization was carried out for New Akhmim City utilizing the MASW technique. For calculating velocity of the shear-wave, sixteen MASW sections were carried out in the study site using Geometric strata visor-NZ 48 channels with vertical geophones of 4.5 Hz and the inter-geophone spacing was 3 m. The recorded data were analyzed using the SurfSeis software. The calculation of the degree of soil compaction or rock consolidation were valued based on velocity of seismic waves and densities and were used to determine the foundation stability.

The proposed site contains two engineering subsurface layers; the first one is the upper most layer and consists of intercalations of unconsolidated material (gravels and sands) of different shear wave velocities. The second layer is more compact with higher velocity (bedrock). From the results of all MASW survey, elastic moduli and geotechnical parameters, the authors concluded that the eastern part of the first and the second layers is more competent than the western part. The degree of competence of the second layer is higher than that of the first one. Therefore the second layer (compact shale) is favored as a most qualified layer for engineering purpose and constructions design.

Keywords: Constructions, Elastic moduli, Geotechnical, MASW, New akhmim city, Shear wave velocity.
Journal of African Earth Sciences, Volume 157, September 2019, Article number 103512

Revised (miospores-based) stratigraphy of the Lower Cretaceous succession of the Minqar-IX well, Shushan Basin, north Western Desert, Egypt: Biozonation and correlation approach

Magdy S. Mahmoud[a], Amr S. Deaf[a], Mohamed A. Tamam[b], Miran M. Khalaf[b]

[a]Geology Department, Faculty of Science, Assiut University, Assiut, 71516, Egypt

[b]Geology Department, Faculty of Science, Sohag University, Sohag, Egypt

Abstract: Shushan Basin is recently considered one of the important petroliferous basins in the north Western Desert of Egypt, where it contains multiple clastic reservoirs. National and international exploration companies are carrying out extensive correlations within the basin to detect the almost similar clastic reservoirs Alam El Bueib and Kharita formations. Stratigraphy of the Lower Cretaceous of Minqar-IX well in Shushan was previously established based on dinoflagellate cysts recovered from a few and widely spaced samples, where clastic units could not be differentiated. However, the current collection of a large number of closely spaced samples enabled the identification of five informal Lower Cretaceous spore-pollen palynozones (PZ) with high resolution. These zones are used to recognize unidentified clastic rock units and to provide an intrabasinal biostratigraphic correlation of the formations. Three palynozones (PZ 1-PZ 3) identify Alam El-Bueib Formation (?Berriasian-early Aptian). PZ4 identifies Alamein Formation (late Aptian). PZ 5 corresponds to Kharita Formation (middle Albian). Results reflect the miospores as a powerful stratigraphic tool for dating the largely non-marine sequences, where diverse dinoflagellate cysts are almost lacking and/or facies-controlled. The use of biostratigraphic correlation of strata successions with monotone lithologies was helpful in identifying problematic formations, tracing their lateral facies change, and in detecting an unrecognized hiatus in the studied well.

Keywords: Palynostratigraphy, Miospores, Cretaceous, Shushan basin, Western desert, Egypt.
Journal of African Earth Sciences, Volume 151, March 2019, Pages 18-35

Geoelectrical Characterization of the Al-Kawamil New Settlement, Sohag, Egypt

Mohammed A. Mohammed[1] and Abdelbaset M. Abudeif[1]
[1]Sohag University, Faculty of Science, Geology Department, 82511, Sohag, Egypt

Abstract: Electrical resistivity tomography (ERT) is one of the most effective geophysical methods used to acquire detailed pictures of subsurface conditions without drilling. Site investigation using two- and three-dimensional electrical resistivity imaging is now a fundamental step before the design and construction of campus buildings at the University of Sohag in Egypt. In this study, an ERT survey was implemented at two pre-defined sites with the aim of selecting the most favorable location for construction of a new educational building on the university campus. The resistivity results were confirmed with boreholes drilled at both sites. RES2DINV and RES3DINV software were used for data processing and interpretation. The results show that the near surface sedimentary succession beneath both sites consists of four geoelectrical and lithological units. From the surface to a depth of 20 m, these layers are: unit 1) unconsolidated boulders and gravels intercalated with percentages of sand and reddish clay; unit 2) fine crushed calcareous gravels and sands with clays intercalations; unit 3) dry sand and clayey sand; and unit 4) shale, at the base. According to an evaluation of the presence and abundance of shale and sand contents cracks, fissures and faults, the second site is identified as more suitable for construction.

Keywords: ERT, 2D, 3D, Construction, Sohag City, Egypt
J. Environmental and Engineering Geophysics, Volume 24, Issue 2,1 June 2019, Pages 327-332

Pore and fracture pressure modeling using direct and indirect methods in Badri Field, Gulf of Suez, Egypt

A.E. Radwan[a] , A.M. Abudeif[b], M.M. Attia[b], M.A. Mohammed[b]
[a]Exploration Department, Gulf of Suez Petroleum Company, Cairo, Egypt
[b]Sohag University, Faculty of Science, Geology Department, Sohag, Egypt

Abstract: Abnormal formation pressure is one of globally dominant drilling hazards because of its direct impact on the drilling operations and exploration risk. An adequate pore pressure and fracture gradient modeling are considered the heart of the well planning and execution. Safe drilling to reach total depth of any well is the main concern for both engineers and geoscientists. Consequently, the main objectives of this paper are evaluation of pore pressure and fracture gradients as well as identification of the geo-pressured zones (over-pressured) in the subsurface sedimentary section. The pore pressure and fracture gradients were evaluated using well logging data namely density, resistivity, gamma-ray and sonic logs obtained from offshore wells in Badri Field. The overburden (overburden stress) was calculated using Amoco overburden equation, while sonic and resistivity logs were used for pore pressure and fracture gradient calculations using Eaton's method. The results of this study revealed that: 1) integration of direct and indirect method can lead to adequate and accurate pore pressure modeling; 2) pore pressure regime shows over-pressured, normal pressure and subnormal horizons; 3) over-pressured zones was detected in the base of Zeit Formation, South Gharib Formation, Hammam Faraun Member and Kareem Formation, pore pressure were 10.3, 10.5, 9.3 and 9.6 ppg equivalent density in arrange; 4) Reservoirs of Hammam Faraun Member and Kareem Formation indicated Sub-normal pressure zones where pore pressure values are varying from 5.5 to 6.2 ppg for Hammam Faraun reservoir and from 5.2 to 8 ppg in Kareem Formation in equivalent density; 5) Normal pressure regime was detected in the upper part of Zeit Formation and Feiran, Sidri and Baba members, where pore pressure value was recorded as 8.7 ppg; 6) Best fitting parameter for Eaton resistivity and sonic logs are 0.9 and 1.65 respectively while for Amoco overburden empirical equations, the Amoco exponent best fit is 0.85 where the mud line density is 2.15 g/cm3. Finally, it is highly recommended to use low mud weight against the under compaction zones and high mud weights against the identified over-pressured intervals.

Keywords: Pore pressure, Fracture pressure, Geo-pressure, Well logging, Overburden, Under compaction
J. African Earth Sciences, Volume 156, August 2019, Pages 133-143

Development of formation damage diagnosis workflow, application on Hammam Faraun reservoir: A case study, Gulf of Suez, Egypt

A.E. Radwan[a], A.M. Abudeif[b], M.M. Attia[b], M.A. Mahmoud[c]

[a]Gulf of Suez Petroleum Company (GUPCO), Egypt

[b]Geology Department, Sohag University, Egypt

[c]Petroleum Engineering Department, King Fahd University of Petroleum & Minerals, Saudi Arabia

Abstract: Numerous studies carried out on Formation damage, but fewer investigations were conducted for the ideal diagnosis workflow. More understanding of geology, reservoir characteristics, and production data is essential to define the source, causes, and suitable treatment technique of formation damage for each well. In this paper, a workflow for the formation damage diagnosis is introduced to find location, potential source even natural or induced damage, root causes and recommend a suitable treatment method of the formation damage. The suggested workflow depends on vital steps including (1) planning and organizing the delivered data for solving the investigated problem, (2) collecting and analyzing all available data, (3) integration of the all geological, reservoir and production data, in addition the suggested workflow was applied on Hammam Faraun reservoir in El-Morgan oil field. In this reservoir, an integration of the available geological, reservoir, and production data was performed to make confident prognosis or diagnoses of formation damage and achieve a complete vision of the sources of formation damage and suggest solutions and treatments. Therefore, in assessing formation damage in the studied well, all aspects of the well and its history were integrated in this study, including: core analysis, XRD, mineralogy, water chemistry, reservoir geology, offset well production, reservoir fluids, production history, drilling fluids, cementing program, completion, stimulation and workover history, perforation reports. The diagnosis of the formation damage problem revealed that the suggested workflow was effective and can help diagnose formation damage problems in the entire oil and gas wells. The integration of geological, reservoir, production data led to accurate analysis, two sources of damage could be responsible for the damage in the studied well based on the geological and engineering data analysis and integration. Firstly, low quality water, secondly the using of an inappropriate stimulation fluid and sensitive formation minerals to fluids, and finally treatment with proper additives is highly recommended.

Keywords: XRD, Stimulation, Formation damage, Workflow, Integration

Journal of African Earth Sciences, Volume 153, May 2019, Pages 42-53

Chemical speciation of heavy metals of quaternary sediments in Sohag Governorate, Egypt

Shaymaa Montaser AbdelRaheem[1] **and Mohamed Hassan Ali**[1]

[1] Faculty of Science, Sohag University, Sohag, Arab Republic of Egypt

Abstract: The speciation patterns of heavy metals were assessed with a view to providing information on the accessibility of metals in the sediment matrix. This work investigated the distribution and speciation of Fe, Mn, Zn, Cu, Cd m Pb and Cr in the Quaternary sediments of Sohag, Egypt. That is useful in finding the available source of heavy metals in sediments bearing groundwater. Well sediments were collected for this purpose. The fine fraction (<60 μm) was analyzed for the total metal content (Fe, Mn, Zn, Cu, Cd , Pb, and Cr) and Organic matter. Metal speciation of selective samples was determined using five-step sequential extraction technique. They display variable concentrations in the different speciation extractions, depending upon the source and geochemical behavior of metals.

The results exposed significant positive correlation between the different fractions and heavy metals Fe ($p<0.001$), Mn ($p<0.001$), Zn ($p<0.001$), Cu ($p<0.001$), Cd ($p<0.001$), Pb ($p<0.001$) and Cr ($p<0.001$).The results indicate that iron, manganese, chromium are speciated into organic and Fe–Mn oxide fractions. While copper and zinc are speciated into residual and Fe–Mn oxide fractions. Cadmium is speciated in carbonate fractions. Lead presents in sediments with moderate amounts.

Journal of National Research Tomsk Polytechnic University, Russia

Remote sensing-based geological mapping and petrogenesis of Wadi Khuda Precambrian rocks, South Eastern Desert of Egypt with emphasis on leucogranite

Asran M. Asran[a], S.M. Hassan[b]

[a]Geology Department, Faculty of Science, Sohag University, Sohag 82524, Egypt

[b]National Authority for Remote Sensing and Space Sciences, Cairo, Egypt

Abstract: The exposed Precambrian rocks along Wadi Khuda area, South Eastern Desert of Egypt, comprise gneisses, amphibolites and migmatites associations (infrastructural rocks) which are intruded by diorite, tonalite, syenogranite and leucogranite (LG). LG forms homogeneous boss like bodies, devoid to xenoliths, except along the outer margins. Chemically and mineralogically they are dissimilar to the surrounding gneisses. In the current study, band ratio and Decorrelation Stretch image processing algorithms were proposed and applied on Landsat-8, Advanced Spaceborne Thermal Emission and Reflection Radiometer (ASTER) and Sentinel-2 remote sensing data to discriminate the widely exposed lithological units in the mapped area. Geochemically, I-type classification and volcanic arc environment were revealed. LG is peraluminous (ASI average of 1.09) with normative corundum up to 1.38 for LG. The LG displays limited major and trace element variations (SiO_2 = 74.5–76.2%, AI_2O_3 = 13.4–14.4%), MgO = 0.03–0.19%, Na_2O = 3.6–4.6%), and Rb = 55–85 ppm) probably due to textural and mineralogical homogeneity. The contents of REE in the leucogranite are low (∑REE = 21–37), but the REE patterns are [(La/Yb)n = 2.45–9.03], [(La/Sm)n = 1.09–2.6], with negative Eu anomaly, (Eu/Eu* = 0.19–0.78). The negative Eu anomaly and the low Sr content (16–92 ppm) may be attributed to the plagioclase feldspars fractionation. The leucogranites represent residual melt of syenogranite which forms Um Itly pluton at the southern flank of Wadi Khuda entrance.

Keywords: Leucogranites, Khuda, I-type, Remote sensing, Eastern Desert, Egypt.

The Egyptian Journal of Remote Sensing and Space Sciences, Available online 19 July 2019

Alluvial karstification and paleodoline development in Eocene limestones, a case study from west Sohag City, Egypt: implications for causes and impacts

Tawfiq M. Mahran[1] and Abdallah M. Hassan[1]

Geology Department, Faculty of Science, Sohag University, Sohag, Egypt

Abstract: The Late Oligocene pre-Eonile paleoriver flows northwesterly over the Eocene Limestone Plateau in the east central Western Desert, west of the Nile Valley (Sohag), building an alluvial plain and leading to the karstification of the limestone bedrock, as paleoerosional surfaces and paleodolines. Knowledge of this alluvial karstification is completed with the detailed studies of the sedimentary evolution of the fluvial system and its contemporary deposition. Analysis of the sedimentological and geomorphological features allows discussing the natural environmental conditions that favored karst in the past and its main genetic mechanisms. The architectural elements of the fluvial deposits indicate that they were deposited in a gravel-dominated braided fluvial system, characterized by high availability of water and sediment supplies. The current study proves that genesis of paleodolines was mainly related to this high water supply. Some of them were progressively filled by syn-sedimentary deformed unconsolidated deposits. Such deformation is due to dissolution of the underlying sagging synclinal limestone, conditioning the location of sinking waters where preferential dissolution and later suffosion took place. A model for the evolution of the paleodoline fills is proposed and interpreted in three different stages: (1) gravitational processes developed and disorganized gravels were remobilized and dragged toward the created paleodolines; (2) flooding of the paleodolines acted as lakes where Gilbert-type deltas and gravel slope deposits accumulated, exhibiting several unconformities interpreted as a result of continued subsidence of the paleodoline related to dissolution; and (3) nondeformed fluvial facies sealed the whole deposits, marking the end of the karstification process. Combinations of different types of factors that could cause karstic subsidence and associated hazards include soluble rock lithology, paleoclimate, and deformational structure.

Keywords: Karstification . Nile Valley. Paleodolines . Geomorphology. Geohazards . Pre-Eonile

Arabian Journal of Geosciences , Volume 12, Issue 7, Article number 240

Flood-Hazard Assessment Modeling Using Multicriteria Analysis and GIS: A Case Study-Ras Gharib Area, Egypt

Ahmed M.Youssef[1,2], Mahmoud A.Hegab[3]

[1]Geology Department, Faculty of Science, Sohag University, Sohag, Egypt

[2]Geological Hazards Department, Applied Geology Sector, Saudi Geological Survey, Jeddah, KSA

[3]Geography Department, Faculty of Arts, Sohag University, Sohag, Egypt

Abstract: Nowadays, the use of Geographic Information Systems (GIS) is emerging as a powerful tool for assessment of different types of natural hazards. Flash floods are among the most severe natural hazards, and have disastrous socioeconomic impacts. Therefore, it is urgent for flash flood susceptibility maps to be developed to delineate flood-prone areas. These maps would help the authorities, planners, and decision makers to make rapid assessments and take appropriate actions to reduce and minimize the consequences of potential impacts from flash floods. This study addresses the characterization of flash flood susceptibility along some watersheds that drain their water towards the RasGharib area, located along the west coast of the Gulf of Suez, Egypt. The RasGharib area is frequently affected by flash floods, causing death, and damage to buildings, infrastructures, and vehicles. One of these flash floods happened on October 18, 2016, when the area was impacted by a disastrous flash flood causing a death toll of 22 people and enormous damage to infrastructure and residential areas. In the current study, multi criteria analysis, using the Analytical Hierarchy Process (AHP) and GIS techniques, was carried out to establish a flood susceptibility map for the study area, through the combination of different flood-related factors. Different methods were applied to assess the reliability and credibility of the proposed model. The validation datasets extracted from high-resolution images acquired after the catastrophic flood event on October 18, 2016, using a slicing technique were used to evaluate the flood susceptibility map using the prediction rate method. The results of the accuracy assessment showed a prediction rate of 83.3% for the AHP model. In addition, another verification method was used by comparing the historical records of flash flood events with the susceptibility of flash flood zones. The results indicated that 76% of the historical data plotted into high and very high susceptible zones, 19.1% appearing in the moderately susceptible zone, and 4.7% falling in the low and very low susceptibility zones. Our findings state that the proposed model is very suitable for flash flood susceptibility analysis and could be useful for engineers, planners, and decision makers in spatial planning and flash flood-hazard management.

Key words: Multi-criteria analysis, Analytical Hierarchy Process; Flash flood hazard assessment; susceptibility map; RasGharib area, Egypt

Book title: Spatial Modeling in GIS and R for Earth and Environmental Sciences. (Chapter 10; pp: 229-257)

Chemical speciation of heavy metals of Quaternary sediments in Sohag Governorate, Egypt.

Ahmed.A.Abdel Moneim, A.M. Hassan, Mohamed H. Ali, Shaymaa Rezk

Geology department Faculty of Science, Sohag University

Abstract: The speciation prototypes of heavy metals were assessed in Sohag Governorate with a view to provid information on the accessibility of heavy metals in the sediment of the Quaternary aquifer. This work investigated the distribution and speciation of Fe , Mn, Zn, Cu, Cd , Pb and Cr in the Quaternary sediments of Sohag, Egypt to identify the available source of heavy metals in sediments bearing groundwater. Well sediments were collected for this purpose. The fine fraction (<60 μm) was analyzed for the total heavy metals content (Fe, Mn, Zn, Cu, Cd , Pb, and Cr) and organic matter. Heavy metals speciation of 16 selective samples was determined using five-step sequential extraction technique. Samples display variable concentrations in the different speciation extractions, depending upon the source and geochemical behavior of heavy metals. The results showed significant positive correlation between the different fractions and heavy metals Fe ($p<0.001$), Mn ($p<0.001$), Zn ($p<0.001$), Cu ($p<0.001$), Cd ($p<0.001$), Pb ($p<0.001$) and Cr ($p<0.001$).The results indicate that Fe, Mn and Cr are speciated into organic and Fe–Mn oxide fractions. while copper and zinc are speciated into residual and Fe–Mn oxide fractions. Cd is speciated in the carbonate fractions. Pb presents in sediments with moderate amounts relatively.

Keywords: heavy metals, speciation, availability, sediment, Quaternary aquifer, sequential extraction.

Annals of the Geological Survey of Egypt, 36 no. ISSN 1110-0435, (2019)

Multi-hazard assessment modeling via multi-criteria analysis and GIS: a case study

Hariklia D. Skilodimou[1], George D. Bathrellos[1], Konstantinos Chousianitis[2], Ahmed M. Youssef [3], Biswajeet Pradhan[4, 5]

[1]Department of Geography and Climatology, Faculty of Geology and GeoenvironmentNational and Kapodistrian University of AthensZografouGreece, [2]Institute of GeodynamicsNational Observatory of AthensLofos NymfonGreece, [3]Department of Geology, Faculty of ScienceSohag UniversitySohagEgypt, [4]The Centre for Advanced Modelling and Geospatial Information Systems (CAMGIS), Faculty of Engineering and Information TechnologyUniversity of Technology SydneyUltimoAustralia, [5]Department of Energy and Mineral Resources EngineeringSejong UniversitySeoulRepublic of Korea

Abstract: Multi-hazard assessment modeling comprises an essential tool in any plan that aims to mitigate the impact of future natural disasters. For a particular area they can be generated by combining assessment maps for different types of natural hazards. In the present study, the analytical hierarchy process (AHP) supported by a Geographical Information System (GIS) was utilized to initially produce assessment maps on hazards from landslides, floods and earthquakes and subsequently to combine them into a single multi-hazard map. Evaluation of the reliability of the proposed model predictions was performed through uncertainty analysis of the variables that we used for producing the final model. The drainage basin of Peneus (Pinios) River (Western Peloponnesus, Greece), an area that is prone to landslides, floods and seismic events, was selected for the implementation of the aforementioned approach. Our findings revealed that the high hazard zones are mainly distributed in the western and north-eastern part of the region under investigation. The calculated multi-hazard map, which corresponds to the potential urban development suitability map of the study area, was classified into five classes, namely of very low, low, moderate, high and very high suitability. The most suitable areas for urban development are distributed mostly in the eastern part, in agreement with the low and very low hazard level for the three considered natural hazards. In addition, by performing uncertainty analysis we showed that the spatial distribution of the suitability zones does not change significantly. Ultimately, the final map was verified using the actual inventory of landslides and floods that affected the study area. In this context, we showed that 80% of the landslide occurrences and all the recorded flood events fall within the boundaries of the moderate, low and very low suitability zones. Consequently, the predictive capacity of the applied method is quite good. Finally, the spatial distribution of the urban areas and the road network were compared with the derived suitability map and the results revealed that approximately 50% of both of them are located within areas susceptible to natural hazards. The proposed approach can be useful for engineers, planners and local authorities in spatial planning and natural hazard management.

Keywords: Analytical hierarchy process, Natural hazard assessment maps, Suitability map for urban development · Peneus River, Western Peloponnesus, Greece

Environmental Earth Sciences, Volume 78, Issue 2, 1 January 2019, Article number 47

Environmental Hazards of Sand Dunes, South Jeddah, Saudi Arabia: An Assessment and Mitigation Geotechnical Study

Ammar Amin[1], El-Sayed Sedek Abu Seif[1,2]

[1]Faculty of Earth Sciences, King Abdulaziz University, P.O. Box 80206, Jeddah, Saudi Arabia

[2]Geology Department, Faculty of Science, Sohag University, P.O. Box 82524, Sohag, Egypt

Abstract: This study presents a concise evaluation of sand dune environmental hazards in Al-Lith area, Jeddah (Saudi Arabia), where active sand dune migration forms serious environmental risks. The study area represents a strategic and very well promising area for extension of urbanization. The study area was characterized by hyper-arid climate where wind erosion plays a critical task in the formation and migration of sand dunes. The most frequent forms of aeolian sands are sand sheets, asymmetrical barchans, longitudinal dune and star-like shape dunes. These dunes are composed mainly of fine sands, medium sands and coarse sands with scarcely amounts of silts and clays. Texturally, the sand particles consist of sub-angular, sub-rounded, rounded, angular, well rounded and very angular. These sands are composed of mono-crystalline quartz with few grains of carbonate rock fragments. The environmental hazards of dune migration need integrated studies to assess and reduce these hazards through successfully long-term stabilization methods.

Keywords: Sand dunes, Environmental hazards, South Jeddah, Saudi Arabia.

Earth Systems and Environment, Volume 3, Issue 2, 1 August 2019, Pages 173-188

Statistical Analysis of Rainfall Patterns in Jeddah City, KSA: Future Impacts

Mazen M. Abu Abdullah[1], Ahmed M. Youssef[1,2], FawzyNashar[1], Emad Abu AlFadail[1]

[1]Geology Department, Faculty of Science, Sohag University, Sohag, Egypt

[2]Geological Hazards Department, Applied Geology Sector, Saudi Geological Survey, Jeddah, KSA

Abstract: Recently, the Kingdom of Saudi Arabia (KSA) has been facing significant changes in rainstorm patterns (rainstorm intensities, frequencies, distributions) causing many flash flood events. The city of Jeddah is located in a coastal plain area, in the middle of the western side of the KSA, which represents a clear case of changing grain storm patterns. Jeddah has been hit by many rainstorm events, which increased dramatically since 2009 (e.g., one in 2009, one in 2011, one in 2015, and another one happened in 2017). However, in 2018 about six rainstorms occurred. Two major flashflood events occurred in the city in November 2009 and in January 2011. There were significant impacts of these two events causing severe flooding. During these events,113 persons were announced dead (in the 2009 event), and infrastructures and properties were damaged (roads and highways, more than 10,000 homes and 17,000vehicles). In addition to that, dam failure occurred in the 2011 event. This situation gives clear evidence in changing the climate system that could cause more storms in the future across the KSA. Generally, Jeddah city has a lack of short-duration data in rainfall stations. In addition to that, there are a limited number of studies that have been done in determining rainstorm patterns. Consequently, the approach of the current study will focus on understanding and determining rainstorm patterns in the period between 2011 and 2017 depending on some digital rainfall stations that have been installed recently in Jeddah city. Rainstorm pattern and the method of distribution are the most crucial factors affecting peak flow and volume calculations. Our findings showed that there are two pattern types for the rainstorms in Jeddah city. Finally, a comparison with SCS-type II distribution was carried out.

Keywords: rainfall patterns, floods, impacts, Jeddah, KSA, statistical analysis

Book Title: (Rainfall - Extremes, Distribution and Properties, Chapter 2)

Flood Hazard Assessment of the Urban Area of Tabuk City, Kingdom of Saudi Arabia by Integrating Spatial-Based Hydrologic and Hydrodynamic Modeling

Ashraf Abdelkarim[1], Ahmed F. D. Gaber[2,3], Ahmed M. Youssef[4,5], Biswajeet Pradhan[6,7]

[1]Research Center, Ministry of Housing, Riyadh, Saudi Arabia, [2]Department of Geography, Faculty of Art, Sohag University, Sohag 82524, Egypt, [3]Geography and GIS Department, College of Arts, Imam Abdulrahman Bin Faisal University, Saudi Arabia, [4]Department of Geology, Faculty of Science, Sohag University, , Egypt, [5]Geological Hazards Department, Applied Geology Sector, Saudi Geological Survey, Jeddah, Saudi Arabia, [6]Centre for Advanced Modelling and Geospatial Information Systems (CAMGIS), Faculty of Engineering and IT, University of Technology, Sydney, Australia, [7]Department of Energy and Mineral Resources Engineering, Choongmu-gwan, Sejong University,, Gwangjin-gu, , Korea

Abstract: This study deals with the use of remote sensing (RS), geographic information systems(GISs), hydrologic modeling (water modeling system, WMS), and hydraulic modeling (Hydrologic Engineering Center River Analysis System, HEC-RAS) to evaluate the impact of flash flood hazards on the sustainable urban development of Tabuk City, Kingdom of Saudi Arabia (KSA). Determining the impact of flood hazards on the urban area and developing alternatives for protection and prevention measures were the main aims of this work. Tabuk City is exposed to frequent flash flooding due to its location along the outlets of five major wadis. These wadis frequently carry flash floods, seriously impacting the urban areas of the city. WMS and HEC-HMS models and RS data were used to determine the paths and morphological characteristics of the wadis, the hydrographic flow of different drainage basins, flow rates and volumes, and the expansion of agricultural and urban areas from 1998 to 2018. Finally, hydraulic modeling of the HEC-RAS program was applied to delineate the urban areas that could be inundated with floodwater. Ultimately, the most suitable remedial measures are proposed to protect the future sustainable urban development of Tabuk City from flood hazards. This approach is rarely used in the KSA. We propose a novel method that could help decision-makers and planners in determining inundated flood zones before planning future urban and agricultural development in the KSA.

Keywords: sustainable urban development; remote sensing; GIS; hydrologic modeling; hydraulic modeling (HEC-RAS); flood hazard; Tabuk City; Kingdom of Saudi Arabia

Sensors , Volume 19, Issue 5, 1 March 2019, Article number 1024

Agriculture Sprawl Assessment Using Multi-Temporal Remote Sensing Images andIts Environmental Impact; Al-Jouf, KSA

Ahmed M. Youssef[1,2], Mazen M. Abu Abdullah[1], Biswajeet Pradhan[3,4], Ahmed F. D. Gaber[5,6]

[1]Geological Hazards Department, Applied Geology Sector, Saudi Geological Survey, SA, [2]Geology Department, Faculty of Science, Sohag University, Egypt, [3]Centre for Advanced Modelling and Geospatial Information Systems (CAMGIS), School of Information, Systems and Modelling, Faculty of Engineering and IT, University of Technology Sydney, Sydney, NSW 2007, Australia, [4]Department of Energy and Mineral Resources Engineering, Choongmu-gwan, Sejong University, Korea, [5]Department of Geography, Faculty of Art, Sohag University, Egypt, [6]Geography and GIS Department, College of Arts, Imam Abdulrahman Bin Faisal University, Saudi Arabia

Abstract: In this paper, multispectral and multi-temporal satellite data were used to assess the spatial and temporal evolution of the agriculture activities in the Al-Jouf region, Kingdom of Saudi Arabia (KSA). In the current study, an attempt was made to map the agriculture sprawl from 1987 to 2017using temporal Landsat images in a geographic information system (GIS) environment for better decision-making and sustainable agriculture expansion. Our findings indicated that the agriculture activities developed through two crucial stages: high and low rise stages. Low rise stages occurred during three sub-stages from April 1987 to April 1988, from September 1993 to August 1998, and from April 2008 to May 2015, with overall change rates of 37.9, 44.4, and 30.5 km2/year, respectively. High rise stages occurred during three sub-stages from April 1988 to February 1993, from September2000 to March 2006, and from April 2016 to August 2017, with overall change rates of 132.4, 159.1, and 119.5 km2/year, respectively. Different environmental problems due to uncontrolled agriculture activities were observed in the area, including substantial depletion of the groundwater table. Another environmental impact observed was the appearance of sinkholes that occurred suddenly with no warning signs. These environmental impacts will increase in the future if no regulated restrictions are implemented by decision-makers.

Keywords: agriculture mapping; Landsat images; GIS; aquifer; sinkholes

Sustainability , Volume 11, Issue 15, Article number 4177

Desertification Risk Assessment of Sand Dunes in Middle Egypt: A Geotechnical Environmental Study

El-Sayed Sedek Abu Seif[1,2] · Mohamed H. El-Khashab[2]

[1]Faculty of Earth Sciences, King Abdulaziz University, Jeddah, Saudi Arabia

[2]Geology Department, Faculty of Science, Sohag University, P.O. Box 82524, Sohâg, Egypt

Abstract: The evaluation of aeolian desertification of sand dunes in north Assiut, Middle Egypt, has been achieved throughout a variety of detailed field investigations and laboratory measurements. The study area lies in hot dry desert climatic conditions where the sand dunes migration represents an effective threat cultivated lands, reclaimed lands, asphaltic roads and the systems of human distribution. Its mean annual rainfall is about 51mm. Except the Nile Valley, Egypt is mostly considered as dry desert lands so about 4% of its surface area is under plough. The study barchans are mainly composed of poorly graded sands and consist of fine sand, medium sand and a negligible amount of coarse sand, silts and clays. Compositionally, the studied sand dunes are mainly consist of quartz, rock fragments and negligible amounts of feldspars with the absence of any chemically active constitutes (e.g. chert, flint, chalcedony and dolomite). These sands are also free of organic matter. The removal of dune sands in hazardous sites considers a short-term solution method of the aeolian desertification problem.

Keywords: Sand dunes, Desertification hazards, Dune stabilization, Middle Egypt

Arabian Journal for Science and Engineering, Volume 7, Issue 44, pp. 357-375

Sources and behavior of trace elements in groundwater in the South Eastern Desert, Egypt

Embaby, A., Redwan, M.

Geology Department, Faculty of Science, Sohag University, Sohag, 82524, Egypt

Abstract: Due to water scarcity, the groundwater will represent an essential source of water in many communities worldwide. This study was carried out to investigate the main hydrogeochemical characteristic of trace elements composition, their sources, and its vulnerability in groundwater to the human population. Fifteen groundwater samples were collected from boreholes and hand dug wells from the South Eastern Desert, Egypt, and analyzed for Al, As, B, Fe, Mn, Cd, Co, Cr, Cu, Hg, Ni, Pb, Rb, Sb, Sr, Th, U, V, and Zn using inductively coupled plasma mass spectrometry. Multivariate analyses were applied to identify the distribution and potential source of trace elements. The groundwater is tapped from the Miocene and the fractured basement rock aquifers. The mean concentrations of trace elements exceed the guideline values of all organizations, except in some wells for Zn, Cu, and Co. Cationic trace elements declined in the order of Mn > Fe > Zn > Al > V > Ni > Rb > Sr > U > Cu > Cr > Co > Cd > Pb > Th > Sb > Hg. Oxyanions As (mean 15.48 mg/L) and B (mean 1.24 mg/L) showed very high concentrations and higher than the average WHO concentrations in water suggesting potential adverse toxicity to all aquatic organisms. Five factor analyses indicated that different geochemical contributions are involved in the chemical characteristics of groundwater in the study area. Water–rock interaction and dissolution processes in bed rocks from different coastal Miocene deposits, meta-volcanics, basic-ultrabasic rocks, granitic and meta-sediments, seawater intrusion, residential wastes, and mining activities, in addition to the pH/Eh conditions, adsorption, and surface complexation during the chemical weathering are the main factors influence the trace elements distribution in groundwater. Results from this study for the six different groundwater aquifers are a unique insight into the sources and mobility of the observed trace elements in the groundwater and can be used in the assessment of contamination for drinking water wells. The association of trace elements from different aquifers might be useful in tracers studies of water-rock interaction. Due to the enrichment of trace elements in nearshore and crystalline groundwater aquifers in the study area and in similar areas worldwide, treatment technologies, and sustainable water management processes should be applied to prevent severe risks to the communities.

Keywords: Groundwater aquifers, Trace element, Multivariate analyses, Geochemistry, Treatment, South Eastern Desert, Egypt.

Environmental Monitoring and Assessment, Volume 191, Issue 11, 1 November 2019, 686

Geological and Engineering Characteristics of Expansive Soils in Western Desert, Egypt

A. Elshater[1], M.A. Khashab[1], M.A. El-Sherif[2] and E.S. Abu Seif[1]

[1]Geology Department, Sohag University, Egypt

[2]Civil Engineering Department, Assiut University, Egypt

Abstract: Expansive shale has been found extensively in all over the world especially in arid and semi-arid regions. Egypt as a country from north Africa has alot areas having expansive soil. Superficial clay soil with the potential to shrink or swell with different degree of expansion covers large areas of many cities in New Valley Government such as Garb El-Mawhoob area. These problems include cracking, break-up of pavements, heaving, and damaging building foundations. Different laboratory tests were carried out on this soil including, natural water content, grain size distribution, Aterberge limits, unconfined compressive strength, swell potential and swelling pressure. These tests were supported by mineralogical investigations such as X-ray diffraction (XRD), scanning Electron Microscopy (SEM) and Differential thermal analysis (DTA). These soils were evaluated based on physico-chemical and geotechnical measurements. Its swelling potentiality (free swelling, swelling percent and swelling pressure) has a direct relationship with clay fraction content, plasticity index (PI) and cation exchange capacity (CEC). Furthermore, the clay fraction percent has a strong direct proportional relation to free swelling, plasticity index (PI) and cation exchange capacity (CEC). Also, the results of these tests showed that the clay in this area has considerable quantities of smectite resulting in the expansive character of these soils

Keywords: Garb El-Mawhoob area, X-ray diffraction, Smectite, Expansive soil.

Civil Engineering Research Journal, Volume 7 - Issue 2 - February 2019

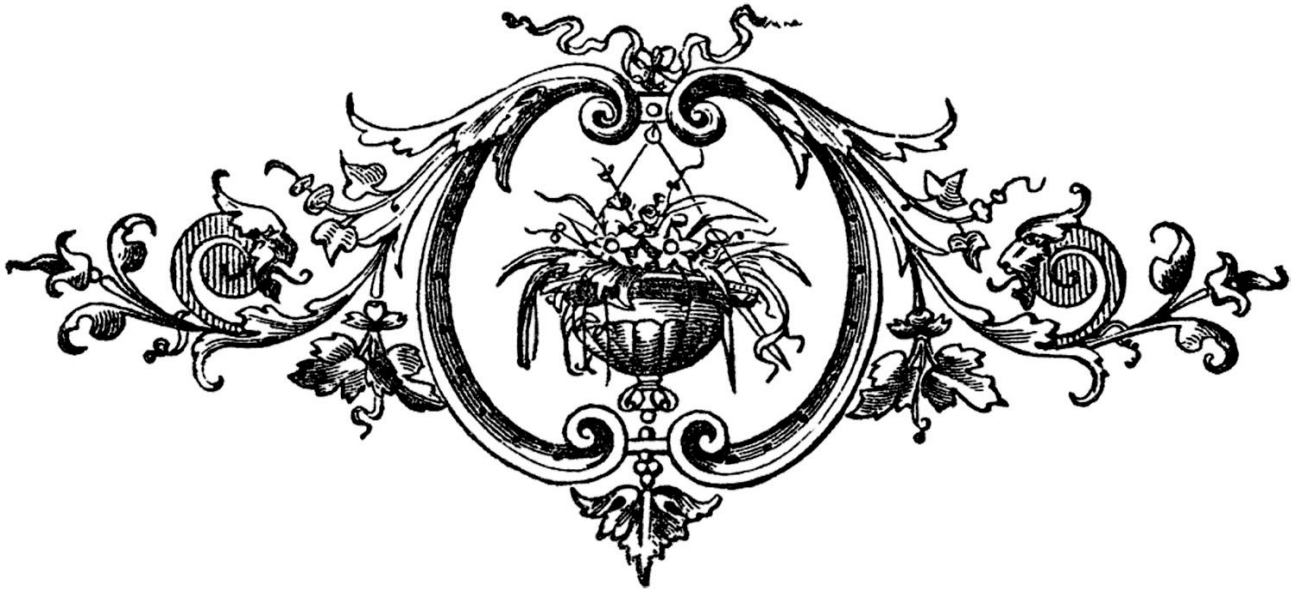

Book Chapters

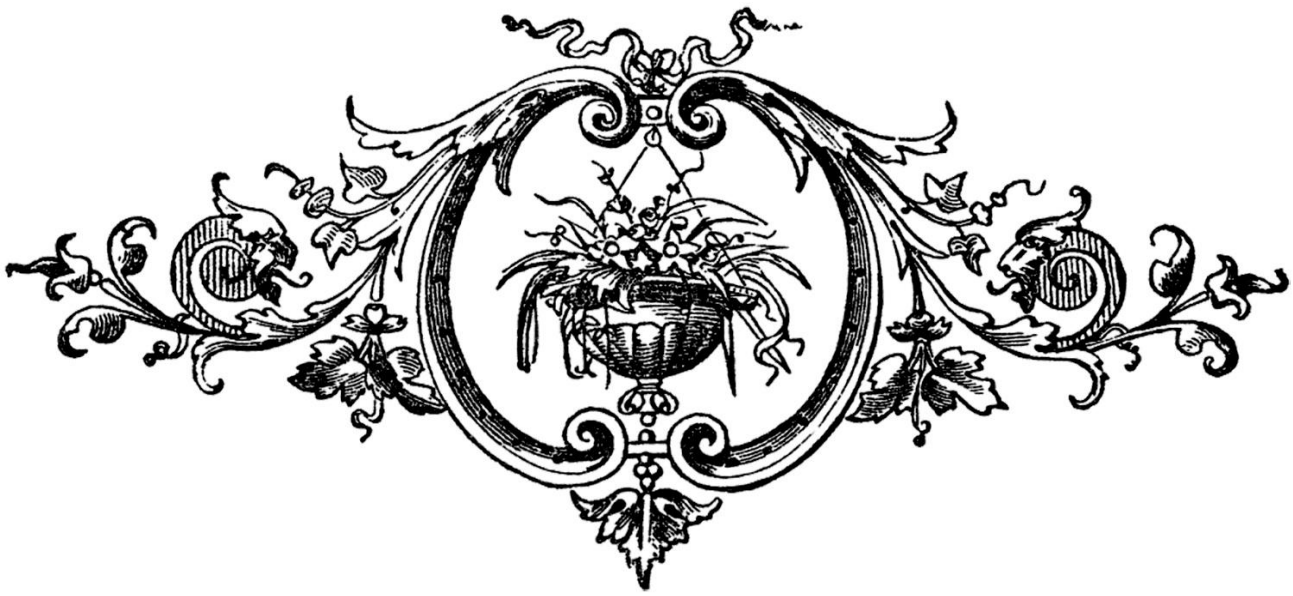

Encyclopaedia of Nuclear Physics of Stars

Ritu Tamta, Khaled S. A. Hassaneen, Johan H. Knapen

Synopsis: Astrophysicists distinguish between three different types of compact stars. These are white dwarfs, neutron stars, and black holes. Most compact stars are the endpoints of stellar evolution and are thus often referred to as stellar remnants, the form of the remnant depending primarily on the mass of the star when it formed. These objects are all small in volume for their mass, giving them a very high density. The former contain matter in one of the densest forms found in the Universe which, together with the unprecedented progress in observational astronomy, make such stars superb astrophysical laboratories for a broad range of most striking physical phenomena. These range from nuclear processes on the stellar surface to processes in electron degenerate matter at sub nuclear densities to boson condensates and the existence of new states of baryonic matter--like color superconducting quark matter at super nuclear densities. More than that, according to the strange matter hypothesis strange quark matter could be more stable than nuclear matter, in which case neutron stars should be largely composed of pure quark matter possibly enveloped in thin nuclear crusts. Another remarkable implication of the hypothesis is the possible existence of a new class of white dwarfs. Thermonuclear fusion drives stars through many stages of combustion; the hot center of the stars allows hydrogen to fuse into helium. Once the core has burned all available hydrogen it will contract until another source of support becomes available. As the core contracts and heats, transforming gravitational energy into kinetic (or thermal) energy, the burning of the helium ashes begins. For stars to burn heavier elements, higher temperatures are necessary to overcome the increasing Coulomb repulsion and allow fusion through quantum-mechanical tunneling. This 1st volume of Encyclopaedia of Nuclear Physics of Stars explores the diverse forms that such compact stars can possibly take, as constrained by the laws of nature: the general principles of relativity and quantum mechanics, the properties of nuclear matter deduced from nuclei, and the asymptotic freedom of quarks at high density. It reviews general relativity, essential aspects of nuclear and particle physics, and general features of white dwarfs, neutron stars and black holes; the discovery of pulsars and associated phenomena, and the strange-matter hypothesis.

Publisher: Auris Reference (ISBN: 9781788022415), 1st Ed., 1 Apr 2018, http://www.aurisreference.com/42-physics

Nuclear Physics the Core of Matter and the Fuel of Stars

Khaled S. A. Hassaneen

Synopsis

The light emitted by the stars is a direct result of the nuclear reactions that naturally occur when massive clouds of gas collapse and heat, whether it be the constant shine of our Sun, or the newly observed flares of gamma-ray bursters. Nuclear physics plays a fundamental role in astrophysics. Vast amounts of energy in the Universe are produced in nuclear reactions. For example, understanding the burning of stars, the dynamics of nucleosynthesis and the structure of neutron stars all require detailed knowledge of nuclear properties. The precise masses of atomic nuclei, their half-lives, and key nuclear reaction rates as well as the equation of state of nuclear matter are all important ingredients in stellar models. Nuclear Physics: The Core of Matter and The Fuel of Stars presents comprehensive coverage in understanding nuclear structure and symmetries, the behavior of matter at extreme densities, the role of nuclear physics in astrophysics and cosmology, and the instrumentation and facilities used by the field. It makes recommendations on the resources needed for experimental and theoretical advances in the coming decade. This volume brings together innovative research and reviews on the compact stars, such as white dwarfs and neutron stars. In addition description of dark matter and dark energy and the connection to the cosmical constant, proposed by Einstein, will be given.

Publisher: Auris Reference, ISBN: 9781788022439, 1st Ed., 01 Apr 2018, http://www.aurisreference.com/42-physics

Cyanotoxins in Egypt and Saudi Arabia

Zakaria A Mohamed

Abstract:
The presence of toxic cyanobacteria and their cyanotoxins in drinking, recreational, or irrigation water sources pose a risk to human health and agriculture; particularly in arid and semi-arid countries where water is limited. This article describes the cyanotoxins and their known producers, and the potential health risks in arid and semi-arid regions, with a special focus on Saudi Arabia and Egypt. The main bloom-forming cyanobacteria that have been detected in these water bodies included; *Anabaena*, *Anabaenopsis*, *Cylindrospermopsis*, *Microcystis*, *Oscillatoria*, and *Raphidiopsis*. The main cyanotoxins related to these cyanobacteria are microcystins, cylindrospermopsin, anatoxin-a-like toxins and saxitoxins. This study investigated the presence of microcystins in treated drinking waters, groundwater wells and hot springs, and their accumulation in edible tissues of fish and vegetables. Toxin concentrations generally exceeded WHO guidelines for maximum daily intake. These findings suggest a significant risk to human health could be occurring upon exposure to these potent toxins.

Encyclopedia of Environmental Health (2nd Ed.), 2019, 796-804